JULY 2017 M. Sc. in Mechanical Engineering ÖZKAN KİREÇ

UNIVERSITY OF GAZİANTEP

GRADUATE SCHOOL OF

NATURAL AND APPLIED SCIENCES

HEAT TRANSFER PERFORMANCE OF POROUS COPPER FOAM

M. Sc. THESIS

IN

MECHANICAL ENGINEERING

ÖZKAN KİREÇ

JULY 2017

Heat Transfer Performance of Porous Copper Foam

M. Sc. Thesis

in

Mechanical Engineering

University of Gaziantep

Supervisor

Prof. Dr. Melda ÇARPINLIOĞLU

by

Özkan KİREÇ

July 2017

T.C.
UNIVERSITY OF GAZİANTEP
GRADUATE SCHOOL OF
NATURAL & APPLIED SCIENCES
MECHANICAL ENGINEERING DEPARTMENT

Name of the thesis: Heat Transfer Performance of Porous Copper Foam

Name of the student: Özkan KİREÇ

Exam date: 06.07.2017

Approval of the Graduate School of Natural and Applied Sciences

Prof. Dr. Ahmet Necmeddin YAZICI

Director

I certify that this thesis satisfies all the requirements as a thesis for the degree of Master of Science.

Prof. Dr. M. Sait SÖYLEMEZ

Head of Department

This is to certify that we have read this thesis and that in our consensus opinion it is fully adequate, in scope and quality, as a thesis for the degree of Master of Science.

Prof. Dr. Melda ÇARPINLIOĞLU

Supervisor

Examining Committee Members	Signature
Prof. Dr. Melda ÇARPINLIOĞLU	....
Prof. Dr. Ahmet TANDIROĞLU	....
Yrd. Doç. Dr. Abdülaziz KAYA	....

I hereby declare that all information in this document has been obtained and presented in accordance with academic rules and ethical conduct. I also declare that, as required by these rules and conduct, I have fully cited and referenced all material and results that are not original to this work.

Özkan KİREÇ

İmza

ABSTRACT

HEAT TRANSFER PERFORMANCE OF POROUS COPPER FOAM

KİREÇ, Özkan
M.Sc. in Mechanical Engineering
Supervisor : Prof. Dr. Melda ÇARPINLIOĞLU

July 2017
211 pages

The main objective of this study is to investigate the heat transfer characteristics of porous copper foams described as a function of temperature, T_H geometry, porosity, ε thickness, t micro-structure and time, ϴ.

An experimental investigation which is based upon a modeling approach through the measurements of local temperatures by using thermal imaging camera along the x-y-z axis of the porous copper foam samples is conducted. This study characterizes a variety of plate type copper foam samples with 40 PPI and porosity, ε of 95 % ; samples with a size of 150 mm, (L) 30 mm, (W) and thicknesses of 3 mm, 4 mm and 5 mm and copper foil samples as a reference items with a size of 150 mm, (L) 30 mm, (W) and 0.4 mm thickness are studied at different heating surface temperatures, T_H in the range of $50\ ^\circ C \leq T_H \leq 100\ ^\circ C$. The microstructures of the foams are characterized with a scanning electron microscopy (SEM). Thermal image analyses and time dependent local changing of the thermal conductivity, k heat capacity, C and thermal diffusivity, α are calculated.

The experimental results showed that, k, C and α values of the porous copper foam and copper foil samples change between $140\ W/m.K \leq k \leq 651\ W/m.K$ and $32\ W/m.K \leq k \leq 98\ W/m.K$, $250\ J/K \leq C \leq 1270\ J/K$ and $3\ mm^2/s \leq \alpha \leq 42\ mm^2/s$ and $0.1\ mm^2/s \leq \alpha \leq 0.8\ mm^2/s$ depending on the T_H, t and ϴ.

Keywords : Copper Foam, Porosity, Thermal Conductivity, SEM, Thermal Analysis

ÖZET

GÖZENEKLİ BAKIR KÖPÜĞÜN ISI TRANSFER PERFORMANSI

KİREÇ, Özkan
Yüksek Lisans Tezi, Makina Mühendisliği Bölümü
Danışman: Prof. Dr. Melda ÇARPINLIOĞLU
Temmuz 2017
211 sayfa

Bu çalışmanın temel amacı, gözenekli bakır köpüklerin ısı transfer karekteristiğinin sıcaklık, T_H geometri, gözeneklilik, ε kalınlık, t mikro yapı ve zaman, ϴ açısından incelemektir.

Gözenekli bakır köpük numunelerinin x-y-z ekseni boyunca termal görüntüleme kamerası kullanılarak lokal sıcaklıkların ölçümleri yoluyla modelleme yaklaşımına dayanan deneysel bir araştırma yapılmıştır. Bu çalışma, çeşitli plaka tipi bakır köpük örneklerini, 40 PPI ve gözeneklilik,% 95 ε özelliklerine sahip; 150 mm, (U) 30 mm, (G) boyutlarında ve 3 mm, 4 mm ve 5 mm kalınlıklarda ve bakır folyo örnekleri 150 mm, (U) 30 mm (G) boyutunda ve 0.4 mm kalınlığında bir referans öğe olarak, 50 °C ≤ T_H ≤ 100 °C aralığında farklı ısıtma yüzey sıcaklıklarında incelenmiştir. Köpüklerin mikroyapıları bir taramalı elektron mikroskobu (SEM) ile karakterize edilmiştir. Termal görüntü analizleri ve termal iletkenlik, k ısı kapasitesi, C ve termal difüzivitenin, α zamana bağımlı lokal değişimi hesaplanmıştır.

Deney sonuçları gözenekli bakır köpük ve bakır folyo numunelerinin T_H, t ve ϴ' ye bağlı olarak, k, C ve α değerlerinin 140 W/m.K ≤ k ≤ 651 W/m.K ve 32 W/m.K ≤ k ≤ 98 W/m.K, 250 J/K ≤ C ≤ 1270 J/K ve 3 mm^2/s ≤ α ≤ 42 mm^2/s ve 0.1 mm^2/s ≤ α ≤ 0.8 mm^2/s aralıklarında değiştiğini göstermiştir.

Anahtar Kelimeler : Bakır Köpük, Gözeneklilik, Isı İletimi, SEM, Termal Analiz

ACKNOWLEDGEMENTS

I would first like to sincerely thank Prof. Dr. Melda Carpinlioğlu for supervision, guidance and interest throughout the my master thesis studies.

I want to also thank, Gaziantep University, Mechanical Engineering Department which gave me an opportunity for my researches and studies.

Finally, I would like to thank my family, who took on many extra responsibilities so that I could concentrate on my Ms. study. Their supports and helps are invaluable.

And I would like to thank me . . .

TABLE OF CONTENTS

LIST OF TABLES

Page

LIST OF FIGURES

Page

LIST OF SYMBOLS / ABBREVATIONS

Cu	Copper
ε	Porosity, %
d_{pore}	Pore diameter, m
d_{face}	Interior pore diameter, m
L_L	Ligament lenght, m
d_{edge}	Pore edge thickness, m
PPI	Pores per inch
ρ^*	Specific gravity
ρ_{foam}	Foam density, kg/m^3
ρ_{metal}	Density of base material, kg/m^3
A_{pore}	Cross-sectional area of the pores, m^2
A_{foam}	Cross-sectional area of the flow channel, m^2
V_{pore}	Volume of the pores, m^3
V_{foam}	Total volume of the foam, m^3
d_p	Pore size, mm
K	Permeability, m^2
μ	Dynamic viscosity of fluid, Pa.s

Q	Fluid flow rate, m^3s^{-1}
ΔL	Flow length, m
A	Cross-sectional area to fluid flow, m^2
ΔP	Pressure drop, Pa
q	Heat flux, kW/m^2
h	Mean heat transfer coefficient, $W/m^2.K$
Nu	Nusselt number
Re	Reynolds number
Q	Heat transfer rate, Watt
A_{base}	Cross sectional area of the base plate, m^2
T_{wall}	Average temperature of the base plate, ˚C
$T_{air,in}$	Temperature of the inlet air, ˚C
L_H	Heated length of the base plate, m
k	Thermal conductivity, W/m.K
q	Density of fluid, kg/m^3
V	Mean velocity of fluid, m/s
Q_{conv}	Convective heat transfer rate, kJ
m_{air}	Mass of air, kg
$C_{p, air}$	Specific heat of air, kJ/(kg/K)
T_o	Outlet temperature, ˚C
T_{in}	Inlet temperature, ˚C
k_A	Overall thermal conductivity of porous metal, W/m.K
k_f	Thermal conductivity, fluid phase, W/m.K

k_s	Thermal conductivity, solid phase, W/m.K
C	Heat capacity, J/K
C_{mol}	Molar heat capacity, J/mol.K
C_p	Specific heat capacity, J/Kg.K
α	Thermal diffusivity, mm^2/s
t	Copper foam thickness, mm
T_H	Heater surface temperature, ˚C
L	Copper foam length, mm
W	Copper foam width, mm
D	Copper foam diameter, mm
n_p	Number of pore
d_h	Hole diameter, mm
L_H	Lenght of heater unit, cm
W_H	Width of heater unit, cm
t_H	Thickness of heater unit, cm
x_p	Sample location, cm
ρ_b	Bulk density, kg/m^3
ε_m	Material emissivity
m	Mass of material, kg
V	Volume of material, m^3
d_i	Inner hole diameter, mm
Θ	Time, min
T_R	Room temperature, ˚C

Θ_e Exposed time, min

T_p Numbers of measured local temperature point

ω_R Uncertainty, %

T_{edge} Copper foam edge temperature, ˚C

ΔT_{edge} Copper foam upper and contact surface edge temperature difference, ˚C

ΔT_{cf} Mean temperature difference between upper and contact surface of the copper foam, ˚C

$T_{m,upper}$ Upper surface mean temperature, ˚C

$T_{m,\ contact}$ Contact surface mean temperature, ˚C

ΔT_H Temperature differences between upper and contact surfaces of the heater, ˚C

T_{upper} Upper surface temperature, ˚C

$T_{contact}$ Contact surface temperature, ˚C

Q_{cond} Conduction heat transfer, W

T_{min} Minumum temperature, ˚C

T_{max} Maximum temperature, ˚C

ΔT_{foil} Mean temperature difference between upper and contact surfaces of the copper foil, ˚C

$\Delta T_{foil,hole}$ Mean temperature difference between upper and contact surfaces of the copper foil with holes, ˚C

$T_{edge,upper}$ Upper surface edge temperature, ˚C

$T_{edge,contact}$ Contact surface edge temperature, ˚C

T_{ave} Average temperature of heater, ˚C

T_i	Initial temperature of heater, ˚C
T_f	Final temperature of heater, ˚C
A	Surface area of sample, m^2
x_d	Nearest distance between 2 points on sample surface, m
ΔT	Temperature difference, K
$T_{f,cf}$	Final temperature of the copper foam sample after the specified time period, ˚C
k_i	Initial value of thermal conductivity at a specified time, W/m.K
k_f	Final value of thermal conductivity at a specified time, W/m.K

CHAPTER 1

INTRODUCTION

Along with the rise of today's issues such as energy-efficiency and thermal balance of machinery, the interest on cellular solids in engineering applications has increased. Porous metals are cellular structural materials with a large volume fraction of pores. The main advantages of metal foams lie on their low density, large surface area, high strength structure, good impact energy, sound absorption and excellent thermal management abilities. From characteristic properties of the metal foam, recent researches show the emerging importance of open cell metal foams especially for fluidic and thermal application fields. For that reason, many scientists and engineers have recently related to porous medium by means of open cell metal foams.

1.1 Motivation of Research

During the last decades, open cell metal foams have been widely used in many engineering fields and become important materials in innovative research and development studies. However, open cell metal foams require advanced researches and further studies to define the thermal characteristics properties. The characterization and design of porous structures is critical for many industries, but generalized prediction of their properties is extremely difficult due to their random nature and geometric complexity. At this point, experimental investigations may help to gain a deep insight and understanding.

Literature studies show that there are few researches on open cell Cu foam materials to define the thermal characteristics of the porous material which enable to study on it is motivation of the research.

1.2 Objectives of Research

The main objectives of the research are experimental investigations of thermal characteristic of the Cu foam materials, showing the time dependent effects of porous medium, Cu foam shapes, sizes, thicknesses and heat source temperatures on heat transfer performances.

Several parameters including, thermal conductivity, heat storage capacity and thermal diffusivity are necessary and important to define the heat transfer characteristics of the porous metal foams. The experimental results compared with Cu foil and Cu foil with holes reference items to show the porous medium effects on heat transfer.

1.3 Outlines of The Thesis

Thesis study includes six chapters. Chapter 2 reviews the literature on porous medium and basic definitions of properties and potential usage of metal foams and importance of thermal characteristics of open cell metal foams for many engineering fields are introduced. Material and heat transfer characteristics of porous metal foams with basic equations and researches are presented. Experimental and numerical studies on heat transfer characteristics and performances of porous medium by means of thermal conductivity, heat capacity and thermal diffusivity are also given. Finally, literatüre studies are analyzed and discussed in detail for the presented study.

Chapter 3 gives a detailed description and properties of the Cu foams & Cu foil reference items. Micro-structure analyses of Cu foams with different thicknesses are presented by SEM unit and Bruker microCT software programme. A detailed descriptions of the experimental study and methodology for thermal analyses of the test samples by means of heating and cooling processes are explained. Finally, uncertainty analysis of the experimental studies are given.

Chapter 4 presents the thermal image analysis results of the Cu foam samples as a function of different parameters. Time dependent thermal profiles of the Cu foam upper and contact surfaces and time dependent temperature difference between upper and contact surfaces of the test samples with respect to different heater temperatures are given in detail. Thermal images and histogram temperatures and also comparisions of the Cu foam samples are presented. Finally, time dependent variation of the (T_{edge} / T_H) and (ΔT_{edge} / T_H) for Cu foam samples & Cu foil reference items are given.

Chapter 5 discusses and presents a detailed analysis of the thermal characteristic of the Cu foam samples and Cu foil reference items by means of thermal conductivity, heat capacity and thermal diffusivity. Time dependent effects of the thicknesses and heater temperatures on thermal properties are investigated and presented. In the last part of the chapter, cooling performances of the test samples are introduced.

Finally, Chapter 6 summarizes the thesis study and makes some recommends for future researches and studies.

CHAPTER 2

LITERATURE SURVEY ON THE USAGE OF POROUS MEDIUM

2.1 Introduction

Heat transfer behaviour or characteristics of metal foams by means of thermal conductivity, heat capacity and thermal diffusivity are important parameters for defining and enhancement of the heat transfer performance. In this chapter, general characteristics and properties of porous medium were defined. Firstly, some information and researches were given about the porous medium and their applications in the engineering fields. After defining the porous medium, metal foam and its classifications were presented with basic terminology. Basic formulations and researches were given in the related studies. Finally, literature studies were analyzed and some conclusions were presented for the basics of the conducted experimental study.

2.2 Porous Media

A porous medium or porous material by definition consists of a solid metal matrix with pores/voids. They are low cost and lightweight structures with distinctive mechanical, thermal, electrical and acoustical properties.[1-4]

Porous media are used in many areas of applied science and engineering. Usage of porous media to extend the heat transfer area, improve effective thermal conductivity, mix fluid flow and thus enhance heat transfer is an enduring theme in the field of thermal fluid science. Particularly, the metallic porous medium exhibits excellent thermal performance because of many unique advantages such as low relative density, high strength, high surface area per unit volume, high solid thermal conductivity, and good flow-mixing capability. [5]

Porous medium may be used in many practical applications for heat transfer enhancement, such as catalyst supports, filters, biomedical implants, heat shield devices for space vehicles, novel compact heat exchangers, and heat sinks, et al. [6-9]

A metallic porous medium is the subject of this study, it can be called as porous metal foam as an industrial term.

2.3 Metal Foams

Metal foams can be made from almost all base materials, such as aluminium, magnesia, tin and copper. The cell structure of metal foam is of statistical nature, where the cells and the pore sizes are more or less statistically scattered, depending on the related manufacturing process. Two major foam types can be distinguished, namely;

i) Closed cell

ii) Open cell

Closed cell foams are characterised by segregated pores that are not linked or connected, as can be seen from Figure 2.1 (a). These foams typically have almost exclusively spherical cells, a very good mass to stiffness ratio, low density and excellent energy absorption properties. Therefore, closed cell foams are suited for the applications in numerous fields within the scope of weight optimisation and impact energy absorption, e.g. automobile and aerospace sectors.

Open cell foams are permeable materials with metallic properties. High porosity open-cell metal foam is a relatively recent development. The characteristic features like high surface area density, low weight and ability to mix fluids have accredited metal foam a potential choice in a variety of thermal engineering applications. [10-19] They feature a very homogeneous structure as can be seen from Figure 2.1 (b) enable constant characteristics over a wide range. Open-cell metal foams can be produced with a large range of pore sizes, types and properties depending on the application. Because of the structure's high variability and functional properties like mechanical strength, sound absorption and high thermal properties, enormous application of fluid and heat transfer studies and researches exist. [20] For example, copper and copper alloys are used for the applications with high heat conductivities.

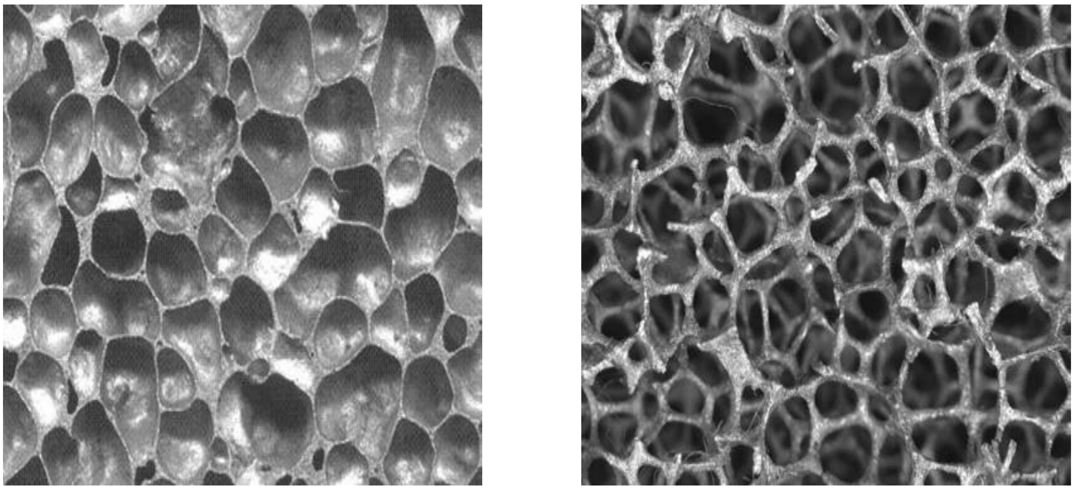

(a) (b)

Figure 2.1 : (a) Closed cell foam and (b) Open cell foam [1]

(This images were taken from: [1] http://commons.wikimedia.org/wiki/File:Closed_cell_ metal_foam_with_large_cell_size.

Figure 2.2 shows the characteristic measures of open cell metal foams. As can be seen from the image, pore size, d_{pore} which defines the unit cell diameter, edge thickness, d_{edge} defines the strut thickness, d_{face} defines the interior pore diameter and ligament length, L_L defines the length of edge of the pore. A certain number of pores can be achieved by both, small pores with thick struts, as well as by large pores with small struts or ligaments. Despite having the same pore density, this results in very different ratios of void volume, V_{pore} and volume of the parent metal, V_{foam} of the foam.

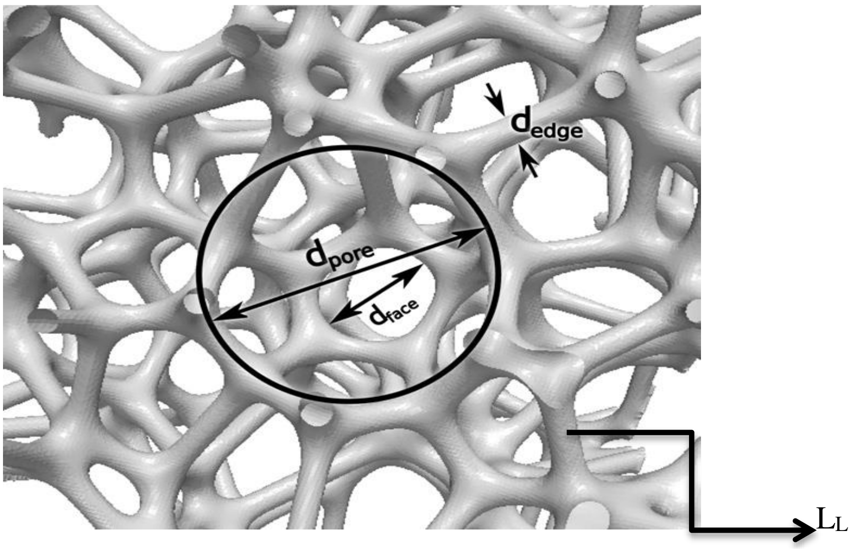

Figure 2.2 : Characteristic measures of open cell metal foams

(This image was taken from, [10] page 8, Figure 2.2)

Prior research in the metal foam literature has generally regarded the Kelvin unit cell as the idealized foam structure best describing metal foams [21, 22, 23, and 24]. This unit cell is relatively easy to model as a single pore described by a regular polyhedral. Some prior work has been done regarding the classification of closed-cell metal foam structures using X-rays and computed tomography (X-ray CT) [25, 26].

The current approach is to obtain geometric data for metal foam samples of varying porosity using X-ray CT, and to use the results for a comparison to idealized geometries.

Thermo-physical and flow properties depend strongly on local morphology of both pore and solid matrix. Local change in the structure could govern the properties (e.g. constriction, strut cross section, surface roughness, etc.). Accurate evaluation of these properties becomes critical for various uses. Yet, solid foam structure and properties are still incompletely characterized (As can be seen from Hugo and Topin [27]), hence induce lot of discrepancies in thermophysical properties.

Metal foams are novel heat transfer surfaces with potential use as heat sinks and heat exchangers. Their inherently high surface area enable effective dissipation of heat to passing air streams. In this manner, they have been recently come to be used especially heat exchanger sectors, aerospace and power electronics companies. Because of its naturally properties, porous metals can be used in wide range of engineering fields such as mechanical, electrical, biological, energy storage and thermal management applications. For that reason, characterization and design of porous metal foams are the key points for many industries.

In order to simulate the heat transfer in porous metal foams, modelling of open cell foams with X-ray microtomography is vital. In the last decade, both stochastic and periodic open cell metal foams have been largely studied through experimentation and analysis. [28]

New and innovative heat transfer techniques are needed for heat transfer enhancement and pressure drop research and development studies. In this view, porous metal foams are good candidate to reach these purposes.

2.4 Material Characteristics of Metal Foams

Characterization of the metal foam samples with regard to their specific properties is significant for the subsequent investigations, gaining more detailed information on the structural composition and on the permeable volume. The micro structure of metal foams consists of small solid or hollow ligaments forming a network of inter-connected dodecahedral-like cells [29, 30]. The shape and size of these open cells vary throughout the medium which make the structure random and anisotropic. Three of the parameters that describe such media are:

1) Specific gravity,
2) Porosity or relative density
3) Pore density which is typically expressed in the unit of pores per inch (PPI).

The specific gravity, ρ^* is defined as ratio of the density of the foam, ρ_{foam} and density of the base material, ρ_{metal} [31,32] as

$$\rho^* = \rho_{foam} / \rho_{metal} \tag{2.1}$$

The porosity, ε is the ratio of the cross-sectional area of the pores, A_{pore} and the cross-sectional area of the flow channel, A_{foam}. According to [33] ε is defined as,

$$\varepsilon = A_{pore} / A_{foam} \tag{2.2}$$

Based on the volume of the pores, V_{pore} and the total volume of the foam, V_{foam} ε is written as [34, 35]

$$\varepsilon = V_{pore} / V_{foam} \tag{2.3}$$

PPI is usually employed to characterize the pore size of the foam metal which is defined by

$$PPI = 25.4 / d_p \tag{2.4}$$

where d_p is the pore size.

Another important parameter is the permeability, K, which is part of the proportionality constant in Darcy's equation. Darcy equation is satisfactory when flow through a porous medium is slow enough, pressure drop is solely due to viscous drag. K is an important parameter for open cell porous metals that effects the convective heat transfer properties, and shows how easy a fluid can flow through the porous material formulated from well-known Darcy equation as follows,

$$K = \frac{\mu . Q . \Delta L}{A . \Delta P} \tag{2.5}$$

where, K is the permeability of a medium (m^2), μ is the dynamic viscosity of the fluid (Pa.s), Q is fluid flow rate (m^3s^{-1}), ΔL is the flow length (m), A is the cross-sectional area to fluid flow (m^2) and ΔP is the pressure drop (Pa).

2.5 Thermal Properties and Heat Transfer Characteristics of Metal Foams

Metal foam provides an extended surface with high surface area and complex flow paths. These properties enable excellent convective heat transfer performance. If metal foams are to be widely used in thermal and fluid systems, their pressure-drop and heat transfer characteristics must be known for design purposes.

In this section, the heat transfer performance of porous metal foams were explained. Many different research groups have studied the heat transfer characteristics of these porous media both experimentally and analytically. It is a widely held view that metal foams are still incompletely characterized because of their specific structure. The information repository is improving with time whereas the widespread use of the high porosity media in modern technological devices makes the need for fully characterizing them more urgent. Developments on this issue will certainly help engineering researchers, especially in terms of heat transfer area [36,37].

Heat transfer can be defined as thermal energy in transit due to spatial temperature difference. They [38] explained that, heat transfer proceeds if there is a difference in temperature in a medium or between media through conduction, convection or radiation.

Heat transfer performance in porous metals can be explained by four mechanisms:

(i) Heat conduction through the metal cell walls,
(ii) Heat radiation through the metal cell walls,
(iii) Heat conduction through the pores in the sample and through the interlinked channels
(iv) Convection within the pores.

Numerous researchers have been interested in the thermal performance of open cell metal foams, and several studies are available in the literature. Kurtbas et al. [39] conducted an experimental study for investigating the heat and exergy transfer characteristics of forced convection in a horizontal rectangular channel with inserted aluminum open cell metal foam under constant heat flux, using different pore densities of 10, 20, 30. They found that the aluminum open cell metal foam has a considerable effect on the thermal performance when they compare their results with an empty channel. Ghosh [40] performed a systematic study to give an overview related to heat transfer in a metal foam and asked ‘‘How good is open-cell metal foam as a heat transfer surface?’’. In his study, the effect of area density as functions of pore size and strut diameter were discussed. He concluded that foams are a promising alternative for compact heat exchangers due to the ideal thermodynamic characteristics. As noted by Mancin et al. [41,42], the normalized mean wall temperate, and the pumping power per unit of heat transfer area can be used to compare the different heat transfer behavior of metal foams. In addition, the global heat transfer coefficient, q increases as the porosity, ε decreases at PPI = 10. Similarly, many researchers have argued that the usage of metal foams in air channel is an effective method for heat transfer from boundary [43,44]. Calmidi *et al.* [45, 46] characterized the heat transfer behavior of different aluminum foams in a wind tunnel. The measurements were conducted by heating the base of the foam and using air as the coolant. The seven tested aluminum foams were designated to range from PPI = 5 to PPI = 40, with a ε that varied between

$0.89 \leq \varepsilon \leq 0.97$, respectively. They found that if air velocity increases, heat transfer will enhance. Furthermore, at a constant frontal velocity, the heat transfer coefficient, h increased with decreasing ε. Hsieh *et al.* [47] carried out an experimental study to characterize the heat transfer behavior of several heat sinks made of aluminum metal foams of height 60 mm with different ε and PPI changing between $0.87 \leq \varepsilon \leq 0.96$ and $10 \leq PPI \leq 40$. They experimentally analyzed the effect of ε on heat transfer, and as part of their work measured the heat transfer performance of four samples with PPI = 20 and differing ε. At constant ε, they found that the heat transfer performance is better at higher PPI. Boomsma and Poulikakos [48] investigated the effective or overall thermal conductivity, k_A of three-dimensionally structured metal foam saturated with liquid. Nawaz *et al.* [49] considered open-cell aluminum metal foam as a highly compact replacement for conventional fins in brazed aluminum heat exchangers. Heat transfer and pressure drop data were obtained from wind-tunnel experiments in order to make the comparisons. The target application was for air-cooling systems, and the authors demonstrated that metal foams have promise. Moofat [50] showed that three parameters must be known to calculate the heat transfer performance of a foam-fin: the convective conductance per unit volume, the effective conductive conductance as a fin, and the effective thermal resistance between the foam and the surface to which it is attached. He developed a new test method, which, in conjunction with an older well established type of test, allows all three parameters to be measured using one specimen. Experimental h values were measured during air flow for seven different aluminum open-cell foam samples with different PPI, ε, and foam core height, h under a wide range of air velocity, V. Three imposed heat fluxes, q were considered for each foam sample, q = 25.0, q = 32.5 and q = 40.0 kW/m^2. The collected heat transfer data were analyzed to obtain the global heat transfer coefficient and normalized mean wall temperature. He selected a model and compared to experimental data, and a new model for the global h and surface area efficiency was presented.

Calmidi and Mahajan [51] developed a model to compare the thermal performance of metal foam heat sinks. They defined a mean h, an average Nusselt number, Nu and a Reynolds number, Re based on the square root of K in order to demark the limit for darcy flow that flow through porous medium is slow, are shown in the following equations.

$$h = Q / A_{base} (T_{wall} - T_{air,in}) \quad (2.6)$$

where, h is the mean heat transfer coefficient characterize the heat transfer by means of convection. Q is the heat transfer rate, A_{base} is the cross sectional area of the base plate, T_{wall} is the average temperature of the base plate and $T_{air,in}$ is the temperature of the inlet air.

$$Nu = hL_h / k \quad (2.7)$$

where, Nu is the nusselt number, which is usually used for characterization of convective heat transfer, Q_{conv}. h is the mean heat transfer coefficient, L_h is the heated length of the base plate and k is the thermal conductivity of the sample.

$$Re = qV\sqrt{K} / \mu \quad (2.8)$$

where, Re is Reynolds number, is often used to describe flow regime, q is the density of fluid, V is the mean velocity of fluid, K is the permeability and μ is the dynamic viscosity of the fluid.

The convective heat transfer rate from electrically heated test surface is calculated as follows

$$Q_{conv} = m_{air} C_{p,air} (T_o - T_{in}) \quad (2.9)$$

Where, m_{air} is mass of air, $C_{p,\,air}$ is specific heat of air, T_o and T_{in} are outlet and inlet temperatures, respectively.

Seyf and Layeghi [52] reported that the heat transfer performance increased with increasing ε and decreasing cell size of metal foams. Zhao et al. [53] experimentally studied the heat dissipation capability of metal foams with forced air convection and found that the cell size has a more significant effect on the overall heat transfer than ε. Mancin et al. [54] investigated forced air convection through heated copper foams and found that the heat transfer coefficient did not depend on the imposed heat flux, q but increased with the fluid flow rate. They also reported the existence of optimal structural parameters (e.g. PPI and surface area) which gave the best heat transfer performance. Tamayol and Hooman [55] theoretically studied the forced convection through metal foams and observed a direct relationship between the heat transfer rate, Q and PPI and solidity, that is, the Q increased with pore density (PPI) and decreased ε. They also added that increasing the foam height enhanced the Q. It is well documented that the heat transfer performance can be significantly enhanced by utilising force cooled metal foams. It was also observed that for metal foams, there exist optimal structural parameters which gave the best heat transfer performance. At this optimal point, a balance between the heat transfer of the fluid and solid phases is achieved.

2.5.1 Thermal Conductivity of Porous Metal Foams

Thermal conductivity, k can be found using a bar with one end of the bar at a higher temperature of T_1 and the other end at a lower constant temperature of T_2. Heat is conducted from the hot end to the cold end at a steady rate as both sides are completely insulated. In steady-state conditions, providing the heat energy passing through any positions is the same within the bar, the heat flow is proportional to the temperature gradient and the area of the cross section [56-57].

$$Q = k\, A\, (dT/dx) \tag{2.10}$$

where Q is the heat flow, k is the thermal conductivity, A is the cross-sectional area perpendicular to the direction of heat flow, and dT/dx is the temperature gradient through the medium conducting heat.

Thermal conductivity is an important parameter for defining the thermal characteristic properties of metal foam. The widespread range of applications of metal foams has led to increase in the interest of modeling the heat transfer phenomena in porous media. It is pointed out that the precise calculation of thermal conductivity is required for accurate modeling of thermal transport through open-cell metal foam as well as foam heat exchangers. Many researches investigated the thermal conductivity of the porous medium including fluid phase (air/water).

A group of studies considered a specific geometry and distribution of pores and/or particles, and/or used the analogy between thermal, electrical, and mass transport phenomena. Using the analogy between mass diffusion and heat conduction, Hsu et al. [58] proposed a complex correlation to determine k_A of sponge like porous media using b as a shape factor which is a function of the ε. Calmidi and Mahajan [59] have proposed one dimensional conductivity model considering the porous medium to be formed by a two dimensional array of hexagonal cells with square lumps at nodes for high porosity metal foams. The models can predict accurately the thermal conductivity for Al foams but they overestimate the k for other foam structures. [60] Kaviany gives the following expression to describe the k_A of porous metal as follows,

$$k_A = \varepsilon k_f + (1 - \varepsilon)k_s \quad (2.11)$$

where, k_A is the overall conductivity, ε is porosity, subscripts *f* and *s* show the fluid and solid phase.

2.5.2 Heat Capacity of Porous Metal Foams

Heat capacity is known as the internal energy of a system, or the systems microscopic kinetic and potential energy. Heat capacity or thermal capacity, C is a measurable physical quantity of a substance that characterizes the amount of heat needed to change the temperature of the substance to a given degree, in other words the ratio between the amount of heat transferred to the sample Q, and the resulting increase in temperature ΔT, by the absorbed heat. [61-64] General heat capacity equation is given as,

$$C = Q / \Delta T \quad (2.12)$$

The property can be specified in different terms, molar heat capacity, which is per mole of a pure substance, and the specific heat capacity, which is per unit mass of a material.

C_{mol} – Molar heat capacity (J/mol.K)

c – Specific heat capacity (J/Kg.K)

Heat capacity measurements can be made theoretically or experimentally. For experimental heat capacity measurements, differential scanning calorimeter (DSC) are used. DSC measurements are normally quite simple, fast and accurate, but heat capacity measurements usually require a minimum of three experiments and a normal accuracy provided is typically only ± 10 % [65]. It is important to know the heat capacity of porous metal foam for defining the thermal behaviour of the material.

There are limited researches related with heat capacity of porous materials. For that reason, in this study, heat capacities of the Cu foam samples were calculated and detaily analyzed in the next chapters.

2.5.3 Thermal Diffusivity of Porous Metal Foams

Thermal diffusivity, α is the thermophysical property that defines the speed of heat propagation by conduction during changes of temperature. The higher the α, the faster the heat propagation. The thermal diffusivity is related to the k, C_p and ρ.

Thermal diffusivity of a material can be defined as the thermal conductivity divided by the product of specific heat capacity and density which can be expressed mathematically as [66] ;

$$\alpha = k \,/\, (\rho . Cp) \tag{2.13}$$

where, α is thermal diffusivity (m^2/s) or (mm^2/s), k is thermal conductivity (W/m.K), ρ is density (kg/m^3) and Cp is specific heat capacity (J/kg.K).

In literature, there are limited number of studies related with thermal diffusivity of porous medium, On the other hand, there are several methods to measure thermal diffusivity of porous materials ; some uses the modification of the initial condition [67], some uses specimen thickness correction [68,69], and some uses the sandwich structure to measure α [68]. Moreover, there is a prediction method for determining thermal properties using a numerical and an analytical approach [70]. The α can also be obtained by pulsed thermography measurements in transmission and reflection mode. In transmission mode a time-domain procedure is applied which is closely related to the standardized Parker's method [71]. For that reason in the present study, a detailed analyses of thermal diffusivity of the Cu foam samples depending on the different thicknesses of t = 3 mm, 4 mm and 5 mm and temperatures of T_H = 50 ˚C, 80 ˚C and 100 ˚C were given, respectively.

2.6 Analysis of Literature In Terms of Experimental Research

There have been many investigations which are based on the heat transfer performance of porous medium by means of porous material in the engineering applications fields. Some of the researches are related with material characteristics of the metal foams which describes the porous medium by analysing the micro-structure of the material. Similarly, many different research groups have studied the heat transfer characteristics of the porous medium, experimentally and analytically. Their studies generally includes the effects of area density as a function of d_p and d_{edge}, cell size, ε, h and k which were discussed for heat transfer performances.

In the experimental studies, aluminium metal foams are mostly used in air channel for characterization of the heat transfer behaviour of different aluminum foams as a function of a variety of ε to observe the effects of ε on heat transfer. The other studies which include the k_A of porous metal foams saturated with liquid, pressure drop relations in channel, calculation of h, comparisions of the thermal performance of metal foam heat sinks, heat dissipation capability of metal foams with forced air convection, optimum ε for Δ_p and heat transfer performance and effects of specific geometry and pore distributions on the best heat transfer performances. Related other important studies were summarized as follows,

Boomsma et al. [72] experimentally studied the heat performance of open-cell aluminum foam heat exchangers during forced convection heat transfer by using liquid coolant, and they investigated the effect of aluminum foam ε on thermal performance. Their findings indicated that the pressure dropped significantly at the highest solid friction (lowest ε), and Nu number increased with increasing coolant velocity. Jiang et al. [73] experimentally studied forced air and water convection in porous plate channels. The effects of porous medium type, particle diameter, fluid velocity, and fluid properties on heat transfer enhancement and forced convection were investigated.

Their findings indicate that heat transfer was enhanced with increased water and air flow rates. Tzeng and Jeng [74] experimentally studied forced convection and Δ_p in porous media channels with a 90_ turned flow during isoflux heating on the bottom wall. The effects of aluminum foam PPI, entry width to porous sink height ratio, and Re number were investigated. They found that an increase in Re number increased the Nu number and that aluminum foam PPI and the ratio of entry width to porous sink height had negligible effects on Nu number. Mohammed and Salman [75] experimentally studied mixed convection in a horizontal circular cylinder for hydrodynamically fully developed, thermally fully developed, and thermally developing laminar air flow. The effect of mixed convection parameters on heat transfer rate was investigated. They found that Nu number increased with q increase in all entrance sections. In addition, the effects of natural convection tended to decrease the heat transfer results at low Re number whereas the opposite was observed at high Re number. Kurtbas and Celik [76] experimentally analyzed mixed convective heat transfer and fluid flow through a horizontal aluminum foam plate in a rectangular channel with varying PPI. Their findings indicate that average Nu number increased in proportion to PPI and rapidly increased at a critical Re number. Wu and Wang [77] numerically studied two-dimensional unsteady forced convection heat transfer with uniform heat generation on the bottom surface of a non-permeable cylinder with an incompressible laminar flow across a porous square cylinder in the middle of a channel. They investigated the effects of Re, ε, and cylinder-to-channel height ratio (B/H) and found that heat transfer increased with increase in Re number and ε. Kamath et al. [78] experimentally studied mixed convection in a vertical channel containing aluminum foams of varying PPI and ε in the range 90–95%. In their study, the effects of Re numbers and ε on heat transfer were investigated and their findings indicated that a porous medium in small inlet velocities does not enhance heat transfer, and porous matrix conduction marginally enhances heat transfer. The average surface temperature of the aluminum plate dropped and h increased with increasing power input. Jeng et al. [79] has experimentally studied the heat transfer and pressure drop in a 180-deg round turned channel fitted with aluminum foam blocks installed with different arrangements. The ε and the PPI of the samples used were ε = 0.90 and PPI = 10 respectively. They found that the average Nu number was from 74 to 140 % higher than that obtained with an empty channel. Furthermore, the staggered configuration of the aluminum foam blocks was found to enhance the heat transfer capacity more efficiently with a lower pressure drop than the symmetric configuration. Mancin et al. [80] achieved an experimental study of the heat transfer and fluid flow in a horizontal channel fitted with twenty-one different aluminum and Cu foams with PPI = 5, PPI = 10, PPI = 20 and PPI = 40. They found that for all aluminum foams samples, the global h increases with the air mass flow rate and are not depend on the imposed q. They proposed two correlations which predict accurately the h and the $\Delta_{P.}$

If literature studies are critized, there are some important results. Generally aluminum foam materials are used because of commercially easy to find, light in weight and cheap to buy it. All researches was made to enhance the heat transfer performance of the metal foam. For that reason, effects of the some parameters such as ε changing between $0.87 \leq \varepsilon \leq 0.97$, PPI changing between $5 \leq PPI \leq 40$ inlet velocity of air / water on heat transfer are main subject. From previous studies it can be seen that, Nu number increases in proportional to Re number and heat transfer enhanced with increased with air or water flow rates. Although some experimental and theoretical researches have been carried out on the heat transfer performance of metal foams, still there are very limited studies available for heat transfer characteristics of porous Cu foam materials. For that reason, the aims of the present study are experimentally investigate the effects of the Cu foam thicknesses, t on the heat transfer behaviour of the material and define the heat storage and thermal characteristics of the porous Cu foam as a function of geometry, ε, T_H and different time periods, Θ.

2.7 Conclusions

Literature studies about porous medium show some important results which summarized as follows;

1. Experimental studies show that the open cell metal foams have a considerable effect on the thermal performance when results compared with the empty channel.
2. Metal foams are a promising alternative for compact heat exchangers due to the ideal thermodynamic characteristics.
3. Nu number increased with an increase of the ε. At constant ε, heat transfer performance is better at higher PPI.
4. Heat transfer performance increased with increasing ε and decreasing cell size of metal foams.
5. Cell size has a more significant effect on the overall heat transfer than ε.
6. Heat transfer rate increased with PPI and decreased ε.
7. Increasing the foam height, h enhanced the heat transfer rate. It is well documented that the heat transfer performance can be significantly enhanced by utilising force cooled metal foams. It was also observed that for metal foams, there exist optimal structural parameters which gave the best heat transfer performance.
8. Precise calculation of k_A is required for accurate modeling of thermal transport through open-cell metal foam as well as foam heat exchangers.
9. Heat capacity of porous metal foam for defining the thermal behaviour of the material is vital.
10. Thermal diffusivity, α shows the relation between k and C of the porous material.

From the results, more attention and a detailed analysis of the porous Cu foam materials are necessary for exactly defining the heat transfer characteristics and performances as a function of different variables and conditions.

CHAPTER 3

EXPERIMENTAL STUDY AND MEASUREMENTS

3.1 Introduction

In this section, the properties, dimensions, microstructure and material analysis results (SEM, microCT and EDX Analysis) of copper (Cu) foam and Cu foil samples were given. A detailed description of the experimental study and procedures for thermal analysis were also presented with the range of the measurements.

3.2 Properties of The Tested Copper Foam / Foil Samples

A variety of Cu foam samples and home-made Cu foil plate and Cu foil plate with drilled holes as reference items were used. Cu foam samples were purchased from manufacturing company, Beijing Shunyuan Wangda Trade Co., China. They have plate and cylindrical forms. Photographs of the tested samples were shown in the Figure 3.1.

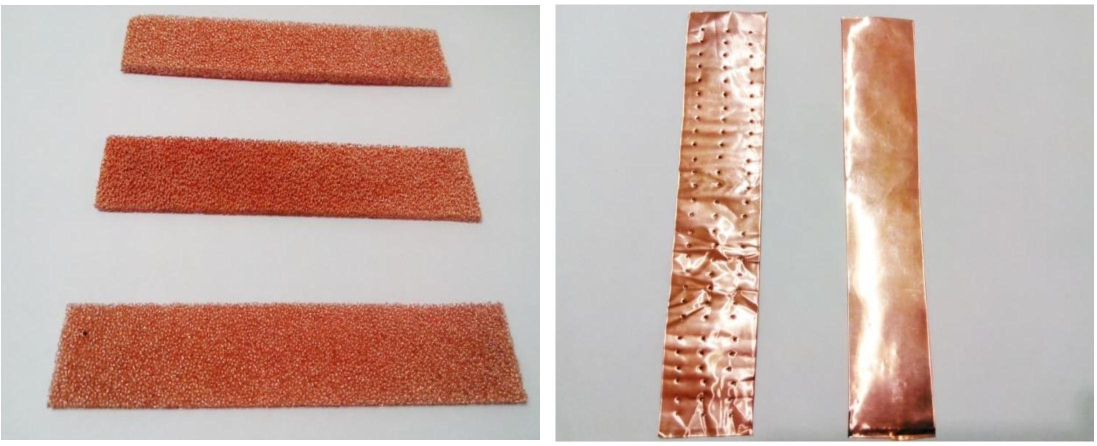

a) b)

Figure 3.1 Photographs of the Cu foam and foil samples with different thicknesses.
a) Plate type Cu foams, b) Cu foil plates

Figure 3.1a shows the tested plate type Cu foam samples with three different thicknesses, t, t = 3 mm, t = 4 mm and t = 5 mm. Cu foam length, L is 150 mm and Cu foam width, W is 30 mm.

Figure 3.1b shows the Cu foil reference plates which, L = 150 mm, W = 30 mm and t = 0.4 mm. Cu foil with drilled holes, which have n_p = 84 holes with hole diameter of d_h = 0.7 mm. Holes are drilled with 0.5 cm distances at horizontal and 1 cm at vertical directions respectively.

Geometric scale of the Cu foam samples with the preferred directions were shown in the Figure 3.2.

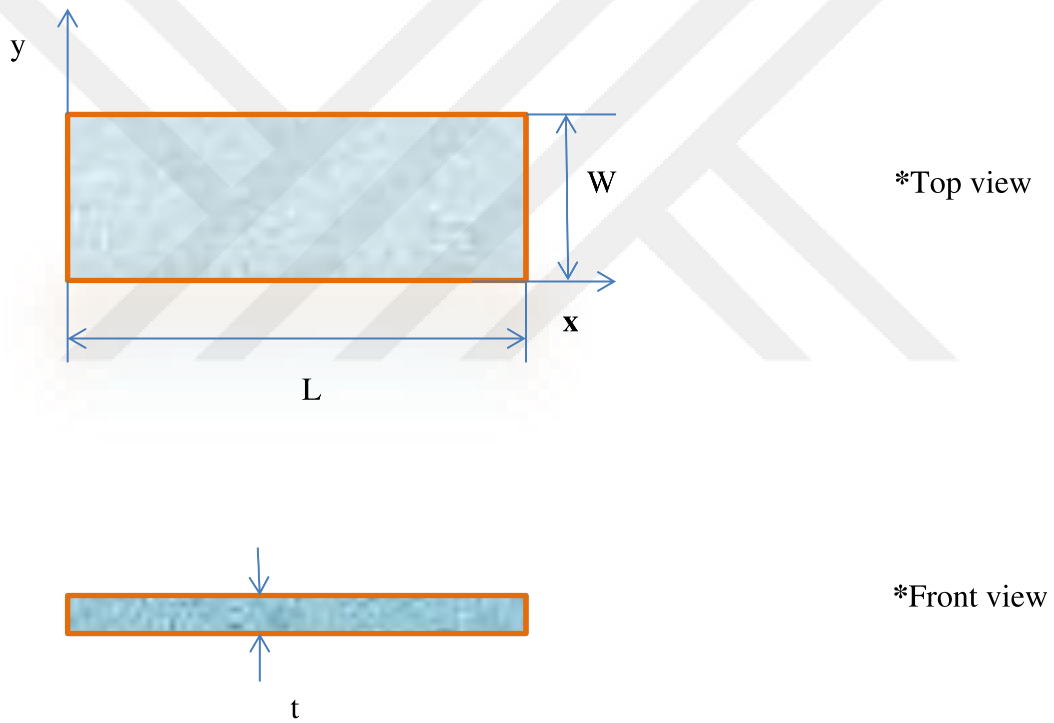

Figure 3.2 Geometric scales and top and front views of the plate sample

It is seen from the Figure 3.2 that, L, W, and t show length, width, and thickness of the tested Cu foam samples. The test samples were located along the heater unit as shown in the Figure 3.3.

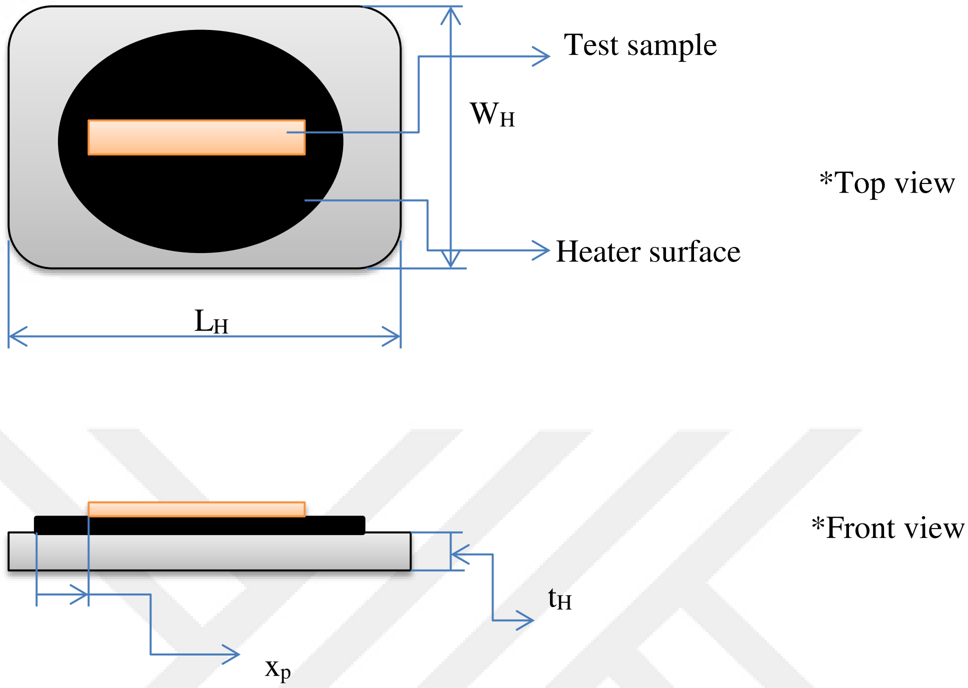

Figure 3.3 Geometric scales and top and front views of the heater unit

It is seen from the Figure 3.3 that, L_H, W_H and t_H show length, width and thickness of the heater unit and x_p shows the sample location.

The geometrical characteristics of the Cu foam and Cu foil samples were given in Table.3.1.

Table 3.1 : Properties and dimensions of the Cu foam and Cu foil samples

Test Sample	Sample Description	Shape	Dimension (mm)	Thickness, t (mm)	Porosity, ε (%)	PPI	Bulk Density, ρ_b (kg/m^3)	Material Emissivity, ε_m
1	Cu Foam	Plate	L =150, W = 30	3	95*	40*	715.555***	0.45**
				4			639.444***	
				5			616.444***	
2	Cu Foil Reference Items			0.4	0	0	2072.222***	0.1**
3	Cu Foil with Drilled Holes				0.72***	6***	2183.333***	

* Values were given by manufacturing company, Beijing Shunyuan Wangda Trade Co., China

** Material emissivity values were taken from Mikron Instrument Company on web

*** Calculated for presented study

Specifications of the test samples were shown in the Table 3.1 and sample dimensions were measured with ruler to compare the manufacturing company values. Results of the measurement showed that all given informations are correct.

It was stated that, bulk density, ρ_b is a physical properties of a granular solid and it was calculated by dividing the weight of a given volume of the material by the volume it occupies. ρ_b was given as,

$$\rho_b = m / V \tag{3.1}$$

where, ρ_b is the bulk density of material, kg/m^3, m is the mass of material, kg and V is the volume of material, m^3. Bulk densities of the samples were calculated by using the equation 3.1. Mass values of the samples were measured by sensitive scale and shown in the Table 3.2.

Table 3.2 : Measured mass values of the Cu foam / Cu foil test samples

<table>
<tr><th>Sample</th><th>Shape</th><th>Thickness, t
(mm)</th><th>Mass, m
(gr)</th></tr>
<tr><td>Cu Foam</td><td rowspan="3">Plate</td><td>3, 4, 5</td><td>9.660, 11.510, 13.87</td></tr>
<tr><td>Cu Foil
Reference Items</td><td rowspan="2">0.4</td><td>3.73</td></tr>
<tr><td>Cu Foil with
Drilled Holes</td><td>3.93</td></tr>
</table>

Volume values of the samples were calculated by using the following equations.

$$V = L.W.\,t \tag{3.2}$$

Where, V is the volume of the plate material, m^3, L is the length of the material, m, W is the width of the material, m and t is the thickness of the material, m. And,

$$V = \pi . r^2 . t \qquad (3.3)$$

where, V is the volume of the cylindrical material, m^3 , π is the mathematical constant, 3.14, r is the radius of the material, m and t is the thickness of the material.

Material emissivity, ε_m may be defined as the ratio of the radiance from the surface to that from a black body viewed under identical optical and geometrical conditons and at the same temperature. The ε_m used in single color thermometry to achieve a correct temperature reading. The ε_m of a surface varies with both temperature and wavelength for a metal. Often surface finish plays a major influence on emissivity values. The values of the ε_m may show some differences depending on the use of different techniques and samples.[81]

Cu foam material emissivity values varies between $0.02 \leq \varepsilon_m \leq 0.88$ depending on the surface conditons and temperature values.

3.3 Micro Structure and Material Analysis of The Copper Foam Samples (SEM & EDX Analysis)

In this section, micro-structure and material analysis results of the cylindrical Cu foam samples were given.

3.3.1 Scanning Electron Microscopy (SEM) Analysis

SEM analyses of the Cu foams were made by using JEOL 6390LV scanning electron microscopy at the Gaziantep University Physics laboratory. The SEM is a type of electron microscope that creates various images by focusing a high energy beam of electrons onto the surface of a sample and detecting signals from the interaction of the incident electrons with the sample’s surface. The primary function of the SEM is an imaging platform that can image using secondary electrons (SE) or backscattered electrons (BSE). Compositions of the material can be found, when coupled with X-ray detectors. Thermal characteristic’ properties of Cu foams depend on the micro-structure of the material. To observe the characteristics of the Cu foams, SEM analysis results of the Cu foam samples are needed. Analysis results for t = 2 mm, t = 3 mm and t = 5 mm cylindrical Cu foams were given in the Figures 3.4 through 3.6.

3.3.1.1 JEOL 6390LV Spectro Electron Microscopy

The JEOL 6390LV SEM unit has a magnification of 300,000x, where fine details of specimen can be observed. The SEM unit has high performance with a high resolution of 3.0 nm, and can accomodate up to 6 – inches in diameter. Standart automated features include auto focus, auto gun, automatic contrast and brightness.

For t = 2 mm Thickness Cylindrical Cu Foam

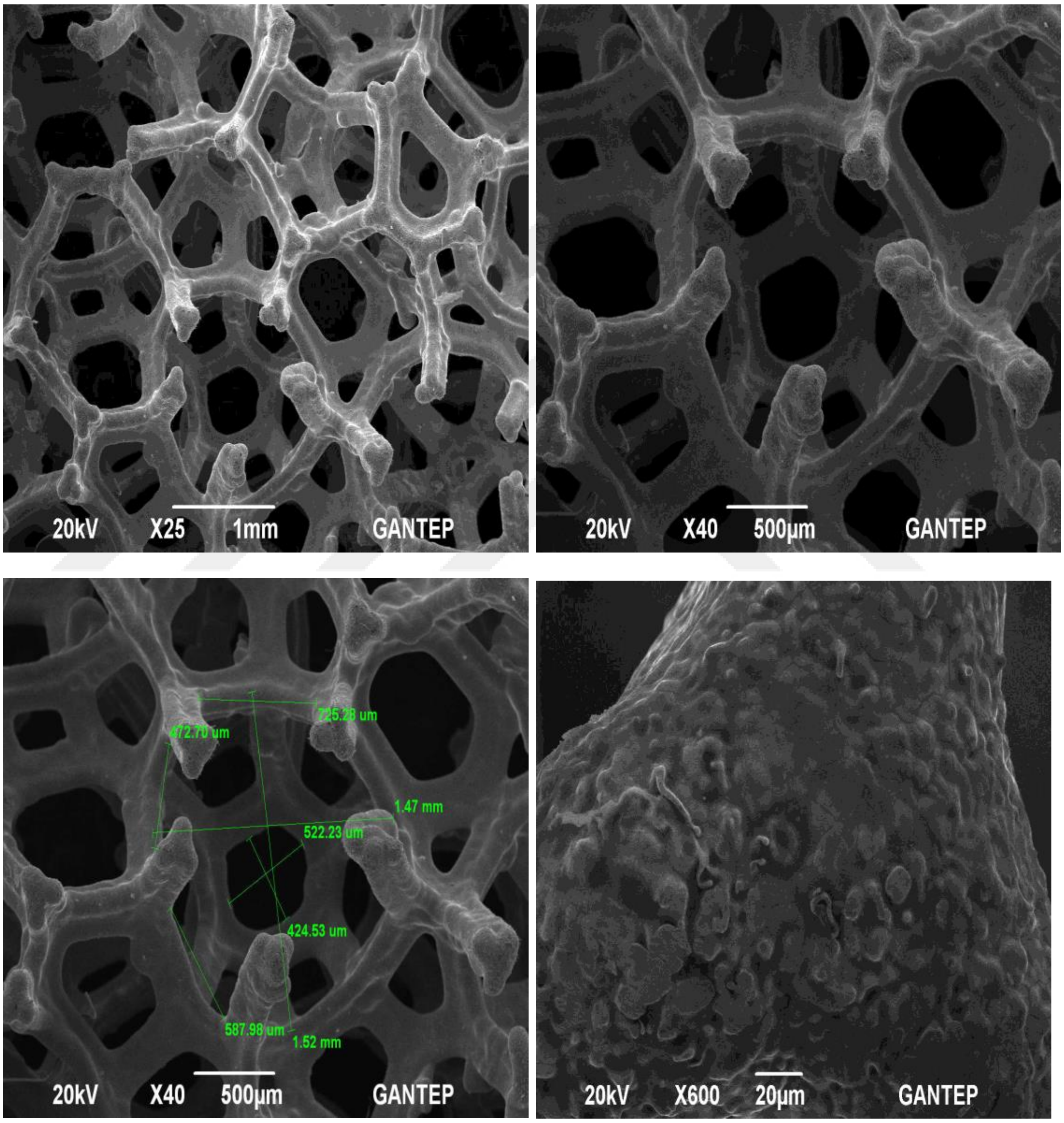

Figure 3.4 SEM images of 2 mm thickness Cu foam with different scales and measured dimensions

For t = 3 mm Thickness Cylindrical Cu Foam

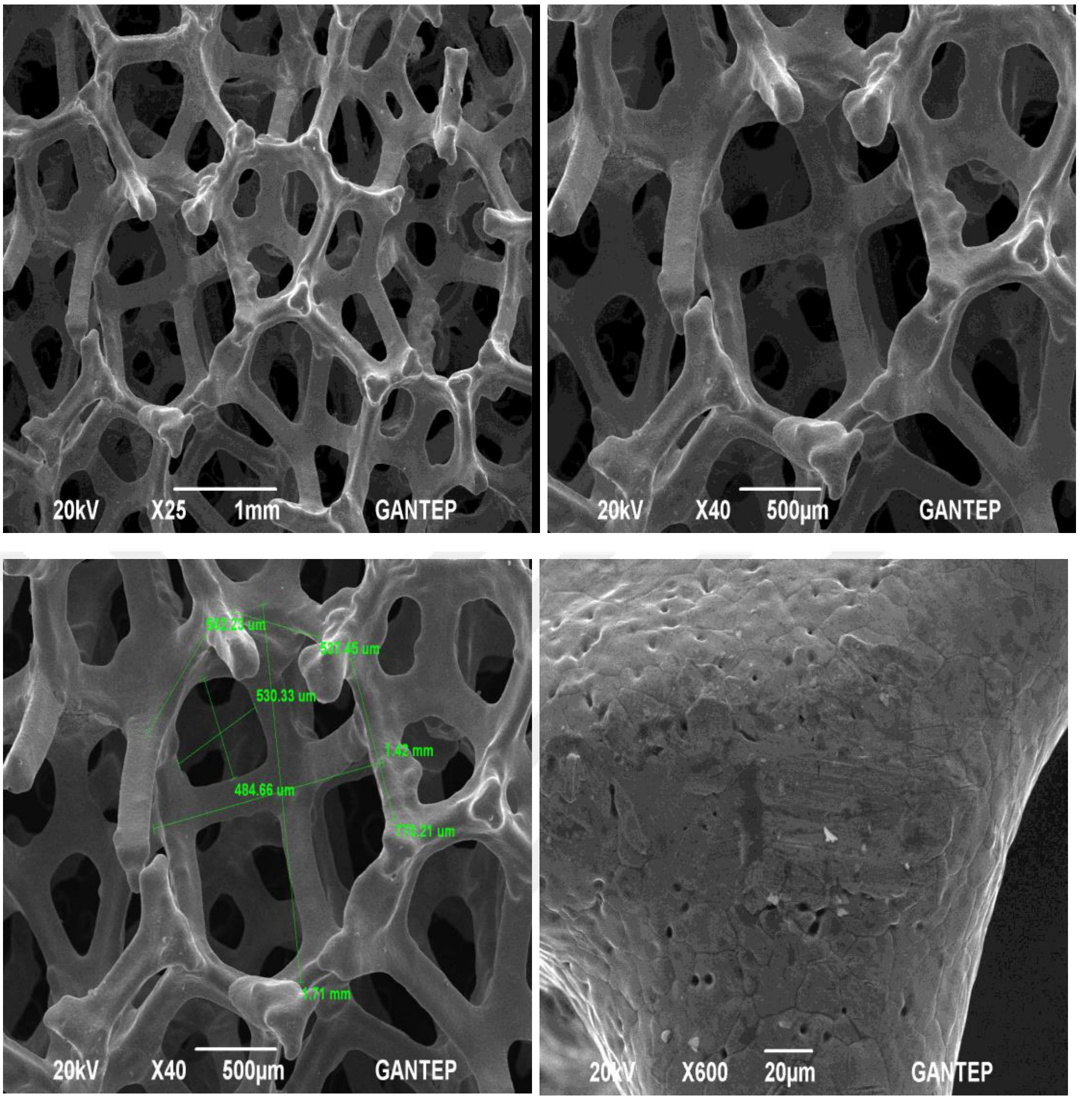

Figure 3.5 SEM images of 3 mm thickness Cu foam with different scales and measured dimensions

For t = 5 mm Thickness Cylindrical Cu Foam

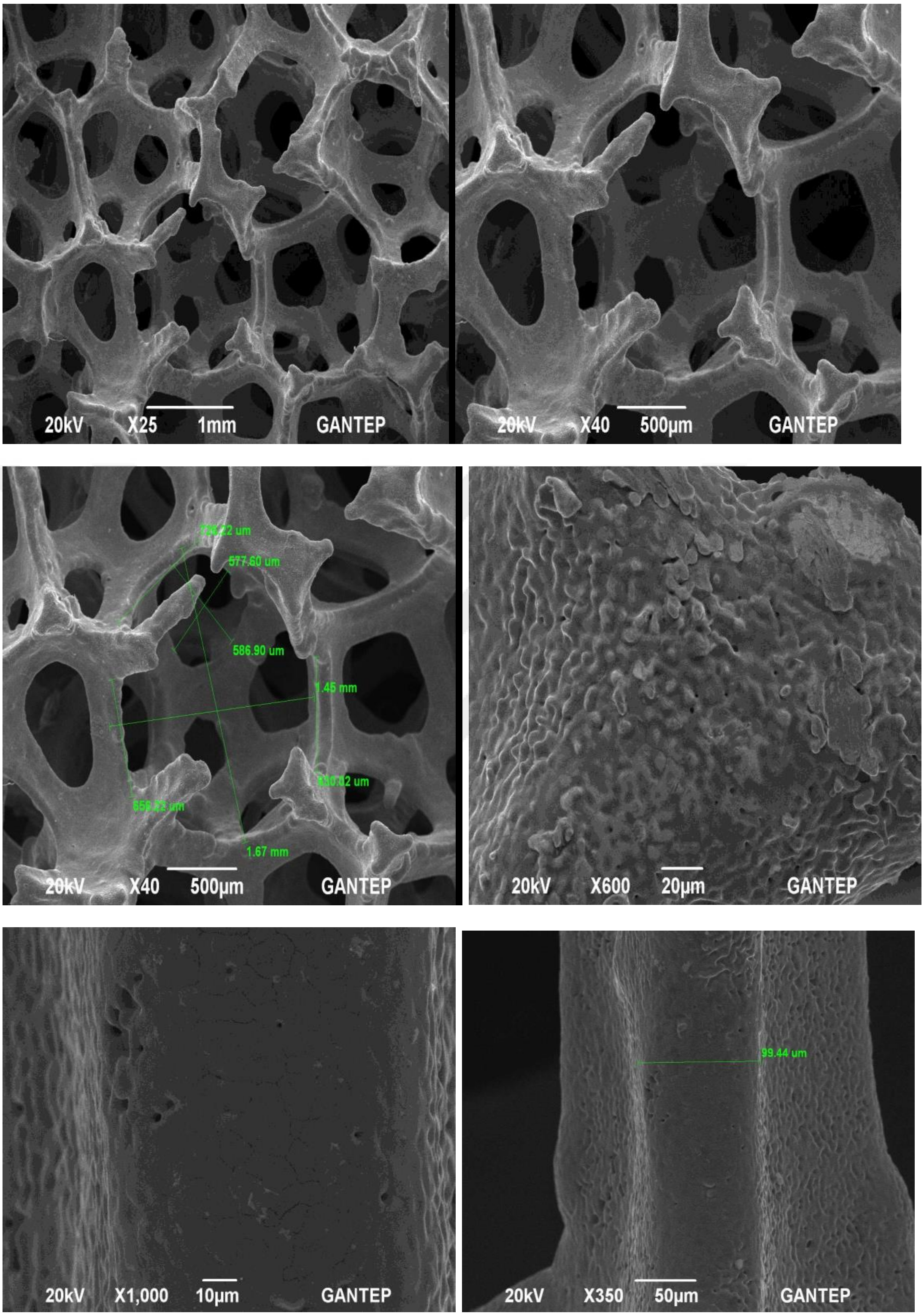

Figure 3.6 SEM images of 5 mm thickness Cu foam with different scales and measured dimensions

SEM analysis results of the Cu foam samples gave some information about the micro structures properties of the sample. These are, pore shape, pore size, connection between the pore structures, pore distribution and material characteristics. In addition to the these properties, some micro pores can be seen depend on the manufacturing or design conditions. In order to define the physical or thermal characteristic properties of the Cu foam material, detailed analysis of the micro-structure is vital for further heat transfer enhancement studies.

A variety of micro-structure images of the Cu foam samples with different scales can be seen from the Figure 3.4 through 3.6. Analysis results and comparisons were given in the following sections.

3.3.2 Energy Dispersive X-Ray Spectroscopy (EDX) Analysis

EDX (Energy Dispersive X-Ray Spectroscopy) is an x-ray technique used to identify the elemental composition of materials. Applications include materials and product research, troubleshooting, deformulation, and more. EDX systems are attachments to SEM instruments where the imaging capability of the microscope identifies the specimen of interest. The data generated by EDX analysis consists of spectra showing peaks corresponding to the elements making up the true compositon of the sample being analysed. Cu foam material compositions were found by using EDX analysis shown in the Figure 3.7 and Table 3.3.

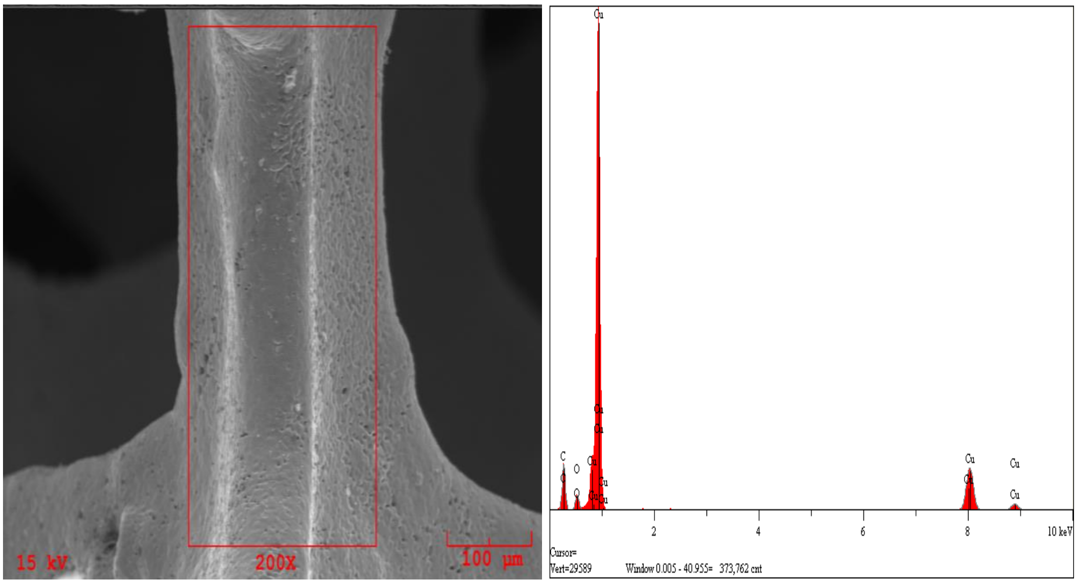

Figure 3.7 Images of EDX analysis of the Cu foam sample

Table 3.3 : EDX analysis results

Element	Concentration	Units
C	26.395	wt.%
O	5.916	wt.%
Cu	67.689	wt.%
Total	100.000	wt.%

It was seen from the table that, material is mostly composed from the Cu element with 67.689 % and remaining is found as C and O.

3.3.3 Micro-Structure Analysis of The Cu Foams Using The Software Programme

To analyse the Cu foam micro-structure, free evaluation version of the Bruker microCT software programme was also used.

3.3.3.1 Bruker microCT Software Programme

CT-Analyser (CTAn) is an application for measuring quantitative parameters and constructing visual models from scanned 3D datasets obtained with SkyScan microCT instruments. It can also be used for 3D and 2D images obtained from other imaging modalities. CTAn allows real time volume rendered model viewing; surface rendered models are also created by CTAn for viewing in another program – CT-Volume ("CTVol"). Quantitative measurement is made both of densitometry (voxel attenuation coefficient or calibrated density) and of morphometry, the latter based on a segmented (black and white) image. Thresholding or "segmentation" is done by simple global or by adaptive methods. Before analysis, adjusting of the pixel size according to magnification of the Cu foam was made. Necessary information taken from CTan user manual. Analysis results were compared with manufacturing company informations. Image analysis views and results were given in the Figures 3.8, 3.9 and 3.10.

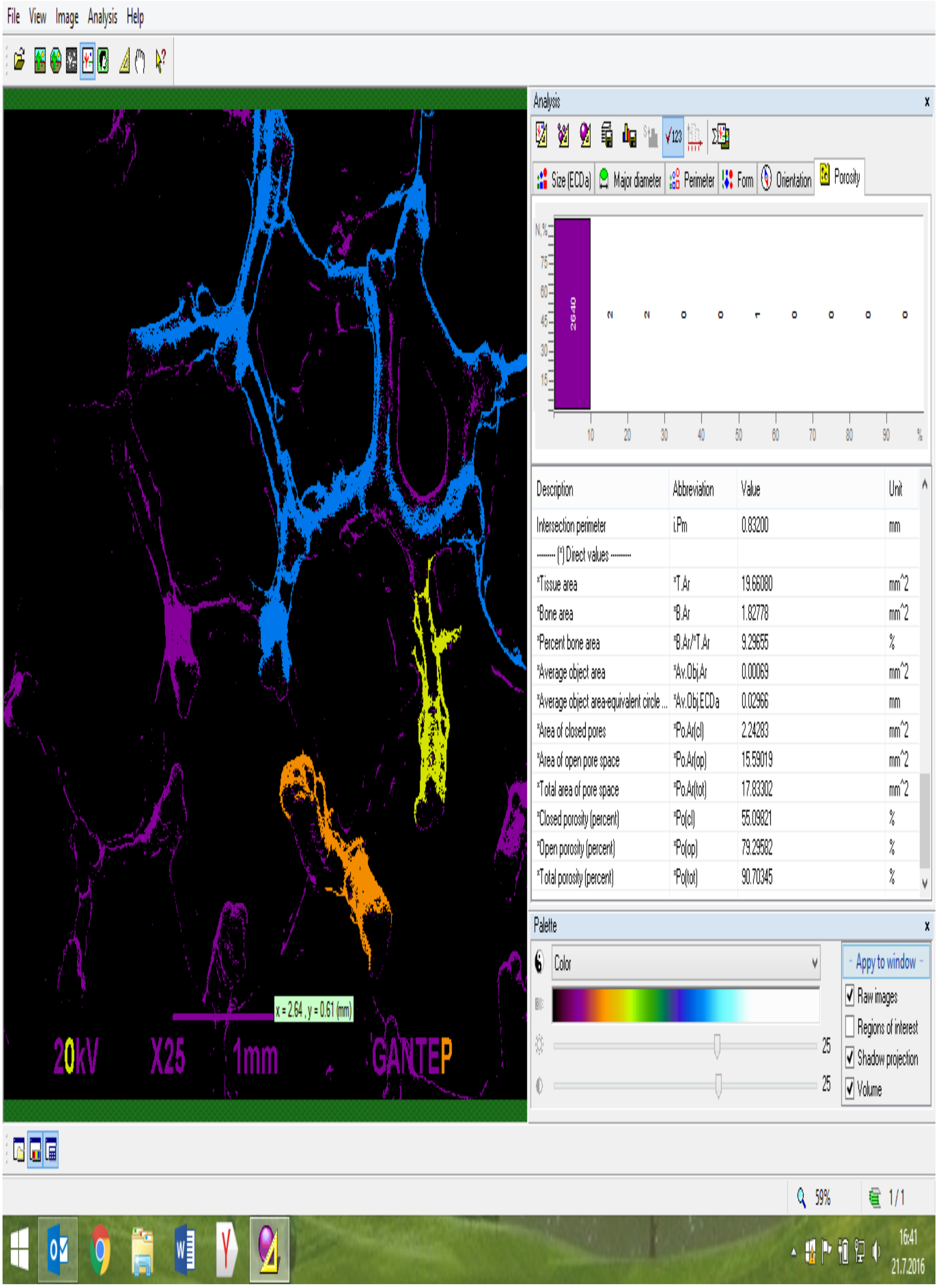

Figure 3.8 Image view of the t = 2 mm cylindrical Cu foam

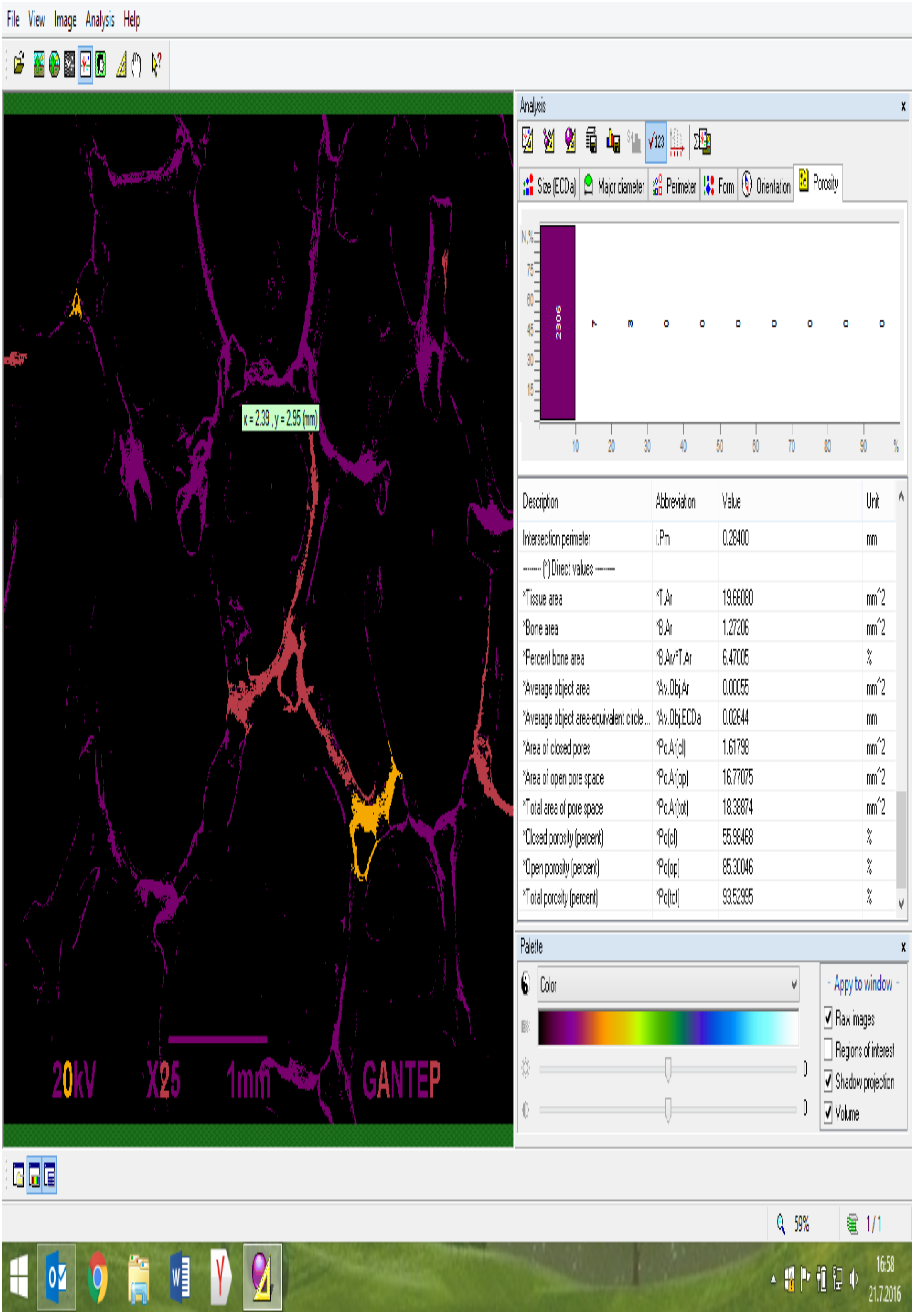

Figure 3.9 Image view of the t = 3 mm cylindrical Cu foam

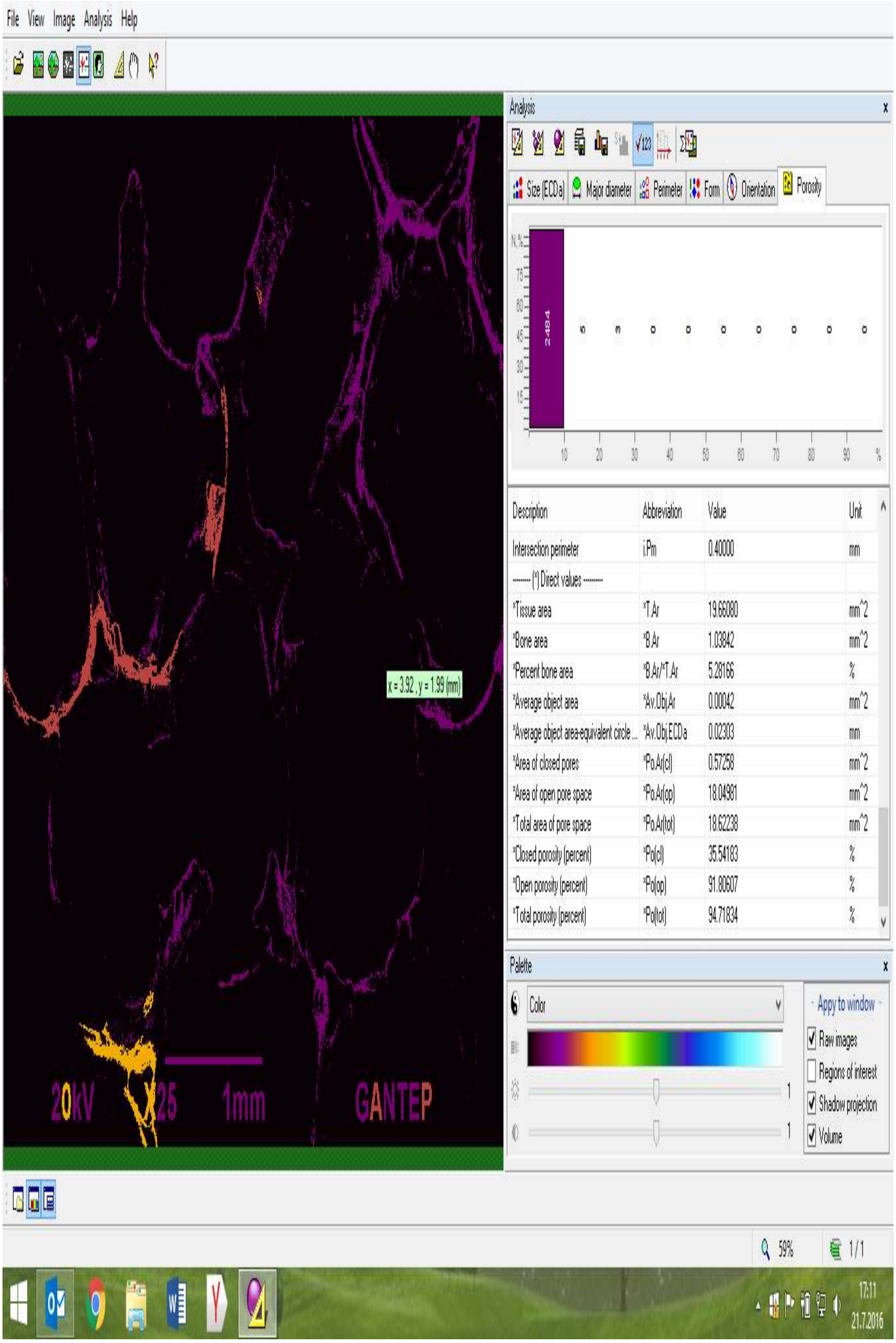

Figure 3.10 Image view of the t = 5 mm cylindrical Cu foam

From the Figures 3.8 through 3.10, micro-structures of the Cu foam samples can be seen. The software program enables the 2D or 3D analysis of the each point or region which needed for micro structure analysis studies which can be selected by analyser. Program gives more information about the Cu foam samples such as, tissue and bone area, area of closed and open pore, total area of pore space, closed porosity and open porosity values. Also, pore size, pore distributions and orientations can be seen in detail.

It is clear from the analysis results, if bone area decreases, total porosity, ε increases. ε change is approximately 4.5 % between t = 2 mm and t = 5 mm Cu foam samples. Depending on the total area of pore space, ε changes. ε increases with increasing pore space area. In addition to these results, particle porosity and number of particles values can be seen from the analysis programme.

Finally, because of the dimension limitation, SEM analysis, EDX analysis and Bruker microCT analyses are applied to cylindrical Cu foam samples. For plate type Cu foams, similar or near results can be seen depending on the manufacturing standarts. After analysing the SEM images of the Cu foams, micro structure properties were given in the Table 3.4.

Table 3.4 : Micro structure properties of the cylindrical Cu foams

Micro Structure Properties of The Cylindrical Cu Foam Samples					
Thickness (mm)	**Pore Diameter, d_p (mm)**	**Inner Hole Diameter, d_i (mm)**	**Ligament Length, L_L (mm)**	**Micro Pores**	**Porosity, ε %**
2	1.4 - 1.5	0.4 - 0.5	(472 - 588 - 725)	-	90.7*
3	1.4 - 1.7	0.4 - 0.6	(537 - 562 - 770)	Available	93.5*
5	1.4 - 1.7	0.5 - 0.6	(630 - 656 - 726)	Available	94.7*

*Porosity values calculated by using the Bruker microCT software programme for SEM image views of t = 2 mm, t = 3 mm and t = 5 mm cylindrical Cu foams.

From Table 3.4, it is clear that pore diameters d_p, inner hole diameters d_i, ligament lengths, L_L and ε show some differences depending on the thickness of the Cu foam samples. It is important to note that t = 3 mm and t = 5 mm Cu foams include some micro pores. These results show the manufacturing of the Cu foams are not same. For this reason, thermal analysis results showed some variations. In this view, design and manufacturing of the Cu foam materials are most important for heat transfer studies in engineering fields and applications. Value of the ε was reported as % 95 by manufacturing company. If analysis was made with usage of the Bruker microCT software programme, results showed little differences but near values for SEM image views of cylindrical Cu foams.

These results show that, given information about the Cu foam samples by manufacturing company are correct. Comparisons of the calculated and reported ε values were given in Table 3.5.

Table 3.5 : Comparisions of the calculated ε values

Calculated Method	**Thickness (mm)**	**Porosity, ε %**
Manufacturing company	2	95
	3	
	5	
Bruker microCT software programme	2	90.7
	3	93.5
	5	94.7
By measurement, $\varepsilon = V_{pore} / V_{foam}$	2	99
	3	
	5	

It was seen from Table 3.5, Bruker microCT sofware programme showed more sensitive results compared with other calculation methods. It is also obvious that, differences in results showed the importance of the precise analysis of the micro-structure of the foam material to obtain the more correct results.

3.4 Basics of The Experimental Study on Thermal Characteristics of Test Samples

This part consists of two sections. In the first section, experimental equipments which were used in the study were given. In the second section, a detailed description of the experimental study and procedures for temperature measurements and thermal analyses of the test samples were explained. All experimental studies were performed in the laboratories of Gaziantep University.

3.4.1 Experimental Equipments and Measurement Devices

In this section, properties and specifications of the Testo 875-2i thermal imaging camera and Sinbo SCO 5030 heater unit will be given.

3.4.1.1 Testo 875-2i Thermal Imaging Camera

The testo 875-2i infrared camera with built-in digital camera shown in Figure 3.11a was used. It can enable completely non-destructive tests on materials and components in industrial applications. The high temperature option extends the measuring range from + 350 ˚C to + 550 ˚C. Using the built-in digital camera, creating of a real image in parallel to the thermal image is possible. The camera is also equipped with voice recording, this means saving of comments to go with images using the headset. Some impressive features of the camera are, digital camera with power LED's guarantee optimum illumination of dark areas, resolution and image quality is high which detector size 160 x 120 pixel and 19,200 temperature measuring points. Super resolution technology enable to take image quality up to next level of 320 x 240 pixel. Thermal sensivity is < 0.05 ˚C so, smallest temperature difference can be seen. High quality 32˚ x 23˚ lens with its manual focusing enables a wide field of view and and ideal overview of the temperature distribution, along with precise focusing of the object being measured. Automatic hot/cold spot detection enables displaying of critical temperature conditions. Pro software programme for image evaluation on the PC is included.

In this study, usage of the thermal imaging camera played the key point and most important for precise temperature measurements from the tested Cu foam samples, and useful for analysing the thermal profiles to observe the heat transfer characteristics of the Cu foam samples. Thermal view of the tested Cu foam sample with measurement direction was seen in Figure 3.11c.

3.4.1.2 Sinbo SCO 5030 Heater

Sinbo heater shown in Figure 3.11b was used for heating of the tested Cu foam samples. Some properties and specifications of the heater are, power control with thermostat, fast warming up with high efficiency, adjustable (in 5 levels) heat control, operating info led, and maximum 1500 watt power capacity.

a)

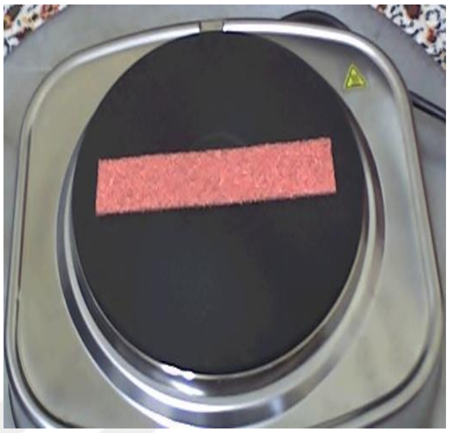

b)

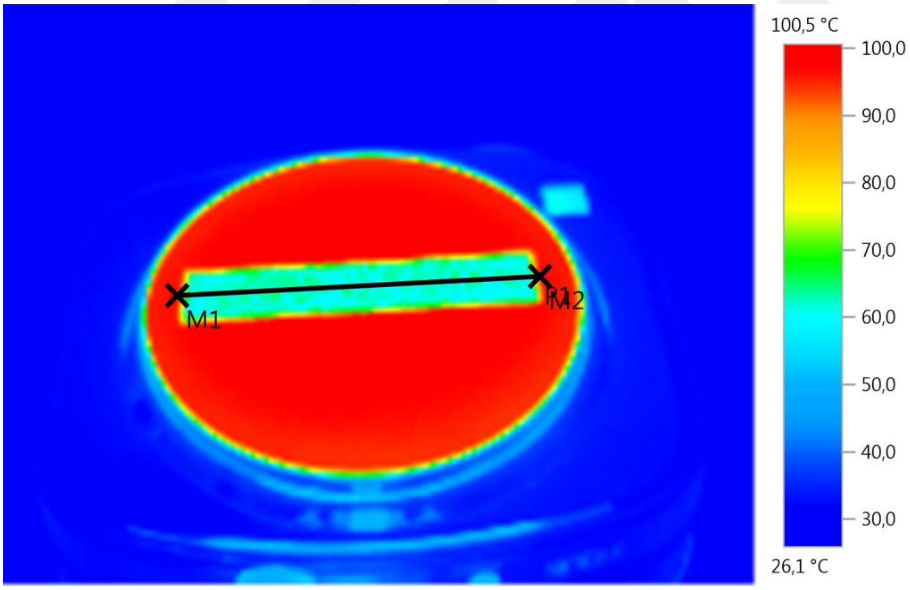

c)

Figure 3.11 Schematic representations of the thermal image camera and Cu foam sample position on heater a) Testo 875-2i thermal imaging camera b) Cu foam arrangement on heater c) Thermal view of the Cu foam with selected measurement direction

Before taking the thermal images of the samples, some parameters were adjusted according to the material properties, such as, temperature ranges, Cu foam and heater surface emissivity, ε_m values (Taken 0.45 for Cu foam samples, 0.1 for reference plate of Cu foil and 0.95 for heater surface from mikron instrument company on web) and related other functions in the thermal imaging camera. It is important to take temperatures from the upper and contact surfaces of the samples correctly. Cu foam and Cu foil upper and contact surface views were shown in Figure 3.12.

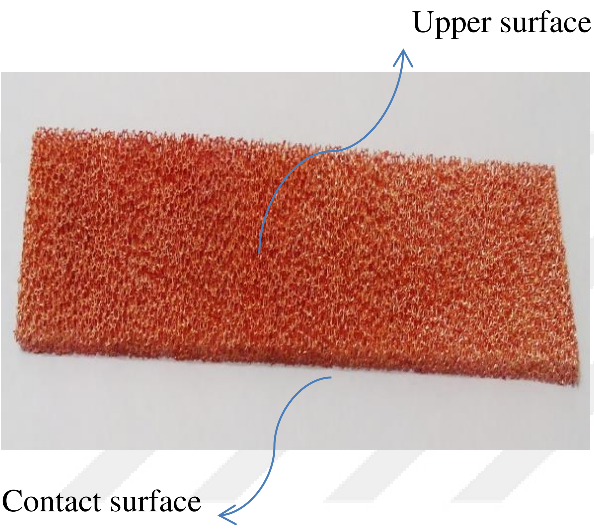

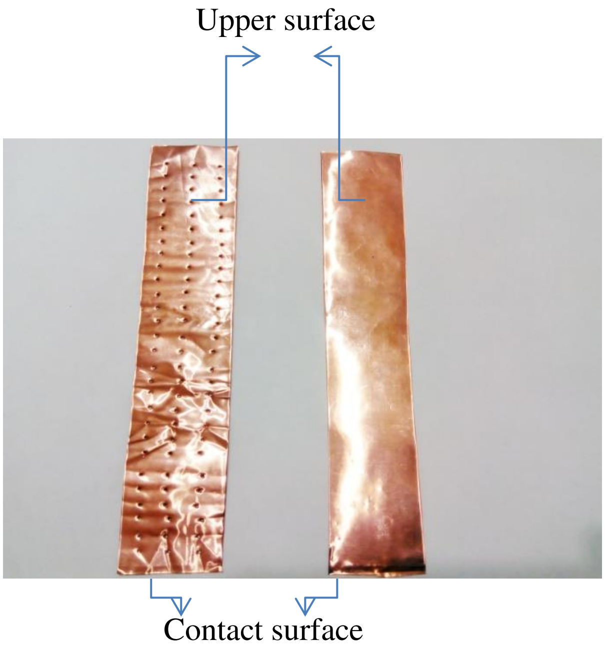

Figure 3.12 Upper and contact surface views of the Cu foam and Cu foil samples

For that reason, thermal camera focused precisely on the Cu foam and foil test samples at the same distance (Approximately 25 cm from the heater surface) and positions (45˚ angle). Image clarity was also set by manually. After taking the thermal images of the samples, all image views were transferred to the computer for thermal analysis. Thermal images analyzed sensitively with testo software program and datas of the local temperature points for all image analysis were transferred to the excell program and profiles of the temperature distributions and histogram picture of the sample's upper surface with respect to selected region or direction were drawn.

Histogram picture and temperature distributions that depend on the selected region were shown in Figure 3.13. From histogram picture, percentage of temperature distribution for selected region/area can be seen and from thermal profiles, local temperature variations along the Cu foam upper and contact surfaces for any directions can also be seen in detail.

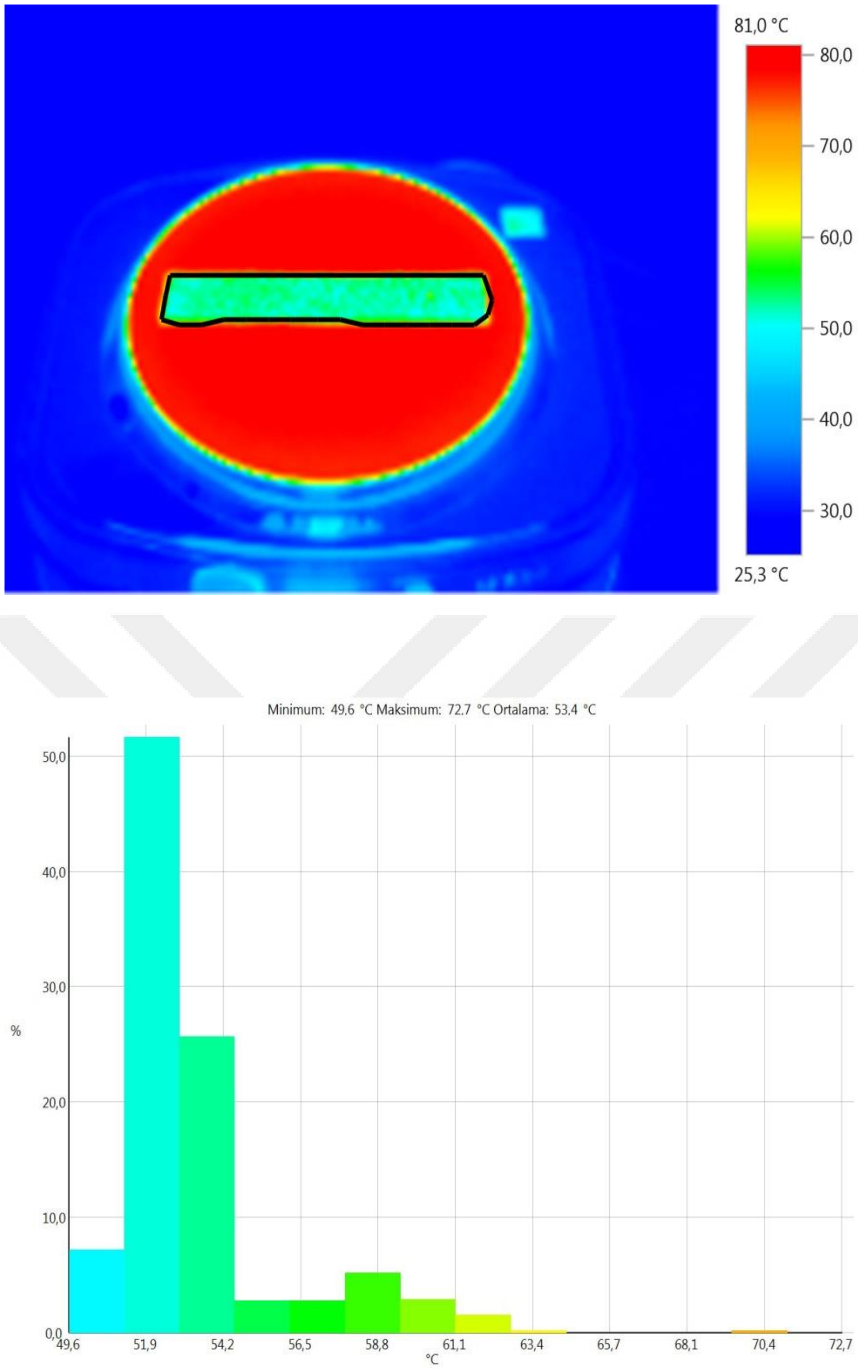

Figure 3.13 Histogram picture and percentage temperature distributions

As can be seen from Figure 3.13, approximately 50 % of the upper surface temperature distribution is 51.9 ˚C, similarly 26 % is 54.2 ˚C for the selected area.

It is necessary to convert the heater temperatures, T_H (˚C) to watt unit. For this aim, heater unit was set to the level 5 and surface temperature of the heater was measured by thermal image camera. Measurement results show that 1500 watt = 575 ˚C. The other T_H temperatures and conversion values were given in Table 3.6.

Table 3.6 : Unit conversion of T_H

T_H, ˚C	Watt
50	130.434
80	208.696
100	260.870
575	1500

And, Table 3.7 showed the measuring instruments range and accuracy values of the instruments.

Table 3.7 : Measuring Instrument Range and Accuracy

Measuring Instrument	Full Scale	Accuracy
Thermal image camera	-20 / + 350 ˚C	+/- 2%
Heater unit	0 – 575 ˚C	+/- 1 ˚C

In the experimental study, calculated parameters are k, C and α were detailed analyzed in chapter 5.

3.4.2 Experimental Procedure and Methodology For Thermal Analysis

In this section, experimental study and temperature measurement were placed for thermal analysis of the test samples were given in a detailed way.

Two different experiments were considered. These are called as heating and cooling experiments. In the heating experiments, test samples were located on to the heater unit with a specified T_H of 50 ˚C, 80 ˚C and 100 ˚C and were waited for 3 different time periods, which ϴ = 10 minutes, ϴ = 20 minutes and ϴ = 30 minutes. Thermal camera views of the test samples were taken at the end of the time periods from the upper surface of the samples and also from the contact surfaces by reversing the sample upper surface. These thermal views were used for analysing the thermal behaviour of the test samples. In the cooling experiments, test samples' contact surfaces, which exposed to a variety of T_H through heating process for 3 different time periods, were located on reference plate of white paper at room temperature until the contact surface temperature comes to room temperature, T_R values. Thermal views of the contact surfaces were taken periodically for ϴ = 0, ϴ = 3, ϴ = 6, ϴ = 10 minutes.

Cu foam samples which used in the experiments are, plate and cylindrical type with same length and width, but different thicknesses, t = 3 mm, t = 4 mm and t = 5 mm for plate type Cu foams and t = 2 mm, t = 3 mm, t = 5 mm for cylindrical Cu foams. Similarly, Cu foils with t = 0.4 mm thickness were used as reference plates.

Heater temperatures (T_H), which used in the experimental studies, were selected as a case temperatures which already mentioned above. Details of the experimental studies are given in the following sections with sequently.

3.4.2.1 Heating and Cooling Experiments

Description of The Case Experiment For T_H = 50 ˚C and ϴ = 10, 20 and 30 minutes

In this part, detailed descriptions of the heating and cooling processes of the t = 3 mm thickness Cu foam test sample were given as a case experiment. Sequences of the experiments were given as follows,

i) Firstly, T_H was set to 50˚C reference temperature

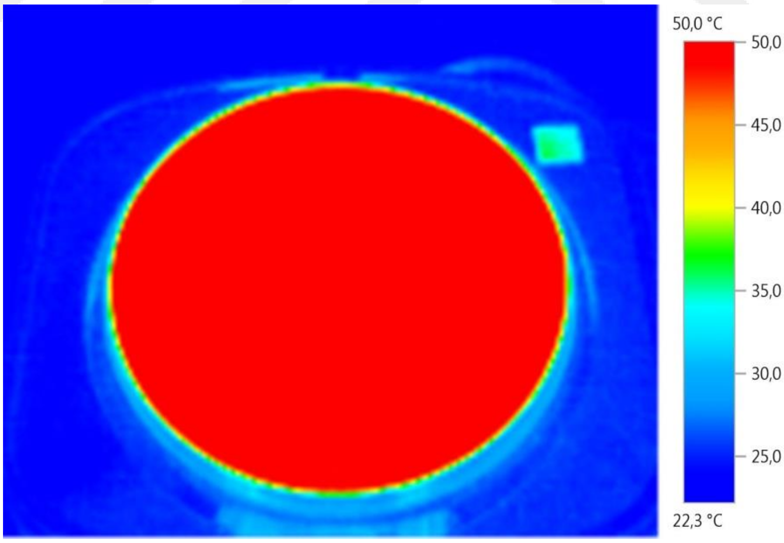

Before T_H was set to 50˚C reference temperature, some parameters of the thermal image camera had beeb adjusted depending on the heater surface.

ii) Test sample with t = 3 mm thickness was located on the heater unit

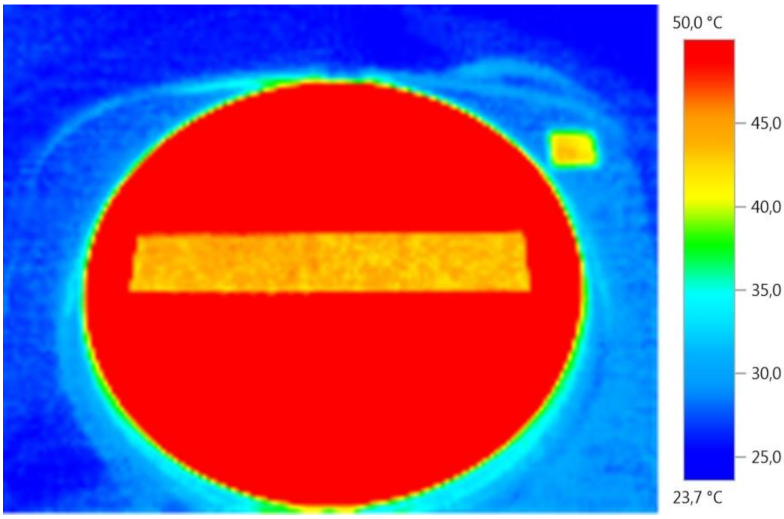

Test sample was sensitively located the hot heater surface of 50 ˚C. Thermal image views were taken at 45 ˚angle to see the effect of the thickness.

iii) Thermal images of the t = 3 mm thickness test sample, which exposed to heating process for ϴ = 10, 20 and 30 minutes, were taken periodically.

<u>For ϴ = 10 min.</u>

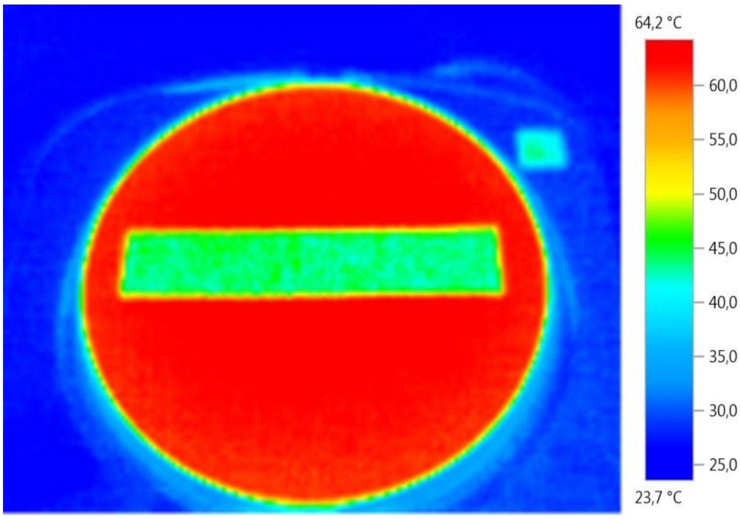

For Θ = 20 min.

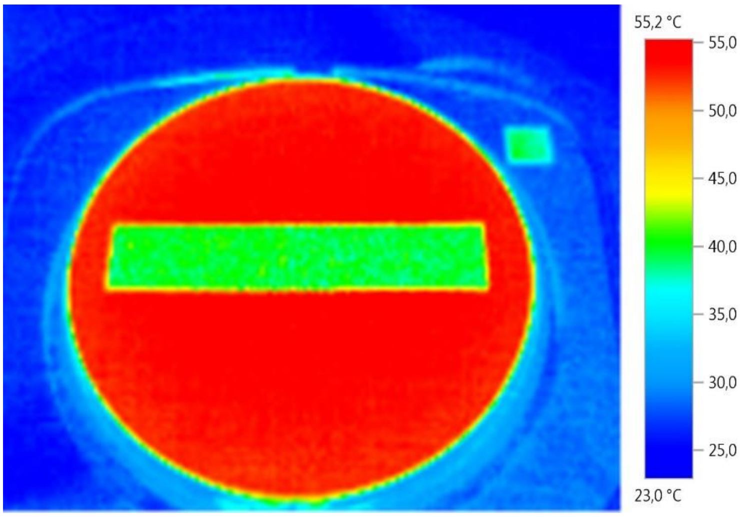

For Θ = 30 min.

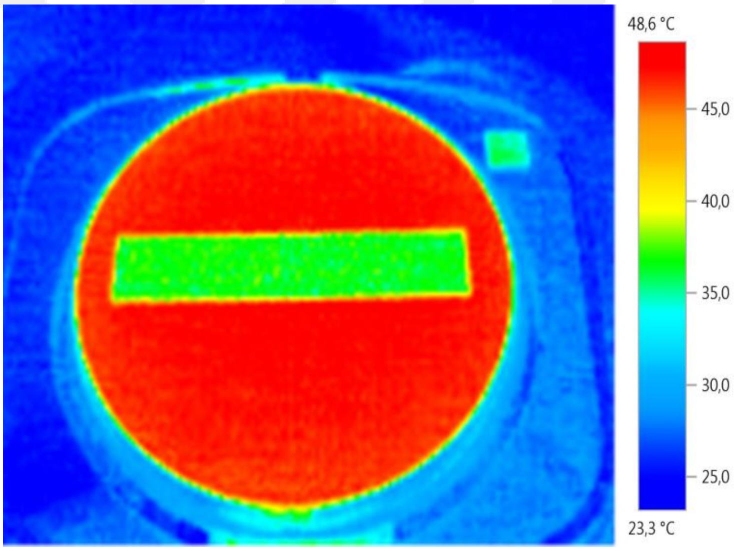

Time dependent thermal image views of the test sample were shown in the above images. Effects of the time were seen from the thermal images. Temperature distributions along the sample upper surface can be seen locally. Local temperature variations showed that, porosity and its distribution were different. Green and open blue colors were stated the hot and cold temperature areas along the sample surface. From the images, temperature variations are more visible for Θ = 10 min.

iv) Thermal profiles of the test sample were taken along the centerline and span of the upper surface.

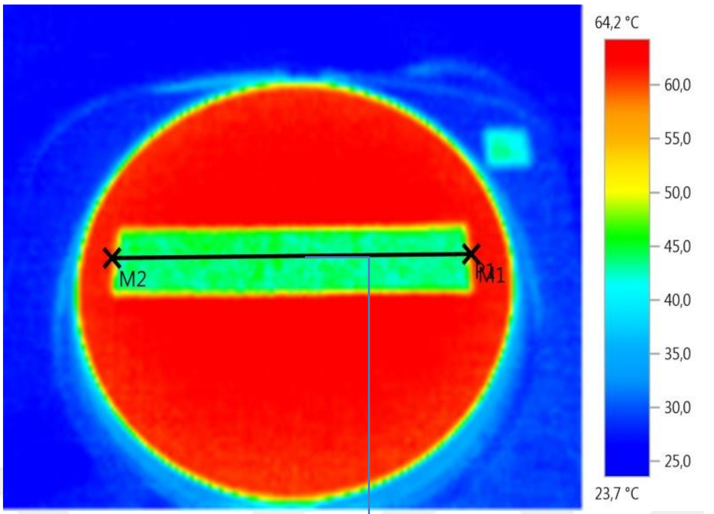

Centerline

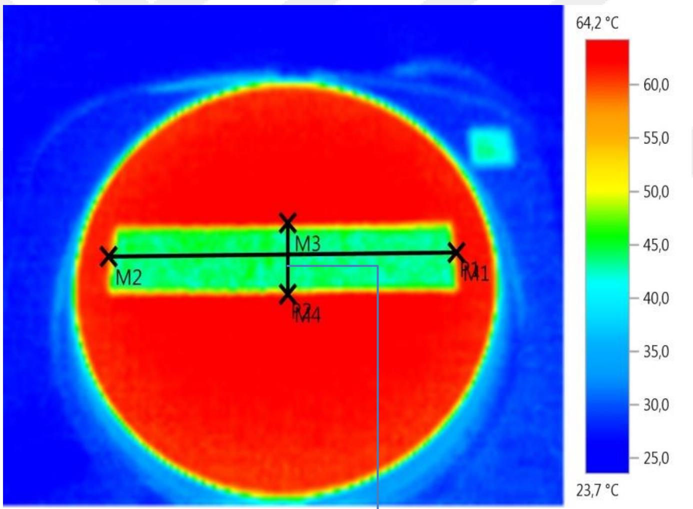

Span

Thermal profiles of the test sample were taken depending on the selected directions, centerline and span for thermal image analysis. Lines were drawn which started just before the sample first point and lasted just after the sample last point. First and last points were indicated with P symbol. For correct image analysis results, emissivity, ε_m values of the points, stated in the above figure M1, M2, M3 and M4 on heater unit were converted to the ε_m values of the test sample.

v) Time dependent thermal profiles along the test sample upper surface were drawn with excell programme by using local temperature point datas

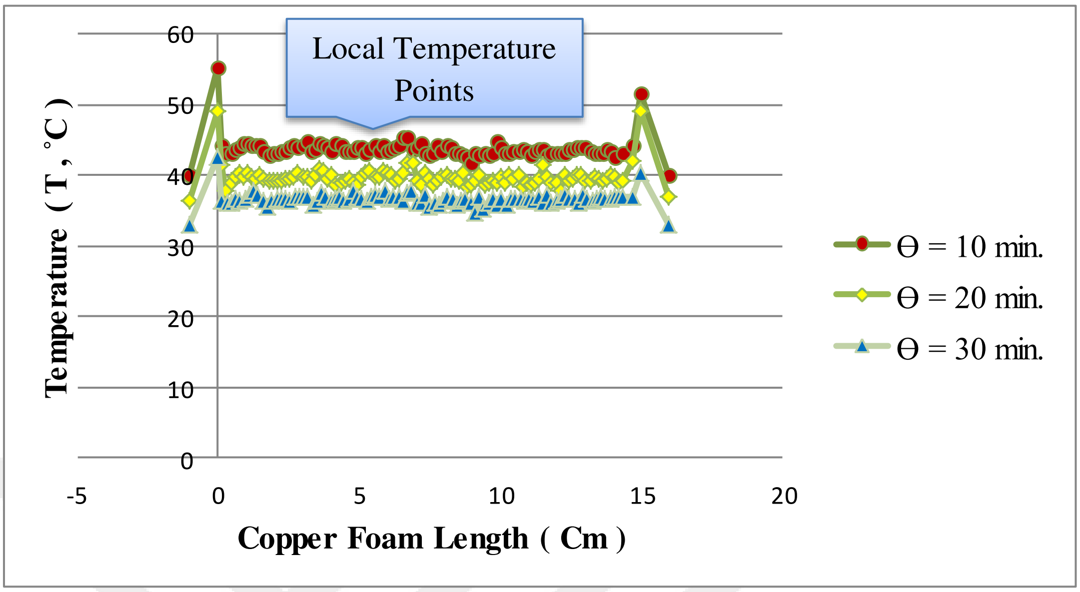

Thermal profiles of the test samples were drawn by using excel programme. All temperature datas were taken from the Testo software programme and transferred to the excel programme. Depending on the number of the local temperature points, length of the sample was equally divided to see the temperature changes corresponding to the each distances along the sample surface.

vi) Histogram picture of the test sample was taken for the selected area

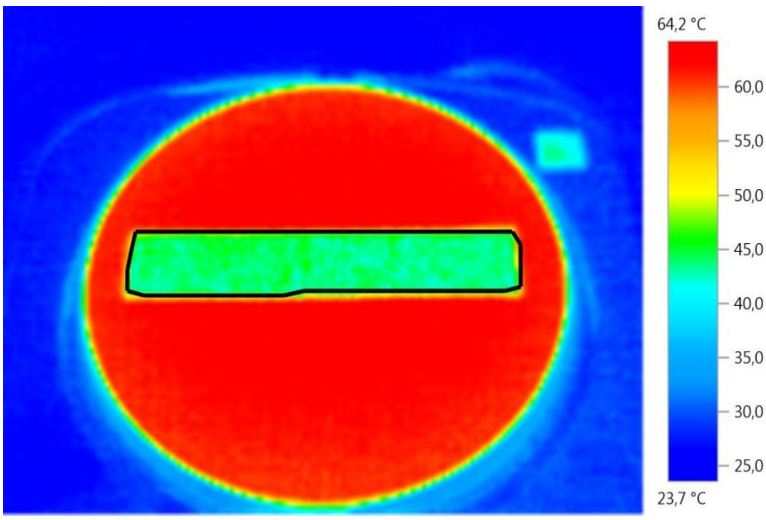

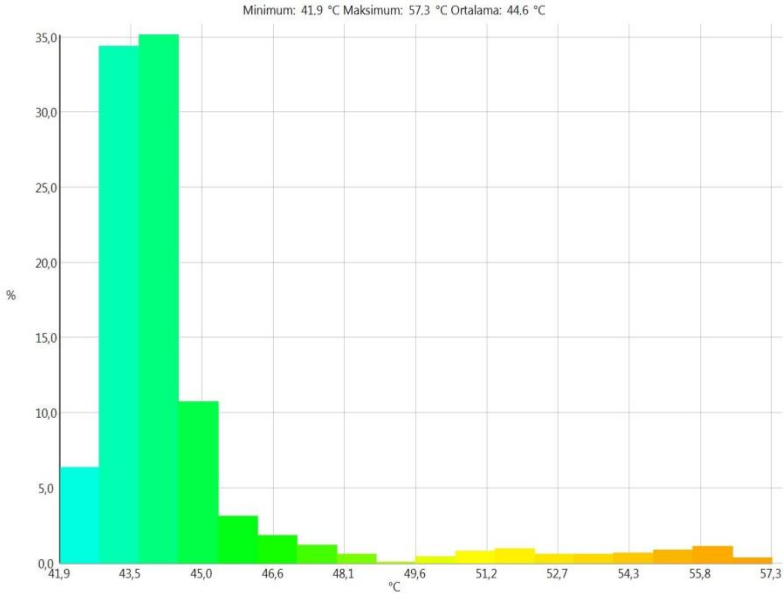

Percentage values of the temperature distributions along the sample surface can be seen by histogram view for the selected region. Histogram results also gave the minimum, maximum and mean temperature values of the sample surface. These results were used for analysing the thermal characteristics of the sample.

vii) After heating process, test samples' contact surface, which was exposed to heating process of $T_H = 50$ ˚C for ϴ = 10 min. was located on the flat paper plate as a cooling medium.

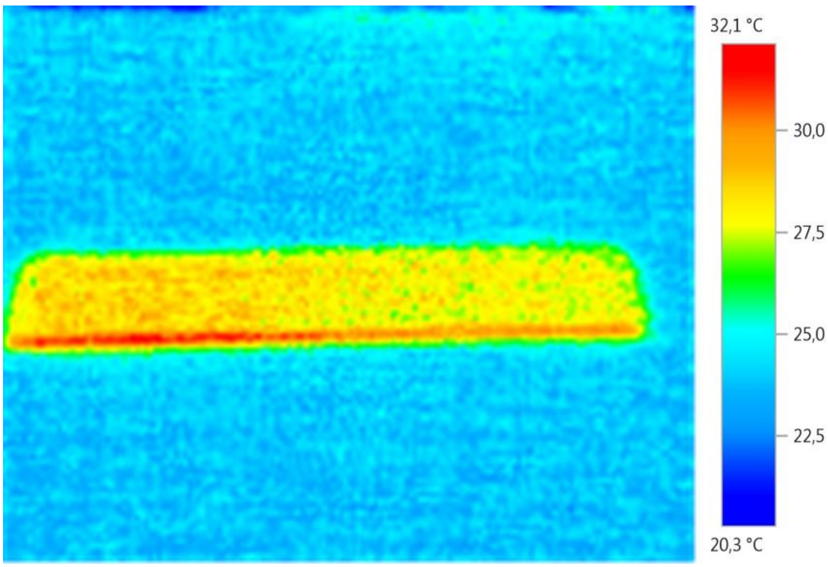

Thermal view of the contact surface of the sample showed the temperature variations along the all surface. It is important to note that, temperature values are higher at edges.

viii) Thermal images of the test samples were taken for ϴ = 0, 3, 6 and 10 min.

For ϴ = 0 min.

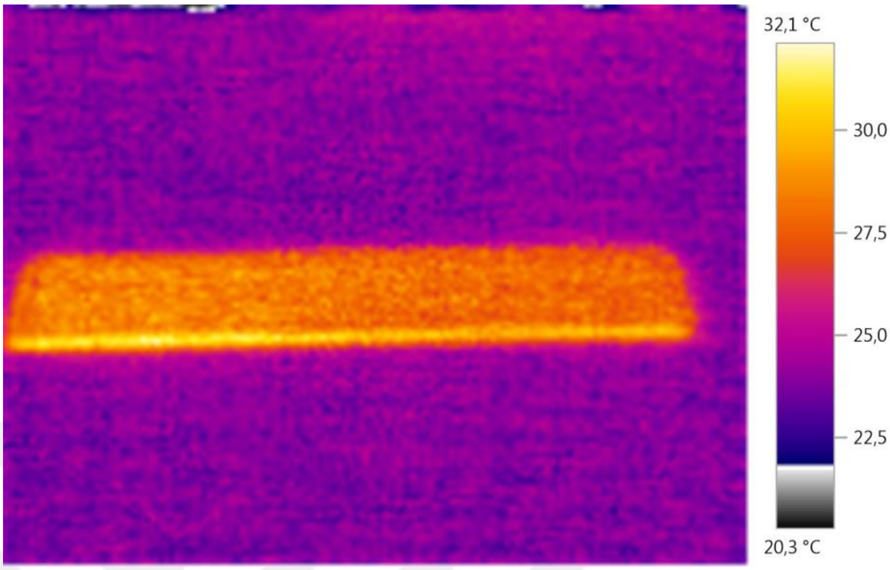

For ϴ = 3 min.

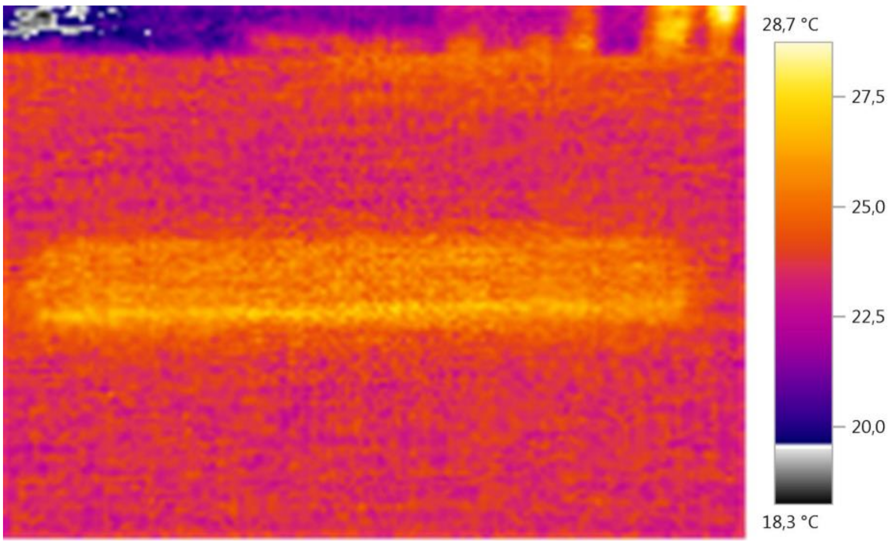

For Θ = 6 min.

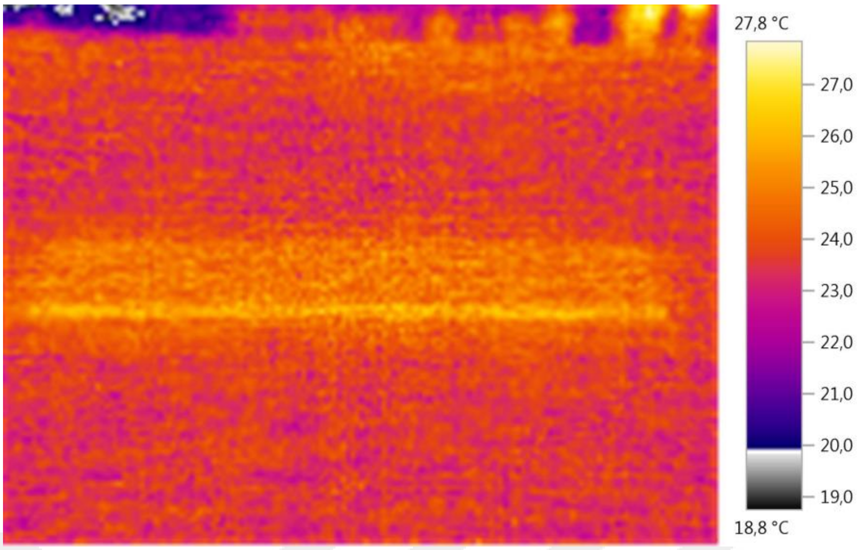

For Θ = 10 min.

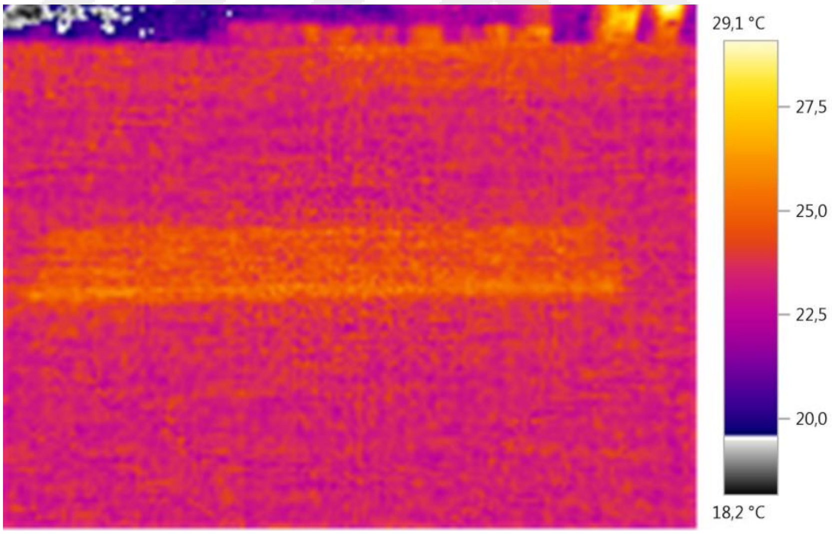

Thermal image views showed the time dependent heat transfer from the all surface of the sample. Analysis results gave information about the heat capacity properties of the sample. From the views and analysis, samples' contact surface temperature came to the surrounding temperature values in a short time.

ix) Thermal profiles of the test sample were taken along the centerline and span of the upper surface.

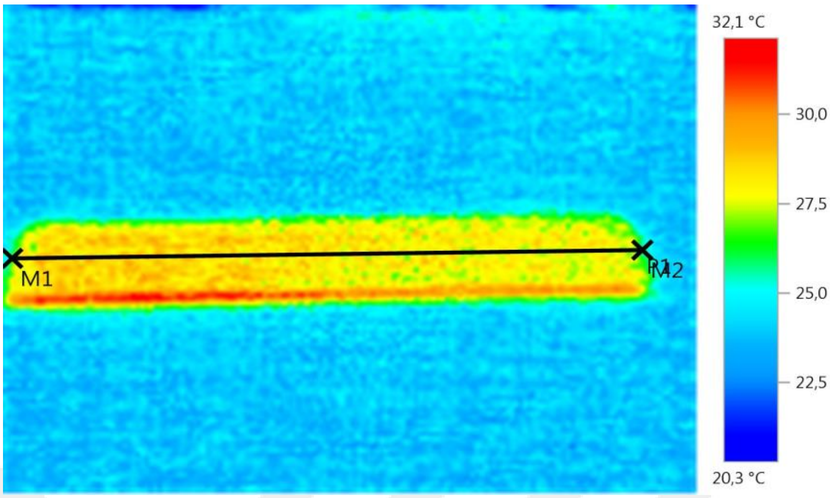

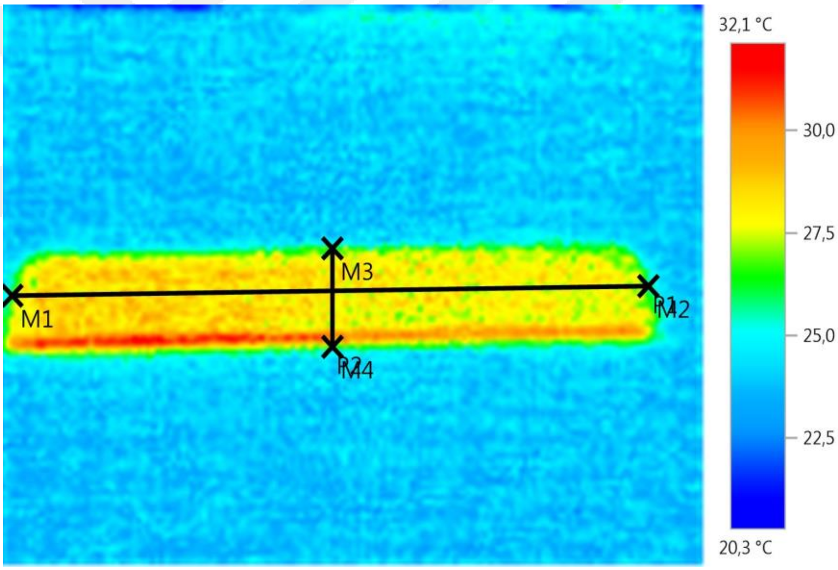

Similarly, thermal profiles of the test sample were taken that depends on the selected directions.

x) Thermal profile along the test sample contact surface was drawn by using local temperature point datas

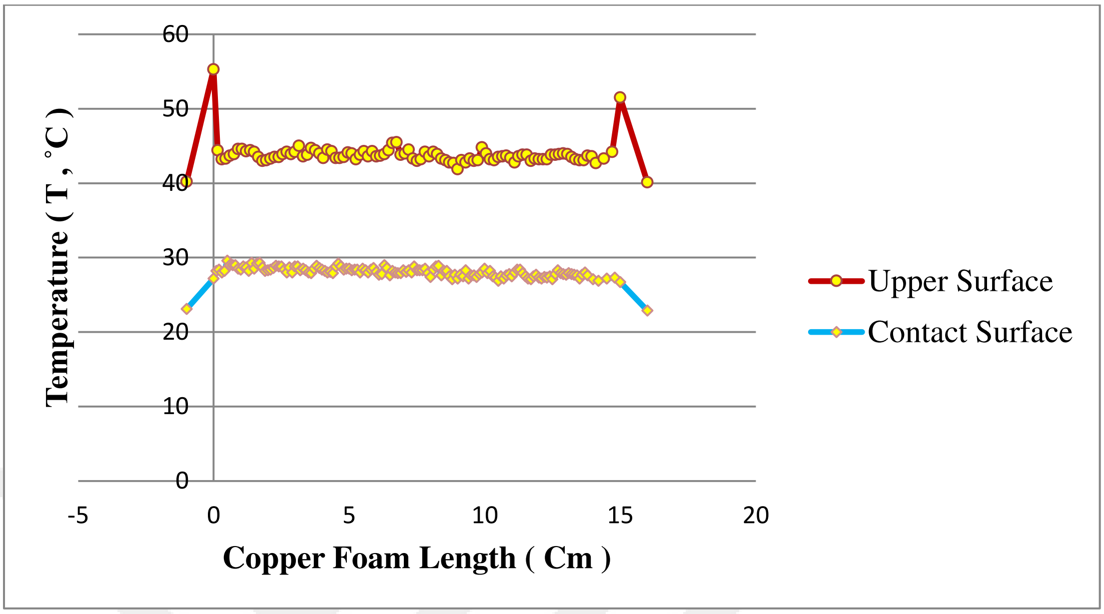

Thermal profile of the contact surface of the sample was plotted as stated heating process. Analysis results showed that, there are large temperature differences between the upper and contact surface of the sample. It is also important, contact surface temperature is lower compared with upper surface temperature.

xi) Histogram picture of the test sample was taken for the selected area

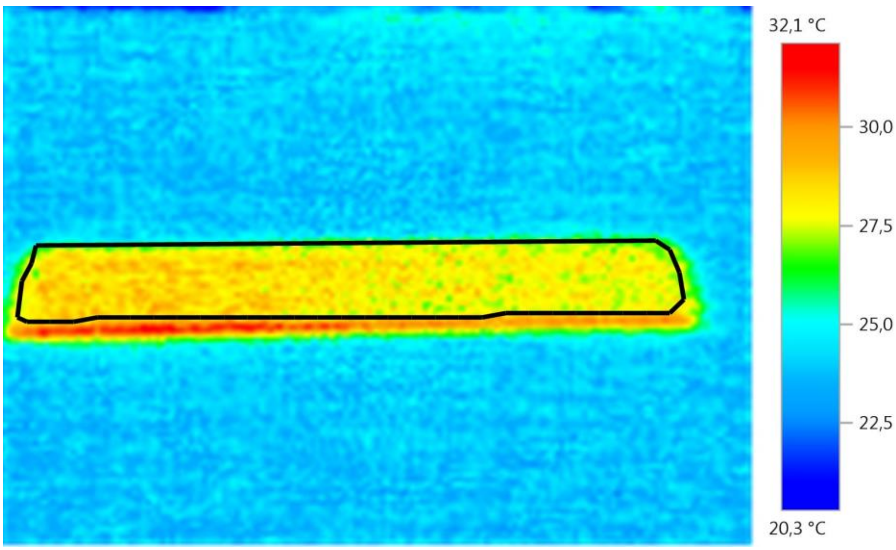

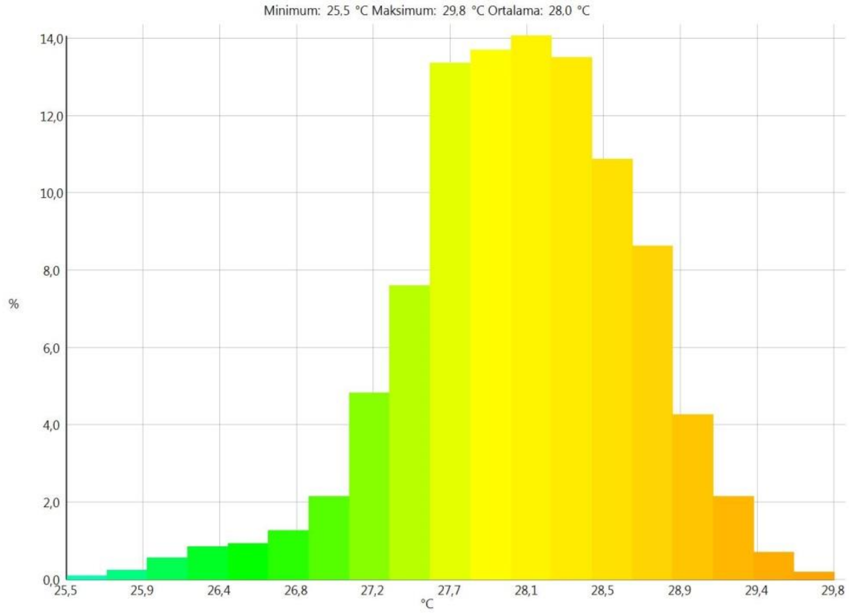

Like heating process, histogram view of the sample showed the percentage value of the temperature distribution on sample surface for selected area. Histogram analysis results showed that temperature distribution range is larger compared with upper surface histogram analysis result.

Heating and cooling experimental method and procedures for Cu foil and Cu foil with drilled holes reference items of t = 0.4 mm are similar to Cu foam experimental studies. Heating and cooling experiment specifications and conditions are given in the Table 3.8. Thermal images and analysis results of the Cu foam test samples for heating and cooling experimental studies were detaily given in the next chapters.

Table 3.8 : Heating and cooling experiment specifications and conditions

<table>
<tr><th>Test Sample</th><th>Test Specification</th><th>Heater Temperature T_H, °C</th><th>Exposed Time Θ_e, min</th><th>Room Temperature T_R, °C</th><th>Measurement Direction</th><th>Numbers of The Measured Local Temperature Point, T_p</th></tr>
<tr><td rowspan="2">Cu Foam Plate</td><td rowspan="4">Heating</td><td rowspan="8">50, 80, 100</td><td rowspan="4">10, 20, 30</td><td rowspan="8">25</td><td>Centerline</td><td>75 - 100</td></tr>
<tr><td>Span</td><td>15 - 30</td></tr>
<tr><td rowspan="2">Cu Foil and Cu Foil with Drilled Holes</td><td>Centerline</td><td>125 - 150</td></tr>
<tr><td>Span</td><td>20 - 30</td></tr>
<tr><td rowspan="2">Cu Foam Plate</td><td rowspan="4">Cooling</td><td rowspan="4">0, 3, 6, 10</td><td>Centerline</td><td>140 - 150</td></tr>
<tr><td>Span</td><td>20 - 30</td></tr>
<tr><td rowspan="2">Cu Foil and Cu Foil with Drilled Holes</td><td>Centerline</td><td>120 – 145</td></tr>
<tr><td>Span</td><td>15 - 25</td></tr>
</table>

It was seen from the Table 3.8, there are many local temperature points depend on the measurement direction which were used for analyzing the local temperature variations along the all sample surface.

3.5 Uncertainty Analysis of The Experimental Studies

The accuracy of the experimental results depend on the measuring instruments. In the present study, sensitivity of the thermal image camera is vital for accurate results. The probable errors in the experimental data refer to values with some uncertainty. The uncertainty in the experimental results with regard to k, C and α were calculated by the equation [82].

$$\omega_R = [((\partial R / \partial x_1) \omega_1)^2 + ((\partial R / \partial x_2) \omega_2)^2 + \ldots + ((\partial R / \partial x_n) \omega_n)^2]^{1/2} \qquad (3.4)$$

Where ω_R is the uncertainty in the result, R is the result is a given function of the independent variables $x_1, x_2, \ldots, x_n$ and $\omega_1, \omega_2, \ldots, \omega_n$ are uncertainties in the independent variables.

Depending on the experimental data, uncertainties associated with k, C and α were estimated to be (2.70 - 2.82) %, 2.82 % and 2.82×10^{-6} %, respectively.

3.6 Conclusion

In this chapter, basic description of the Cu foam and Cu foil sample's material properties, geometric dimensions, micro-structure analysis and results (SEM Analysis) and some comparisons, as well as explanation of the experimental studies and procedures for thermal image analysis of the Cu foam test samples by means of heating and cooling processes were given in detail.

Heating and cooling experimental studies were composed of basically 30 different experiments. In the heating experiment, a total of 60 thermal camera views were taken and in the cooling experiment, a total of 225 thermal camera views were taken for thermal image analysis and for observing the thermal characteristics of the Cu foam test samples.

It was seen from the experiments that measured local temperature points, T_p from Cu foam and Cu foil test samples surfaces for heating experiment are approximately 315 and for cooling experiments are nearly 375. Numbers of the thermal analyses were 288. It is important to note that measurement of the local temperature points of the test samples sensitively is critical and important to analyze and define the heat transfer characteristics of the porous material. These results may also be used for further researches and studies in the related fields.

CHAPTER 4

TIME DEPENDENT THERMAL IMAGE ANALYSIS

4.1 Introduction

In this chapter, after measuring the temperatures of the Cu foam samples, thermal analysis results of the upper and contact surfaces of the tested samples with respect to different T_H, t and Θ are given. T_H is in the range of 50 ˚C ≤ T ≤ 100 ˚C and Θ is the range of 10 ≤ Θ ≤ 30 minutes.

Firstly, in section 4.1.1, thermal image analysis results of the Cu foam samples along the upper and contact surfaces with experimental sequences are given.

In section 4.2, temperature histogram analysis results are given to see the effects of the $T_{H,}$ t and Θ and after representing the individual analysis of thermal profiles of the Cu foam samples and Cu foil reference items,

In section 4.3, comparisons of the temperature profiles are made to see the effects of the ε, geometry, T_H, t and Θ.

Finally, in section 4.4 and 4.5, time dependent thermal analysis results of the Cu foil reference samples with and without holes for upper surfaces at different T_H and time dependent variation of (T_{edge} / T_H) and (ΔT_{edge} / T_H) for tested Cu foam samples and Cu foil reference items are given in detail.

4.1.1 Time Dependent Thermal Profiles of The Copper Foam Samples

In this section, local temperature variations are given at varying times in the porous medium. Figure 4.2.a shows Cu foam edge temperature, T_{edge} which changes depending on the different parameters. Mean temperature difference between upper and contact surface of the Cu foam, ΔT_{cf} is given in equation 4.1.

$$\Delta T_{cf} = T_{m,upper} - T_{m,contact} \tag{4.1}$$

where, $T_{m,upper}$ is the upper surface mean temperature (˚C) and $T_{m,\ contact}$ is the contact surface mean temperature (˚C). ΔT_{cf} is shown in the Figure 4.2.b.

Similarly, temperature difference between upper and contact surfaces of the heater, ΔT_H is given in equation 4.2.

$$\Delta T_H = T_{upper} - T_{contact} \tag{4.2}$$

where, T_{upper} is the upper surface temperature (˚C) and $T_{contact}$ is the contact surface temperature (˚C). ΔT_H is shown in the Figure 4.2.c.

Figure 4.1 shows the time dependent upper surface temperature distributions of the t = 3 mm Cu foam sample. Figure 4.1 also shows the local temperature points along the foam surface and heater surface points. Figure 4.2.a, 4.2.b and 4.2.c show the time dependent local temperature variations of upper and contact surfaces of the t = 3 mm Cu foam sample at T_H = 80 ˚C.

Firstly, time dependent thermal analysis results along the t = 3 mm Cu foam sample upper and contact surfaces at T_H = 80 ˚C are described through the plots which are given in the Figures 4.1, 4.2.a, 4.2.b, 4.2.c and 4.3.

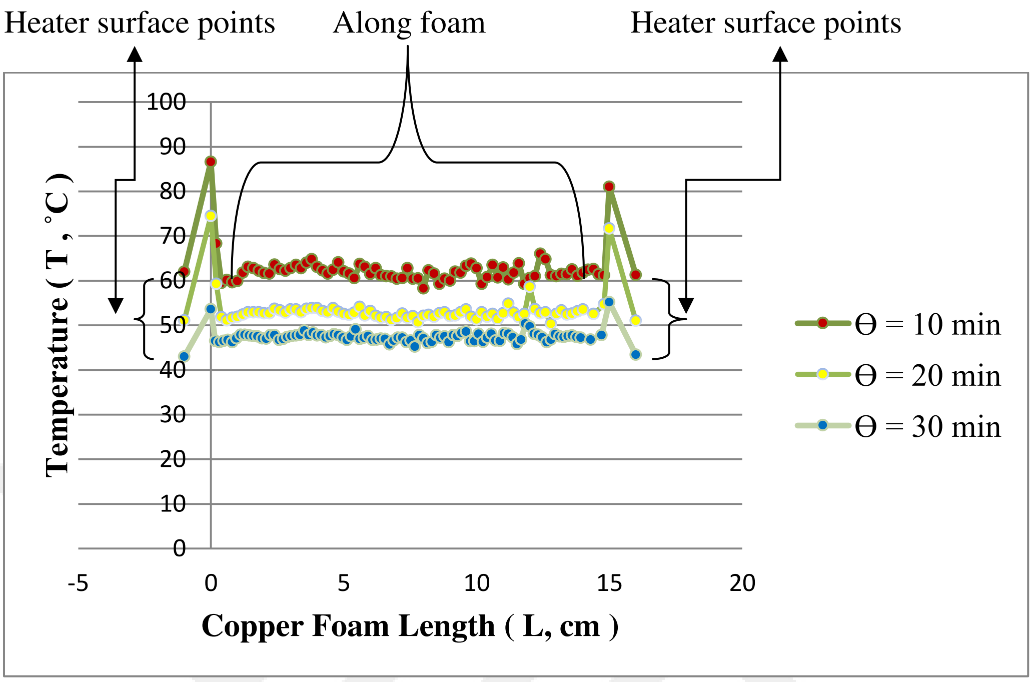

Figure 4.1 Time dependent upper surface thermal profiles of the 3 mm thickness Cu foam plate

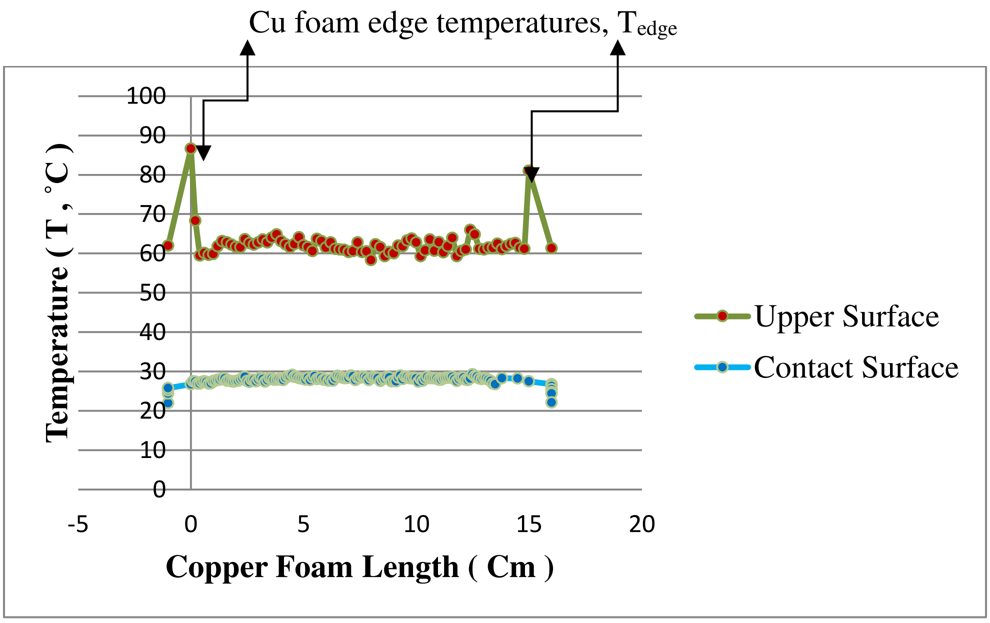

Figure 4.2.a Thermal profiles of the upper and contact heating surfaces of the 3 mm thickness Cu foam plate for ϴ = 10 min.

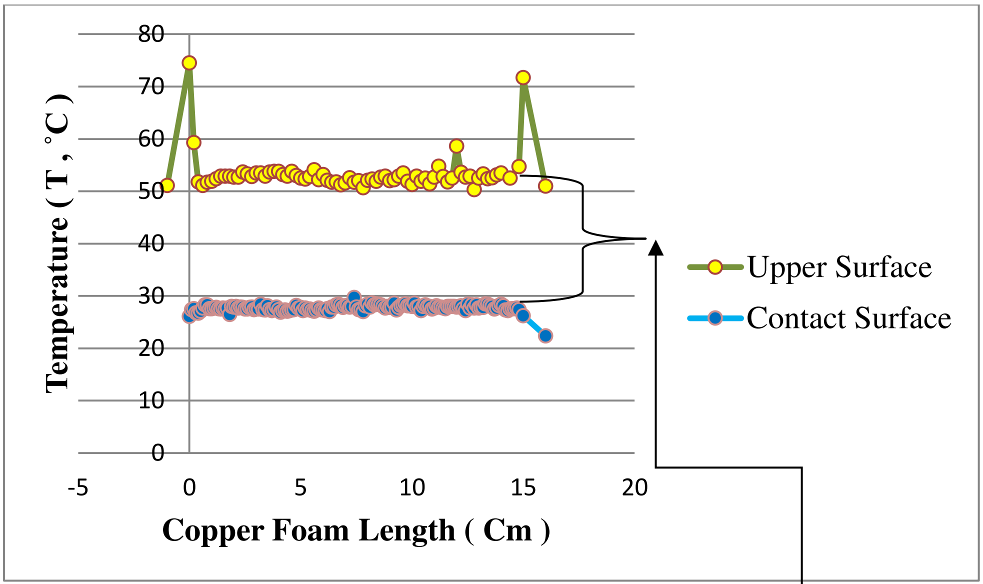

Figure 4.2.b Thermal profiles of the upper and contact heating surfaces of the 3 mm thickness Cu foam plate for ϴ = 20 min.

ΔT_{cf}

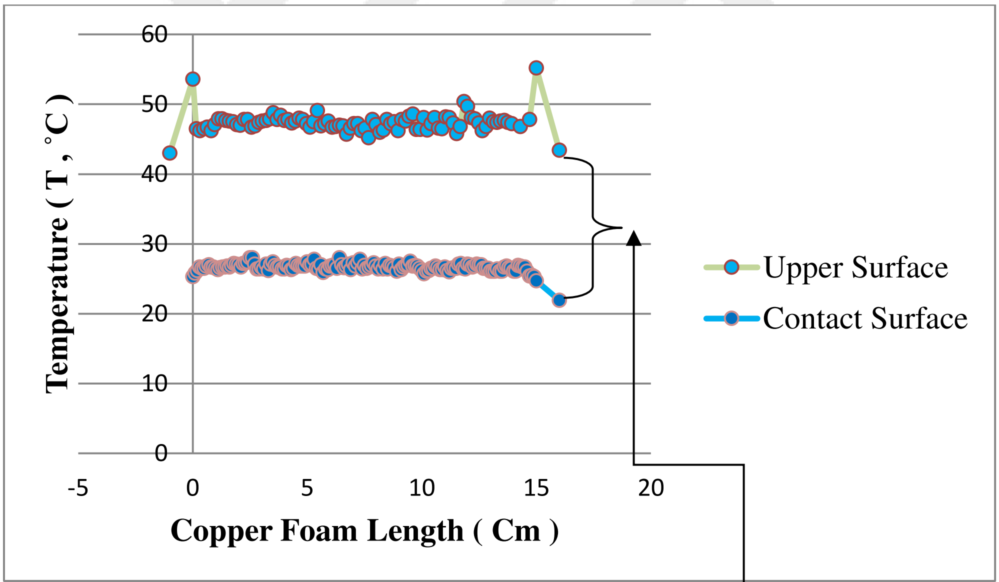

Figure 4.2.c Thermal profiles of the upper and contact heating surfaces of the 3 mm thickness Cu foam plate for ϴ = 30 min.

ΔT_H

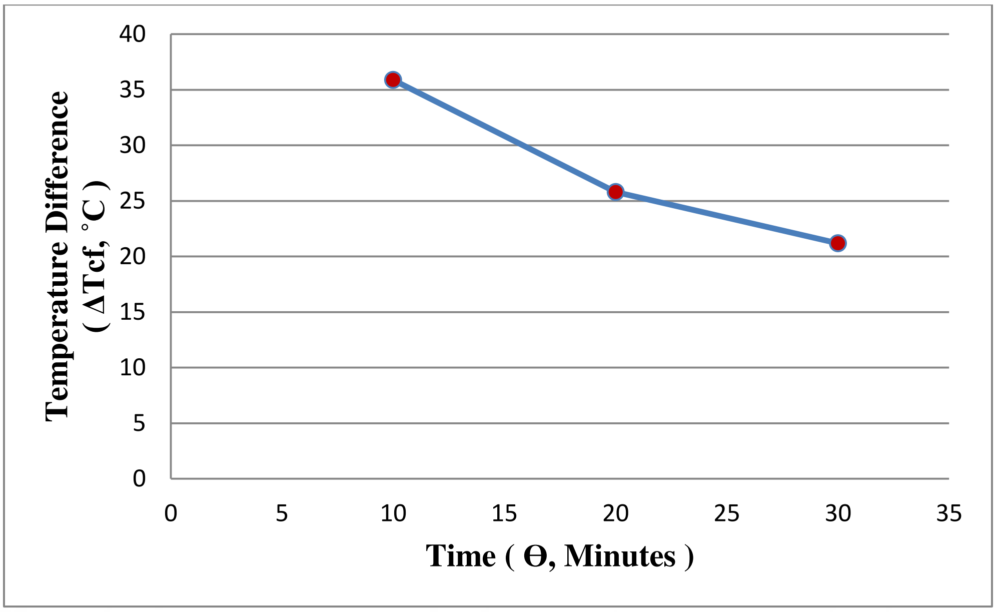

Figure 4.3 Time dependent mean temperature difference (ΔT_{cf}) variations between upper and contact surfaces of the 3 mm thickness Cu foam plate

Analysis results from the Figure 4.1 show that T_H after Θ = 10, 20 and 30 minutes are 64 ˚C, 52.5 ˚C and 45.2 ˚C respectively. Reasons of the temperature decreases are Q_{cond}, between the heater surface and Cu foam sample and Q_{conv}, between the heater surface and surrounding medium. It is seen from the figure that temperature distributions are not same, which mean that porosity also pore shape, size & direction of the Cu foam are distributed non-uniformly along the all surface. Non-uniform variations of the porosity showed the manufacturing and design considerations of the Cu foam were not same. In addition to the porous effect, there was k effect which changes from point to point along the Cu foam surface. It was important to note that, T_{edge}, are higher than the other surfaces. This situation implies that, Cu foam absorbs heat from the heater surface and spreads to all edges of the Cu foam surface depending on the pore directions. For Θ = 10 minutes, T_{edge} are 86.6 ˚C and 81 ˚C. For Θ = 20 minutes, 74.5 ˚C and 71.7 ˚C and for Θ = 30 minutes, 53.6 ˚C and 55.2 ˚C.

It is seen from the Figures 4.2.a through 4.2.c, Cu foam upper surface temperature ranges decrease from Θ = 10 to 30 minutes. The reason is that Q_{cond} between the heater surface and Cu foam plate decreases with decreasing Θ. The other effects are heat losses from the heater surface and Cu foam to surrounding medium by means of heat convection, and changes in k depends on time. Temperature profiles for Θ = 20 and 30 minutes showed similar results compared with that of Θ = 10 minutes. This situation shows the effect of the Θ on heat transfer. It was seen from these figures, T_H decreases rapidly before and after the Cu foam limits. (Points just before 0 cm and just after 15 cm of Cu foam length) which explain the effects of emissivity values of the heater surface which taken 0.95, heat losses from heater surfaces to surrounding medium by means of convection heat transfer and T_{edge} which absorb heat from the other surfaces which changes with Θ and also surrounding conditions.

Figure 4.2.a showed the ΔT_H, are for just before the Cu foam plate (62 – 24.4) 37.6 ˚C and just after the Cu foam plate (61.3 – 26.8) 34.5 ˚C for Θ = 10 minutes heating process. Figure 4.2.b showed the ΔT_H are for just before the Cu foam plate (51.1 – 22.4) 28.7 ˚C and just after the Cu foam plate (51 – 22.4) 28.6 ˚C for Θ = 20 minutes heating process. Similarly, Figure 4.2.c showed the ΔT_H are for just before the Cu foam plate (43 – 21.9) 21.1 ˚C and just after the Cu foam plate (43.4 – 21.9) 21.5 ˚C for Θ = 30 minutes heating process. Temperature variations showed the effects of Θ on heat transfer and importance of the T_{edge} of the Cu foam samples on T_H.

Mean temperature differences between upper and contact surfaces of the Cu foam, ΔT_{cf} are (63.9 – 28) 35.9 ˚C for Θ = 10 minutes heating process, (53.4 – 27.6) 25.8 ˚C for Θ = 20 minutes heating process and (47.9 – 26.7) 21.2 ˚C for Θ = 30 minutes heating process were shown in the Figure 4.3. It was obvious from that figures, ΔT_{cf} decreases with increasing Θ.

Finally, it was clear from the above figures; depending on the ε, pore shape, d_p, and pore direction parameters, ΔT_{cf}, ΔT_H, T_{edge} and k change along the Cu foam surface. From the experimental analysis results, it was clear that there were heat conduction and heat convection heat transfer variations along the all directions inside the Cu foam plate.

Figure 4.4 shows the time dependent upper surface temperature distributions of the t = 4 mm Cu foam sample. Figure 4.5.a, 4.5.b and 4.5.c show the time dependent local temperature variations of upper and contact surfaces of the Cu foam sample at T_H = 80 ˚C . Time dependent thermal analysis results along the t = 4 mm Cu foam sample upper and contact surfaces at T_H = 80 ˚C were described through the plots which given in the Figures 4.4, 4.5.a, 4.5.b, 4.5.c and 4.6.

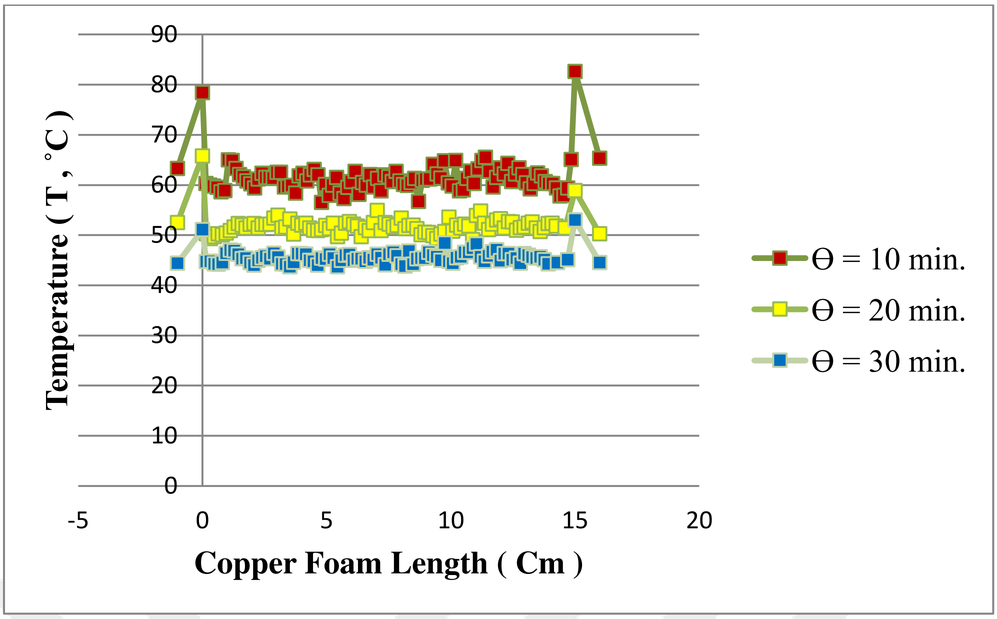

Figure 4.4 Time dependent upper surface thermal profiles of the 4 mm thickness Cu foam plate

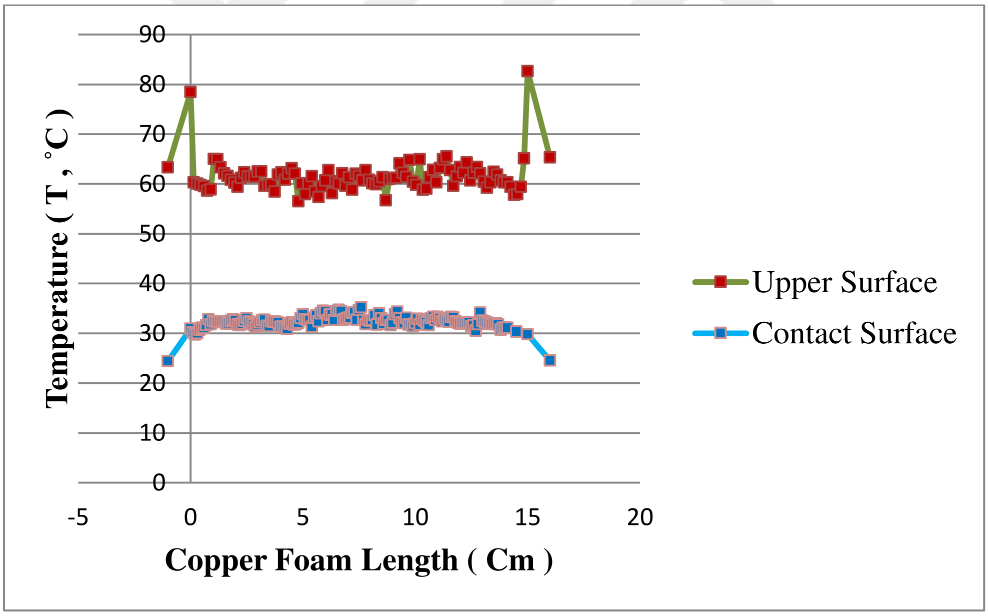

Figure 4.5.a Thermal profiles of the upper and contact heating surfaces of the 4 mm thickness Cu foam plate for Θ = 10 min.

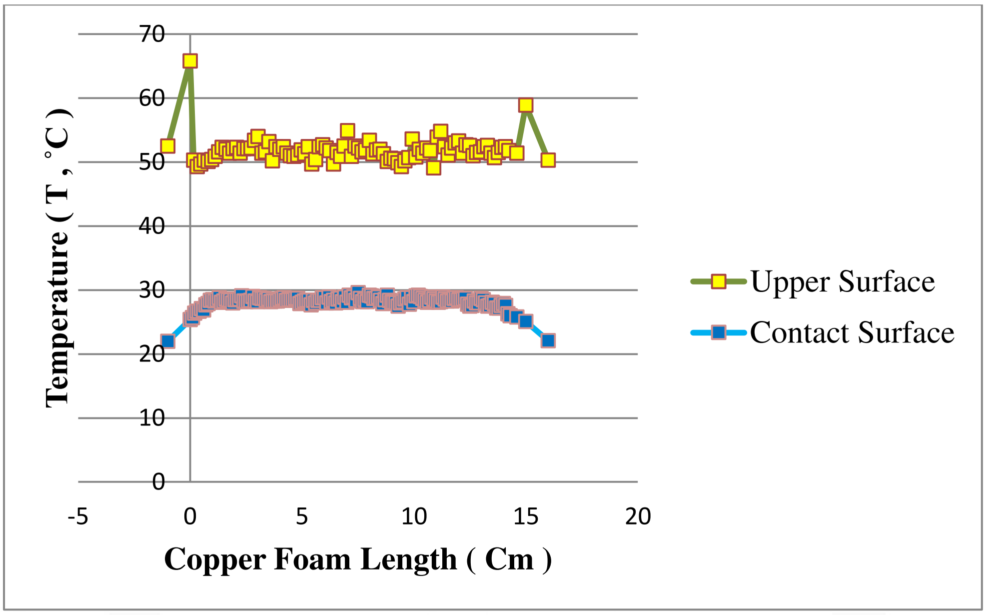

Figure 4.5.b Thermal profiles of the upper and contact heating surfaces of the 4 mm thickness Cu foam plate for ϴ = 20 min.

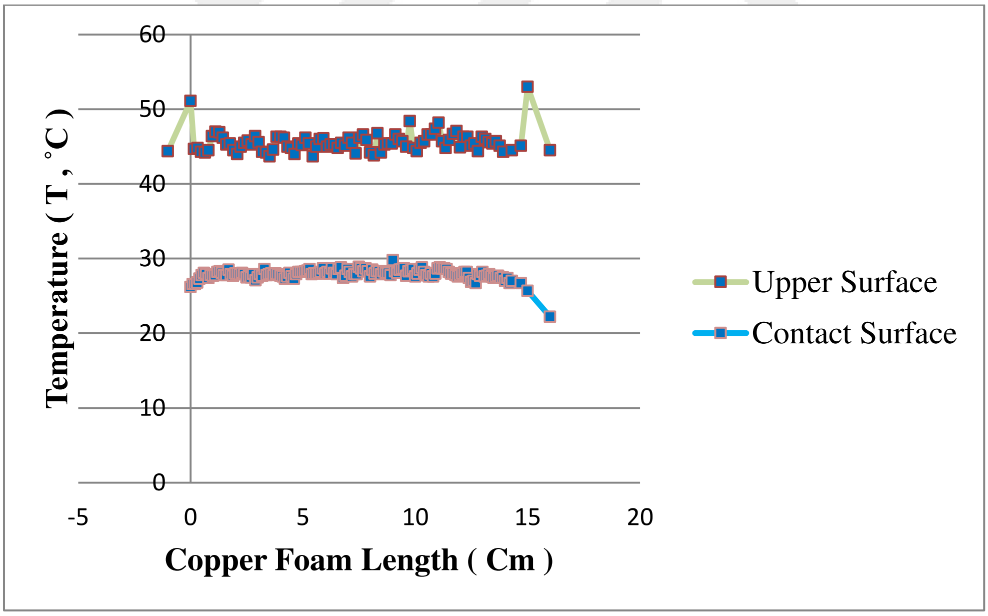

Figure 4.5.c Thermal profiles of the upper and contact heating surfaces of the 4 mm thickness Cu foam plate for ϴ = 30 min.

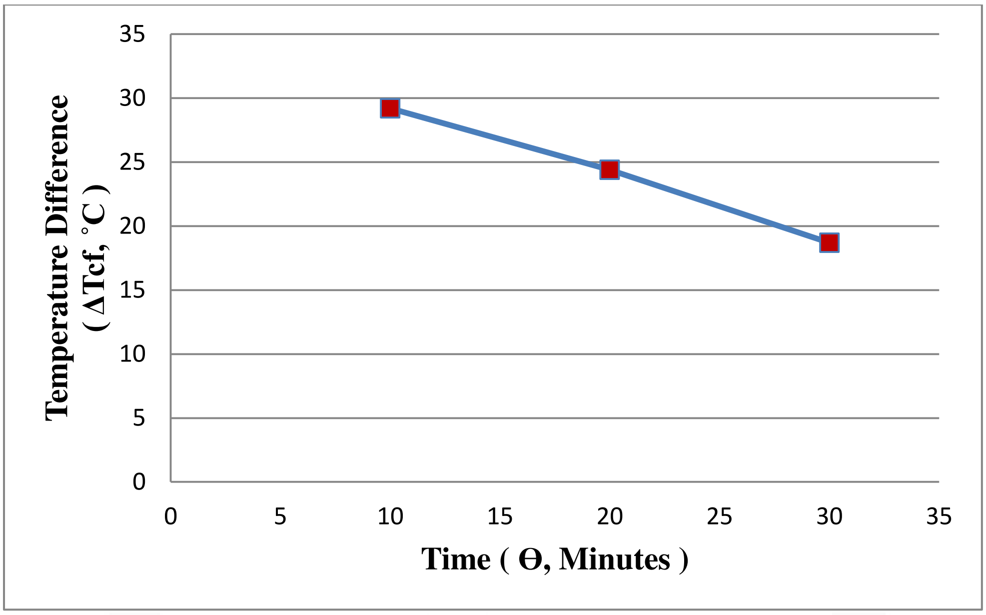

Figure 4.6 Time dependent mean temperature difference (ΔT_{cf}) variations between upper and contact surfaces of the 4 mm thickness Cu foam plate

Figure 4.7 shows the time dependent upper surface temperature distributions of the t = 5 mm Cu foam sample. Figure 4.8.a, 4.8.b and 4.8.c show the time dependent local temperature variations of upper and contact surfaces of the Cu foam sample at T_H = 80 ˚C . Time dependent thermal analysis results along the t = 5 mm Cu foam sample upper and contact surfaces at T_H = 80 ˚C are described through the plots which given in the Figures 4.7, 4.8.a, 4.8.b, 4.8.c and 4.9.

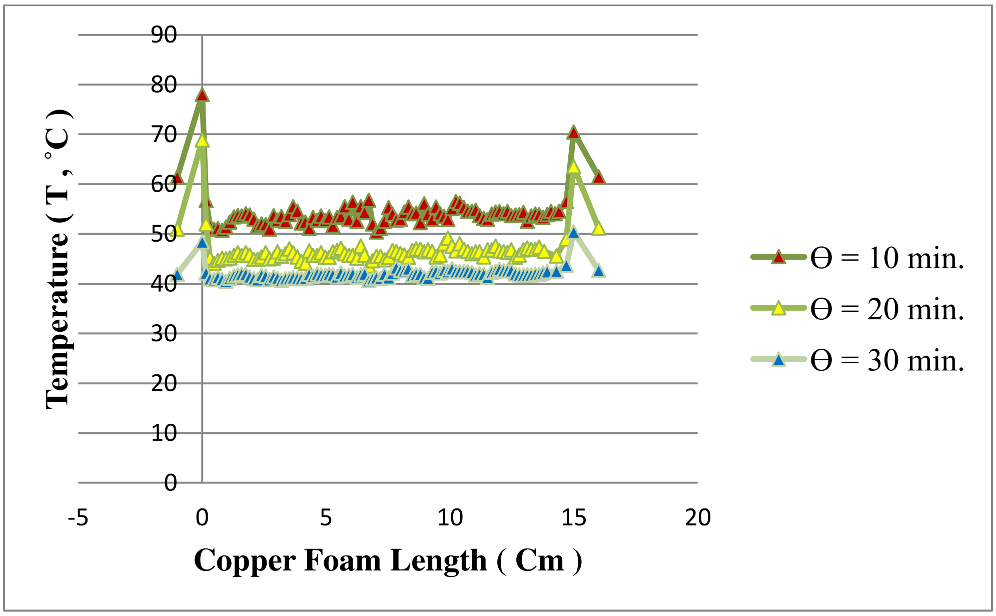

Figure 4.7 Time dependent upper surface thermal profiles of the 5 mm thickness Cu foam plate

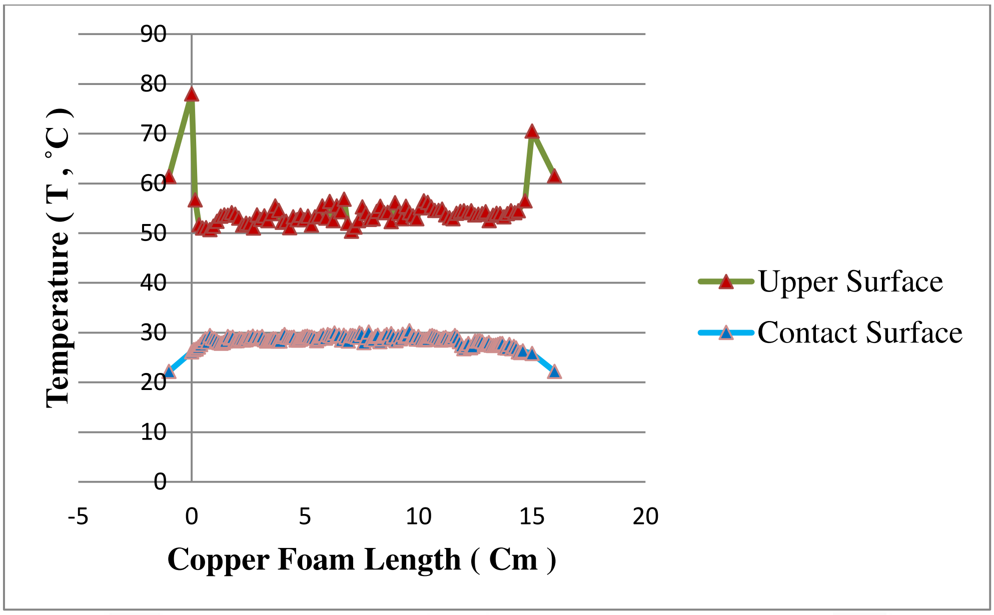

Figure 4.8.a Thermal profiles of the upper and contact heating surfaces of the 5 mm thickness Cu foam plate for Θ = 10 min.

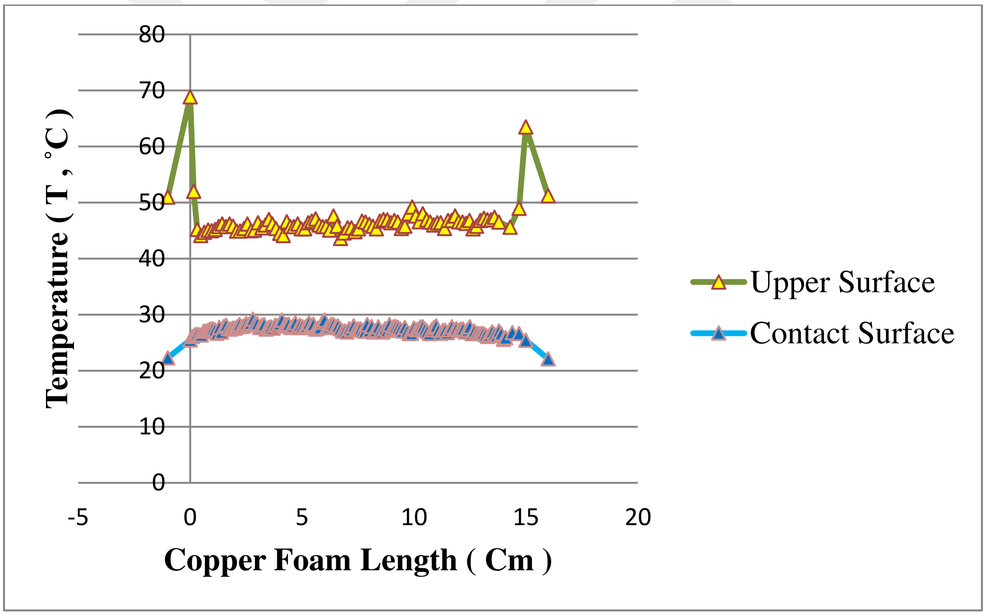

Figure 4.8.b Thermal profiles of the upper and contact heating surfaces of the 5 mm thickness Cu foam plate for Θ = 20 min.

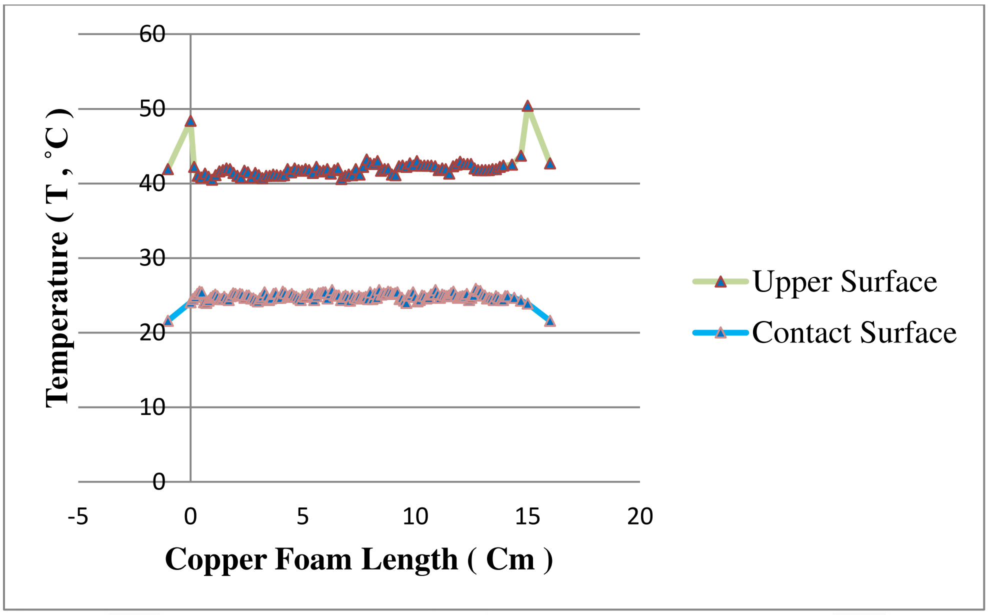

Figure 4.8.c Thermal profiles of the upper and contact heating surfaces of the 5 mm thickness Cu foam plate for ϴ = 30 min.

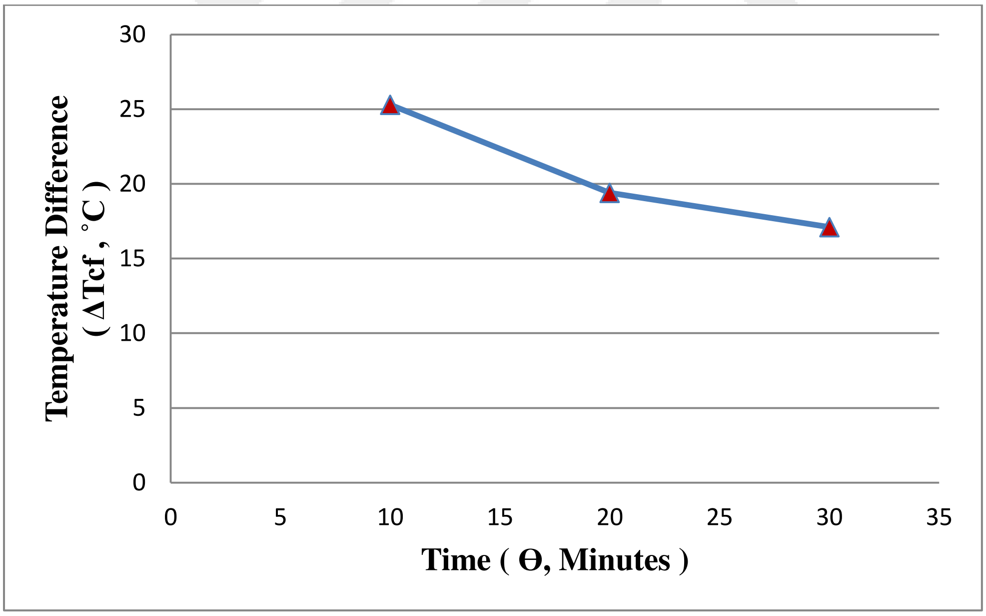

Figure 4.9 Time dependent mean temperature difference (ΔT_{cf}) variations between upper and contact surfaces of the 5 mm thickness Cu foam plate

Figure 4.10 shows the time dependent upper surface temperature distributions of the t = 3 mm Cu foam sample. Figure 4.11.a, 4.11.b and 4.11.c show the time dependent local temperature variations of upper and contact surfaces of the Cu foam sample at T_H = 100 ˚C . Time dependent thermal analysis results along the t = 3 mm Cu foam sample upper and contact surfaces at T_H = 100 ˚C are described through the plots which are given in the Figures 4.10, 4.11.a, 4.11.b, 4.11.c and 4.12.

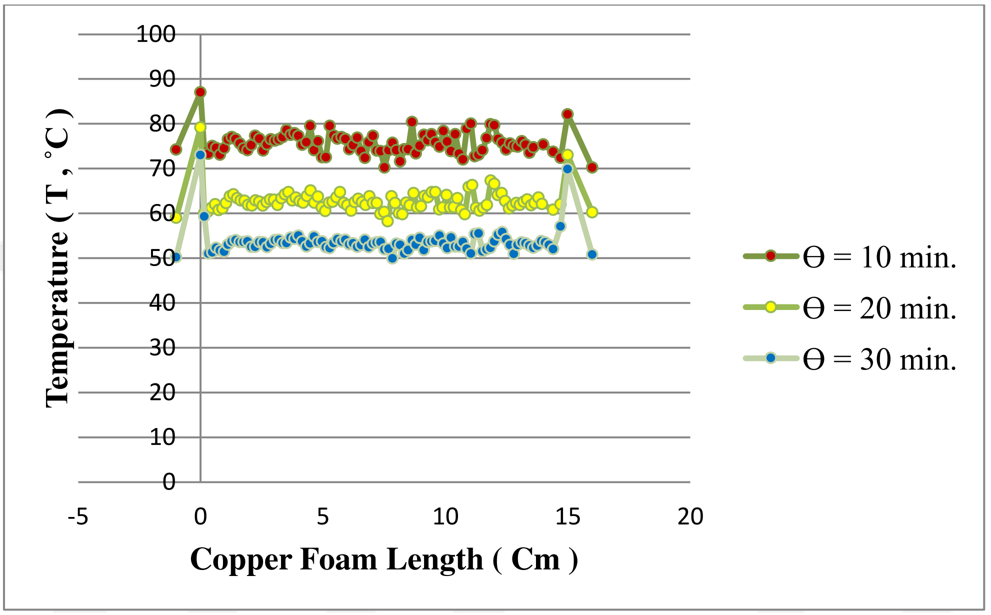

Figure 4.10 Time dependent upper surface thermal profiles of the 3 mm thickness Cu foam plate

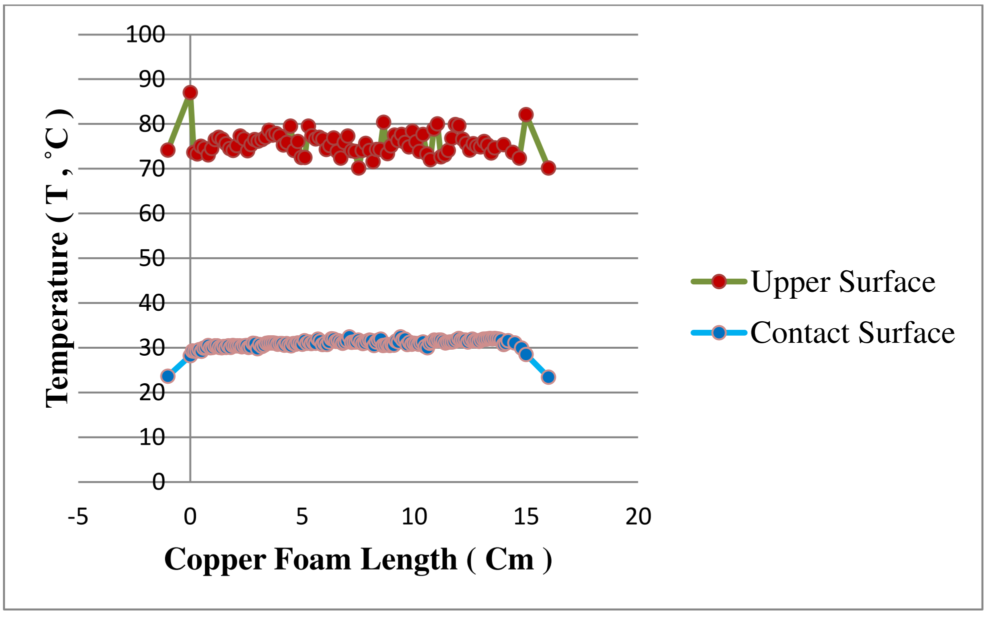

Figure 4.11.a Thermal profiles of the upper and contact heating surfaces of the 3 mm thickness Cu foam plate for ϴ = 10 min.

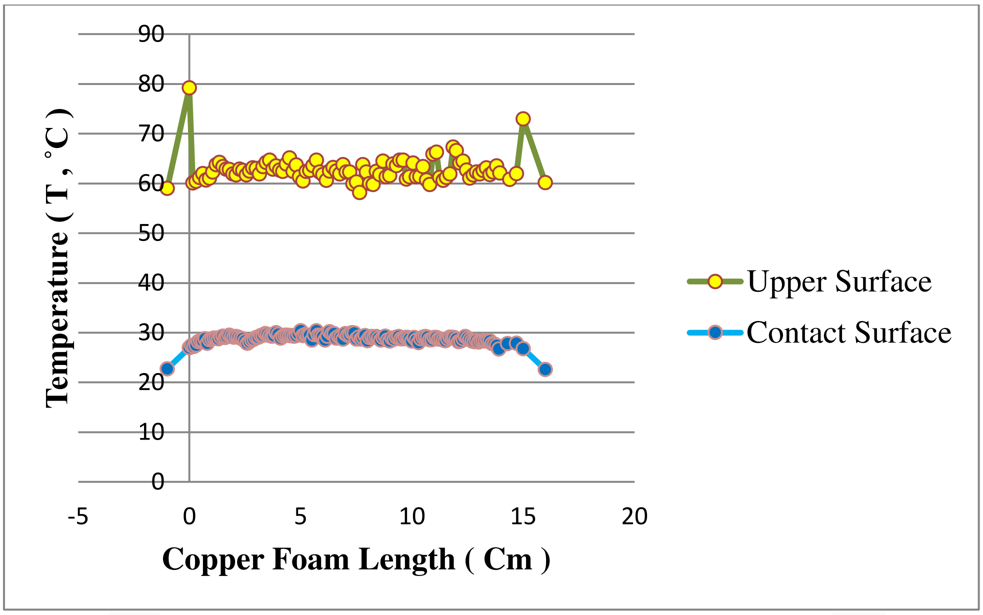

Figure 4.11.b Thermal profiles of the upper and contact heating surfaces of the 3 mm thickness Cu foam plate for ϴ = 20 min.

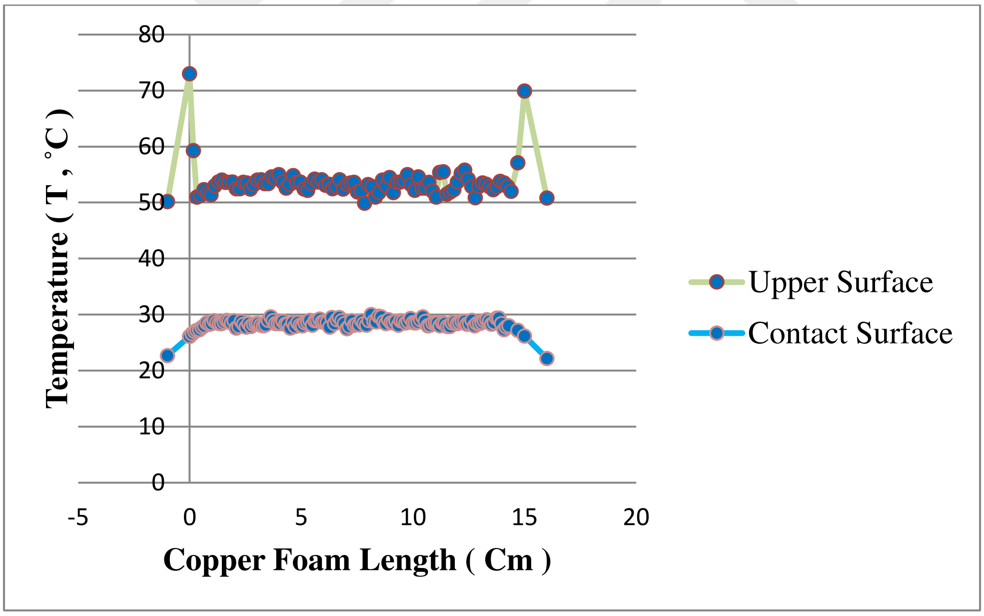

Figure 4.11.c Thermal profiles of the upper and contact heating surfaces of the 3 mm thickness Cu foam plate for ϴ = 30 min.

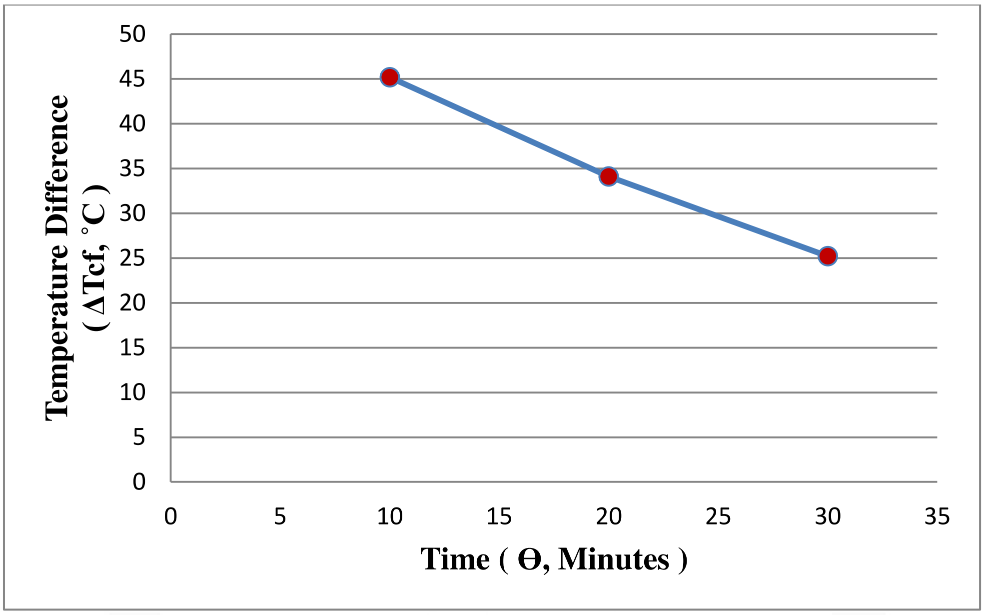

Figure 4.12 Time dependent mean temperature difference (ΔT_{cf}) variations between upper and contact surfaces of the 3 mm thickness Cu foam plate

Figure 4.13 shows the time dependent upper surface temperature distributions of the t = 4 mm Cu foam sample. Figure 4.14.a, 4.14.b and 4.14.c show the time dependent local temperature variations of upper and contact surfaces of the Cu foam sample at T_H = 100 ˚C . Time dependent thermal analysis results along the t = 4 mm Cu foam sample upper and contact surfaces at T_H = 100 ˚C are described through the plots which are given in the Figures 4.13, 4.14.a, 4.14.b, 4.14.c and 4.15.

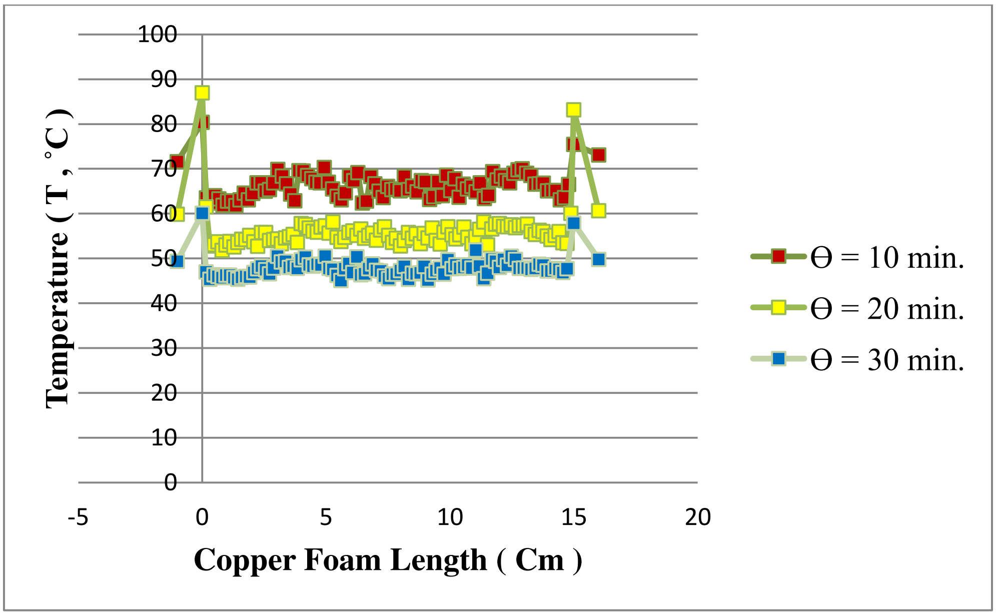

Figure 4.13 Time dependent upper surface thermal profiles of the 4 mm thickness Cu foam plate

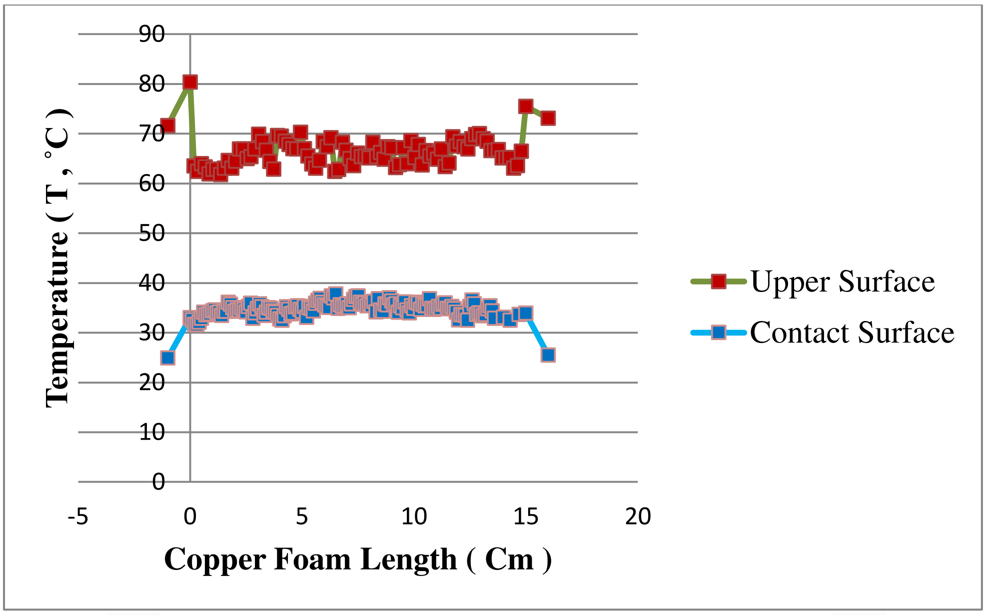

Figure 4.14.a Thermal profiles of the upper and contact heating surfaces of the 4 mm thickness Cu foam plate for ϴ = 10 min.

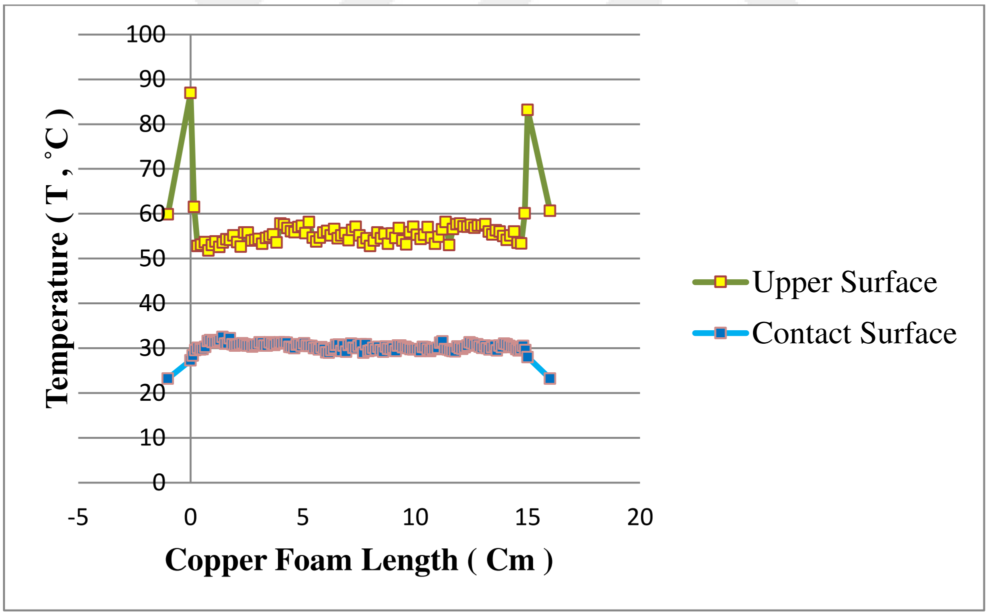

Figure 4.14.b Thermal profiles of the upper and contact heating surfaces of the 4 mm thickness Cu foam plate for ϴ = 20 min.

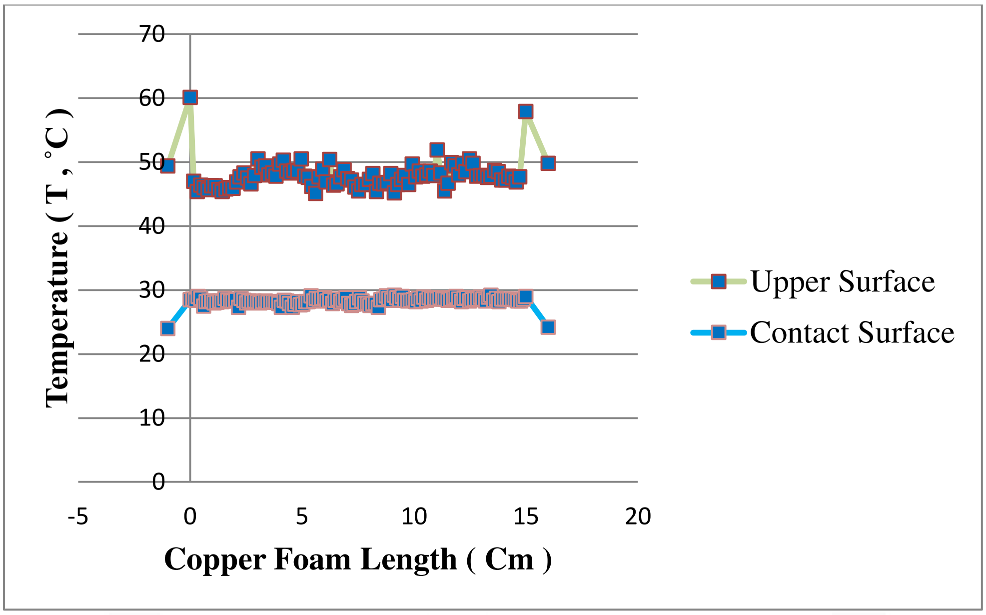

Figure 4.14.c Thermal profiles of the upper and contact heating surfaces of the 4 mm thickness Cu foam plate for ϴ = 30 min.

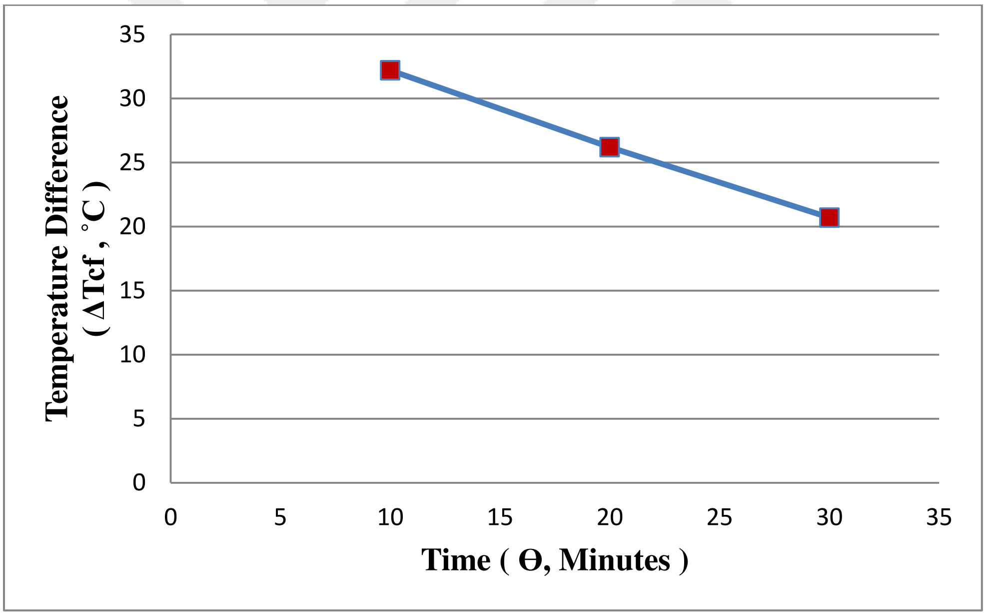

Figure 4.15 Time dependent mean temperature difference (ΔT_{cf}) variations between upper and contact surfaces of the 4 mm thickness Cu foam plate

Figure 4.16 shows the time dependent upper surface temperature distributions of the t = 5 mm Cu foam sample. Figure 4.17.a, 4.17.b and 4.17.c show the time dependent local temperature variations of upper and contact surfaces of the Cu foam sample at T_H = 100 ˚C . Time dependent thermal analysis results along the t = 5 mm Cu foam sample upper and contact surfaces at T_H = 100 ˚C are described through the plots which are given in the Figures 4.16, 4.17.a, 4.17.b, 4.17.c and 4.18.

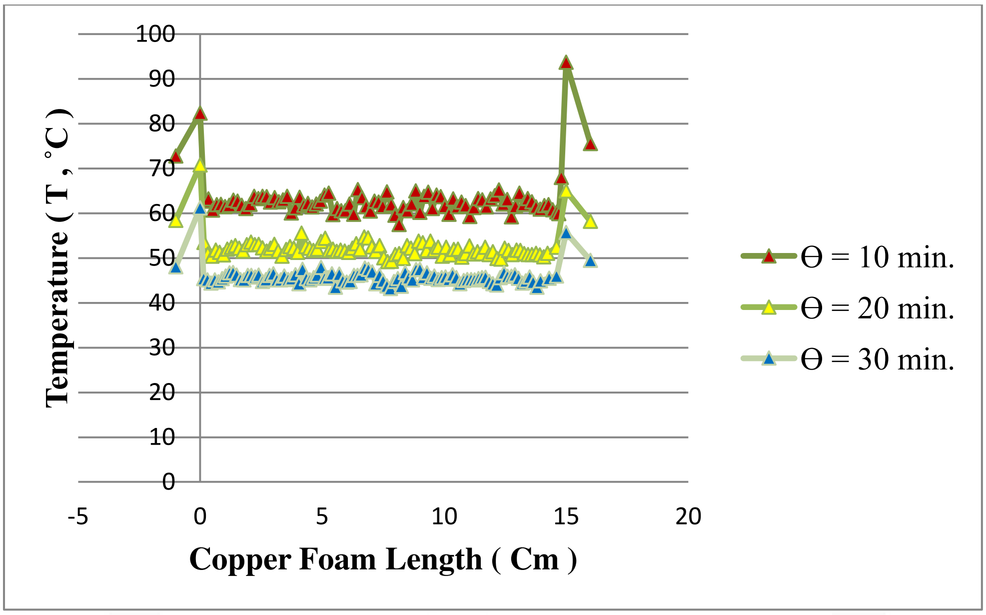

Figure 4.16 Time dependent upper surface thermal profiles of the 5 mm thickness Cu foam plate

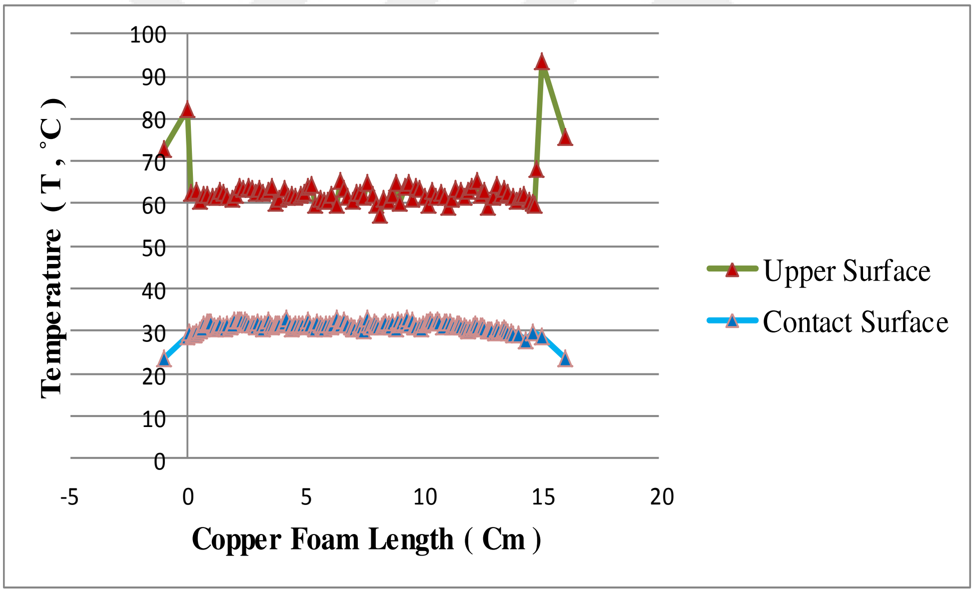

Figure 4.17.a Thermal profiles of the upper and contact heating surfaces of the 5 mm thickness Cu foam plate for Ө = 10 min.

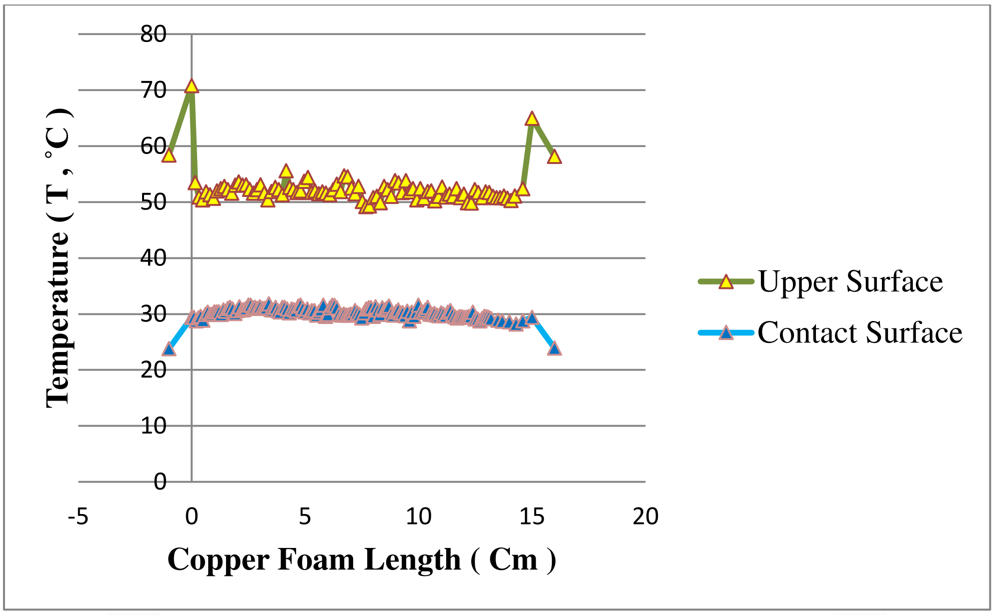

Figure 4.17.b Thermal profiles of the upper and contact heating surfaces of the 5 mm thickness Cu foam plate for Θ = 20 min.

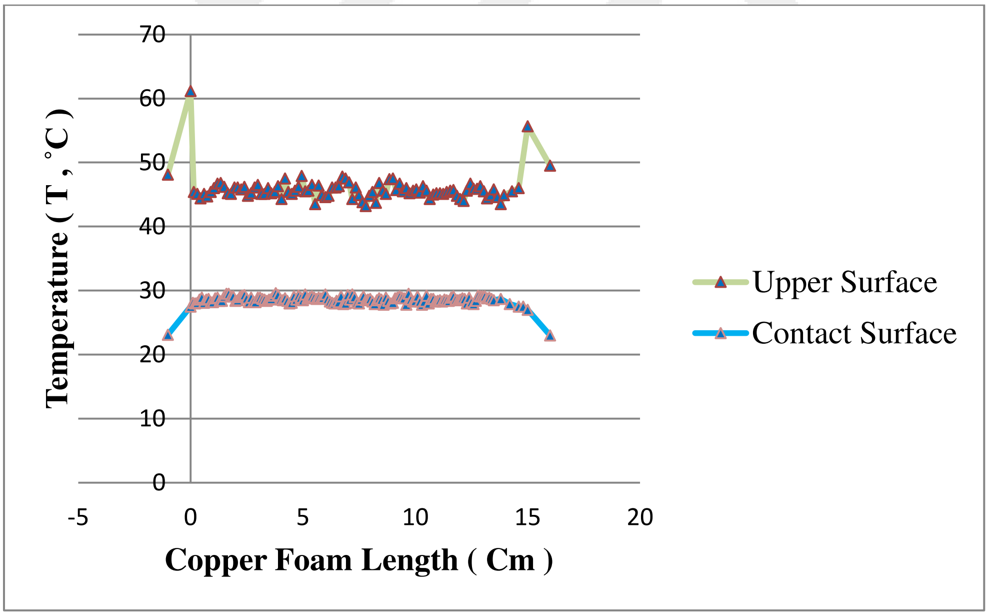

Figure 4.17.c Thermal profiles of the upper and contact heating surfaces of the 5 mm thickness Cu foam plate for Θ = 30 min.

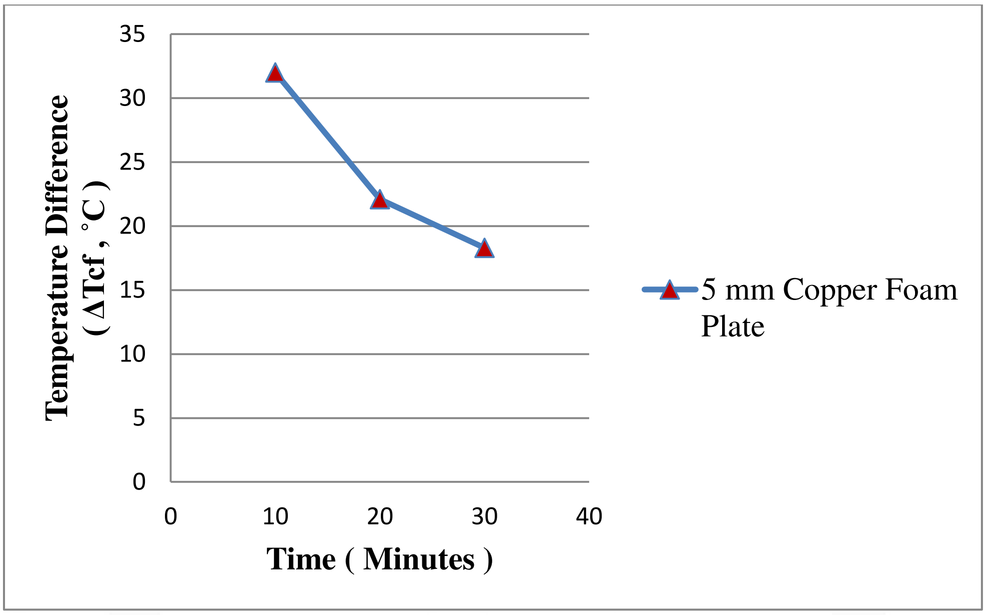

Figure 4.18 Time dependent mean temperature difference (ΔT_{cf}) variations between upper and contact surfaces of the 5 mm thickness Cu foam plate

Figure 4.19 shows the time dependent upper surface temperature distributions of the t = 3 mm Cu foam sample. Figure 4.20.a, 4.20.b and 4.20.c show the time dependent local temperature variations of upper and contact surfaces of the Cu foam sample at T_H = 50 ˚C . Time dependent thermal analysis results along the t = 3 mm Cu foam sample upper and contact surfaces at T_H = 50 ˚C are described through the plots which are given in the Figures 4.19, 4.20.a, 4.20.b, 4.20.c and 4.21.

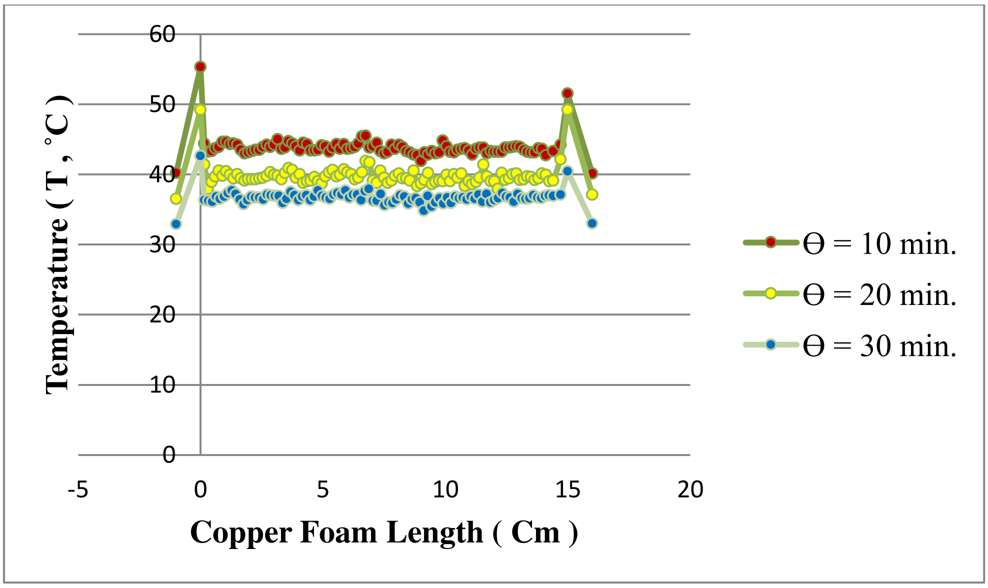

Figure 4.19 Time dependent upper surface thermal profiles of the 3 mm thickness Cu foam plate

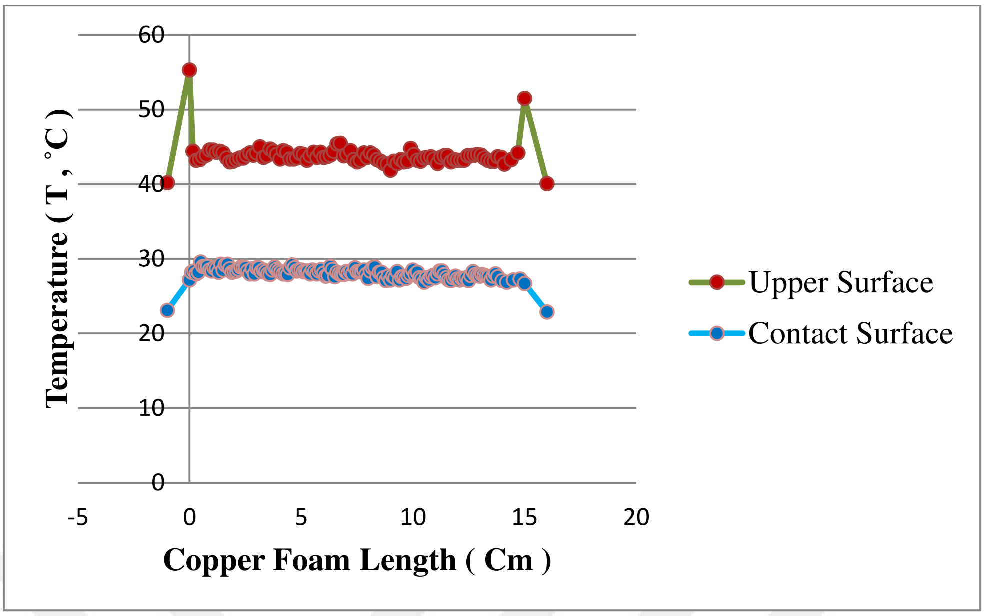

Figure 4.20.a Thermal profiles of the upper and contact heating surfaces of the 3 mm thickness Cu foam plate for ϴ = 10 min.

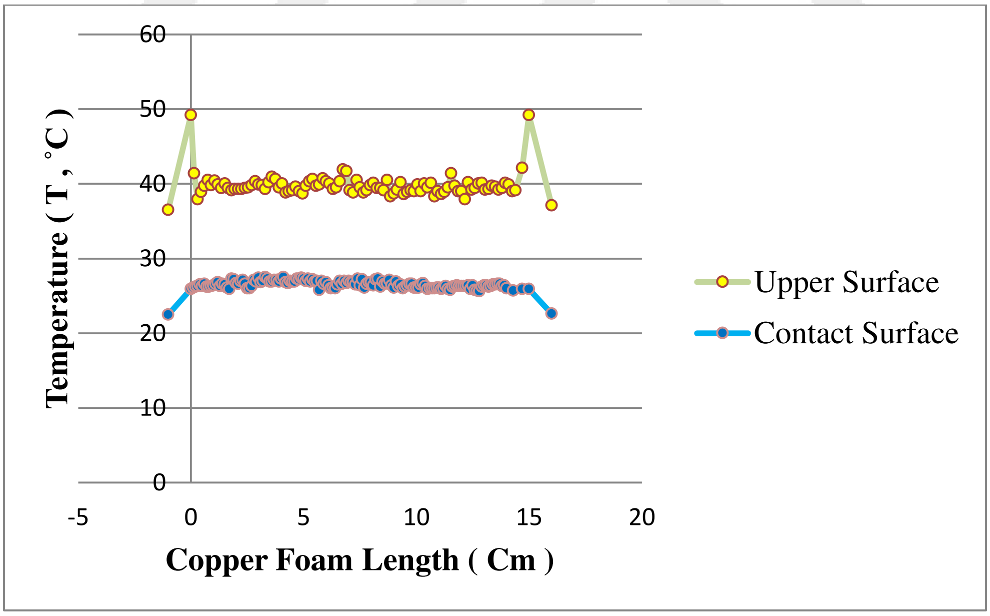

Figure 4.20.b Thermal profiles of the upper and contact heating surfaces of the 3 mm thickness Cu foam plate for ϴ = 20 min.

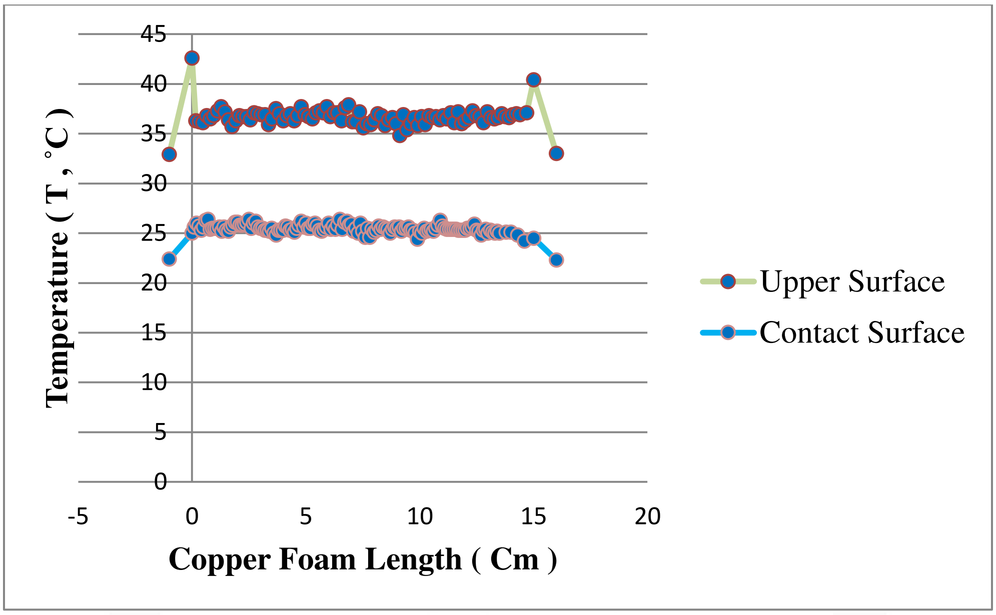

Figure 4.20.c Thermal profiles of the upper and contact heating surfaces of the 3 mm thickness Cu foam plate for ϴ = 30 min.

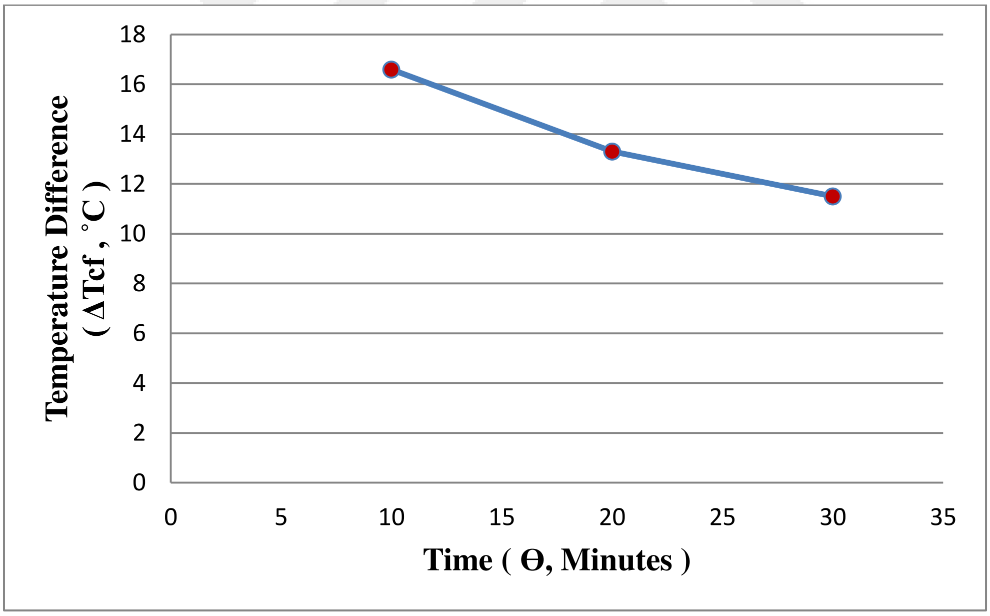

Figure 4.21 Time dependent mean temperature difference (ΔT_{cf}) variations between upper and contact surfaces of the 3 mm thickness Cu foam plate

Figure 4.22 shows the time dependent upper surface temperature distributions of the t = 4 mm Cu foam sample. Figure 4.23.a, 4.23.b and 4.23.c show the time dependent local temperature variations of upper and contact surfaces of the Cu foam sample at T_H = 50 ˚C . Time dependent thermal analysis results along the t = 4 mm Cu foam sample upper and contact surfaces at $T_H = 50$ ˚C are described through the plots which are given in the Figures 4.22, 4.23.a, 4.23.b, 4.23.c and 4.24.

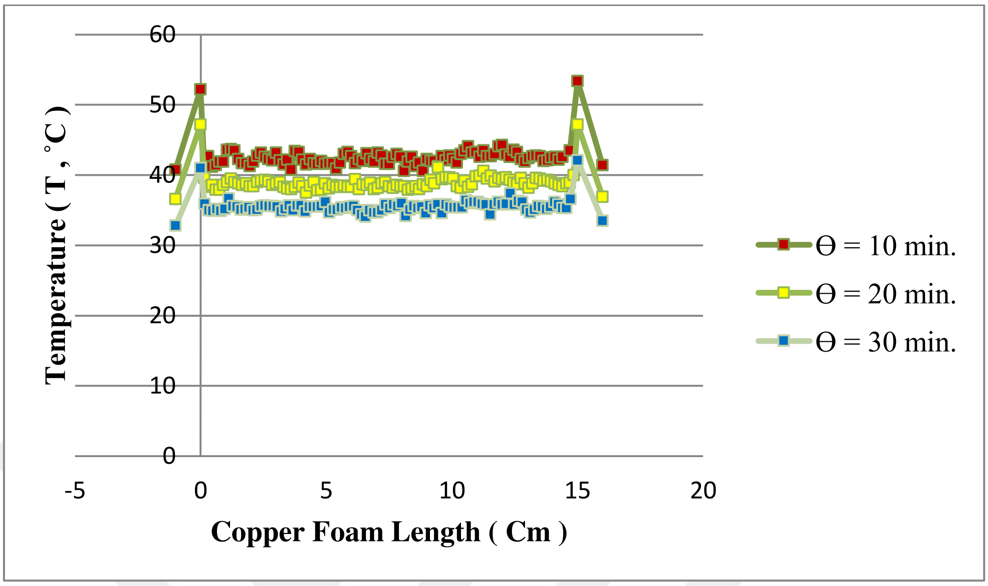

Figure 4.22 Time dependent upper surface thermal profiles of the 4 mm thickness Cu foam plate

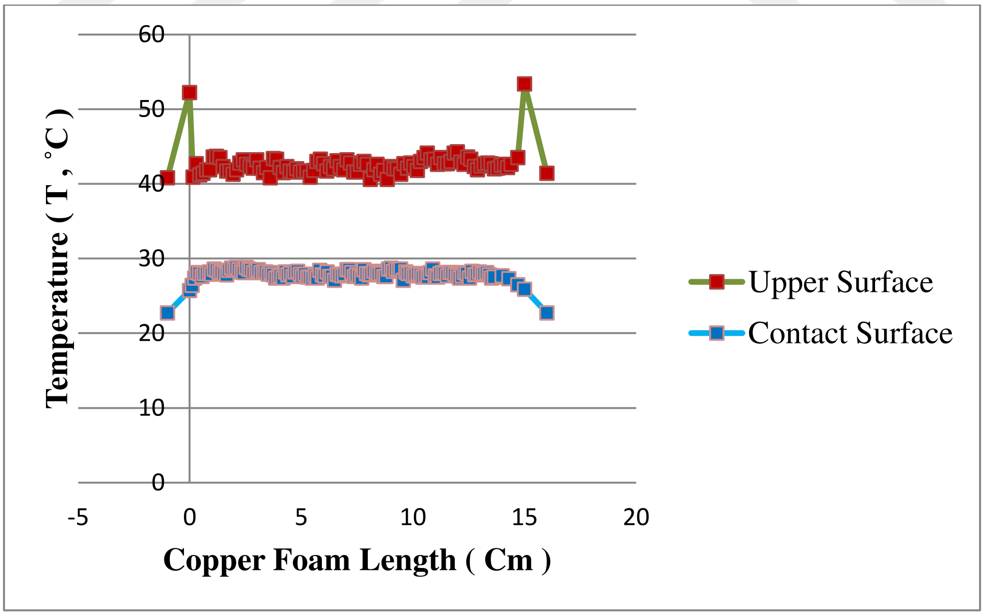

Figure 4.23.a Thermal profiles of the upper and contact heating surfaces of the 4 mm thickness Cu foam plate for ϴ = 10 min.

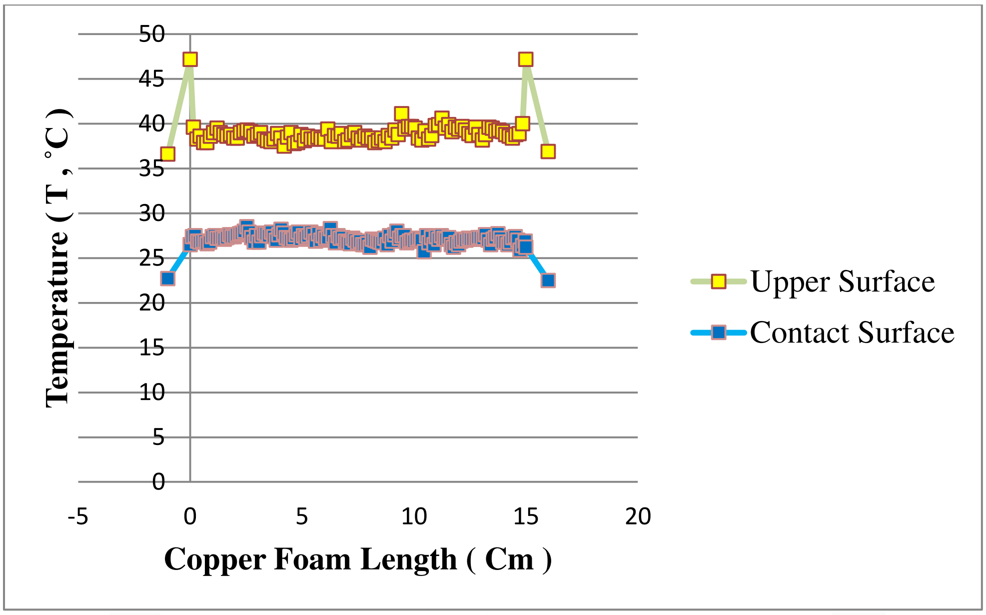

Figure 4.23.b Thermal profiles of the upper and contact heating surfaces of the 4 mm thickness Cu foam plate for ϴ = 20 min.

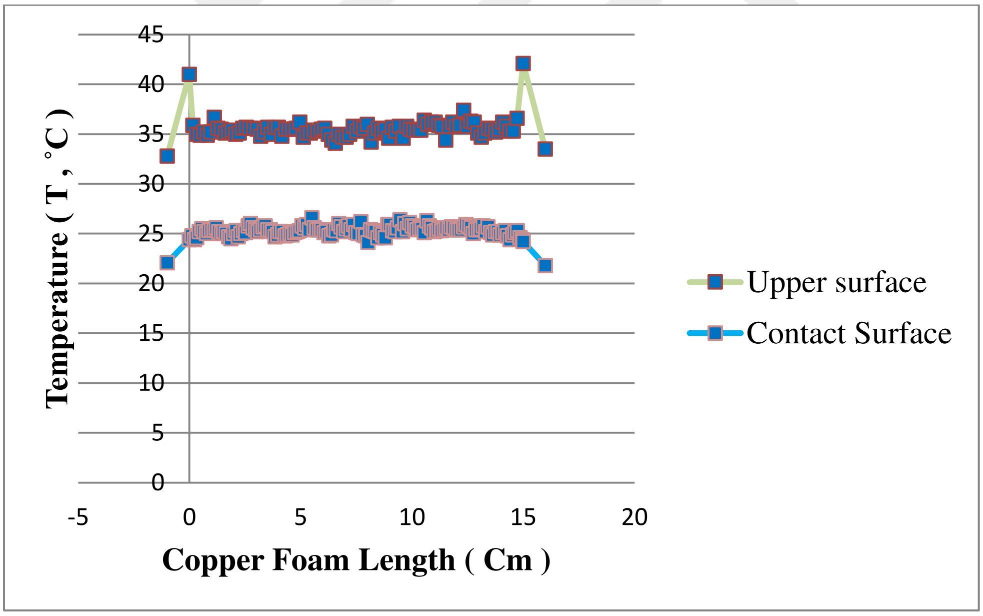

Figure 4.23.c Thermal profiles of the upper and contact heating surfaces of the 4 mm thickness Cu foam plate for ϴ = 30 min.

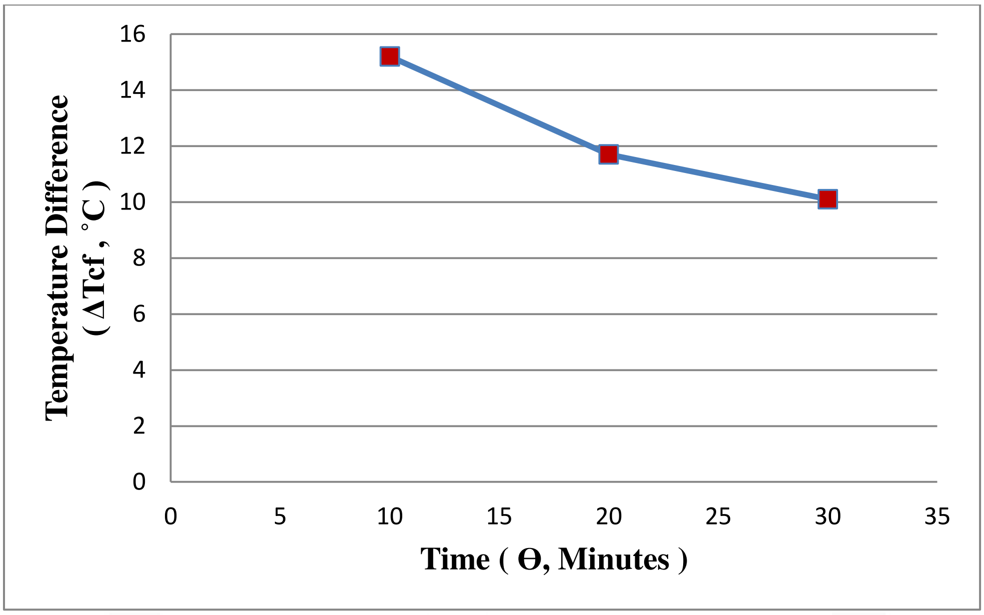

Figure 4.24 Time dependent mean temperature difference (ΔT_{cf}) variations between upper and contact surfaces of the 4 mm thickness Cu foam plate

Figure 4.25 shows the time dependent upper surface temperature distributions of the t = 5 mm Cu foam sample. Figure 4.26.a, 4.26.b and 4.26.c show the time dependent local temperature variations of upper and contact surfaces of the Cu foam sample at T_H = 50 ˚C . Time dependent thermal analysis results along the t = 5 mm Cu foam sample upper and contact surfaces at T_H = 50 ˚C are described through the plots which are given in the Figures 4.25, 4.26.a, 4.26.b, 4.26.c and 4.27.

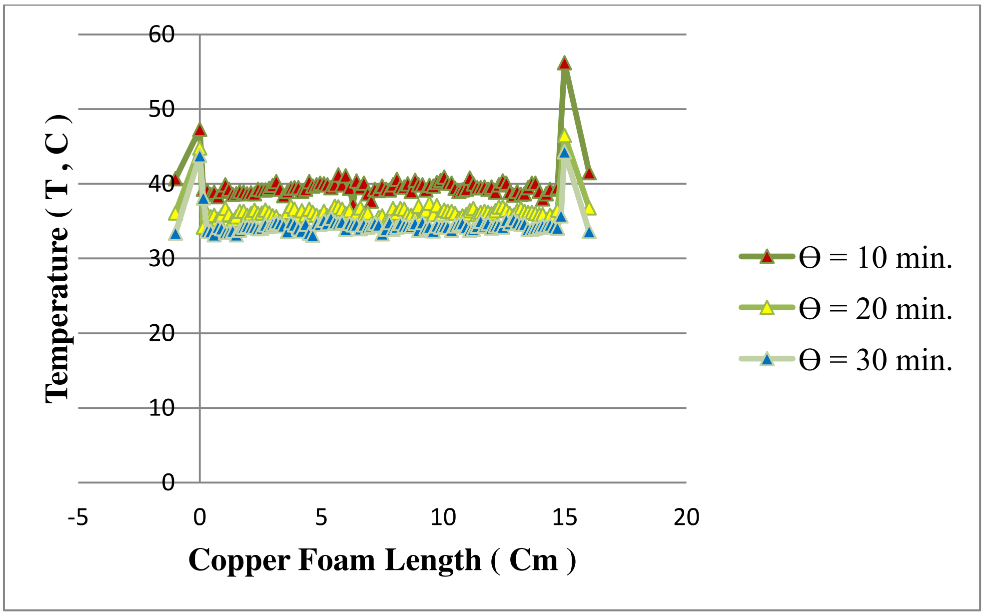

Figure 4.25 Time dependent upper surface thermal profiles of the 5 mm thickness Cu foam plate

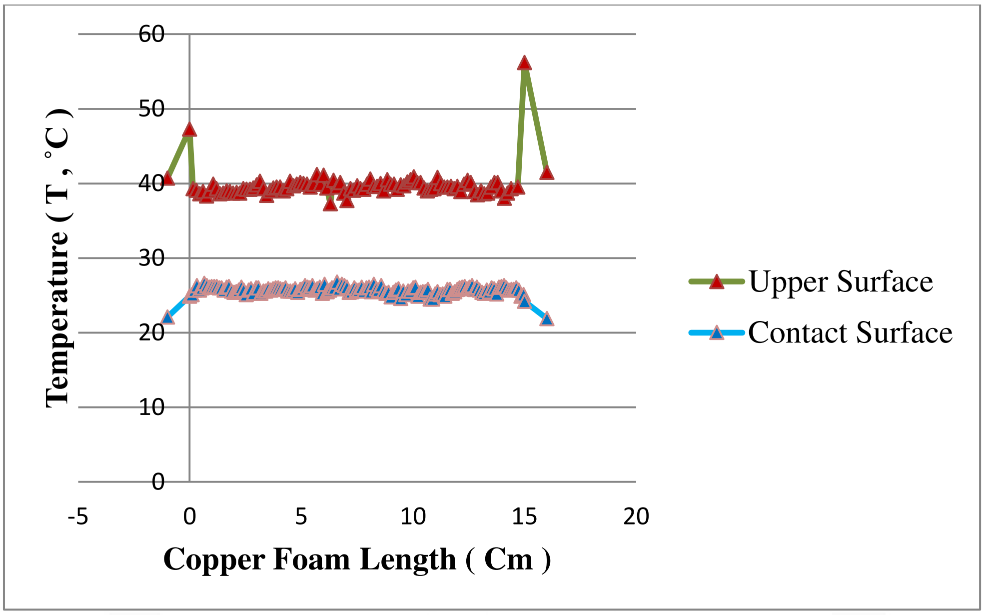

Figure 4.26.a Thermal profiles of the upper and contact heating surfaces of the 5 mm thickness Cu foam plate for ϴ = 10 min.

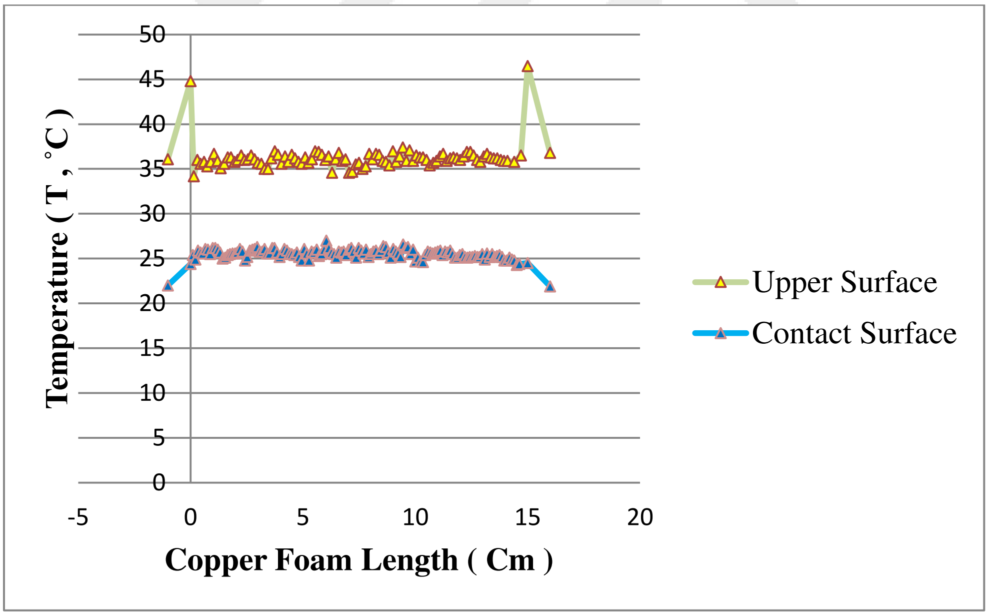

Figure 4.26.b Thermal profiles of the upper and contact heating surfaces of the 5 mm thickness Cu foam plate for ϴ = 20 min.

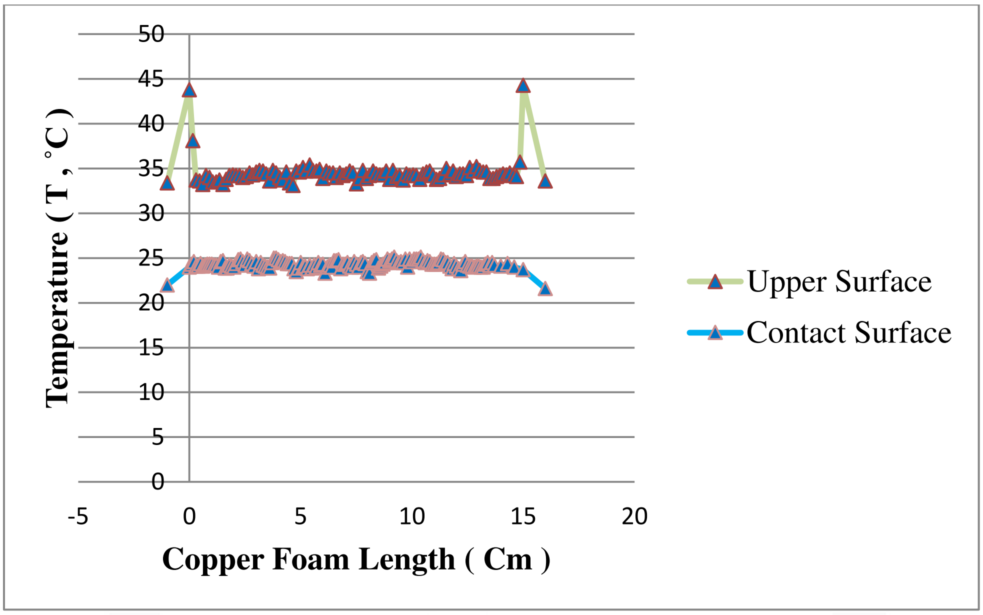

Figure 4.26.c Thermal profiles of the upper and contact heating surfaces of the 5 mm thickness Cu foam plate for ϴ = 30 min.

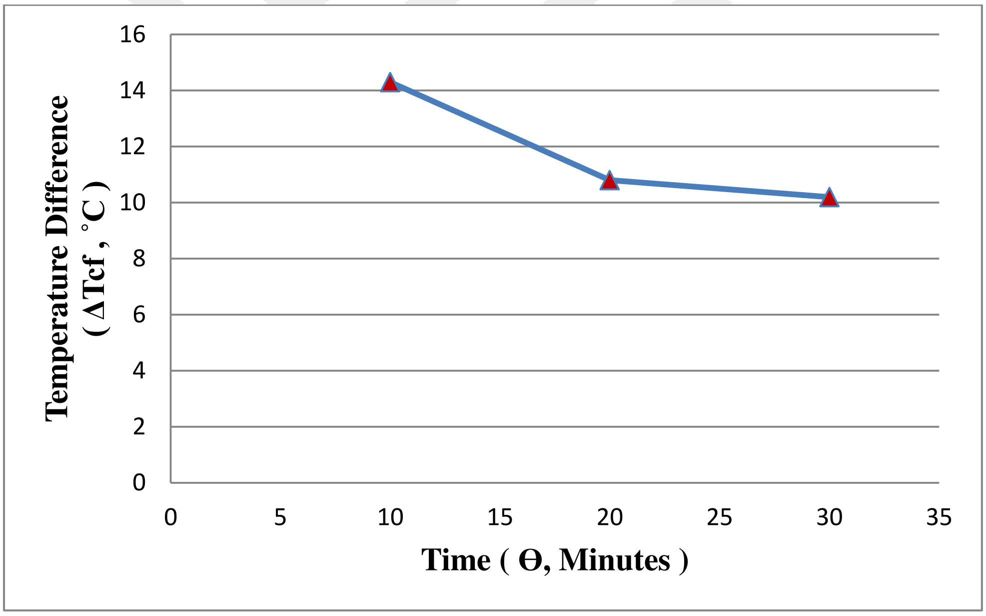

Figure 4.27 Time dependent mean temperature difference (ΔT_{cf}) variations between upper and contact surfaces of the 5 mm thickness Cu foam plate

Thermal image analysis results with different parameters are summarized in Table 4.1 as follows,

Table 4.1 : Time dependent thermal image analysis results

T_H, ˚C	Thickness, t (mm)	Parameter	ϴ = 10 min. (˚C)	ϴ = 20 min. (˚C)	ϴ = 30 min. (˚C)
50	3,4,5	T_H	42.5, 43.1,42.8	37.7,37.8,37.7	34, 34, 34.2
		T_{edge}	55.3 – 51.5 52.2 – 53.4 47.3 – 56.2	49.2 – 49.2 47.2 – 47.2 44.8 – 46.5	42.6 – 40.4 41 – 42.1 43.8 – 44.3
		ΔT_H	17.1 – 17.2 18.1 – 18.7 18.6 – 19.6	14 – 14.5 13.9 – 14.4 14.1 – 14.9	10.5 – 10.7 10.7 – 11.7 11.4 - 12
		ΔT_{cf}	16.6, 15.2,14.3	13.3, 11.7,10.8	11.5,10.1,10.2
80	3,4,5	T_H	64, 66, 65.5	52.5, 55, 53	45.2,46.4,45.3
		T_{edge}	86.6 – 81 78.4 – 82.6 78 – 70.5	74.5 – 71.7 65.8 – 58.9 68.9 – 63.5	53.6 – 55.2 51.1 – 53 48.4 – 50.4
		ΔT_H	37.6 – 34.5 38.9 – 40.8 39.2 – 39.3	28.7 – 28.6 30.5 – 28.2 28.7 – 29.1	21.1 – 21.5 22.2 – 22.3 20.3 – 21.1
		ΔT_{cf}	35.9, 29.2,25.3	25.8, 24.4,19.4	21.2, 18.7,17.1
100	3,4,5	T_H	79, 77.9, 78.7	63, 62.2, 62.2	52, 51.2, 51.5
		T_{edge}	87 – 82.1 80.4 – 75.5 82.4 – 93.7	79.2 – 73 87 – 83.2 70.8 - 65	73 – 69.9 60.1 – 57.9 61.2 – 55.7
		ΔT_H	50.6 – 46.8 46.7 – 47.6 49 – 52.1	36.3 – 37.6 36.7 – 37.5 34.6 – 34.3	27.5 – 28.6 25.4 – 25.6 25 – 26.5
		ΔT_{cf}	45.2, 32.3, 32	34.1, 26.2,22.1	25.2, 20.7,18.3

It is also important to note that, ΔT_{cf} changes depending on the t and T_H. Figure 4.28 through Figure 4.33 show the time dependent variation of the ΔT_{cf} depending on the different thickness and heater temperatures.

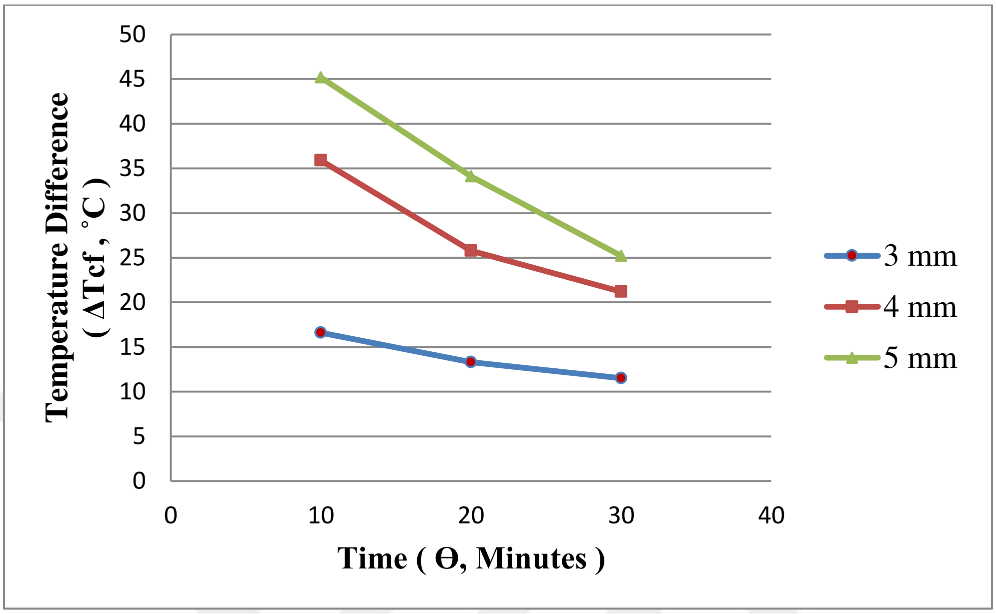

Figure 4.28 Time dependent variations of the ΔT_{cf} for $T_H = 50$ ˚C

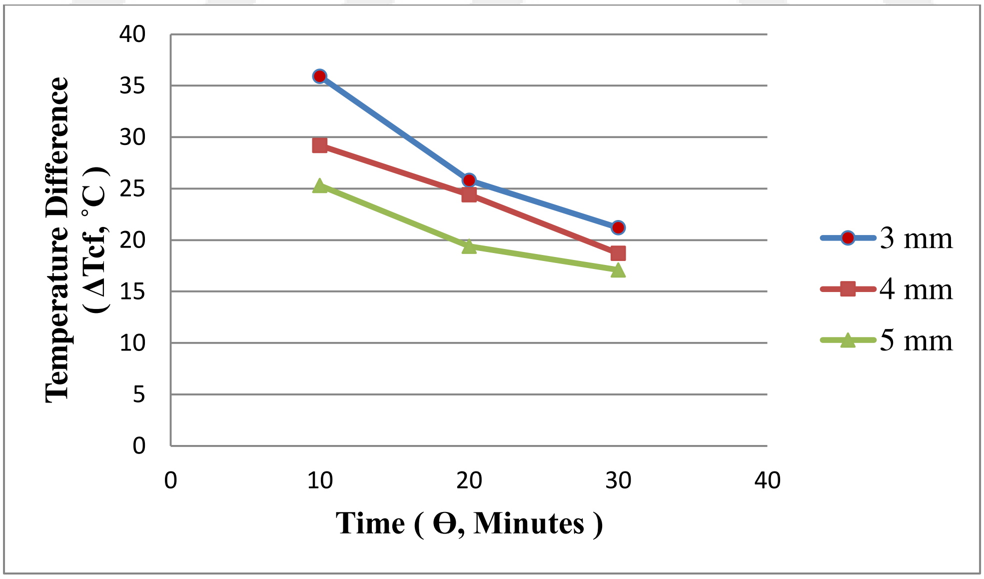

Figure 4.29 Time dependent variations of the ΔT_{cf} for $T_H = 80$ ˚C

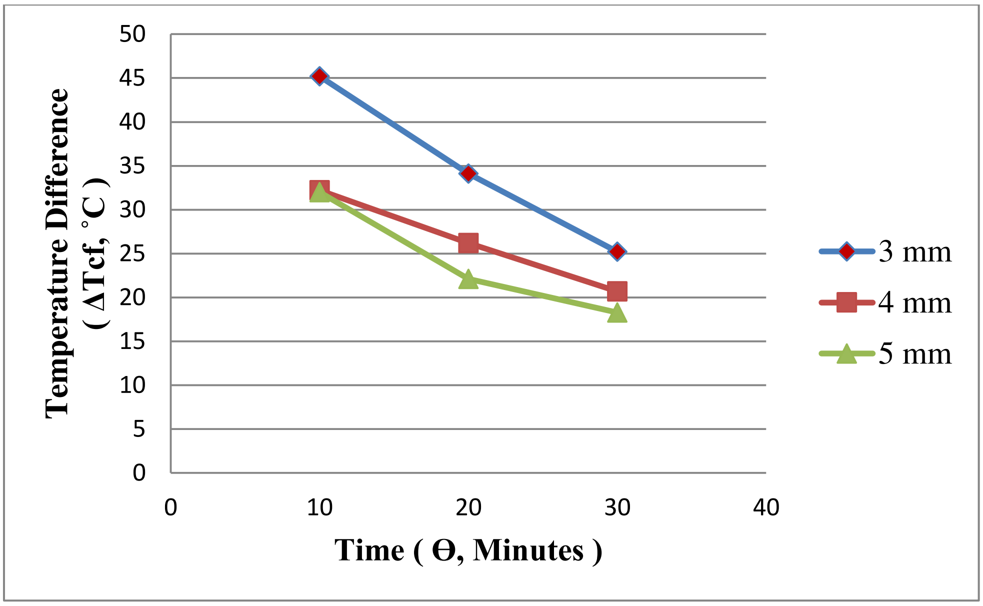

Figure 4.30 Time dependent variations of the ΔT_{cf} for $T_H = 100$ ˚C

Figure 4.28 show the effects of the thickness on the ΔT_{cf}. It is clear that ΔT_{cf} increases with increasing t but decreases with increasing Θ. From that figure, 4 mm and 5 mm thicknesses of Cu foam samples have high values compared with 3 mm Cu foam sample. In contrast, it is seen from the Figure 4.29 that, ΔT_{cf} decreases with increasing t and Θ. ΔT_{cf} values are similar to each other for different thicknesses, especially for Θ = 30 minutes. Figure 4.30 shows the t = 3 mm Cu foam sample has higher ΔT_{cf} values compared with t = 4 mm and t = 5 mm Cu foam samples. Likely, ΔT_{cf} decreases with increasing Θ.

ΔT_{cf} values of the t = 3 mm, 4 mm and 5 mm Cu foam samples change depending on the Θ, between 11 ˚C ≤ ΔT_{cf} ≤ 17 ˚C, 20 ˚C ≤ ΔT_{cf} ≤ 36 ˚C and 25 ˚C ≤ ΔT_{cf} ≤ 45 ˚C for $T_H = 50$ ˚C. 21 ˚C ≤ ΔT_{cf} ≤ 36 ˚C, 18 ˚C ≤ ΔT_{cf} ≤ 30 ˚C and 16 ˚C ≤ ΔT_{cf} ≤ 25 ˚C for $T_H = 80$ ˚C and 25 ˚C ≤ ΔT_{cf} ≤ 45 ˚C, 20 ˚C ≤ ΔT_{cf} ≤ 33 ˚C and 18 ˚C ≤ ΔT_{cf} ≤ 32 ˚C for $T_H = 100$ ˚C respectively.

Figure 4.31, 4.32 and 4.33 show the effects of the T_H on the ΔT_{cf} for different t.

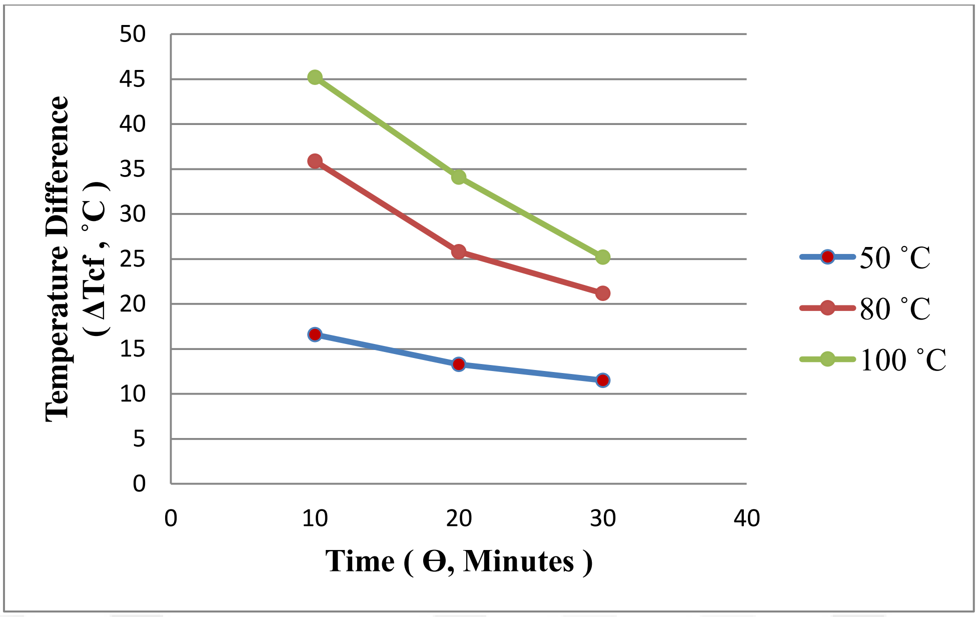

Figure 4.31 Time dependent variations of the ΔT_{cf} for 3 mm thickness Cu foam sample

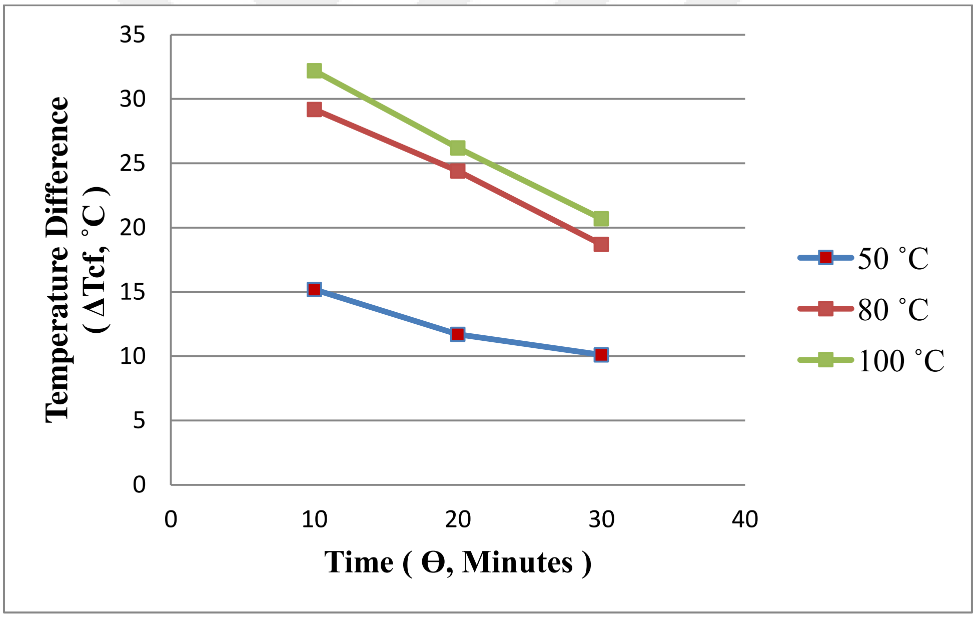

Figure 4.32 Time dependent variations of the ΔT_{cf} for 4 mm thickness Cu foam sample

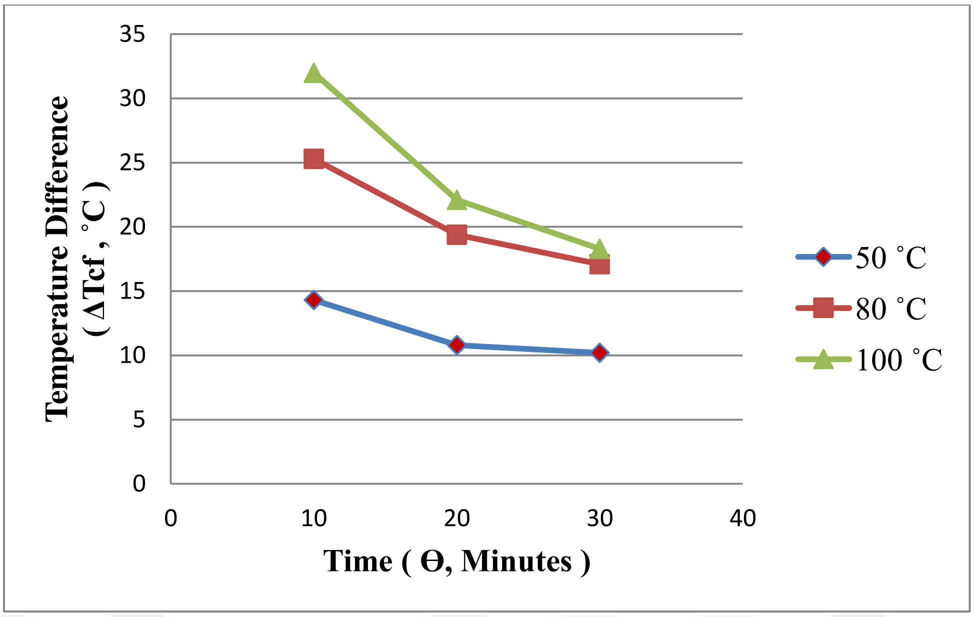

Figure 4.33 Time dependent variations of the ΔT_{cf} for 5 mm thickness Cu foam sample

It is seen from the Figure 4.31 that, ΔT_{cf} values increases with increasing $T_{H.}$ At high heater temperatures, ΔT_{cf} is higher. ΔT_{cf} decreases with increasing Ɵ. It is seen from the Figure 4.32 that, increase in ΔT_{cf} values depends on the T_H and values are comparable to each other at T_H = 80 ˚C and T_H = 100 ˚C. Finally, Figure 4.33 shows the similar results compared with Figure 4.32.

4.2 Thermal Images and Histogram Temperatures of The Copper Foam Samples

4.2.1 Introduction

Thermal images and histogram temperatures of the t = 3 mm Cu foam sample at T_H = 80 ˚C are given in the Figures 4.34 and 4.35 for upper surface and Figures 4.36 and 4.37 for contact surface. Other images and histogram temperature figures for Cu foam samples are given in the **Appendix A.**

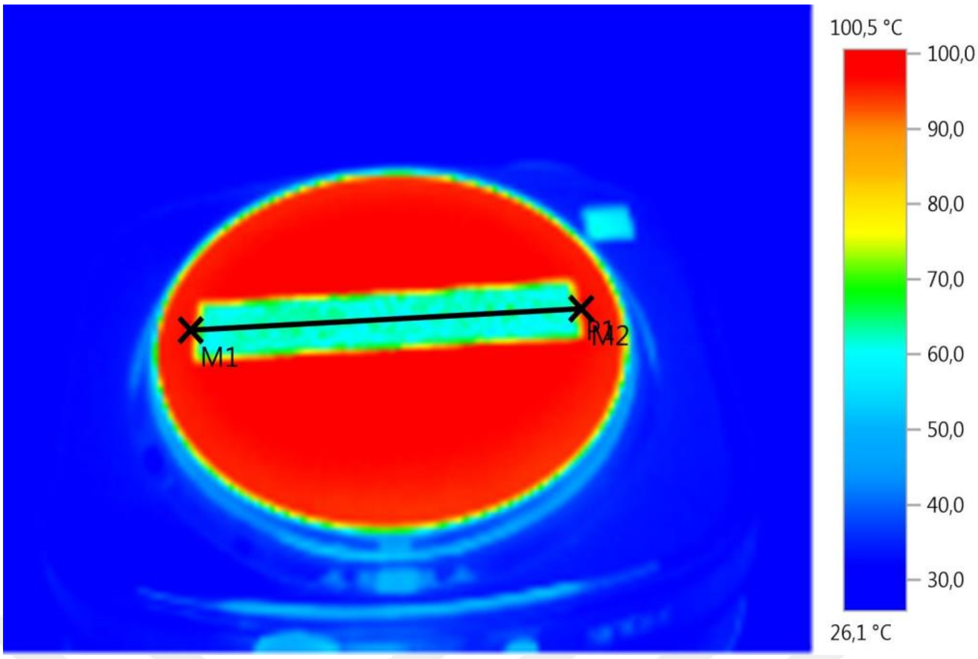

Figure 4.34 Thermal image of the 3 mm thickness Cu foam sample with measurement direction

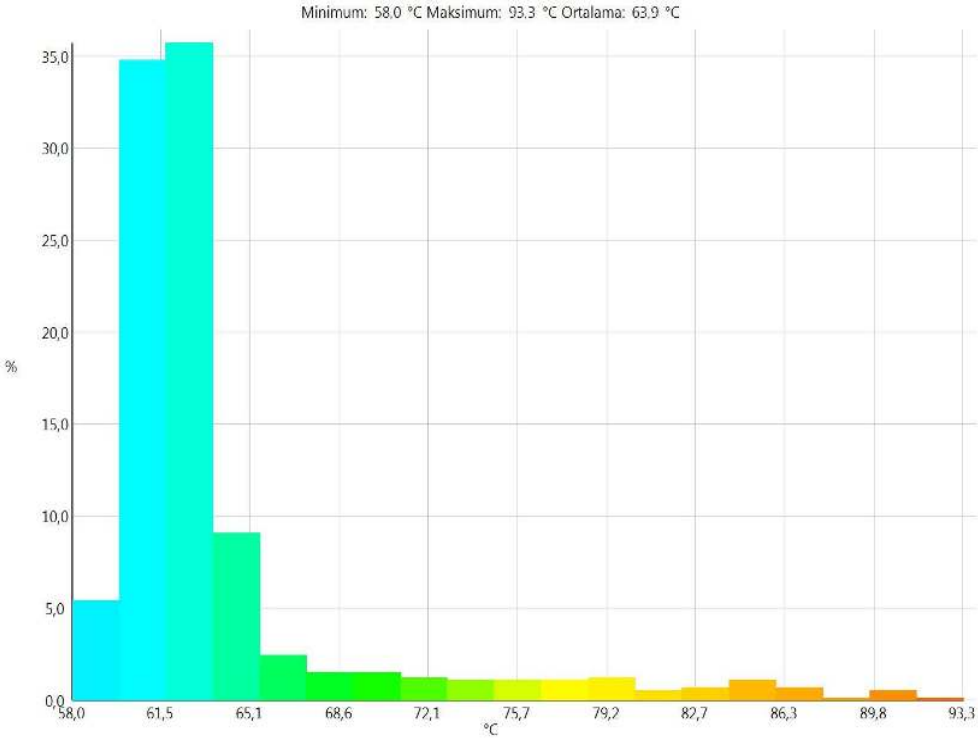

Figure 4.35 Histogram picture of the 3 mm thickness Cu foam sample

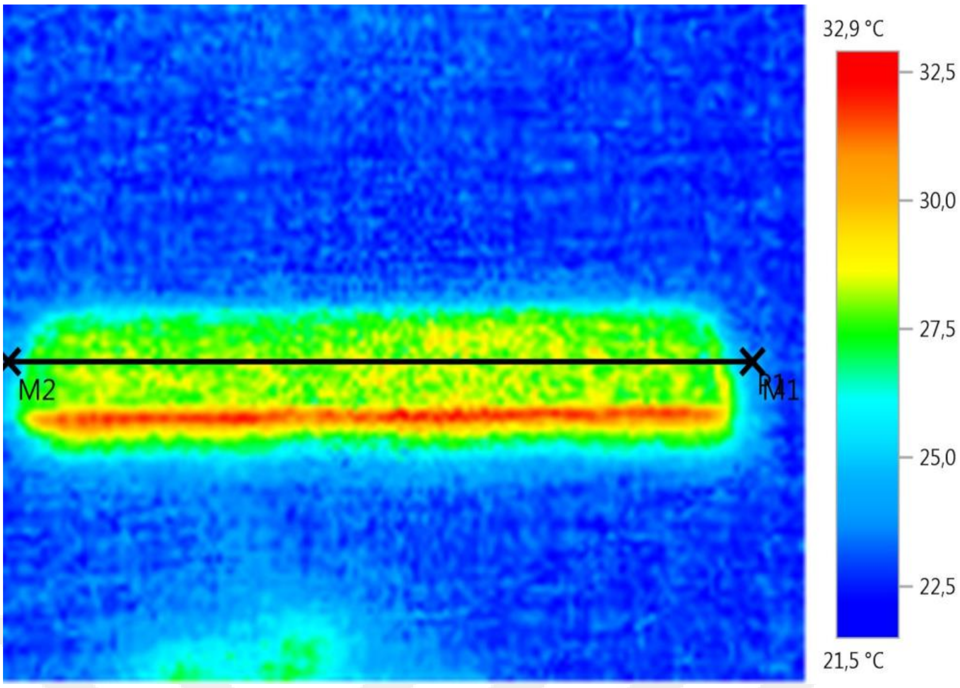

Figure 4.36 Thermal image of the 3 mm thickness Cu foam sample with measurement direction

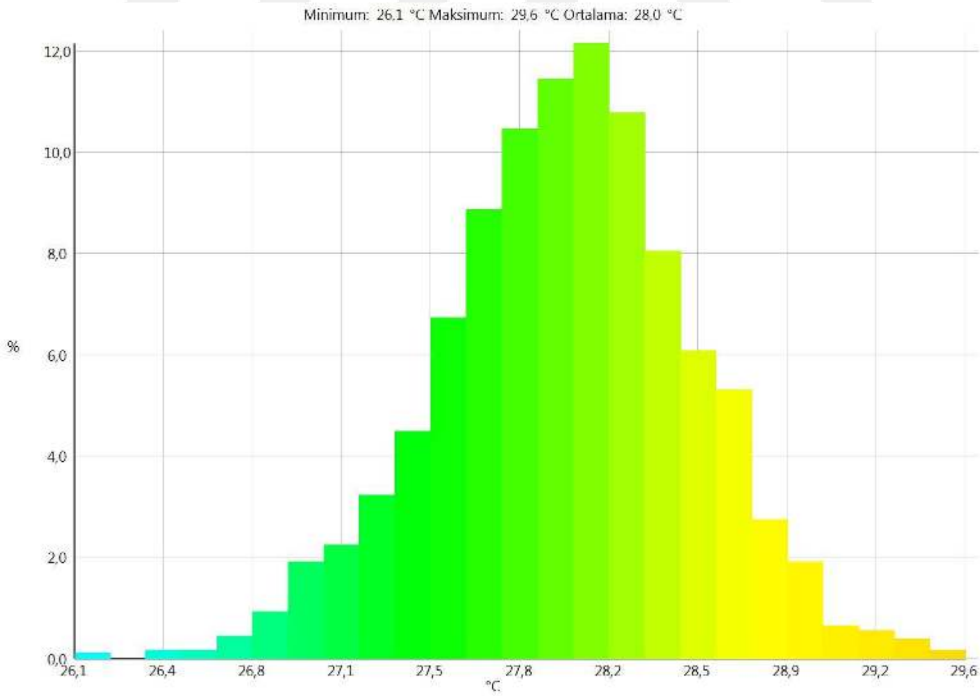

Figure 4.37 Histogram picture of the 3 mm thickness Cu foam sample

Comparison of the percentage distributions of the upper surface temperature of the Cu foam samples are given in Table 4.2.

Table 4.2 Comparisions of the upper surface temperature histogram of the Cu foam samples

Heater temperature, T_H (˚C)	Cu foam thickness, t (mm)	Time, ϴ (Min.)	Percentage of temperature distribution (% - ˚C)	T_{min} (˚C)	T_{max} (˚C)	$T_{m,upper}$ (˚C)
50	3	10	35 – 44	41.9	57.3	44.6
		20	36 – 39.9	37.6	48.9	39.7
		30	30 – 36.8	34.7	43.8	36.9
	4	10	40 – 42.5	40	56.9	43
		20	32 – 38.7	36.8	46.3	38.9
		30	28 – 35	34.1	41.6	35.5
	5	10	43 – 39	37	55.6	39.9
		20	40 – 36	33.9	49.1	36.4
		30	30 – 34.3	32	43.3	34.6
80	3	10	35 – 61.5	58	93.3	63.9
		20	52 – 51.9	49.6	72.7	53.4
		30	40 – 47	44.9	63.9	47.9
	4	10	30 – 60	56.5	81.5	61.5
		20	40 – 52	48.4	74.5	52.6
		30	40 – 45.5	43.2	66.6	46.6
	5	10	32 – 53.1	50.2	79	53.9
		20	36 – 45.5	43.3	60.1	46.7
		30	35 – 41.5	39.8	52	41.9

Heater temperature, T_H (˚C)	Cu foam thickness, t (mm)	Time, ϴ (min.)	Percentage of temperature distribution (% - ˚C)	T_{min} (˚C)	T_{max} (˚C)	$T_{m,upper}$ (˚C)
100	3	10	24 – 75.5	70	97.2	76
		20	29 – 63	58.2	83.8	62.8
		30	28 – 53	49.7	67.6	53.5
	4	10	25 – 66.9	60.1	94	66.9
		20	30 – 55.8	50.8	75.9	56.2
		30	35 – 47.5	44.1	71.9	48.9
	5	10	40 – 61	56.8	96.1	63.1
		20	36 – 52	47.6	69.9	52.2
		30	60 – 45.4	42.2	74.1	46.8

As can be seen from Table 4.2, upper surface mean temperature, $T_{m,upper}$ values of the Cu foam samples decreases with increasing ϴ. Time dependent percentage changes for t = 3 mm, 4 mm and 5 mm Cu foam samples are % 17.2, % 17.4 and % 13.2 for T_H = 50 ˚C, for $T_{H =}$ 80 ˚C are % 25, % 24.2 and % 22.2 and for $T_{H =}$ 100 are % 29.6, % 26.9 and % 25.8 respectively.

From the results, it was obvious that percentage change rate was highest at $T_{H =}$ 100 compared with other $T_{H.}$ It was also important to note that, percentage change of the upper surface temperature of the samples decreases with increasing thickness. These situations showed the temperature and thickness effects on upper surface temperature distribution of the Cu foam samples. Also, T_{min} and T_{max} values showed the effects of the porosity and its distributions in the sample.

As a result of the analyses, time dependent thermal analysis results for different thicknesses of Cu foams along the upper and contact surfaces at different T_H can be seen from the above figures. Experimental analysis results are summarized and listed as,

1. Heater surface and Cu foam upper surface temperatures decrease depending on the increasing time periods.

2. Temperature distributions of all Cu foam samples are not same, these situations mean that porosity also pore shape, size & direction of the Cu foams distributed non-uniformly along the all surface. So porous effects can be seen from the figures.

3. Cu foam upper and contact surface temperature differences showed the importance and effects of the thermal conductivity and Cu foam thicknesses on heat transfer. In the next chapters, a detailed analysis of the thermal conductivity, k, heat capacity, C and thermal diffusivity, α of the tested Cu foam samples are given.

4. Cu foam edge temperatures T_{edge}, are higher than the other surfaces. This implies that, Cu foam absorbs heat from the heater surface and spreads to all edges of the Cu foam surface depending on the pore directions. It is obvious from the figures, T_{edge} change depend on the time, T_H and Cu foam thicknesses. Related comparisions are given in the next sections.

5. Heater temperatures $T_{H,}$ decrease rapidly before and after Cu foam limits (Points just before 0 cm and just after 15 cm of Cu foam length) which imply the effects of emissivity, heat losses from heater surfaces to surrounding medium by means of convection heat transfer and T_{edge} which changing with time and also surrounding conditions.

6. Temperature differences between upper and contact surfaces of the Cu foam, ΔT_{cf}, decreases with increasing Θ.

7. Temperature differences between upper and contact surfaces of the heater, ΔT_h are for just before the Cu foam plate and just after the Cu foam plate decrease with time which Θ = 10, 20 and 30 minutes time periods. Temperature variations show nearly similar results for different thicknesses and little temperature differences can be seen. As a result, if T_H increase, temperature differences between the upper and contact surfaces will increase.

8. There are Q_{cond} and Q_{conv} variations along the all directions inside the Cu foam plate can be seen from the experimental results.

4.3 Effects of The Thickness on Temperature Distribution Along The Copper Foam Surfaces

The effects of the thickness on temperature distributions of the Cu foam samples along the upper and contact surfaces are shown in detail in the following sections. Firstly, comparison of the temperature distributions of the Cu foam sample surfaces with different thicknesses at $T_H = 50$ ˚C for upper and contact surfaces for ϴ = 10, 20 and 30 minutes are shown in the Figures 4.38, 4.39 and 4.40.

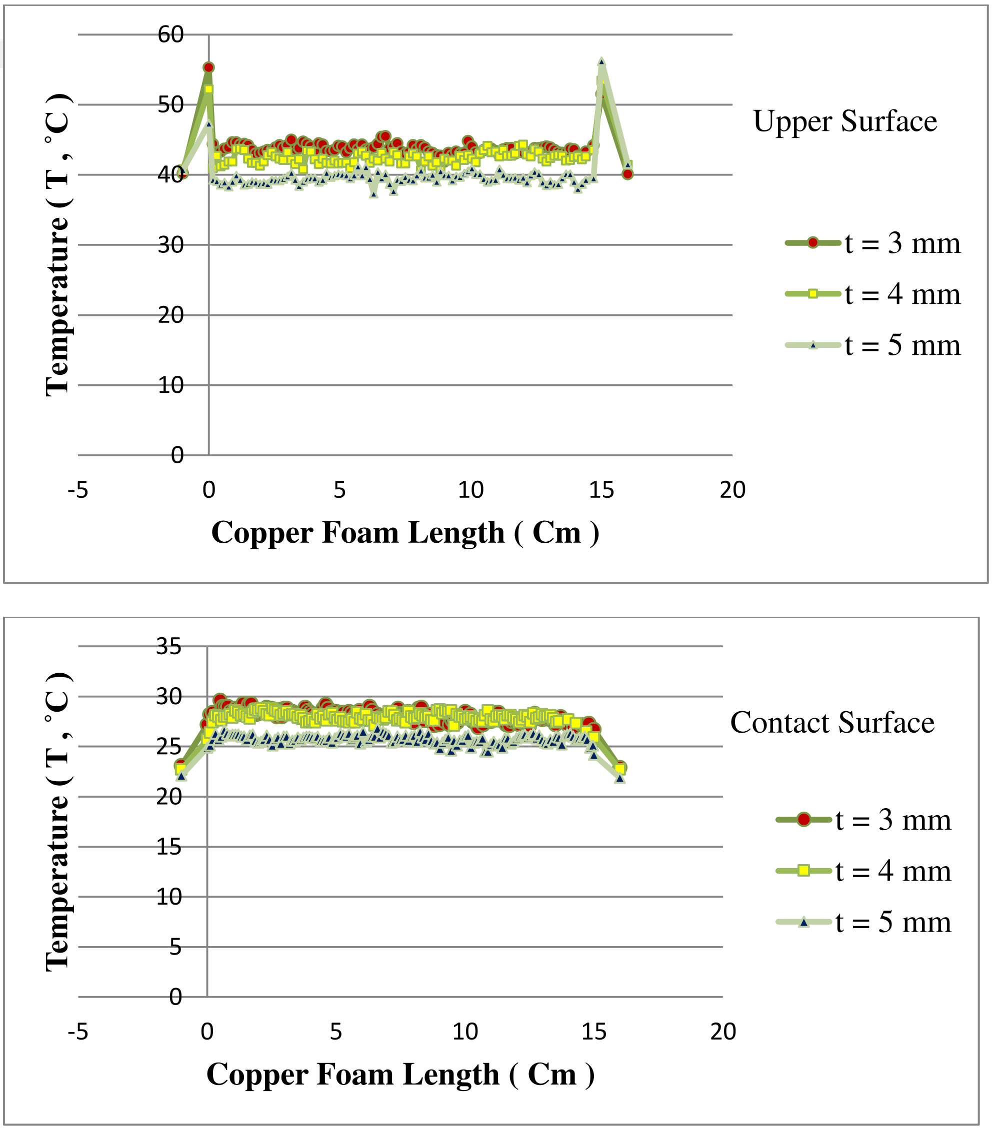

Figure 4.38 Variation of temperature distributions along the upper and contact surfaces of the Cu foam samples as a function of t for ϴ = 10 min

Analysis results for Cu foam samples which were waited on heater surface at T_H = 50 ˚C for Θ = 10 minutes showed some differences shown in the Figure 4.38. Such as, upper surface mean temperatures, $T_{m,upper}$, (shown in the first picture) for t = 3 mm, 4 mm and 5 mm Cu foams are 44.6 ˚C, 43 ˚C and 39.9 ˚C respectively. Contact surface mean temperatures, $T_{m,\ contact}$, (shown in the second picture) for t = 3 mm, 4 mm and 5 mm Cu foams are 28 ˚C, 27.8 ˚C and 25.6 ˚C respectively. From the thermal profiles, it was clear that 3 mm and 4 mm thicknesses Cu foams showed near results compared with 5 mm Cu foam.

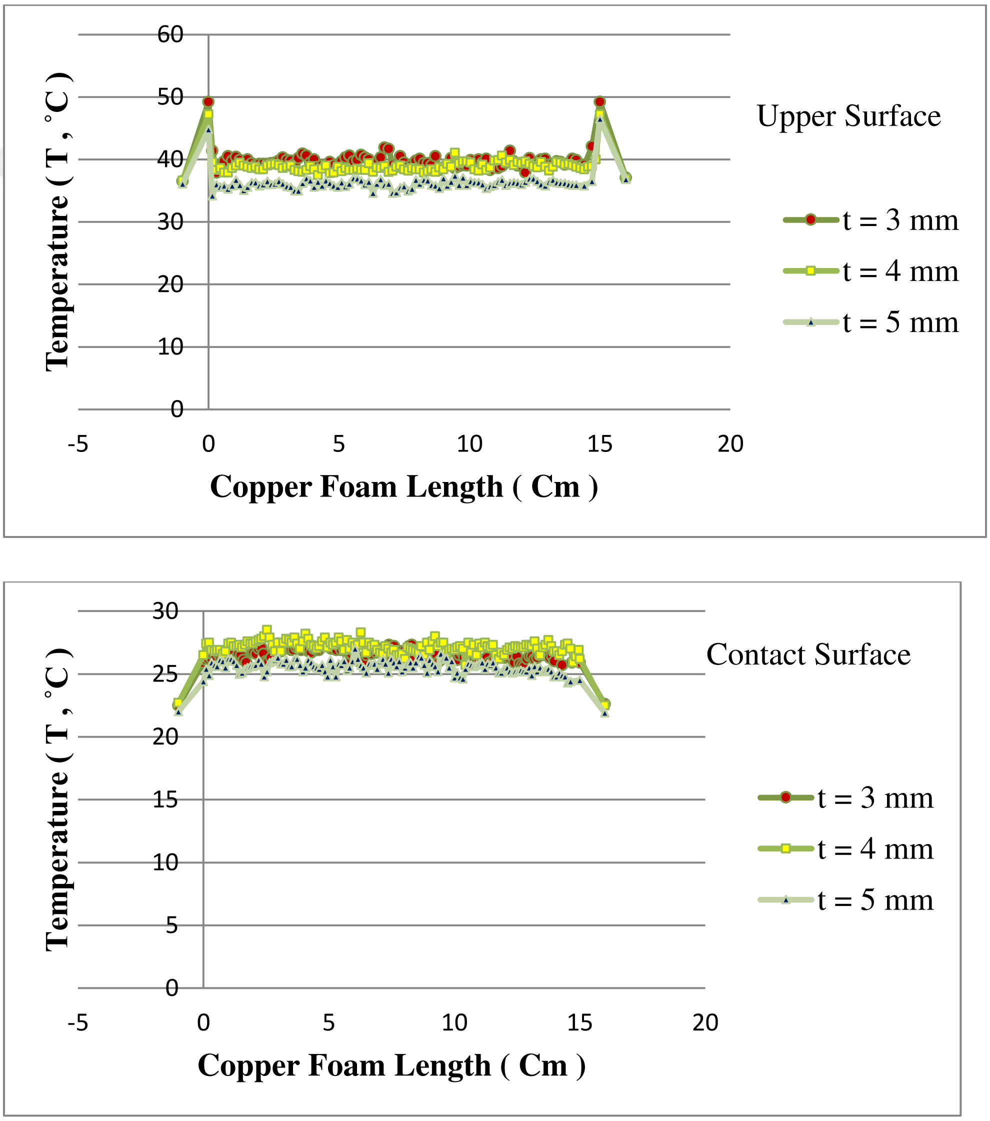

Figure 4.39 Variation of temperature distributions along the upper and contact surfaces of the Cu foam samples as a function of t for Θ = 20 min.

Analysis results for Cu foams which were waited on heater surface at T_H = 50 ˚C for ϴ = 20 minutes showed some differences shown in the Figure 4.39. Such as, $T_{m,upper}$ for t = 3 mm, 4 mm and 5 mm Cu foams are 39.7 ˚C, 38.9 ˚C and 36.4 ˚C respectively. From thermal profiles, 3 mm and 4 mm thicknesses Cu foams showed near results compared with 5 mm Cu foam seen from the figures. $T_{m,\ contact}$ for 3 mm, 4 mm and 5 mm thicknesses Cu foams are 26.4 ˚C, 27.2 ˚C and 25.6 ˚C respectively. From the thermal profiles, it was clear that Cu foams showed near results, there was a little temperature difference seen from the figure.

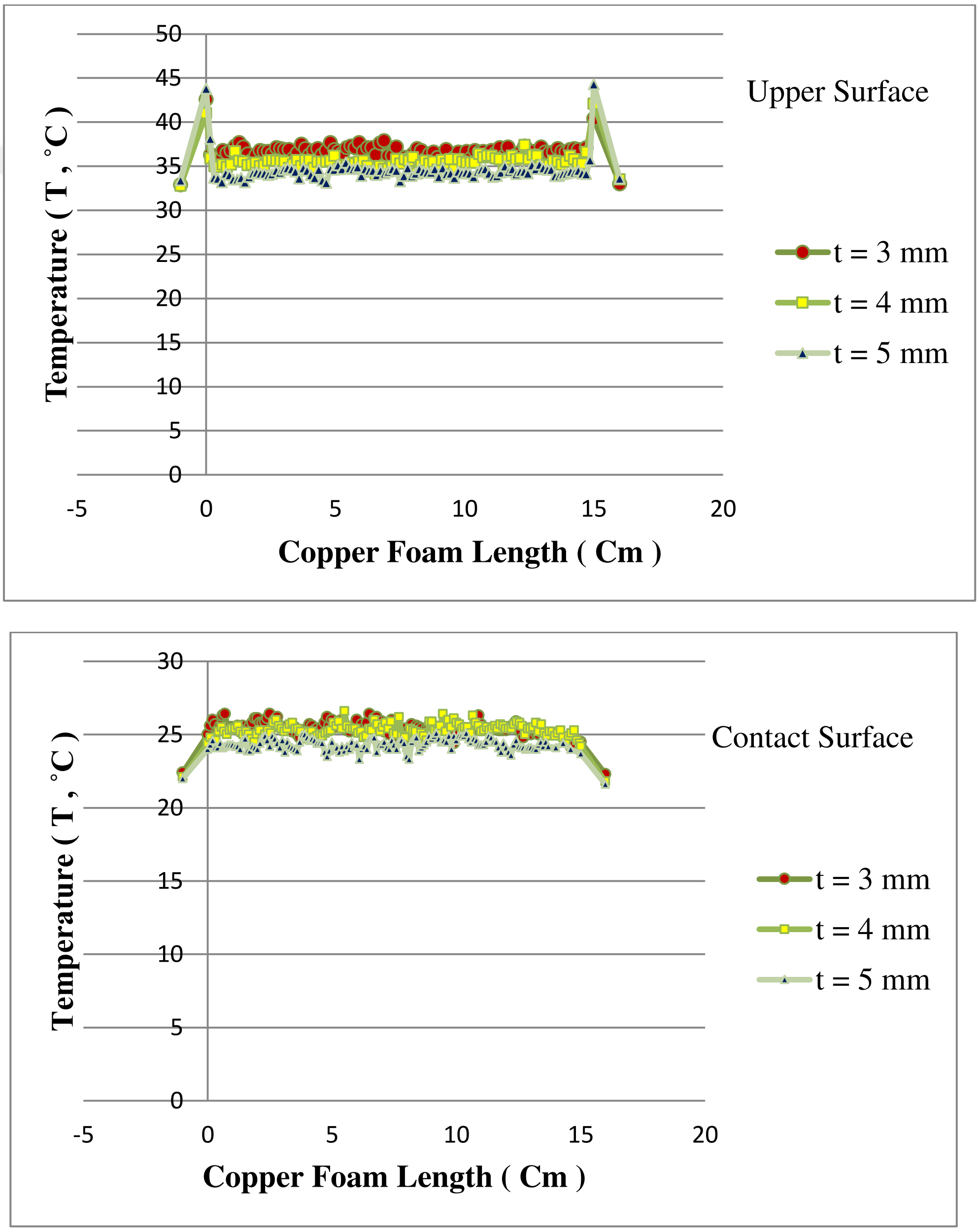

Figure 4.40 Variation of temperature distributions along the upper and contact surfaces of the Cu foam samples as a function of t for ϴ = 30 min.

Analysis results for Cu foams which were waited on heater surface at $T_H = 50$ ˚C for $\Theta = 30$ minutes showed some differences shown in the Figure 4.40. Such as, $T_{m,upper}$ for t = 3 mm, 4 mm and 5 mm Cu foams are 36.9 ˚C, 35.5 ˚C and 34.6 ˚C respectively. From thermal profiles, Cu foams showed nearly 1˚C temperature differences. $T_{m,\ contact}$ for t = 3 mm, 4 mm and 5 mm Cu foams are 25.4 ˚C, 25.4 ˚C and 24.4 ˚C respectively. From the thermal profiles, it was clear that 3 mm and 4 mm Cu foams showed same results compared with 5 mm Cu foam. Comparision of the temperature distributions of the Cu foam sample surfaces with different thicknesses at $T_H = 80$ ˚C for upper and contact surfaces for $\Theta = 10$, 20 and 30 minutes are shown in the Figures 4.41, 4.42 and 4.43.

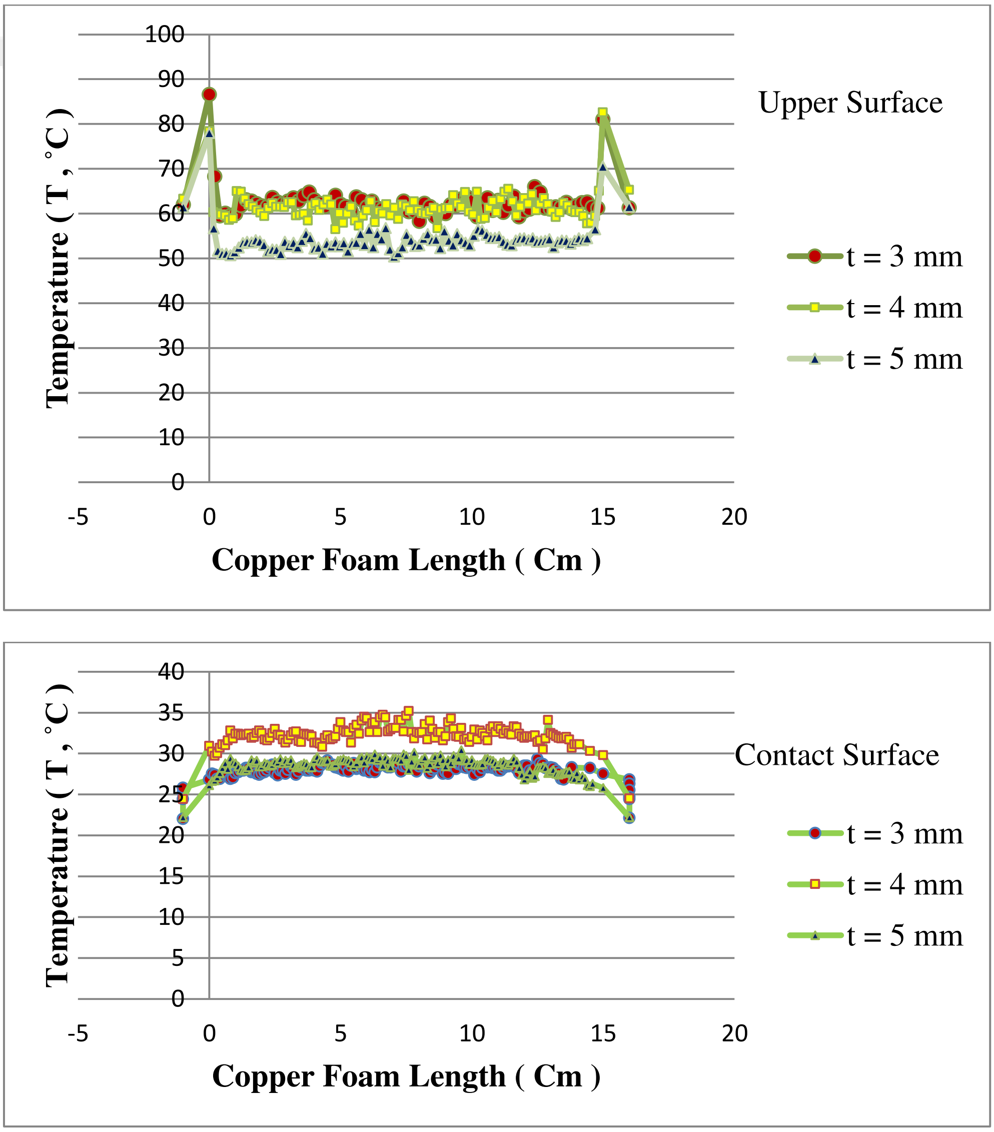

Figure 4.41 Variation of the temperature distributions along the upper and contact surfaces of the Cu foam samples as a function of t for $\Theta = 10$ min.

Effects of the thicknesses on temperature distributions along the Cu foam upper and contact surfaces can be seen which Cu foams were waited on heater surface at $T_H = 80$ ˚C for Θ = 10 minutes. It was seen from the Figure 4.41, Cu foam temperature distributions showed the different variations along the all surfaces. $T_{m,upper}$ for t = 3 mm, 4 mm and 5 mm Cu foams are 63.9 ˚C, 61.5˚C and 53.9 ˚C respectively.

Results showed that if thickness of the Cu foam increases, upper surface temperature of the Cu foam will decreases. From the figure, it was obvious that temperatures along the sample surface change from point to point because of pore shape, d_{p}, pore direction and also pore distributions. These situations showed the importance of the micro-structure of the Cu foams. Thermal profiles for t = 3 mm and 4 mm Cu foams showed similar results compared with that of 5 mm Cu foam. It was most important that edge temperatures of the Cu foams were higher and showed some variations for both surfaces are observed in detail in the next sections.

On the other hand, $T_{m, contact}$ for t = 3 mm, 4 mm and 5 mm Cu foams are 28 ˚C, 32.3 ˚C and 28.6 ˚C respectively. So thermal profiles for 3 mm and 5 mm thicknesses Cu foams showed near results compared with 4 mm Cu foam. From the upper and contact surface figures, contact surface temperatures were lower than the upper surface temperatures mean that heat was absorbed from the heater surface and send to the upper surface of the Cu foam samples rapidly, these results showed the thermal charateristics of the Cu foam materials which have high thermal conductivity properties.

Thermal conductivity analysis of the Cu foam samples are given in the next chapters.

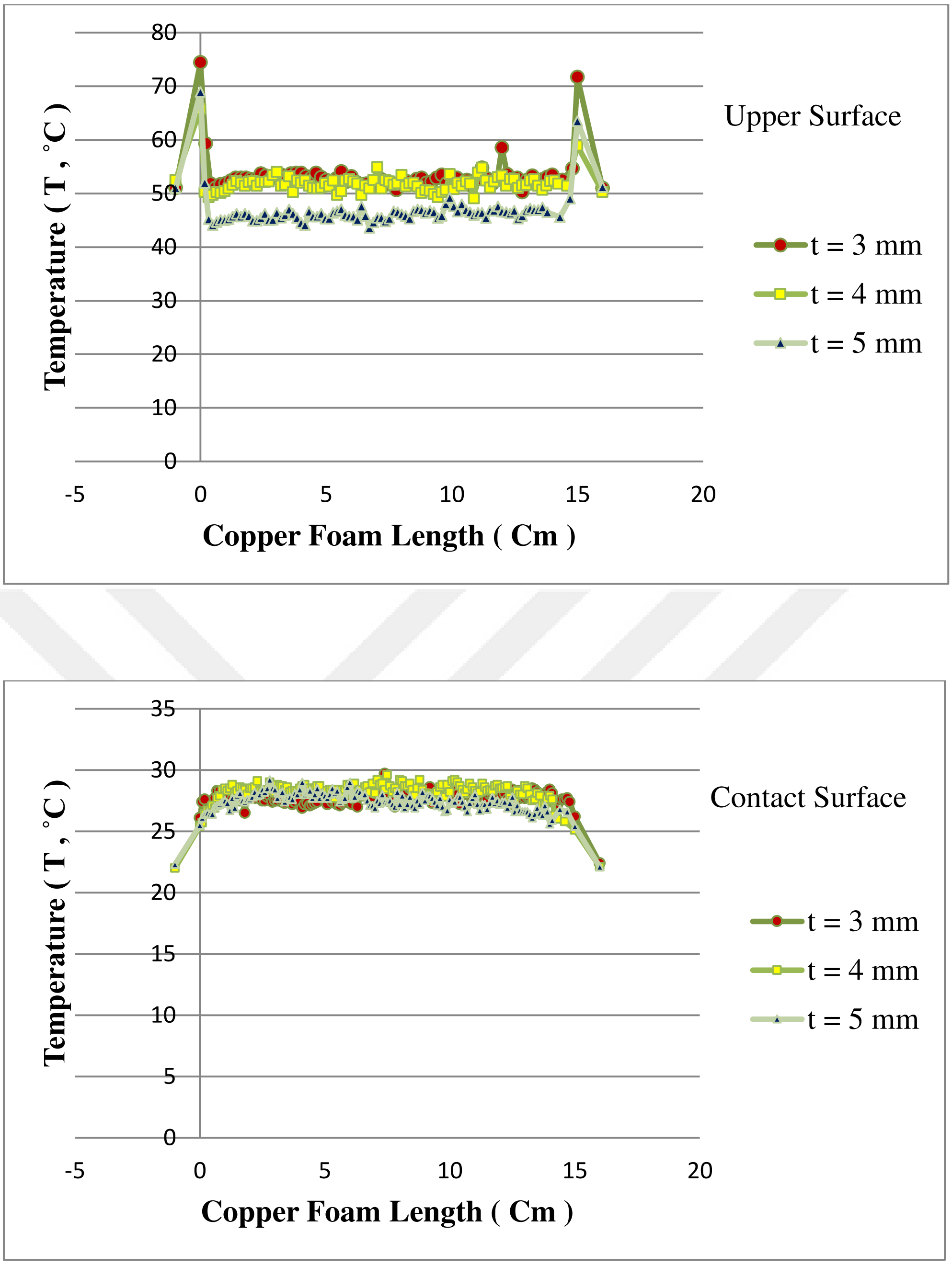

Figure 4.42 Variation of temperature distributions along the upper and contact surfaces of the Cu foam samples as a function of t for ϴ = 20 min.

Similarly, analysis results for Cu foams which were waited on heater surface at T_H = 80 ˚C for ϴ = 20 minutes showed some differences shown in the Figure 4.42. Such as, $T_{m,upper}$ for t = 3 mm, 4 mm and 5 mm Cu foams are 53.4 ˚C, 52.6 ˚C and 46.7 ˚C respectively. Thermal profiles for 3 mm and 4 mm Cu foams showed similar results compared with 5 mm Cu foam. $T_{m,\ contact}$ for t = 3 mm, 4 mm and 5 mm Cu foams are 27.6 ˚C, 28.2 ˚C and 27.3 ˚C respectively. From the thermal profiles, it was clear that Cu foams showed nearly similar results.

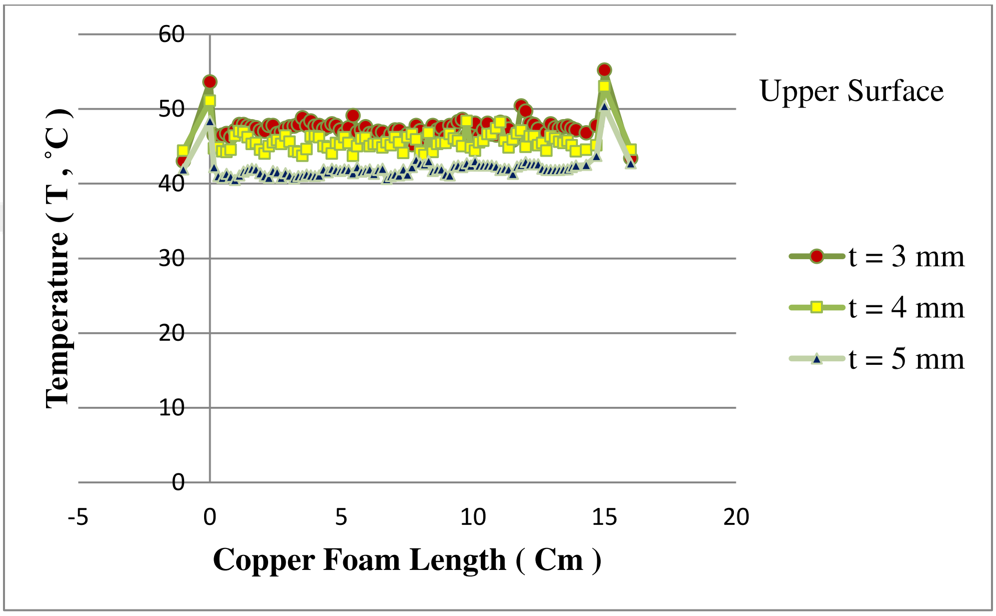

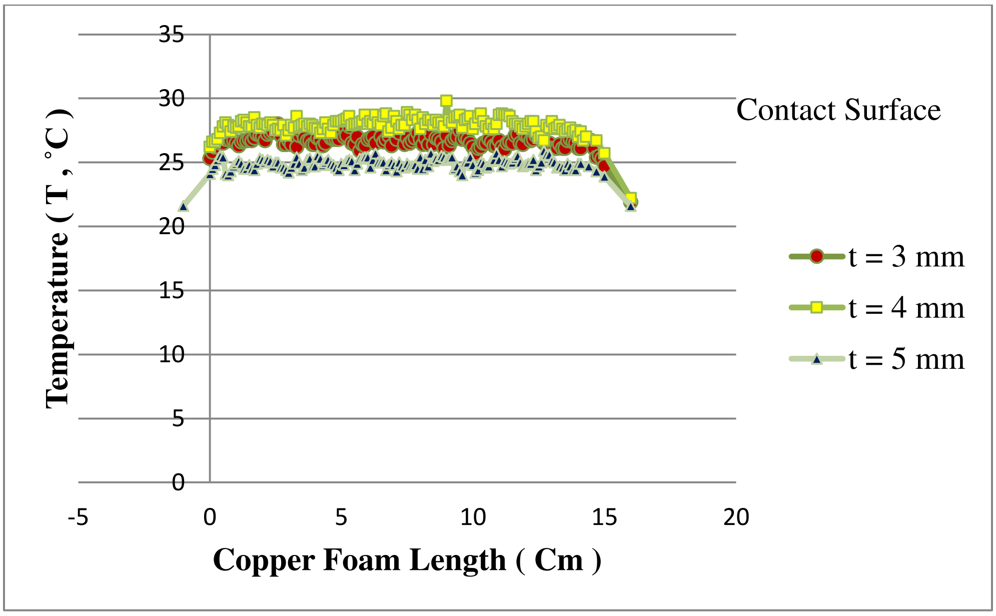

Figure 4.43 Variation of temperature distributions along the upper and contact surfaces of the Cu foam samples as a function of t for ϴ = 30 min.

Analysis results for Cu foams which were waited on heater surface at T_H = 80 ˚C for ϴ = 30 minutes showed some differences shown in the Figure 4.43. Such as, $T_{m,upper}$ for t = 3 mm, 4 mm and 5 mm Cu foams are 47.9 ˚C, 46.6 ˚C and 41.9 ˚C respectively. Thermal profiles for 3 mm and 4 mm Cu foams showed near results compared with 5 mm Cu foam. $T_{m, contact}$ for t = 3 mm, 4 mm and 5 mm Cu foams are 26.7 ˚C, 27.9˚C and 24.8 ˚C respectively. From the thermal profiles, it was clear that Cu foams showed near results. There was a little difference seen between the temperature profiles.

Comparison of the temperature distributions of the Cu foam sample surfaces with different thicknesses at T_H = 100 ˚C for upper and contact surfaces for ϴ = 10, 20 and 30 minutes are shown in the Figures 4.44, 4.45 and 4.46.

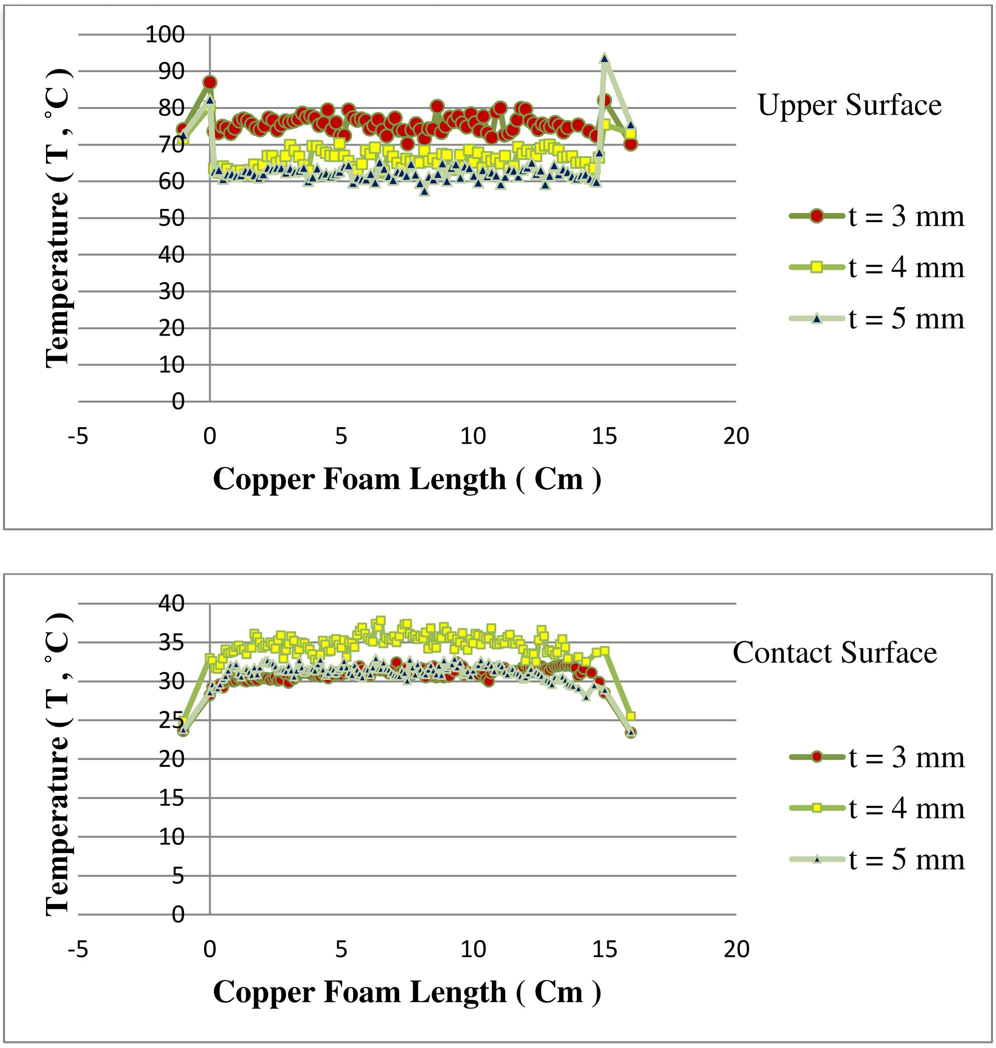

Figure 4.44 Variation of temperature distributions along the upper and contact surfaces of the Cu foam samples as a function of t for ϴ = 10 min.

Analysis results for Cu foams which were waited on heater surface at T_H = 100 ˚C for ϴ = 10 minutes showed some differences shown in the Figure 4.44. Such as, $T_{m,upper}$ for t = 3 mm, 4 mm and 5 mm Cu foams are 76 ˚C, 66.9 ˚C and 63.1 ˚C respectively. Thermal profiles for 4 mm and 5 mm Cu foams showed similar results compared with 3 mm Cu foam. $T_{m, contact}$ for t = 3 mm, 4 mm and 5 mm Cu foams are 30.8 ˚C, 34.6 ˚C and 31.1 ˚C respectively. From the thermal profiles, it was clear that 3 mm and 5 mm Cu foams showed similar results compared with 4 mm Cu foam.

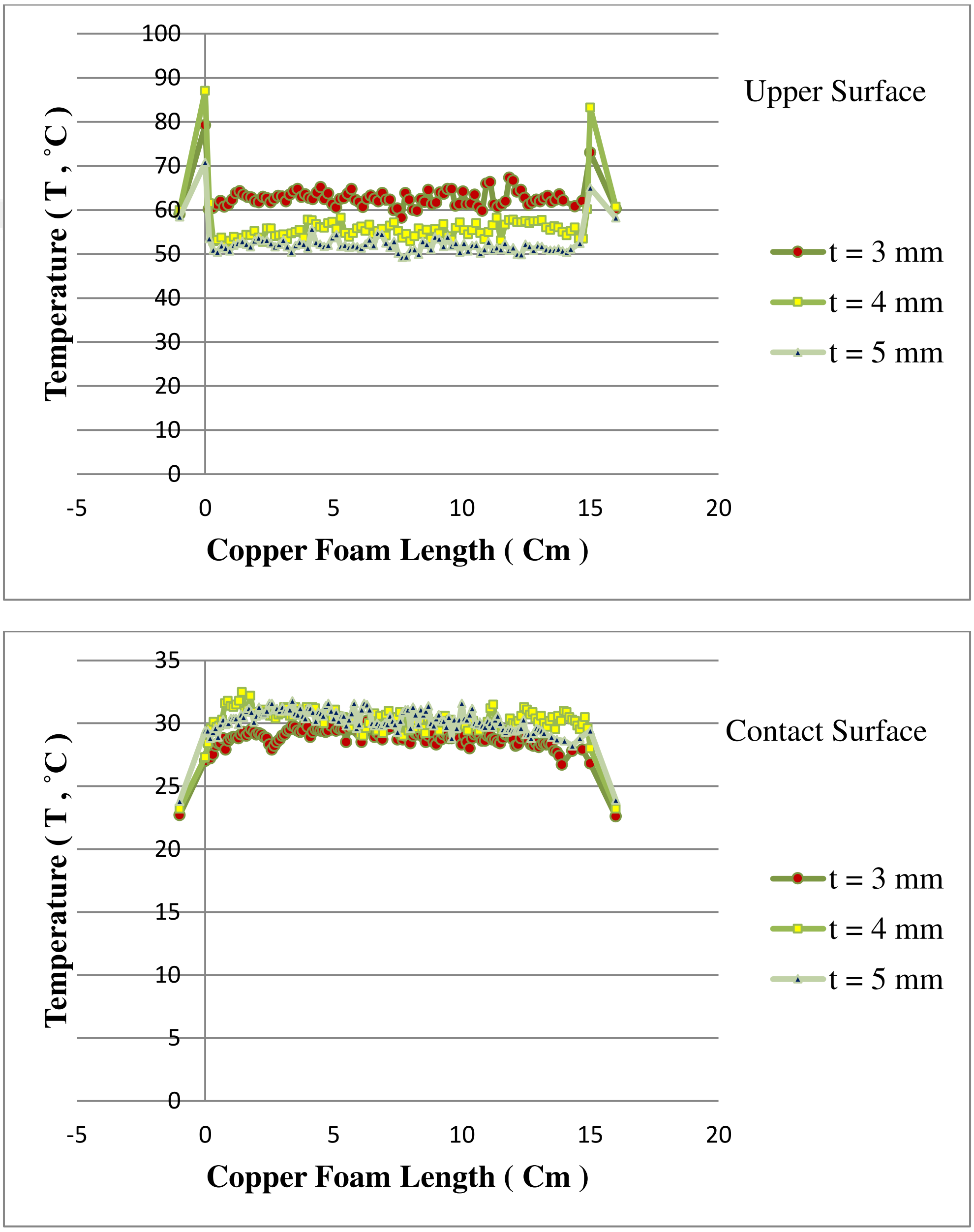

Figure 4.45 Variation of temperature distributions along the upper and contact surfaces of the Cu foam samples as a function of t for ϴ = 20 min.

Analysis results for Cu foams which were waited on heater surface at T_H = 100 ˚C for ϴ = 20 minutes showed some differences shown in the Figure 4.45 Such as, $T_{m,upper}$ for t = 3 mm, 4 mm and 5 mm Cu foams are 62.8 ˚C, 56.2 ˚C and 52.2 ˚C respectively. Thermal profiles for Cu foams showed that there were some temperature differences seen from the figure. $T_{m, contact}$ for t = 3 mm, 4 mm and 5 mm Cu foams are 28.7 ˚C, 30 ˚C and 30.1 ˚C respectively. From the thermal profiles, it was clear that 4 mm and 5 mm thicknesses Cu foams showed similar results compared with 3 mm thickness Cu foam.

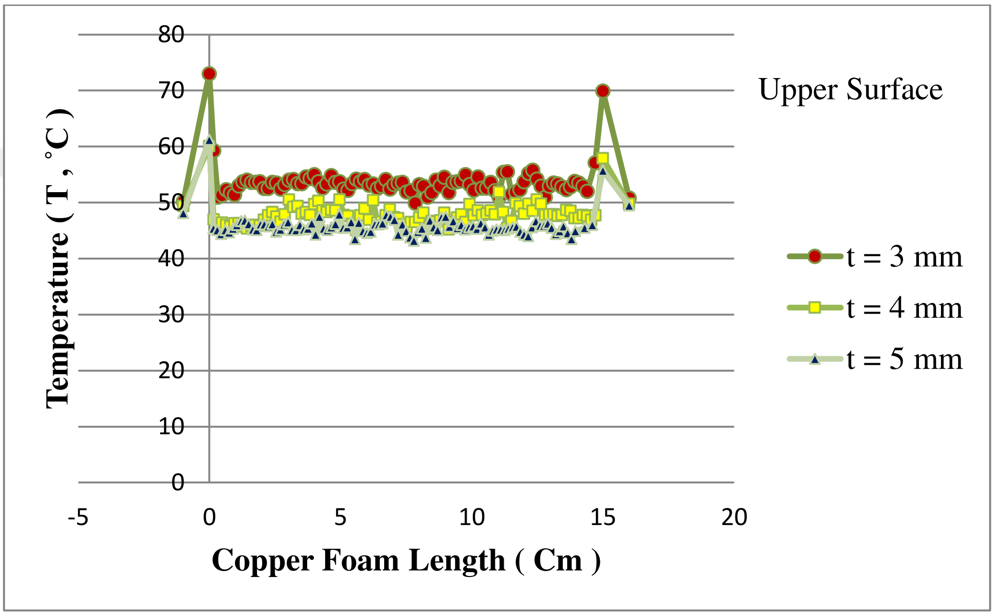

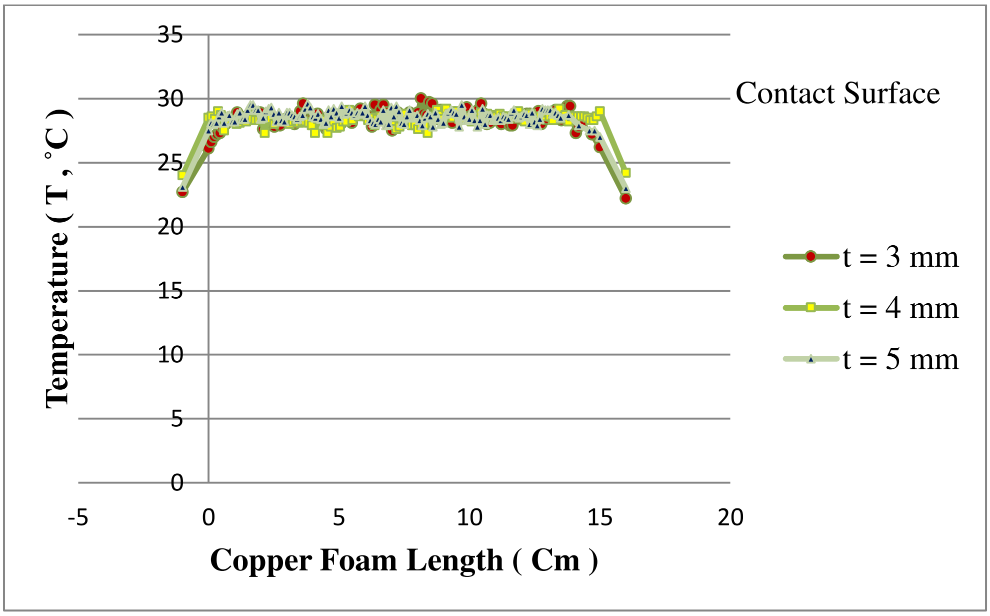

Figure 4.46 Variation of temperature distributions along the upper and contact surfaces of the Cu foam samples as a function of t for ϴ = 30 min.

Analysis results for Cu foams which were waited on heater surface at T_H = 100 ˚C for ϴ = 30 minutes showed some differences shown in the Figure 4.46. Such as, $T_{m,upper}$ for t = 3 mm, 4 mm and 5 mm Cu foams are 53.5˚C, 48.9 ˚C and 46.8 ˚C respectively. Thermal profiles for Cu foams showed some different results seen from the figure. $T_{m,contact}$ for t = 3 mm, 4 mm and 5 mm Cu foams are 28.3 ˚C, 28.2 ˚C and 28.5 ˚C respectively. From the thermal profiles, it was clear that Cu foams showed nearly same results.

As a result of the analyses, effects of the thicknesses on temperature distributions of the Cu foams along the upper and contact surfaces at different T_H and ϴ can be seen from the above figures. Experimental analysis results are summarized and listed as,

1. Cu foam temperature profiles showed the different variations along the upper and contact surfaces of the Cu foams for different T_H.
2. Cu foam upper and contact surface temperatures decrease depending on time periods changing from ϴ = 10 minutes to 30 minutes with respect to t and T_H. For example, $T_{m,upper}$ change between 34 ˚C ≤ $T_{m,upper}$ ≤ 45 ˚C for T_H = 50 ˚C, 40 ˚C ≤ $T_{m,upper}$ ≤ 64 ˚C for T_H = 80 ˚C and 46 ˚C ≤ $T_{m,upper}$ ≤ 76 ˚C for T_H = 100 ˚C. Similarly, $T_{m,contact}$ change between 24 ˚C ≤ $T_{m,contact}$ ≤ 28 ˚C for T_H = 50 ˚C, 24 ˚C ≤ $T_{m,contact}$ ≤ 28 ˚C for T_H = 80 ˚C and 28 ˚C ≤ $T_{m,contact}$ ≤ 35 ˚C for T_H = 100 ˚C.
3. If thickness of the Cu foam increases, upper surface temperature of the Cu foam sample decreases.
4. Cu foam temperatures along the surfaces change from point to point because of the pore shape, pore size, pore direction and also pore distributions, so investigation of the micro-structure of the Cu foams is important in order to know the thermal and physical characteristics of the Cu foam materials.
5. Cu foam upper surface edge temperatures are higher than the other surfaces and showed some variations according to the T_H, t and ϴ. For example, upper surface edge temperatures change between 40 ˚C ≤ T_{edge} ≤ 56 ˚C for T_H = 50 ˚C, 48 ˚C ≤ T_{edge} ≤ 87 ˚C for T_H = 80 ˚C and 55 ˚C ≤ T_{edge} ≤ 94 ˚C for T_H = 100 ˚C.

6. Similarly, contact surface edge temperatures change between 23 ˚C ≤ T_{edge} ≤ 27 ˚C for T_H = 50 ˚C, 24 ˚C ≤ T_{edge} ≤ 31 ˚C for T_H = 80 ˚C and 26 ˚C ≤ T_{edge} ≤ 34 ˚C for T_H = 100 ˚C. A detailed analyses and comparisons are given in the next sections.

7. Contact surface temperatures are lower than the upper surface temperatures means that heat is absorbed from the heater surface and send to upper surface of the samples rapidly, these results estimate the superior thermal charateristics of the Cu foam materials by means of high thermal conductivity and heat storage capacities and properties.

8. Cu foams contact surface temperatures are higher at high T_H.

9. Cu foams contact surface temperatures comparisons showed the various effects of the thicknesses. For T_H = 80 ˚C, 4 mm Cu foam showed the higher contact surface temperatures compared with other thicknesses of samples for all the time periods. On the other side, 3 mm Cu foam has higher contact surface temperatures than 5 mm Cu foam for Θ = 20 and 30 minutes time periods. For T_H = 100 ˚C, generally 4 mm and 5 mm Cu foams showed the higher temperatures than 3 mm Cu foam. For T_H = 50 ˚C, 3 mm and 4 mm thiknesses of Cu foams showed the higher temperatures compared with 5 mm Cu foam.

4.4 Effects of Time on Thermal Profiles of The Copper Foil & Copper Foil with Holes Reference Items

In this section, time dependent thermal analysis results of the t = 0.4 mm Cu foil with and without holes for upper surfaces at different T_H are analyzed in detail. Mean temperature difference between upper and contact surface of the Cu foil reference sample, ΔT_{foil} is given in equation 4.3.

$$\Delta T_{foil} = T_{m,upper} - T_{m,contact} \quad (4.3)$$

Where, $T_{m,\ upper}$ is the upper surface mean temperature of Cu foil reference sample (˚C) and $T_{m,contact}$ is the contact surface mean temperature of the Cu foil reference sample (˚C).

Similarly, mean temperature difference between upper and contact surfaces of the Cu foil reference sample with holes, $\Delta T_{foil,hole}$ is given in equation 4.4.

$$\Delta T_{foil,hole} = T_{m,upper} - T_{m,contact} \quad (4.4)$$

Where, $T_{m,upper}$ is the upper surface mean temperature of Cu foil reference sample with holes (˚C) and $T_{m,contact}$ is the contact surface mean temperature of the Cu foil reference sample with holes (˚C).

Thermal analysis results along the t = 0.4 mm Cu foil reference sample with and without holes upper surface at T_H = 50 ˚C for ϴ = 10, 20 and 30 minutes are given in the Figures 4.47, 4.48 and 4.49.

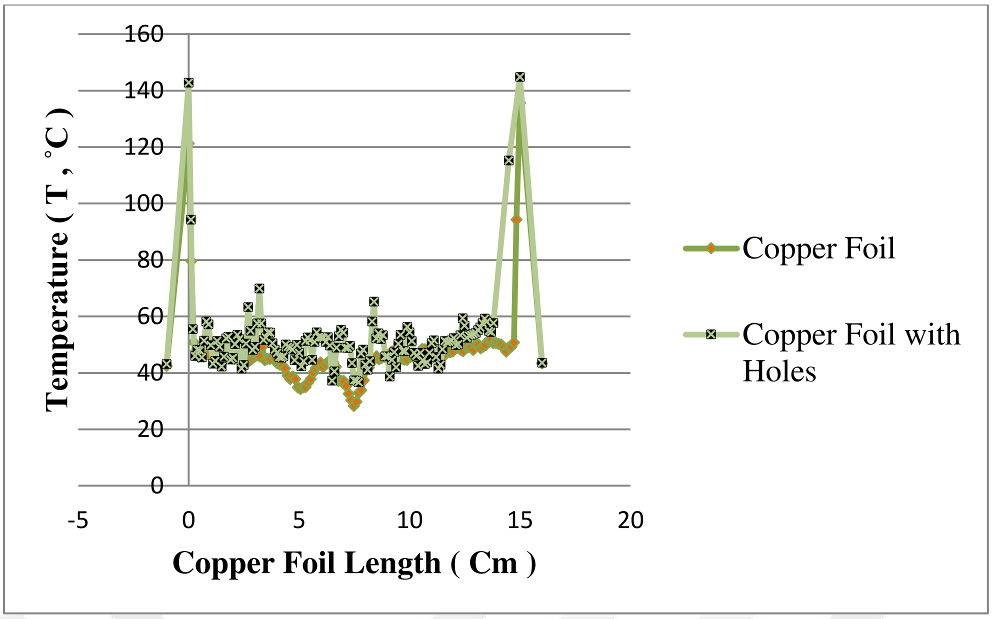

Figure 4.47 Temperature distributions of the Cu foils upper surfaces for Θ = 10 min

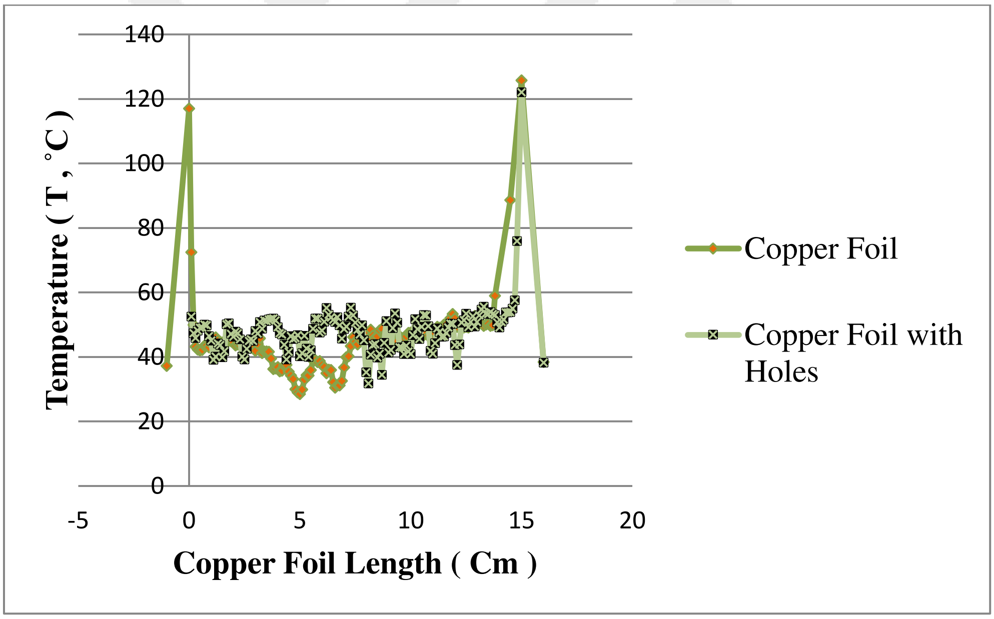

Figure 4.48 Temperature distributions of the Cu foils upper surfaces for Θ = 20 min

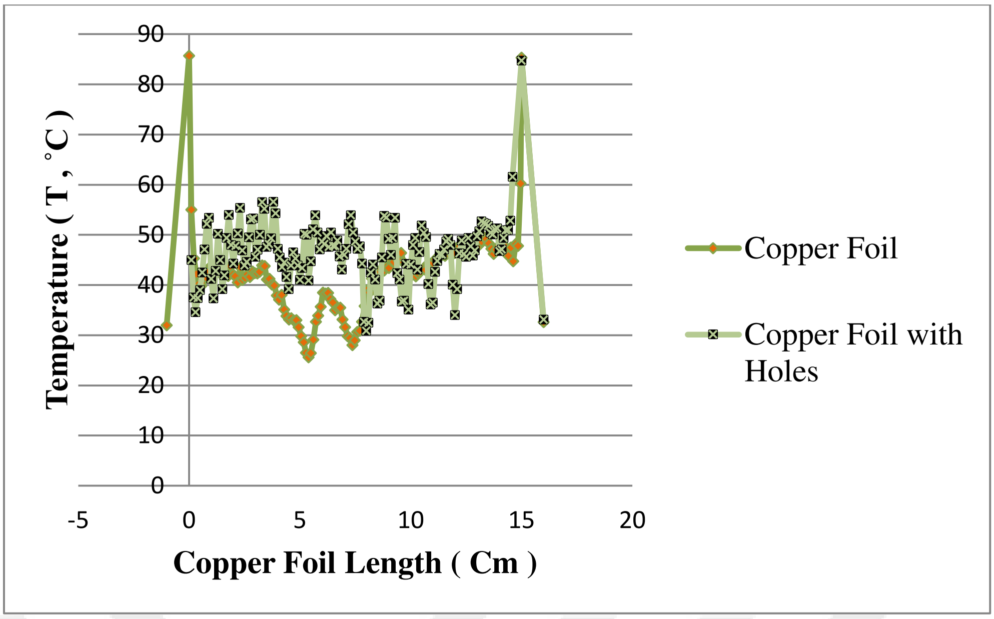

Figure 4.49 Temperature distributions of the Cu foils upper surfaces for ϴ = 30 min

Analysis results from the Figures 4.47, 4.48 and 4.49 showed that T_H, after ϴ = 10, 20 and 30 minutes are 45.1 ˚C, 39.5 ˚C and 35.1 ˚C respectively.

For ϴ = 10 minutes, Cu foil edge temperatures, T_{edge}, are 121.3 ˚C and 135.7 ˚C. For ϴ = 20 minutes, 117 ˚C and 125.7 ˚C. For ϴ = 30 minutes, 85.7 ˚C and 85.3 ˚C.

For ϴ = 10 minutes, T_{edge} of the Cu foil with holes are 142.8 ˚C and 144.8 ˚C. For ϴ = 20 minutes, 117.5 ˚C and 122.1 ˚C and for ϴ = 30 minutes, 83 ˚C and 84.7 ˚C.

Temperature differences between upper and contact surfaces of the Cu foil, ΔT_{foil}, are (46.8 – 37.5) 9.3 ˚C for ϴ = 10 minutes heating process, (45 – 35.2) 9.8 ˚C for ϴ = 20 minutes heating process and (43.5 – 29.6) 13.9 ˚C for ϴ = 30 minutes heating process.

Temperature differences between upper and contact surfaces of the Cu foil with holes, $\Delta T_{foil,hole}$, are (50.6 – 35.6) 15 ˚C for ϴ = 10 minutes heating process, (50 – 34.3) 15.7 ˚C for ϴ = 20 minutes heating process and (47.2 – 28.4) 18.8 ˚C for ϴ = 30 minutes heating process.

From thermal analysis results, temperature distributions were more stable for Cu foil which compared with Cu foil with holes and depend on the ϴ, irregular temperature variations are seen.

Thermal analysis results along the t = 0.4 mm Cu foil with and without holes upper surface at T_H = 80 ˚C for Θ = 10, 20 and 30 minutes are given in the Figures 4.50, 4.51 and 4.52.

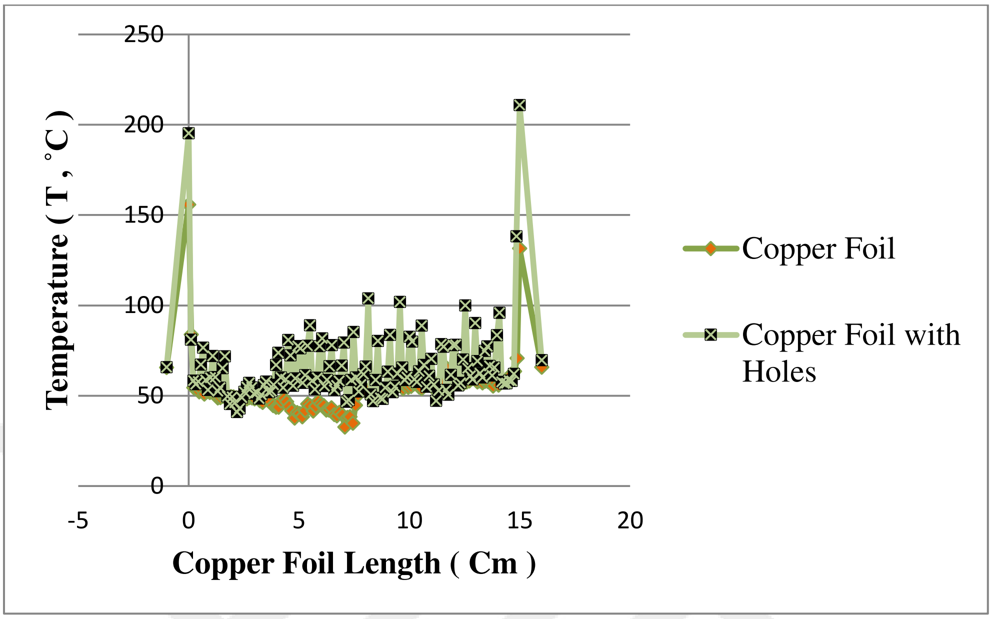

Figure 4.50 Temperature distributions of the Cu foils upper surfaces for Θ = 10 min

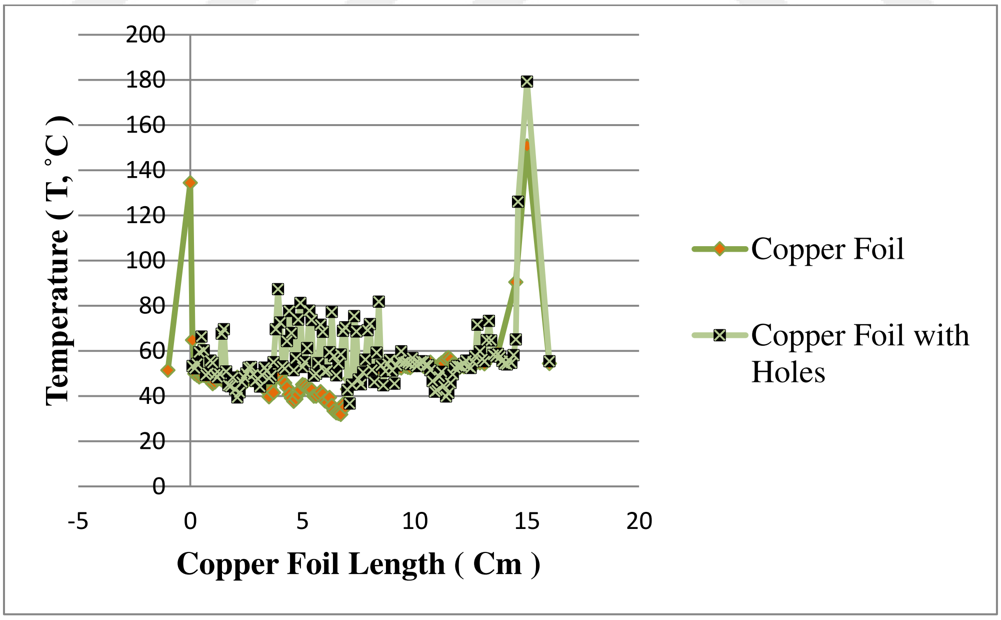

Figure 4.51 Temperature distributions of the Cu foils upper surfaces for Θ = 20 min

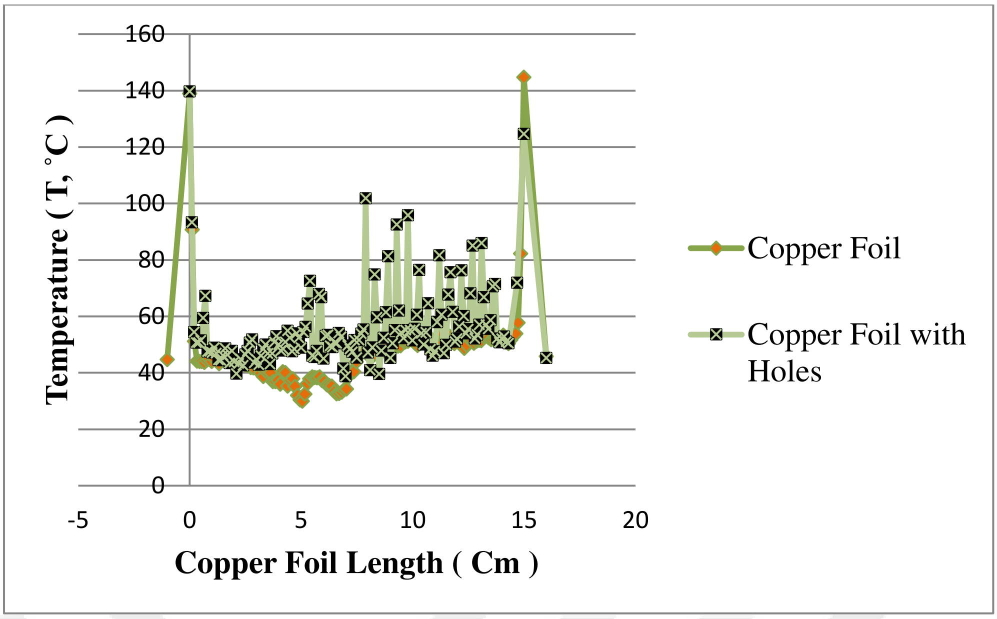

Figure 4.52 Temperature distributions of the Cu foils upper surfaces for ϴ = 30 min

Analysis results from the Figures 4.50, 4.51 and 4.52 showed that T_H after ϴ = 10, 20 and 30 minutes are 72 ˚C, 58.1 ˚C and 48.2 ˚C respectively. Reasons of the decrease in temperature were Q_{cond} between the heater surface and Cu foils, Q_{conv} between the heater surface and surrounding medium. It was seen from the figures that temperature distributions were generally same, but some irregularities can be seen because of the foil surface structures. It was important to note that, Cu foil edge temperatures are higher than the other surfaces. This implies that, Cu foils take heat from the heater surface and spreads to all edges.

For ϴ = 10 minutes, T_{edge} of Cu foil are 155.8 ˚C and 131.4 ˚C. For ϴ = 20 minutes, 134.5 ˚C and 150.7 ˚C and for ϴ = 30 minutes, 138.9 ˚C and 144.7 ˚C. Similarly,

For ϴ = 10 minutes, T_{edge} of Cu foil with holes are 195.2 ˚C and 210.9 ˚C. For ϴ = 20 minutes, 174.5 ˚C and 179.2 ˚C and for ϴ = 30 minutes, 139.7 ˚C and 124.7 ˚C.

It is seen from the figures, Cu foils upper surface temperature range decrease from ϴ = 10 to 30 minutes time periods. Because, Q_{cond} between the heater surface and Cu foil plate which decrease depends on ϴ. The other effects are heat losses from heater surface and Cu foils to surrounding medium by means of heat convection. Temperature profiles showed near results. This situation showed the effect of the time on heat transfer. From the figures, T_H decrease rapidly before and after Cu foils limits. (Points just before 0 cm and just after 15 cm of Cu foil length) which implies the effects of emissivity of the heater surface which taken 0.95, heat losses from heater surfaces to surrounding medium by means of convection heat transfer and T_{edge} of copper foil which take heat from other surfaces which changing with time and also surrounding conditions.

Similarly, ΔT_{foil} are (58.7 – 32.3) 26.4 ˚C for ϴ = 10 minutes heating process, (53.5 – 34.3) 19.2 ˚C for ϴ = 20 minutes heating process and (48.4 – 33.2) 15.2 ˚C for ϴ = 30 minutes heating process. $\Delta T_{foil,hole}$ are (62.8 – 30.7) 32.1 ˚C for ϴ = 10 minutes heating process, (56.9 – 32.1) 24.8 ˚C for ϴ = 20 minutes heating process and (52.4 – 30.7) 21.7 ˚C for ϴ = 30 minutes heating process.

Thermal analysis results along the t = 0.4 mm Cu foil with and without holes upper surface at T_H = 100 ˚C for ϴ = 10, 20 and 30 minutes are given in the Figures 4.53, 4.54 and 4.55.

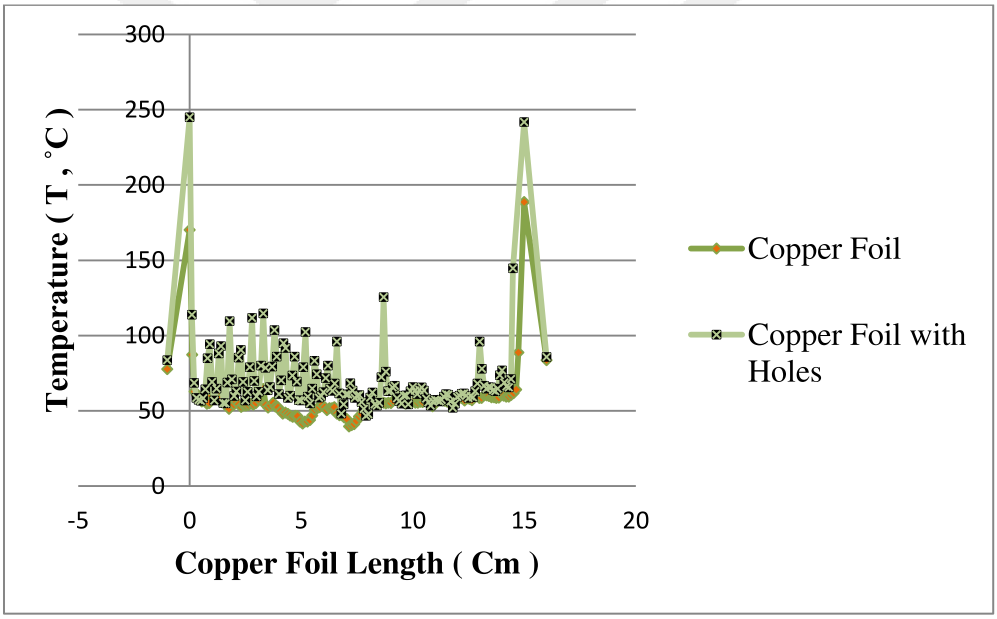

Figure 4.53 Temperature distributions of the Cu foils upper surfaces for ϴ = 10 min

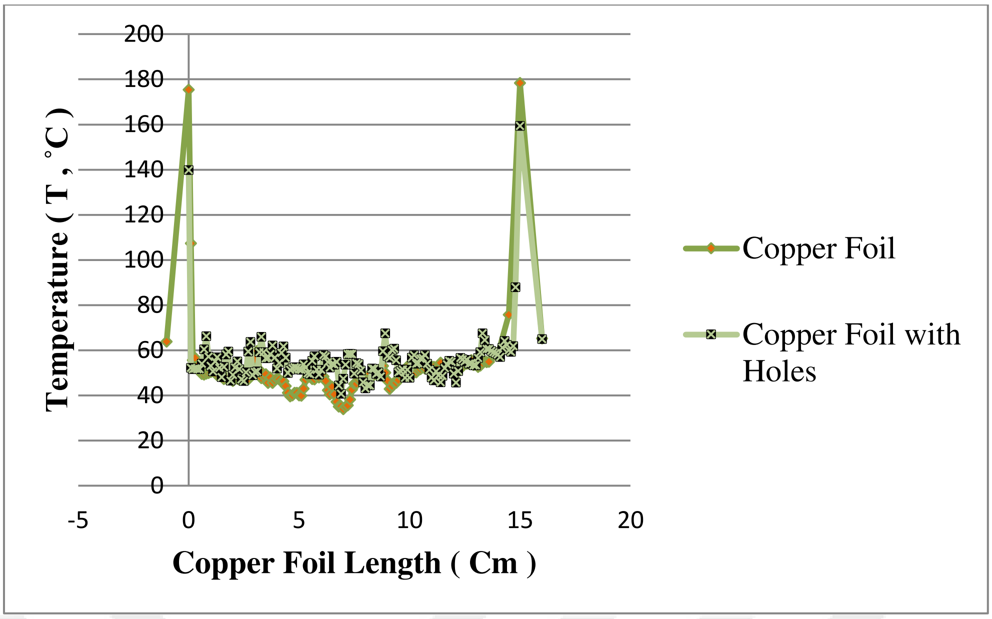

Figure 4.54 Temperature distributions of the Cu foils upper surfaces for ϴ = 20 min

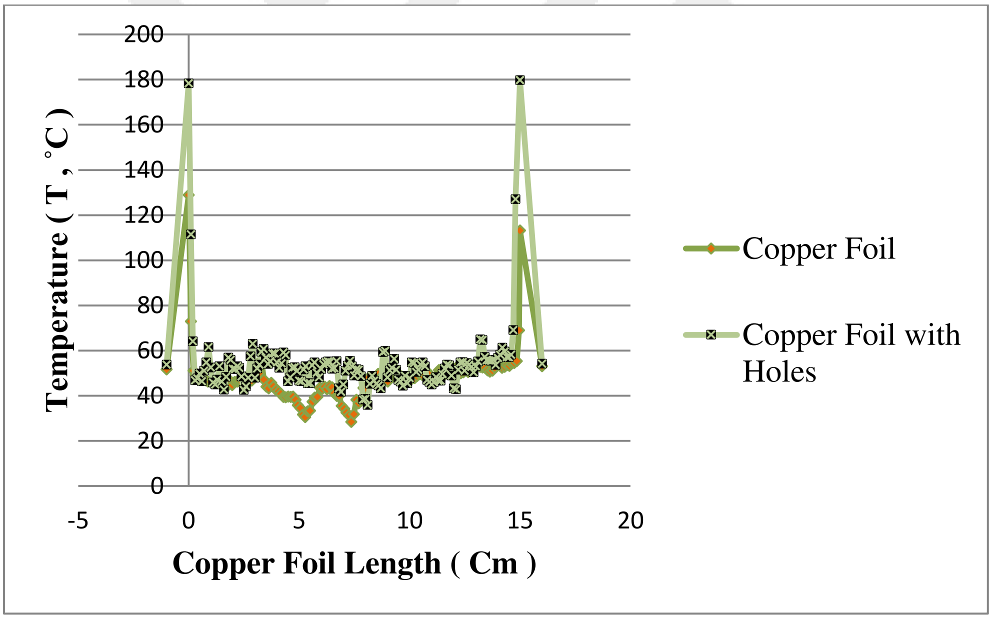

Figure 4.55 Temperature distributions of the Cu foils upper surfaces for ϴ = 30 min

Analysis results from the Figures 4.53, 4.54 and 4.55 showed that T_H after ϴ = 10, 20 and 30 minutes are 91.7 ˚C, 71.7 ˚C and 57 ˚C respectively. Similarly,

For ϴ = 10 minutes, T_{edge} of the Cu foil are 170.1 ˚C and 188.6 ˚C. For ϴ = 20 minutes, 175.4 ˚C and 178.3 ˚C and for ϴ = 30 minutes, 128.9 ˚C and 113.2 ˚C.

For ϴ = 10 minutes, T_{edge} of the Cu foil with holes are 254 ˚C and 241.8 ˚C. For ϴ = 20 minutes, 139.8 ˚C and 159.3 ˚C and for ϴ = 30 minutes, 178.3 ˚C and 179.8 ˚C.

ΔT_{foil} are (63.3 – 34) 29.3 ˚C for ϴ = 10 minutes heating process, (52.4 – 31.6) 20.8 ˚C for ϴ = 20 minutes heating process and (49.3 – 35.9) 13.4 ˚C for ϴ = 30 minutes heating process. $\Delta T_{foil,hole}$ are (65.4 – 31.5) 33.9 ˚C for ϴ = 10 minutes heating process, (59 – 30.5) 28.5 ˚C for ϴ = 20 minutes heating process and (56.6 – 32.1) 24.5 ˚C for ϴ = 30 minutes heating process.

As a result of the analyses, time dependent thermal analysis results of the 0.4 mm thickneses of Cu foil with and without holes for upper surfaces at different T_H can be seen from the above figures, experimental analysis results are summarized and listed as follows;

1. Heater surface and Cu foils upper surface temperatures decreases with increasing ϴ.

2. Temperature distributions along the foil surface are generally uniform, but some irregularities can be seen because of the Cu foil surface structures.

3. Cu foil reference item sample upper and contact surface temperatures decrease with increasing ϴ at different t and T_H values. For example, $T_{m,upper}$ change between 43 ˚C ≤ $T_{m,upper}$ ≤ 47 ˚C for T_H = 50 ˚C, 48 ˚C ≤ $T_{m,upper}$ ≤ 59 ˚C for T_H = 80 ˚C and 49 ˚C ≤ $T_{m,upper}$ ≤ 64 ˚C for T_H = 100 ˚C. Similarly, $T_{m,contact}$ change between 29 ˚C ≤ $T_{m,contact}$ ≤ 38 ˚C for T_H = 50 ˚C, 32 ˚C ≤ $T_{m,contact}$ ≤ 34.5 ˚C for T_H = 80 ˚C and 31 ˚C ≤ $T_{m,contact}$ ≤ 36 ˚C for T_H = 100 ˚C.

4. Cu foil reference item sample with holes upper and contact surface temperatures decrease with increasing ϴ at different t and T_H values. For example, $T_{m,upper}$ change between 47 ˚C ≤ $T_{m,upper}$ ≤ 51 ˚C for T_H = 50 ˚C, 52 ˚C ≤ $T_{m,upper}$ ≤ 63 ˚C for T_H = 80 ˚C and 56 ˚C ≤ $T_{m,upper}$ ≤ 66 ˚C for T_H = 100 ˚C. Similarly, $T_{m,contact}$ change between 28 ˚C ≤ $T_{m,contact}$ ≤ 36 ˚C for T_H = 50 ˚C, 30 ˚C ≤ $T_{m,contact}$ ≤ 32.5 ˚C for T_H = 80 ˚C and 30 ˚C ≤ $T_{m,contact}$ ≤ 32.5 ˚C for T_H = 100 ˚C.

5. It is important to note that, Cu foil with holes upper surface edge temperatures are higher than the Cu foil edge temperatures. For example, upper surface edge temperatures of the Cu foil change between 85 ˚C $\leq T_{edge} \leq$ 135 ˚C for T_H = 50 ˚C, 130 ˚C $\leq T_{edge} \leq$ 156 ˚C for T_H = 80 ˚C and 113 ˚C $\leq T_{edge} \leq$ 189 ˚C for T_H = 100 ˚C. Similarly, upper surface edge temperatures of the Cu foil with holes change between 82 ˚C $\leq T_{edge} \leq$ 145 ˚C for T_H = 50 ˚C, 125 ˚C $\leq T_{edge} \leq$ 210 ˚C for T_H = 80 ˚C and 140 ˚C $\leq T_{edge} \leq$ 245 ˚C for T_H = 100 ˚C.

6. Cu foil contact surface edge temperatures are higher than the Cu foil edge temperatures. For example, contact surface edge temperatures of the Cu foil change between 30 ˚C $\leq T_{edge} \leq$ 40 ˚C for T_H = 50 ˚C, 31 ˚C $\leq T_{edge} \leq$ 40 ˚C for T_H = 80 ˚C and 33 ˚C $\leq T_{edge} \leq$ 42 ˚C for T_H = 100 ˚C. Similarly, contact surface edge temperatures of the Cu foil with holes change between 28 ˚C $\leq T_{edge} \leq$ 38 ˚C for T_H = 50 ˚C, 29 ˚C $\leq T_{edge} \leq$ 37 ˚C for T_H = 80 ˚C and 30 ˚C $\leq T_{edge} \leq$ 45 ˚C for T_H = 100 ˚C.

7. Generally, temperature distributions showed similar profiles at low T_H. But in some cases, temperature distributions showed some irregularities dependinh on ϴ.

4.5 Time Dependent Variation of (T_{edge} / T_H) and (ΔT_{edge} / T_H) For Tested Copper Foam Samples and Copper Foil Reference Items

Cu foam and Cu foil thermal analysis results showed that the T_{edge} of the samples had different values for upper and contact surfaces compared with different t, T_H and ϴ.

Figures 4.56 through 4.60 showed the time dependent variations of T_{edge} of the Cu foams and foils with respect to T_H for different sample thicknesses and first and last surface points.

Similarly, Figures 4.61 through 4.64 showed the time dependent variations of Cu foams and foils upper and contact surface edge temperature differences, ΔT_{edge} , with respect to T_H like for different sample thicknesses and first and last surface points is given in equation 4.5.

$$\Delta T_{edge} = T_{edge,upper} - T_{edge,contact} \tag{4.5}$$

Where, $T_{edge,upper}$ is the upper surface edge temperature of the Cu foam / foil samples (˚C) and $T_{edge,contact}$ is the contact surface edge temperature of the Cu foam / foil samples (˚C).

4.5.1 Time Dependent Variation of The (T_{edge} / T_H) For Copper Foam Samples and Copper Foil Reference Items

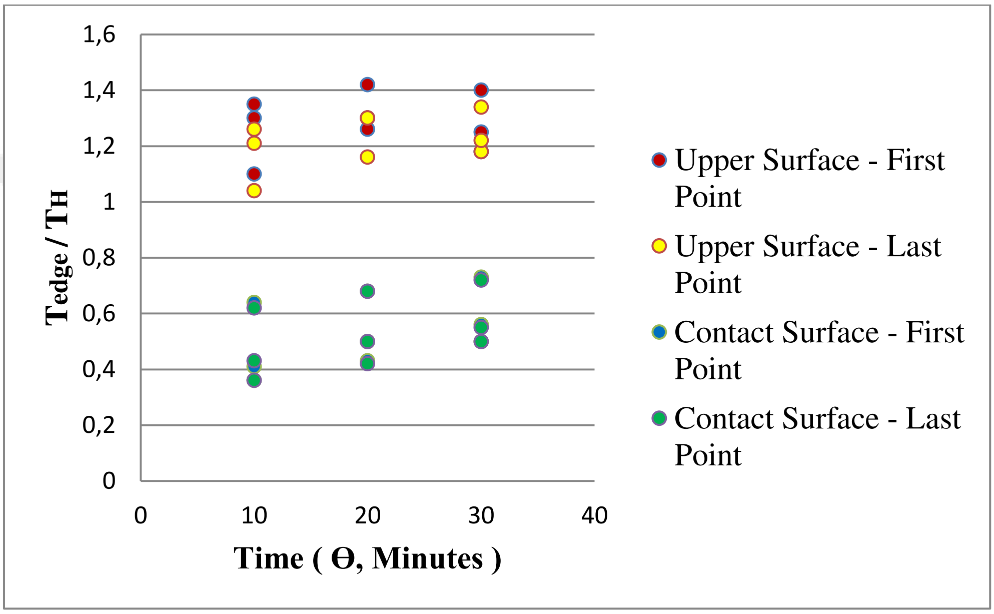

Figure 4.56 Time dependent variations of the (T_{edge} / T_H) for t = 3 mm Cu foam upper and contact surface points

From the Figure 4.56, it is seen that for upper surface, range of the T_{edge}/ T_H decrease depending on the increasing Ɵ. For example, T_{edge}/ T_H change between (1 – 1,4) for Ɵ = 10 min, (1,1 – 1,4) for Ɵ = 20 min. and (1,2 – 1,4) for Ɵ = 30 min. Generally, the upper surface first points values higher than the last points values. These situations showed the effects of the porosity which changing along the Cu foam surface and edges.

For contact surface points, rates of T_{edge}/ T_H increase depending on the increasing Ɵ. Such as, change between (0,38 – 0,62) for Ɵ = 10 min, (0,42 – 0,7) for Ɵ = 20 min. and (0,5 – 0,73) for Ɵ = 30 min.

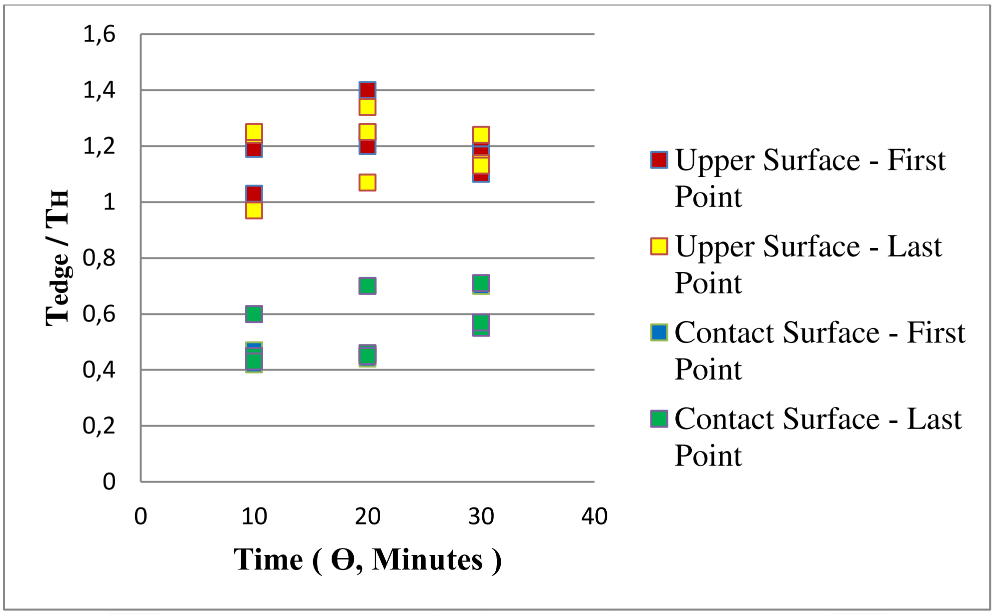

Figure 4.57 Time dependent variations of the (T_{edge} / T_H) for t = 4 mm Cu foam upper and contact surface points

From the Figure 4.57, it is seen that for upper surface, rate of the T_{edge}/ T_H increase depending on the increasing Θ, for 10 min. and 20 min. For example, T_{edge}/ T_H change between (0,98 – 1,25) for Θ = 10 min, (1,05 – 1,4) for Θ = 20 min. and decrease (1,1 – 1,23) for Θ = 30 min.

For contact surface points, rates of T_{edge}/ T_H increase depending on the increasing Θ. Such as, change between (0,42 – 0,6) for Θ = 10 min, (0,43 – 0,7) for Θ = 20 min. and (0,58 – 0,72) for Θ = 30 min.

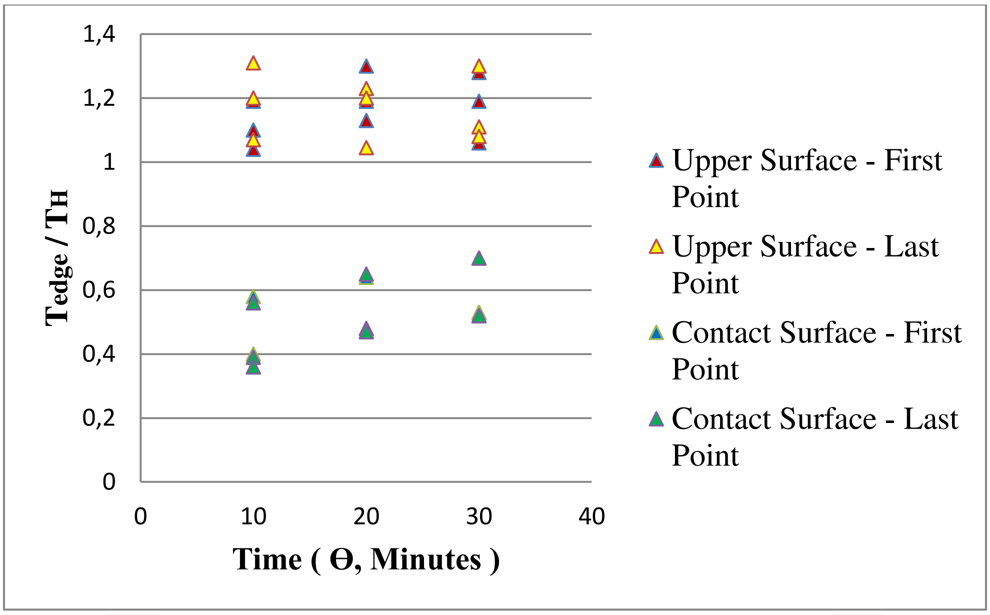

Figure 4.58 Time dependent variations of the (T_{edge} / T_H) for t = 5 mm Cu foam upper and contact surface points

From the Figure 4.58, it is seen that for upper surface, rate of the T_{edge}/ T_H nearly same depending on the increasing Θ. For example, T_{edge}/ T_H change between (1,02 – 1,32) for Θ = 10 min, (1,05 – 1,3) for Θ = 20 min. and (1,08 – 1,3) for Θ = 30 min.

For contact surface points, rates of T_{edge}/ T_H increase depending on the increasing Θ. Such as, change between (0,36 – 0,58) for Θ = 10 min, (0,45 – 0,65) for Θ = 20 min. and (0,55 – 0,72) for Θ = 30 min.

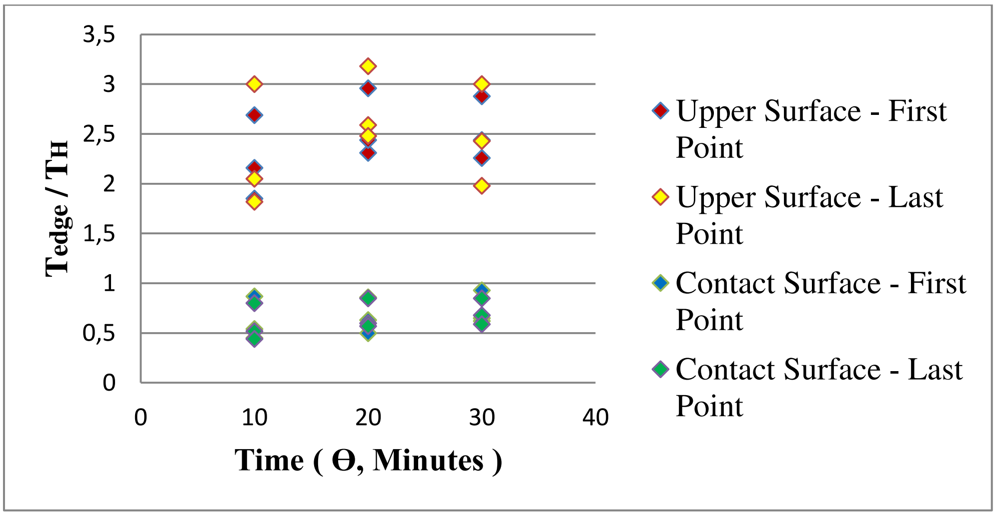

Figure 4.59 Time dependent variations of the (T_{edge} / T_H) for t = 0.4 mm Cu foil upper and contact surface points

From the Figure 4.59, it is seen that for upper surface, rate of the T_{edge}/ T_H increase depending on the increasing ϴ, for 10 min and 20 min. For example, T_{edge}/ T_H change between (1,7 – 3) for ϴ = 10 min, (2,25 – 3,2) for ϴ = 20 min. but decrease (2 – 3) at ϴ = 30 min.

For contact surface points, rates of T_{edge}/ T_H increase depending on the increasing ϴ. Such as, change between (0,4 – 0,8) for ϴ = 10 min, (0,5 – 0,8) for ϴ = 20 min. and (0,52 – 0,9) for ϴ = 30 min. If comparison made with respect to values, generally last points values are higher than the first points values for all the time periods.

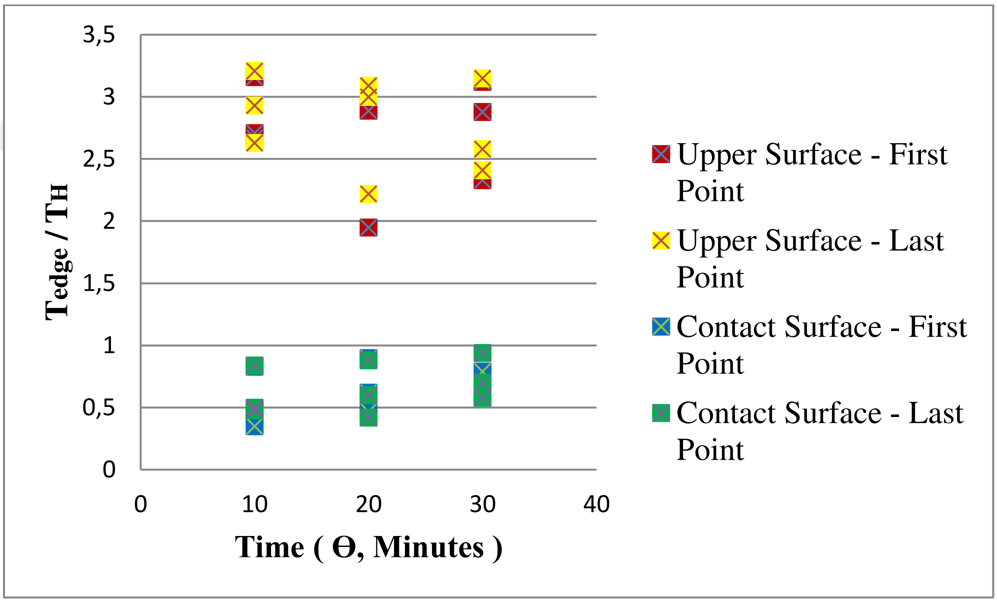

Figure 4.60 Time dependent variations of the (T_{edge} / T_H) for t = 0.4 mm Cu foil with holes upper and contact surface points

From the figure 4.60, it is seen that for upper surface, rate of the T_{edge}/ T_H decrease depending on the increasing ϴ, between 10 min and 20 min. For example, T_{edge}/ T_H change between (2,6 – 3,2) for ϴ = 10 min, (2 – 3,1) for ϴ = 20 min. but increase (2,3 – 3,2) at ϴ = 30 min.

For contact surface points, rates of T_{edge}/ T_H increase depending on the increasing ϴ. Such as, change between (0,35 – 0,8) for ϴ = 10 min, (0,4 – 0,85) for ϴ = 20 min. and (0,6 – 0,9) for ϴ = 30 min. Generally, last points show higher values compared with first points depending on ϴ.

4.5.2 Time Dependent Variation of The (ΔT_{edge} / T_H) For Copper Foam Samples and Copper Foil Reference Items

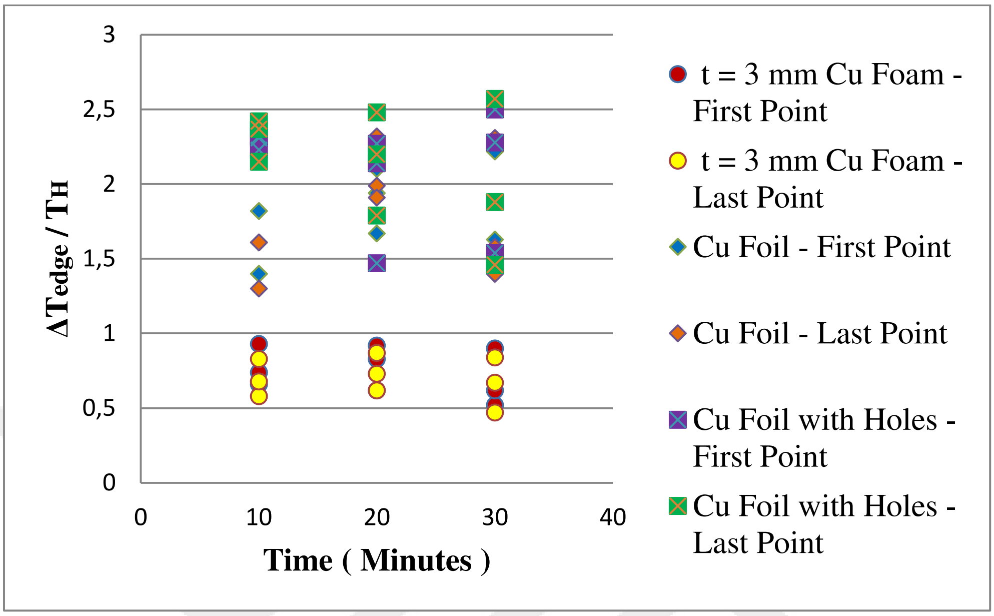

Figure 4.61 Time dependent variations of the (ΔT_{edge} / T_H) for t = 3 mm Cu foam sample and t = 0.4 mm Cu foils reference items surface points

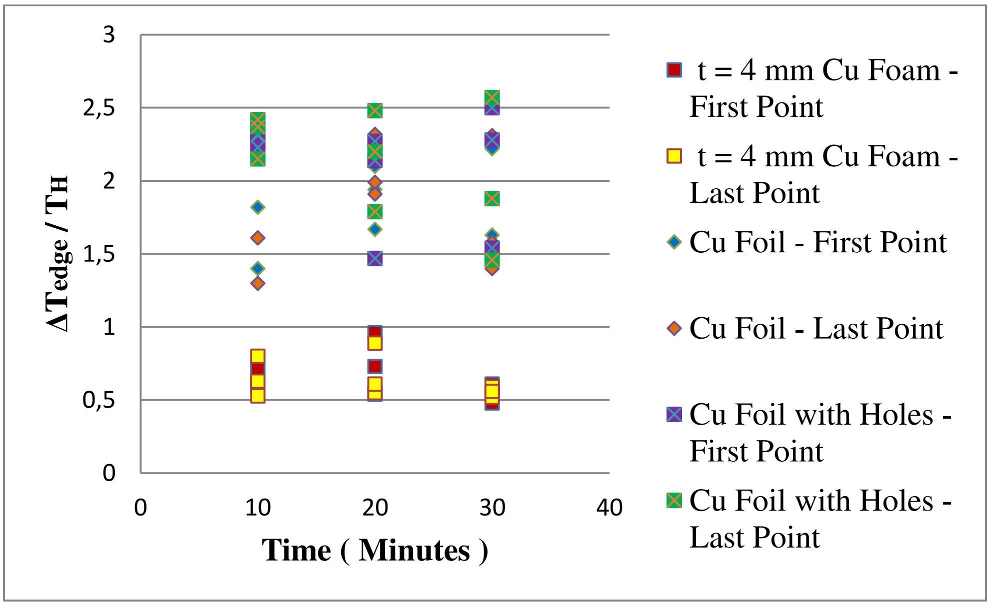

Figure 4.62 Time dependent variations of the (ΔT_{edge} / T_H) for t = 4 mm Cu foam sample and t = 0.4 mm Cu foils reference items surface points

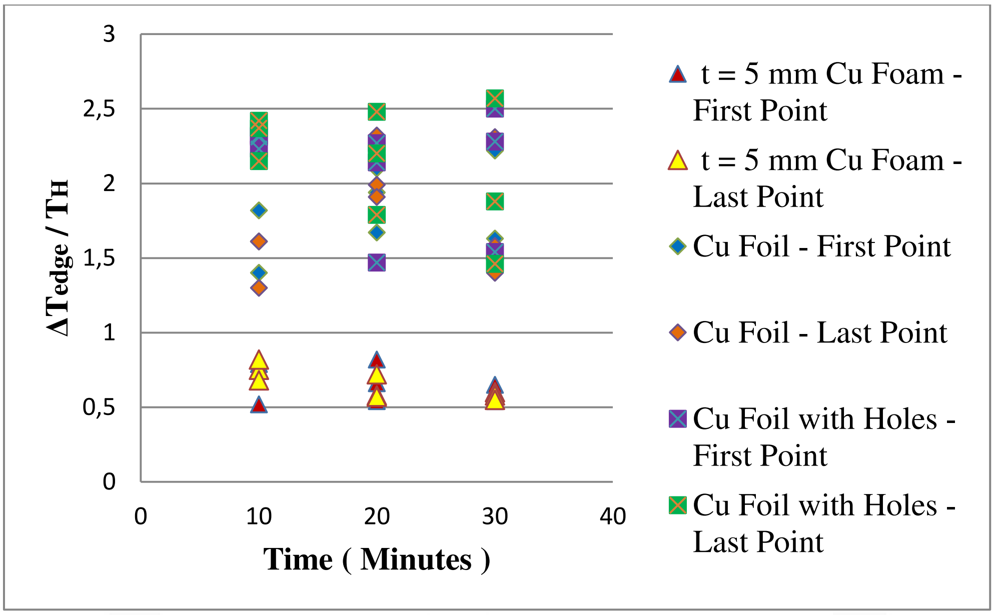

Figure 4.63 Time dependent variations of the (ΔT_{edge} / T_H) for t = 5 mm Cu foam sample and t = 0.4 mm Cu foils reference items surface points

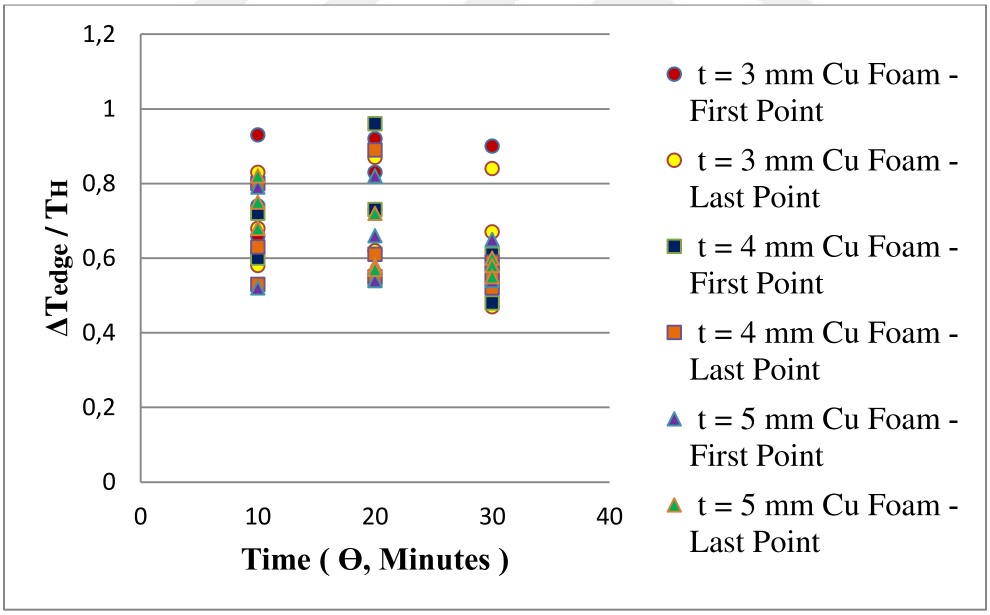

Figure 4.64 Time dependent variations of the (ΔT_{edge} / T_H) for different thicknesses of Cu foam samples surface points

From the Figures 4.61, 4.62 and 4.63, it is clear that ΔT_{edge} / T_H values showed some differences for Cu foam and Cu foil samples, for example values for Cu foam samples changing between (0.5 – 1) range, for Cu foils changing between (1.3 – 2.6) range. These results showed the effects and thermal properties of the porous and non-porous medium on heat transfer. As stated before, depending on the Θ, first and last points values change for the samples.

From the Figure 4.64, if analysis is made for different thicknesses of Cu foams, ranges of the ΔT_{edge} / T_H for t = 3 mm Cu foam higher than the other Cu foams and values are 0,9 and nearly same for all the time periods.

Ranges of the ΔT_{edge} / T_H for t = 4 mm and 5 mm Cu foams showed similar results compared with t = 3 mm Cu foam especially for Θ = 30 min. From Figure 4.64, ΔT_{edge} / T_H results showed very near values for Θ = 30 minutes compared with other time periods. For Θ = 20 min, results show that there are 2 different ranges for example (0,5 – 0,65) and (0,8 – 0,9) respectively.

If analyses are made for Cu foil reference items, values of the Cu foil with holes ΔT_{edge} / T_H higher than the Cu foil values for Θ = 10 min. There are small increase from Θ = 10 min. to 30 min. Results showed that some irregularities for Θ = 20 min. and 30 min. by means of first and last points. Generally, ΔT_{edge} / T_H ratio comes to nearly same values, there are small difference between them.

As a result of the analyses, time dependent variations of T_{edge} and ΔT_{edge} of the Cu foam samples and Cu foil reference items as a function of T_H for different sample thicknesses and first and last surface points can be seen from the above figures. Analysis results are summarized and listed as follows,

1. Ranges of the T_{edge} / T_H for upper surfaces of the samples changes depending on the Θ and sample type and thicknesses.
2. t = 3 mm Cu foam sample upper surface first point values higher than the last point values. On the other hand, first and last points values of the other Cu foams showed some differences depending on the Θ and t.

3. T_{edge} / T_H values of the Cu foil reference items are higher than the Cu foam samples. The values change between $1,8 \leq T_{edge}/T_H \leq 3,2$ for Cu foil reference items and change between $0,9 \leq T_{edge}/T_H \leq 1,4$ for Cu foam samples.

4. Values of the T_{edge} / T_H for Cu foam and Cu foil samples contact surfaces show nearly same results. There are not clear differences for first and last points values.

5. ΔT_{edge} / T_H values showed some differences for Cu foams and Cu foils, for example values for Cu foams changing between (0.45 – 1) range, for Cu foils changing between (1.3 – 2.6) range. These results showed the effects and thermal properties of the porous and non-porous medium on heat transfer.

6. ΔT_{edge} / T_H results of Cu foam samples showed very near values for Θ = 30 min. compared with other time periods.

4.6 Conclusion

In this chapter, firstly, thermal image analysis results of the upper and contact surfaces of the tested samples with respect to different T_H, t and Θ are given. It is clear from the experimental results depend on the ε, pore shape, d_p, and pore direction parameters, ΔT_{cf}, ΔT_H and T_{edge} change along the Cu foam surface. It is also important to note that there are heat conduction and heat convection heat transfer variations along the all directions inside the Cu foam plate.

Analysis results show that, T_H and $T_{m,upper}$ values of the Cu foam samples decrease depending on the increasing Θ. Time dependent percentage changes for t = 3 mm, 4 mm and 5 mm Cu foam samples are % 17.2, % 17.4 and % 13.2 for $T_H = 50$ ˚C, for $T_H = 80$ ˚C are % 25, % 24.2 and % 22.2 and for $T_H = 100$ ˚C are % 29.6, % 26.9 and % 25.8 respectively.

ΔT_{cf} values of the t = 3 mm, 4 mm and 5 mm Cu foam samples change depending on the Θ, between 11 ˚C $\leq \Delta T_{cf} \leq$ 17 ˚C, 20 ˚C $\leq \Delta T_{cf} \leq$ 36 ˚C and 25 ˚C $\leq \Delta T_{cf} \leq$ 45 ˚C for $T_H = 50$ ˚C. 21 ˚C $\leq \Delta T_{cf} \leq$ 36 ˚C, 18 ˚C $\leq \Delta T_{cf} \leq$ 30 ˚C and 16 ˚C $\leq \Delta T_{cf} \leq$ 25 ˚C for $T_H = 80$ ˚C and 25 ˚C $\leq \Delta T_{cf} \leq$ 45 ˚C, 20 ˚C $\leq \Delta T_{cf} \leq$ 33 ˚C and 18 ˚C $\leq \Delta T_{cf} \leq$ 32 ˚C for $T_H = 100$ ˚C respectively.

Secondly, effects of the thickness on temperature distributions of the Cu foams along the upper and contact surfaces at different T_H and Θ are given, analysis results showed some differences depend on the parameters. As can be seen from the analysis results, Cu foam upper and contact surface temperatures decrease depending on the increasing Θ with respect to t and T_H. For example, $T_{m,upper}$ change between 34 ˚C ≤ $T_{m,upper}$ ≤ 45 ˚C for T_H = 50 ˚C, 40 ˚C ≤ $T_{m,upper}$ ≤ 64 ˚C for T_H = 80 ˚C and 46 ˚C ≤ $T_{m,upper}$ ≤ 76 ˚C for T_H = 100 ˚C. Similarly, $T_{m,contact}$ change between 24 ˚C ≤ $T_{m,contact}$ ≤ 28 ˚C for T_H = 50 ˚C, 24 ˚C ≤ $T_{m,contact}$ ≤ 28 ˚C for T_H = 80 ˚C and 28 ˚C ≤ $T_{m,contact}$ ≤ 35 ˚C for T_H = 100 ˚C.

Finally, time dependent thermal analysis results of the Cu foil with and without holes for upper surfaces at different T_H and time dependent variation of (T_{edge} / T_H) and (ΔT_{edge} / T_H) for tested copper foam samples and copper foil reference Items are given in detail. Results showed the effects of the edge temperatures as a function of T_H for a variety of times.

T_{edge} / T_H values of the Cu foil reference items are higher than the Cu foam samples. The values change between 1,8 ≤ T_{edge}/T_H ≤ 3,2 for Cu foil reference items and change between 0,9 ≤ T_{edge}/T_H ≤ 1,4 for Cu foam samples. ΔT_{edge} / T_H values showed some differences for Cu foams and Cu foils, for example values for Cu foams changing between (0.45 – 1) range, for Cu foils changing between (1.3 – 2.6) range. These results showed the effects and thermal properties of the porous and non-porous medium on heat transfer.

CHAPTER 5

A MODELLING FOR THE DETERMINATION OF THERMAL CHARACTERISTICS OF COPPER FOAM SAMPLES

5.1 Introduction

In this chapter, a method for the calculation of thermal characteristics of the Cu foam samples and Cu foil reference items are given. It is obvious that, in order to learn or define the thermal characteristics of a material, thermal conductivity, k (W/m.K) heat capacity, C (J/K) and thermal diffusivity, α (mm^2/s) are important parameters. After analyzing the thermal characteristics of the tested Cu foam samples, cooling performances are also described.

A detailed analyses of the thermal characteristics of the tested Cu foam and Cu foil samples and related comparisons are given in the following sections.

5.2 Time Dependent Thermal Conductivity Changes of The Tested Copper Foam Samples and Copper Foil Reference Items

In chapter 2, basic definition of the thermal conductivity of porous metal foams are given. As stated before, thermal conductivity is an important parameter for defining the thermal characteristics of porous metal foam. In this section, time dependent change of the thermal conductivities of the Cu foam and Cu foil samples depend on the different t and T_H are observed in detail and given in the following sections from 5.2.1 to 5.2.10. Thermal conductivity values of the samples are calculated using the heat conduction equation stated in equations 5.1 and 5.2 as follows,

$$Q = k.A\ (T_{upper} - T_{contact}) / t \qquad (5.1)$$

$$k = Q.t / A (T_{upper} - T_{contact}) \quad (5.2)$$

where, k is thermal conductivity, W/(m.K), Q is heat transfer through material, (Watt), t is thickness of the material, (m), A is surface area, (m^2), T_{upper} is the upper surface temperature of the material (˚C) and $T_{contact}$ is the contact surface temperature of the material (˚C).

From equation 5.2, k values and its changes along the Cu foam sample surface are calculated and analysis results are shown in the following sections. Each of the k values are calculated with locally. 9 different local points are selected for calculation of the change of k which shown in the Figure 5.1.

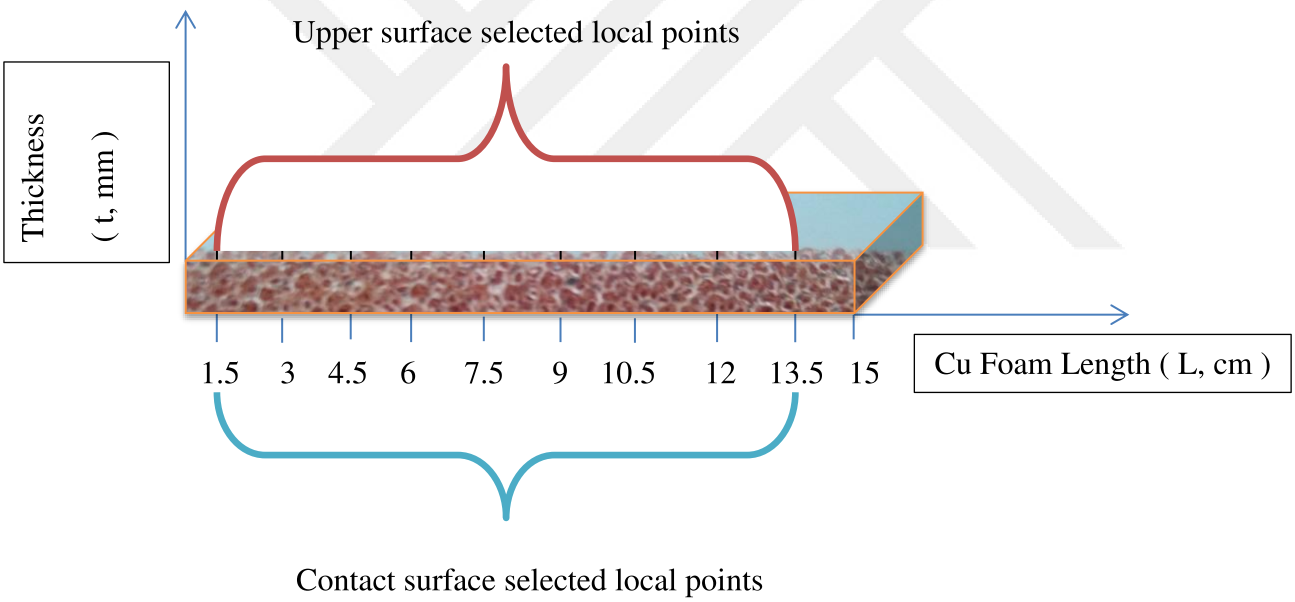

Figure 5.1 Selected local points along the Cu foam samples for calculation of the k

In the equation 5.2, in order to determine the Q, firstly, T_{ave} is calculated by using the Equation 5.3.

$$T_{ave} = (T_i + T_f) / 2 \quad (5.3)$$

where, T_{ave} is the average temperature of the heater, (˚C), T_i is the initial temperature of the heater (˚C) and T_f is the final temperature of the heater after specified time periods(˚C) .

After finding the T_{ave} value, this value is converted to Watt unit by using the Table 3.5 to find the Q values. Area, A is calculated by using the Equation 5.4.

$$A = x_d \, . \, W \tag{5.4}$$

where, A is the surface area, (m^2), x_d is distance between 2 points which nearest to the selected local point on sample surface, (m) and W is the width of the sample (m). T_{upper} and $T_{contact}$ values of the samples are taken according to the selected local points for different t, T_H and ϴ. For each case, 9 different k values are calculated and local changes of the k are shown in the following sections.

5.2.1 Effects of The Thickness on Local Thermal Conductivity Changes of the Tested Cu Foam Samples

In this section, changes of the thermal conductivities of the Cu foam samples and Cu foil reference items at $T_H = 50$˚C are given and results compared for ϴ = 10, 20 and 30 minutes in the Figures 5.2, 5.3 and 5.4.

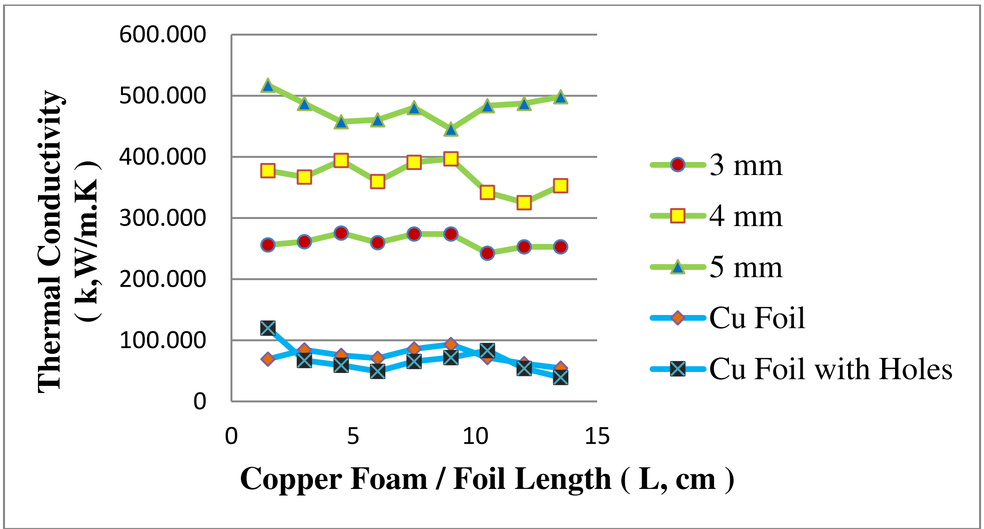

Figure 5.2 Variations of the thermal conductivity of the Cu foams / foils for ϴ = 10 min.

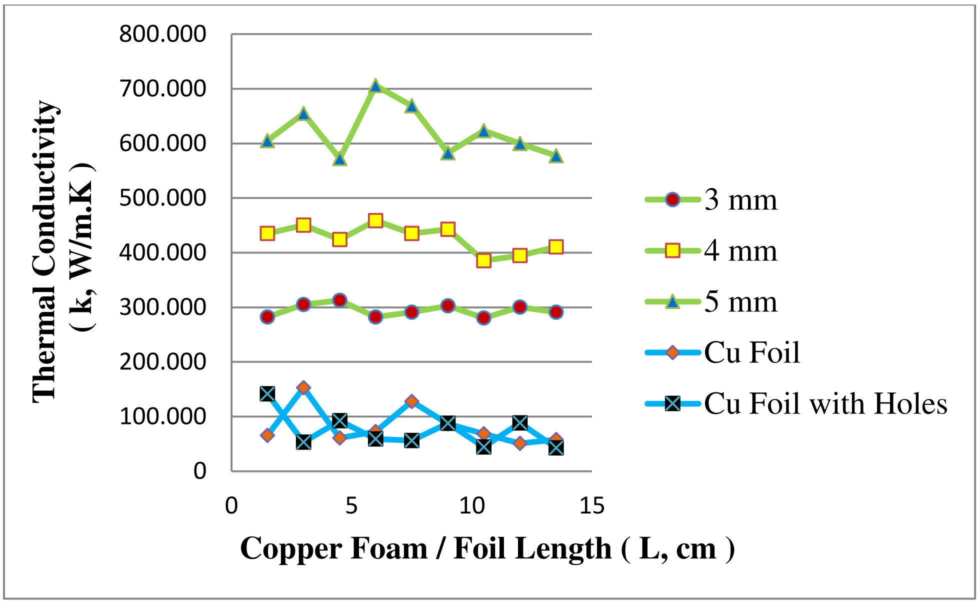

Figure 5.3 Variations of the thermal conductivity of the Cu foams / foils for Θ = 20 min.

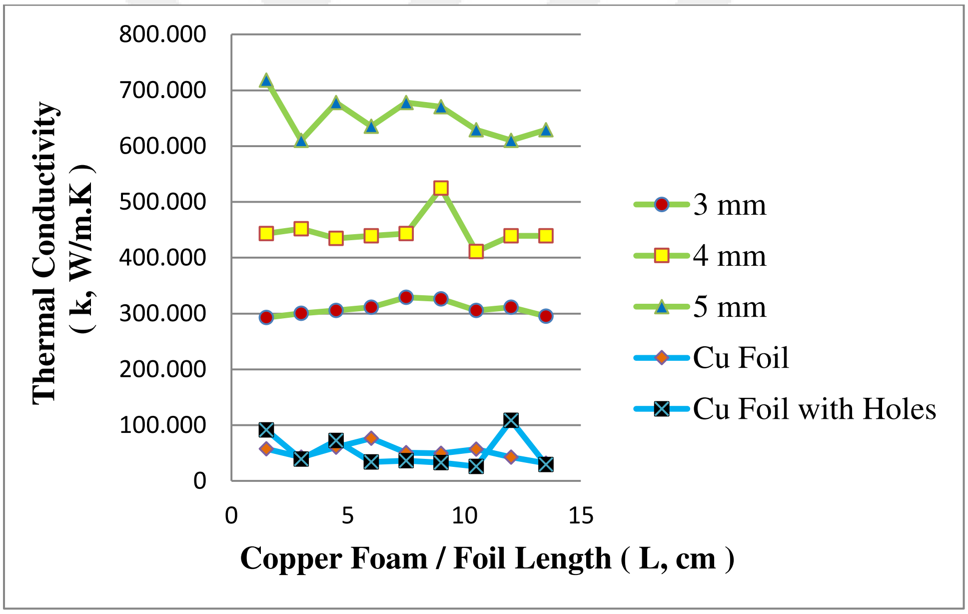

Figure 5.4 Variations of the thermal conductivity of the Cu foams / foils for Θ = 30 min.

Results from the Figures 5.2, 5.3 and 5.4 give some informations; k values of the Cu foam and Cu foil samples change from point to point and depend on the Θ which can be seen along the surface. It is clear from the figures that if thicknesses of the Cu foam increase then k increases. This situation shows the effects of the porous medium on k. k of the Cu foams show an increase depend on Θ which changing from Θ = 10 minutes to 30 minutes.

It is seen from the Figure 5.2 that, t = 5 mm Cu foam sample has higher k than the other thicknesses of the samples. Values of the k change between the (250 W/m.K – 275 W/m.K) for 3 mm, (320 W/m.K – 400 W/m.K) for 4 mm and (440 W/m.K – 517 W/m.K) for 5 mm Cu foam sample. On the other hand, Cu foil reference samples k values change between the (50 W/m.K – 93 W/m.K) for Cu foil and (40 W/m.K – 120 W/m.K) for the Cu foil with holes. Analysis results show the variations of the k are high for t = 4 mm and t = 5 mm samples and low for t = 3 mm sample along the surface. These variations imply the effects of the porous medium on local k changes depending on the sample thickness. It is also important to note that, irregular variations of the k values show the non-uniform distribution of the porosity in the sample and show the effects of the pore size and pore structures on the change of the k values.

Likely, it is seen from the Figure 5.3 that, t = 5 mm Cu foam sample has higher k than the other thicknesses of the samples. Values of the k change between the (280 W/m.K – 310 W/m.K) for 3 mm, (380 W/m.K – 460 W/m.K) for 4 mm and (570 W/m.K – 670 W/m.K) for 5 mm Cu foam sample. On the other hand, Cu foil reference samples k values change between the (50 W/m.K – 150 W/m.K) for Cu foil and (40 W/m.K – 145 W/m.K) for the Cu foil with holes. Analysis results show the variations of the k are high for t = 4 mm and t = 5 mm samples and low for t = 3 mm sample along the surface.

Finally, it is seen from the Figure 5.4 that, t = 5 mm Cu foam sample has higher k than the other thicknesses of the samples. Values of the k change between the (290 W/m.K – 330 W/m.K) for 3 mm, (430 W/m.K – 520 W/m.K) for 4 mm and (600 W/m.K – 710 W/m.K) for 5 mm Cu foam sample. On the other hand, Cu foil reference samples k values change between the (30 W/m.K – 76 W/m.K) for Cu foil and (25 W/m.K – 110 W/m.K) for the Cu foil with holes. Analysis results show the variations of the k are high for t = 4 mm and t = 5 mm samples and low for t = 3 mm sample along the surface. For Cu foil and Cu foil with holes samples, changes of the k values show some irregularities depend on the surface structures and points and there are small differences for k values.

In order to analyze the time dependent percentage change of the k values of the Cu foam and Cu foil samples, mean values of the 9 different k values are calculated and changes summarized for different samples in the Table 5.1. Percentage change of the k values are calculated by equation 5.5

$$\text{Change in } \% = (k_f - k_i) / k_i \times 100 \quad (5.5)$$

Where, k_f and k_i are the final and initial values of thermal conductivity at a specified Θ (W/m.K).

Table 5.1: Time dependent percentage changes of the mean thermal conductivity

T_H (˚C)	**Time, Θ (Min)**	**3 mm (W/m.K)**	**4 mm (W/m.K)**	**5 mm (W/m.K)**	**Cu Foil (W/m.K)**	**Cu Foil with Holes (W/m.K)**
50	10	260.840	367.301	479.719	72.854	68.096
	20	294.205	426.265	621.260	86.991	73.892
	30	308.599	447.348	650.896	51.087	52.283

It is seen from the table that percentage change of the mean k is 29,5 % and highest for t = 5 mm Cu foam sample and lowest with 12,8 % for t = 3 mm Cu foam sample between the Θ = 10 minutes and 20 minutes time periods. It is also seen from the table that, percentages of the change of k are 4,9 % and 4,8 % and nearly same between the Θ = 20 minutes and 30 minutes for all Cu foam samples. In contrast to the Cu foams, Cu foil samples show change negatively between the Θ = 20 minutes and 30 minutes time periods. Percentage changes are 41,2 % and 29.2 % respectively. Percentage change of the Cu foil is 19,8 % and higher than the Cu foil with holes reference items between the Θ = 10 minutes and 20 minutes. These results show that at a specified T_H, effects of the Θ are high for local thermal conductivity changes of the samples.

Changes of the thermal conductivities of the Cu foam samples and Cu foil reference items at T_{H} = 80˚C are given and results compared for Θ = 10, 20 and 30 minutes in the Figures 5.5, 5.6 and 5.7.

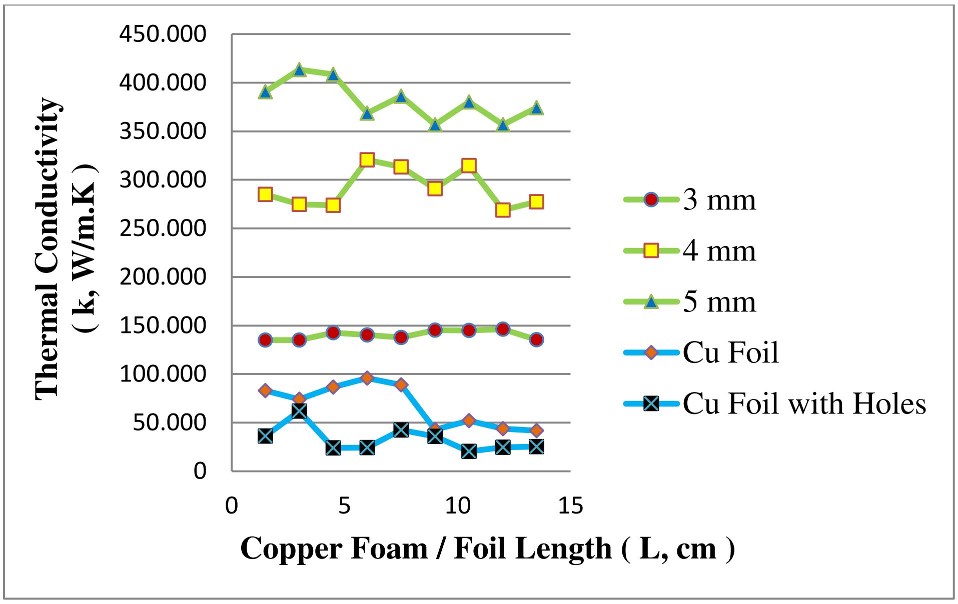

Figure 5.5 Variations of the thermal conductivity of the Cu foams / foils for Θ = 10 min.

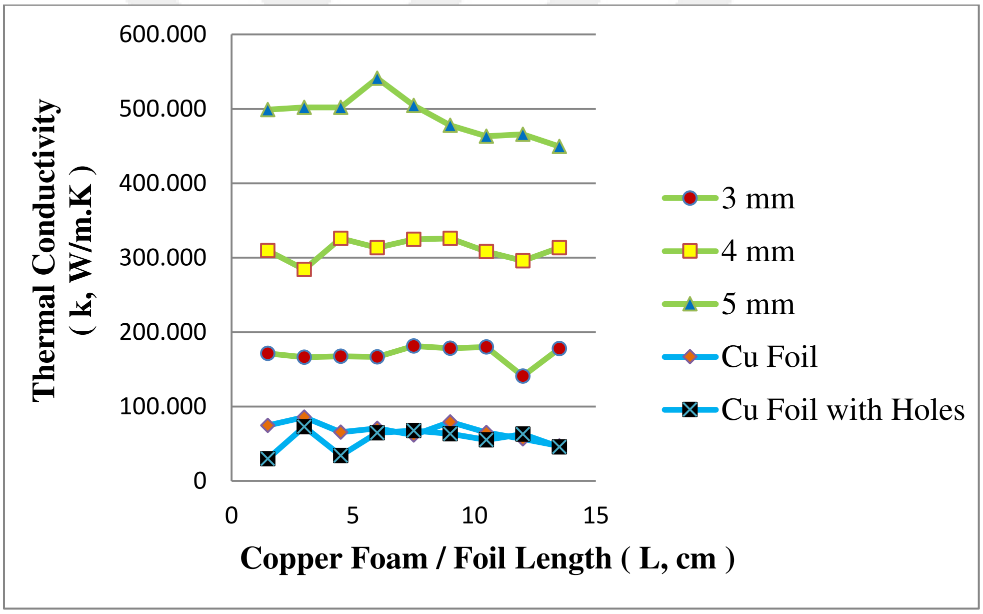

Figure 5.6 Variations of the thermal conductivity of the Cu foams / foils for Θ = 20 min.

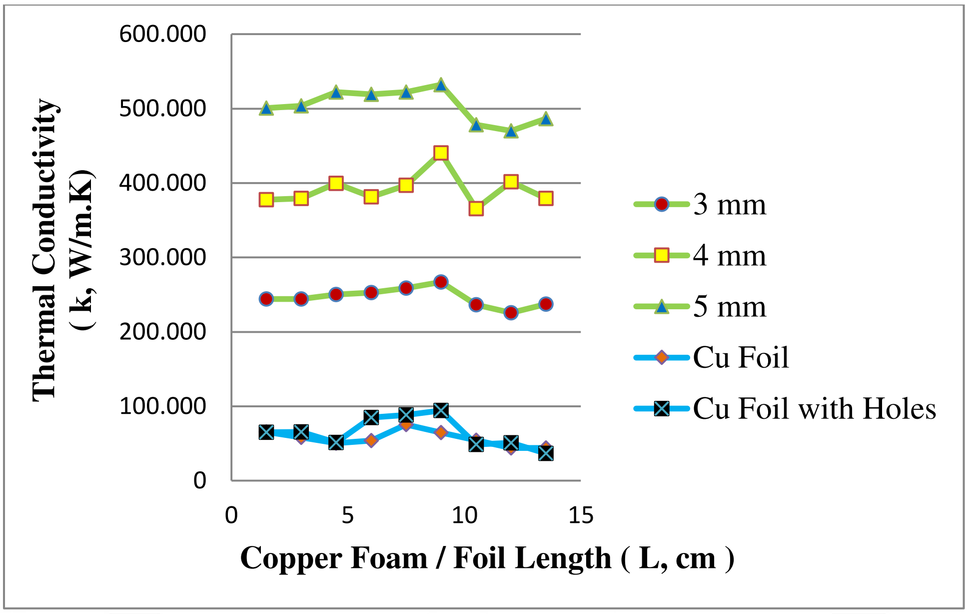

Figure 5.7 Variations of the thermal conductivity of the Cu foams / foils for ϴ = 30 min.

It is seen from the Figure 5.5 that, t = 5 mm Cu foam sample has higher k than the other thicknesses of the samples. Values of the k change between the (134 W/m.K – 146 W/m.K) for 3 mm, (268 W/m.K – 320 W/m.K) for 4 mm and (356 W/m.K – 413 W/m.K) for 5 mm Cu foam sample. On the other hand, Cu foil reference samples k values change between the (40 W/m.K – 95 W/m.K) for Cu foil and (20 W/m.K – 62 W/m.K) for the Cu foil with holes. Analysis results show the variations of the k are high for t = 4 mm and t = 5 mm samples and low for t = 3 mm sample along the surface.

It is seen from the Figure 5.6 that, t = 5 mm Cu foam sample has higher k than the other thicknesses of the samples. Values of the k change between the (140 W/m.K – 180 W/m.K) for 3 mm, (284 W/m.K – 326 W/m.K) for 4 mm and (450 W/m.K – 540 W/m.K) for 5 mm Cu foam sample. On the other hand, Cu foil reference samples k values change between the (45 W/m.K – 85 W/m.K) for Cu foil and (30 W/m.K – 73 W/m.K) for the Cu foil with holes. Analysis results show the variations of the k are high for t = 4 mm and t = 5 mm samples and low for t = 3 mm sample along the surface.

Finally, it is seen from the Figure 5.7 that, t = 5 mm Cu foam sample has higher k than the other thicknesses of the samples. Values of the k change between the (225 W/m.K – 267 W/m.K) for 3 mm, (365 W/m.K – 440 W/m.K) for 4 mm and (470 W/m.K – 532 W/m.K) for 5 mm Cu foam sample. On the other hand, Cu foil reference samples k values change between the (44 W/m.K – 75 W/m.K) for Cu foil and (36 W/m.K – 90

W/m.K) for the Cu foil with holes. Analysis results show the variations of the k are high for t = 4 mm and t = 5 mm samples and low for t = 3 mm sample along the surface. These variations imply the effects of the porous medium on local k changes depending on the sample thickness.

In order to analyze the time dependent percentage change of the k values of the Cu foam and Cu foil samples, mean values of the 9 different k values are calculated and changes summarized for different samples in the Table 5.2.

Table 5.2: Time dependent percentage changes of the mean thermal conductivity

T_H (˚C)	Time, ϴ (min)	3 mm (W/m.K)	4 mm (W/m.K)	5 mm (W/m.K)	Cu Foil (W/m.K)	Cu Foil with Holes (W/m.K)
80	10	140.263	291.046	381.768	64.066	32.699
	20	170.063	311.331	489.508	67.146	55.166
	30	246.312	391.348	503.869	58.131	65.262

It is seen from the table that percentage change of the mean k is 28,2 % and highest for t = 5 mm Cu foam sample and lowest with 6.97 % for t = 4 mm Cu foam sample between the ϴ = 10 minutes and 20 minutes time periods. It is also seen from the table that, percentages of the change of k are 44,8 % and highest for t = 3 mm Cu foam sample and lowest for 2,93 % for t = 5 mm Cu foam sample between the ϴ = 20 minutes and 30 minutes. In contrast to the Cu foams, Cu foil samples show change negatively between the ϴ = 20 minutes and 30 minutes time periods. Percentage change is 13,4 % respectively. Percentage change of the Cu foil with holes is 68,7 % and higher than the Cu foil reference items between the ϴ = 10 minutes and 20 minutes. These results show that at a specified T_H, effects of the ϴ are high for local thermal conductivity changes of the samples.

Changes of the thermal conductivities of the Cu foam samples and Cu foil reference items at T_{H} = 100˚C are given and results compared for ϴ = 10, 20 and 30 minutes in the Figures 5.8, 5.9 and 5.10.

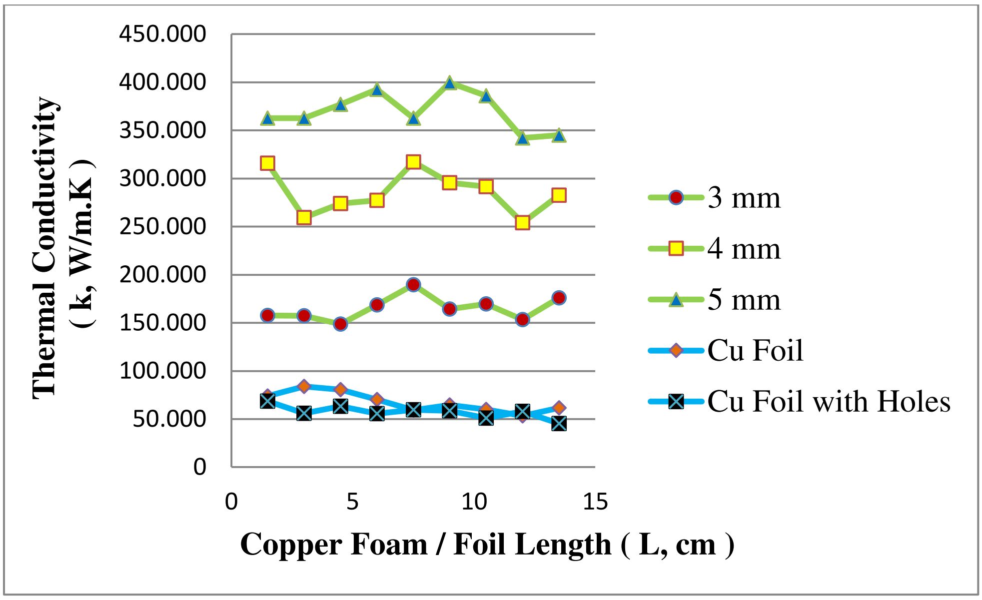

Figure 5.8 Variations of the thermal conductivity of the Cu foams / foils for ϴ = 10 min.

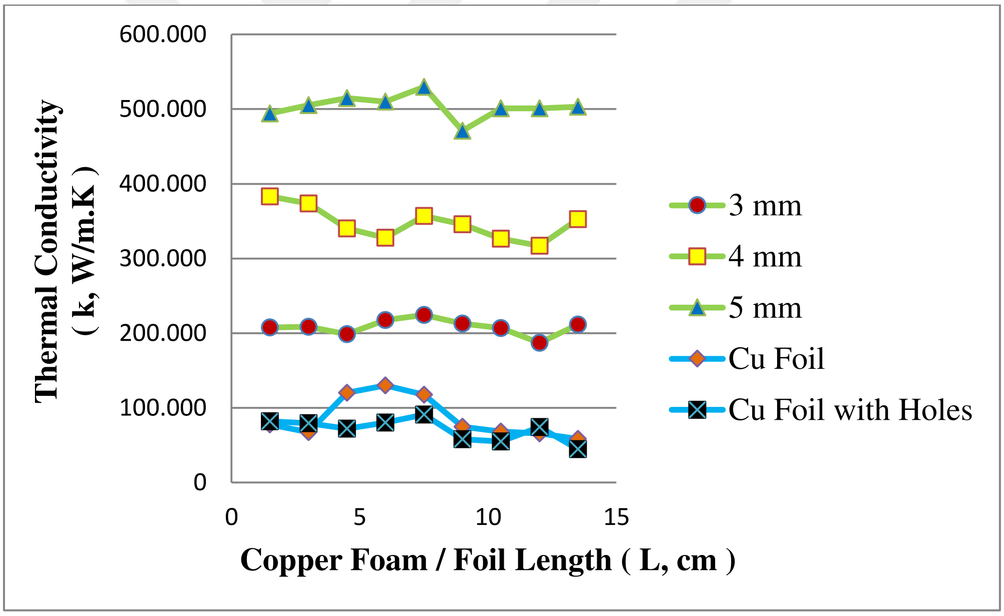

Figure 5.9 Variations of the thermal conductivity of the Cu foams / foils for ϴ = 20 min.

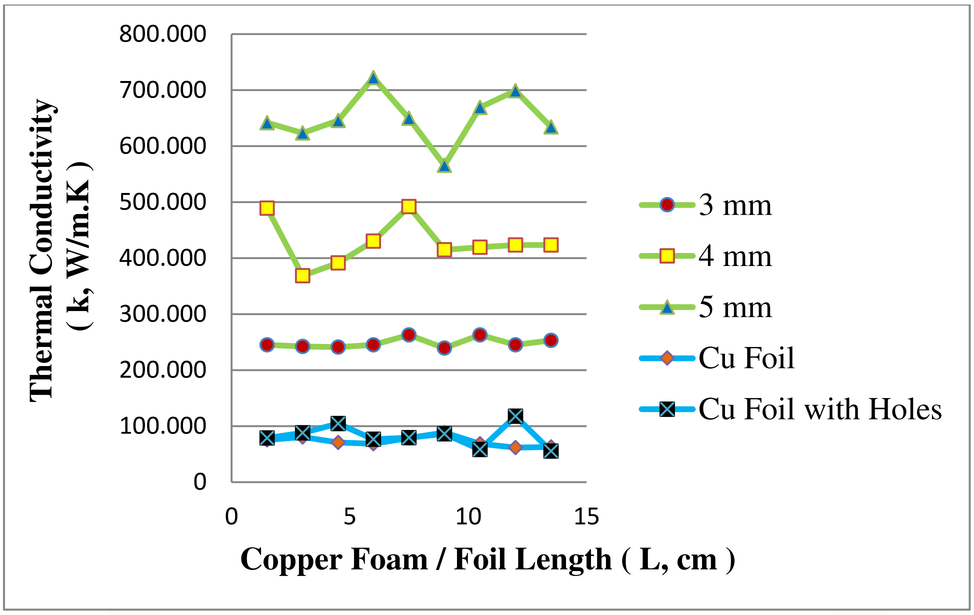

Figure 5.10 Variations of the thermal conductivity of the Cu foams / foils for ϴ = 30 min.

It is seen from the Figure 5.8 that, t = 5 mm Cu foam sample has higher k than the other thicknesses of the samples. Values of the k change between the (148 W/m.K – 190 W/m.K) for 3 mm, (250 W/m.K – 317 W/m.K) for 4 mm and (340 W/m.K – 400 W/m.K) for 5 mm Cu foam sample. On the other hand, Cu foil reference samples k values change between the (53 W/m.K – 83 W/m.K) for Cu foil and (45 W/m.K – 68 W/m.K) for the Cu foil with holes. Analysis results show the variations of the k are high for t = 4 mm and t = 5 mm samples and low for t = 3 mm sample along the surface. These variations imply the effects of the porous medium on local k changes depending on the sample thickness.

Similarly, it is seen from the Figure 5.9 that, t = 5 mm Cu foam sample has higher k than the other thicknesses of the samples. Values of the k change between the (185 W/m.K – 224 W/m.K) for 3 mm, (317 W/m.K – 383 W/m.K) for 4 mm and (470 W/m.K – 530 W/m.K) for 5 mm Cu foam sample. On the other hand, Cu foil reference samples k values change between the (58 W/m.K – 130 W/m.K) for Cu foil and (44 W/m.K – 91 W/m.K) for the Cu foil with holes. Analysis results show the variations of the k are high for t = 4 mm and t = 5 mm samples and low for t = 3 mm sample along the surface.

Finally, it is seen from the Figure 5.10 that, t = 5 mm Cu foam sample has higher k than the other thicknesses of the samples. Values of the k change between the (240 W/m.K – 262 W/m.K) for 3 mm, (360 W/m.K – 490 W/m.K) for 4 mm and (560 W/m.K – 722 W/m.K) for 5 mm Cu foam sample. On the other hand, Cu foil reference samples k values change between the (60 W/m.K – 80 W/m.K) for Cu foil and (55 W/m.K – 120 W/m.K) for the Cu foil with holes. Analysis results show the variations of the k are high for t = 4 mm and t = 5 mm samples and low for t = 3 mm sample along the surface.

In order to analyze the time dependent percentage change of the k values of the Cu foam and Cu foil samples, mean values of the 9 different k values are calculated and changes summarized for different samples in the Table 5.3.

Table 5.3 : Time dependent percentage changes of the mean thermal conductivity

T_H (°C)	Time, Θ (min)	3 mm (W/m.K)	4 mm (W/m.K)	5 mm (W/m.K)	Cu Foil (W/m.K)	Cu Foil with Holes (W/m.K)
100	10	164.949	285.298	370.076	75.715	57.301
	20	208.268	347.070	503.352	82.483	70.752
	30	248.322	428.070	650.282	97.116	82.724

It is seen from the table that percentage change of the mean k is 36 % and highest for t = 5 mm Cu foam sample and lowest with 21,6 % for t = 4 mm Cu foam sample between the Θ = 10 minutes and 20 minutes time periods. It is also seen from the table that, percentages of the change of k are 29,2 % and highest for t = 5 mm Cu foam sample and lowest for 19,2 % for t = 3 mm Cu foam sample between the Θ = 20 minutes and 30 minutes. On the other hand, Cu foil samples show change highly between the Θ = 20 minutes and 30 minutes time periods. Percentage changes are 17,7 % and 16,9 % respectively. Percentage change of the Cu foil with holes is 23,5 % and higher than the Cu foil reference items between the Θ = 10 minutes and 20 minutes. These results show that at a specified T_H, effects of the Θ are high for local thermal conductivity changes of the samples.

As a result, time dependent thermal conductivity changes of the different thicknesses of Cu foams and Cu foils are given in the above figures. Analysis results and thickness effects based on T_H are summarized and listed as follows ;

1. Thermal conductivities of the Cu foam and Cu foil samples change locally from point to point and depend on the ϴ along the surface.

2. If thicknesses of the Cu foam increase, k will increase. 5 mm thicknesses of Cu foam samples show high k values.

3. Thermal conductivities of the Cu foam samples increase depending on the increasing ϴ.

4. There are large differences between Cu foam samples and Cu foil reference items k values due to effects of the porous medium. For example,

   - Time dependent k values of t = 3 mm Cu foam sample change between 260 W/m.K ≤ k ≤ 309 W/m.K for T_H = 50 ˚C, 140 W/m.K ≤ k ≤ 247 W/m.K for T_H = 80 ˚C and 160 W/m.K ≤ k ≤ 250 W/m.K for T_H = 100 ˚C.

   - Time dependent k values of t = 4 mm Cu foam sample change between 360 W/m.K ≤ k ≤ 450 W/m.K for T_H = 50 ˚C, 290 W/m.K ≤ k ≤ 392 W/m.K for T_H = 80 ˚C and 285 W/m.K ≤ k ≤ 430 W/m.K for T_H = 100 ˚C.

   - Time dependent k values of t = 5 mm Cu foam sample change between 479 W/m.K ≤ k ≤ 651 W/m.K for T_H = 50 ˚C, 380 W/m.K ≤ k ≤ 504 W/m.K for T_H = 80 ˚C and 370 W/m.K ≤ k ≤ 650 W/m.K for T_H = 100 ˚C.

   - Time dependent k values of t = 0.4 mm Cu foil reference sample change between 50 W/m.K ≤ k ≤ 87 W/m.K for T_H = 50 ˚C, 58 W/m.K ≤ k ≤ 68 W/m.K for T_H = 80 ˚C and 75 W/m.K ≤ k ≤ 98 W/m.K for T_H = 100 ˚C.

   - Time dependent k values of t = 0.4 mm Cu foil with holes reference sample change between 52 W/m.K ≤ k ≤ 74 W/m.K for T_H = 50 ˚C, 32 W/m.K ≤ k ≤ 66 W/m.K for T_H = 80 ˚C and 57 W/m.K ≤ k ≤ 83 W/m.K for T_H = 100 ˚C.

5. It is obvious from the experimental result that, Cu foam samples have superior thermal conductivity properties, k values can reach to 650 W/m.K values compared with Cu foils materials, this situation show the effects and differences of the porous and non-porous mediums on k.

6. Generally, variations of the k values of the t = 3 mm Cu foam are more low and there are no large changes along the sample surface during the different time periods. On the other hand, t = 4 mm and 5 mm Cu foam samples show different and large variations and changes which percentage changes can be seen from the stated tables.

7. Percentage changes of the k of the Cu foams and Cu foils show some different variations depending on t, Θ and T_H.

8. Basically, changes in k show the effects and importance of micro-structure of the porous Cu foams by means of pore shape, pore size, pore direction, and pore distribution. For that reasons, a detailed analysis of the micro-structures of the Cu foam (SEM Analysis) materials become most important to define the thermal characteristics of the Cu foam samples correctly.

9. In literature, thermal conductivity values of the Cu foam and Cu foil samples are given as 400 W/m.K. There is a few experimental study for determination of the k. For that reason, it is valuable to see the local changing of the k as a function of different parameters are performed in this study.

5.2.2 Effects of The Temperature on Local Thermal Conductivity Changes of The Tested Cu Foam Samples

In this section, changes of the thermal conductivities of the 3 mm Cu foam sample at different T_H values are given and results are compared for Θ = 10, 20 and 30 minutes and are shown in the Figures 5.11, 5.12 and 5.13.

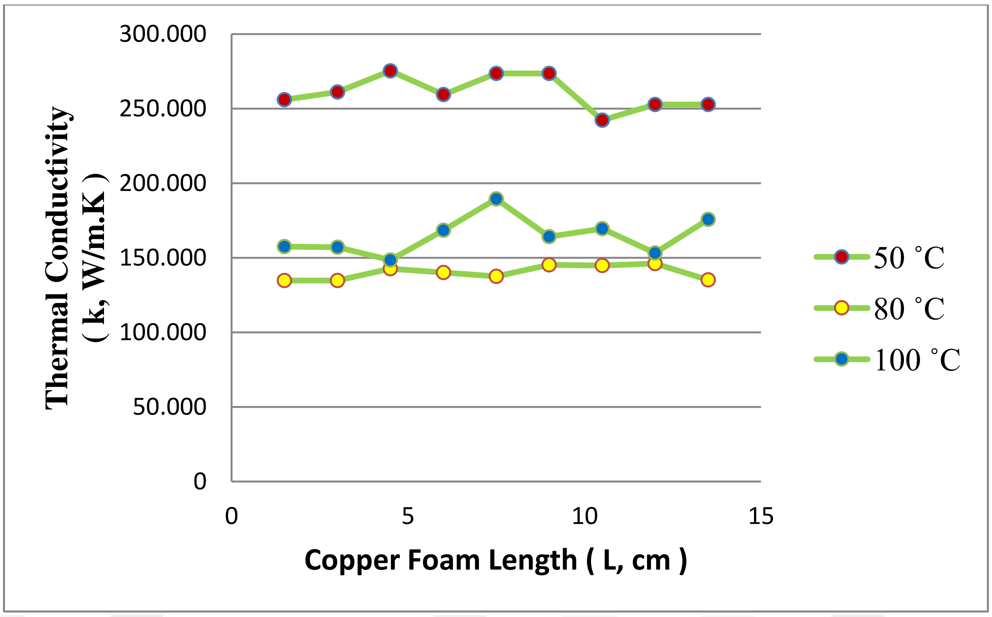

Figure 5.11 Thermal conductivity changes of the t = 3 mm Cu foam sample for ϴ = 10 min.

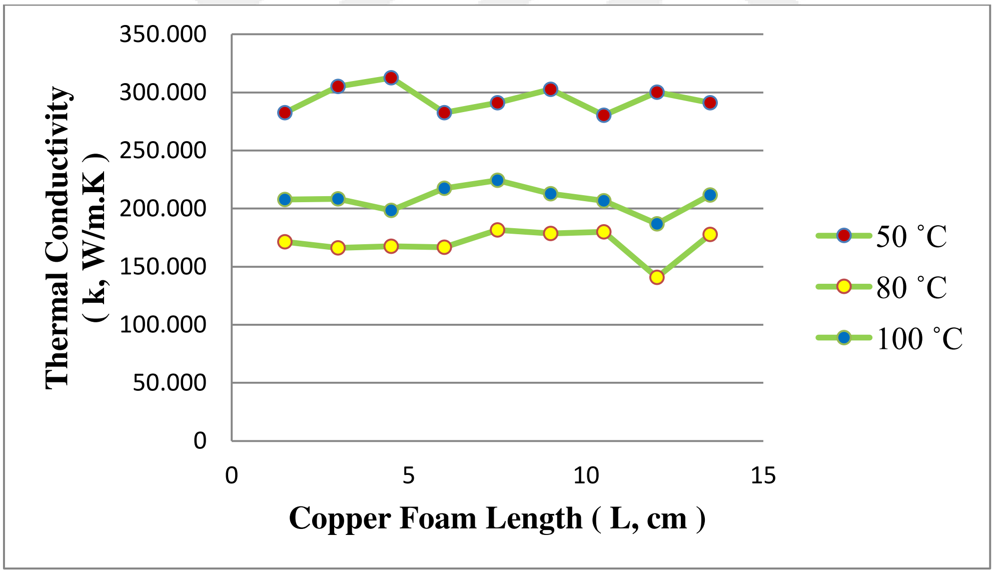

Figure 5.12 Thermal conductivity changes of the t = 3 mm Cu foam sample for ϴ = 20 min.

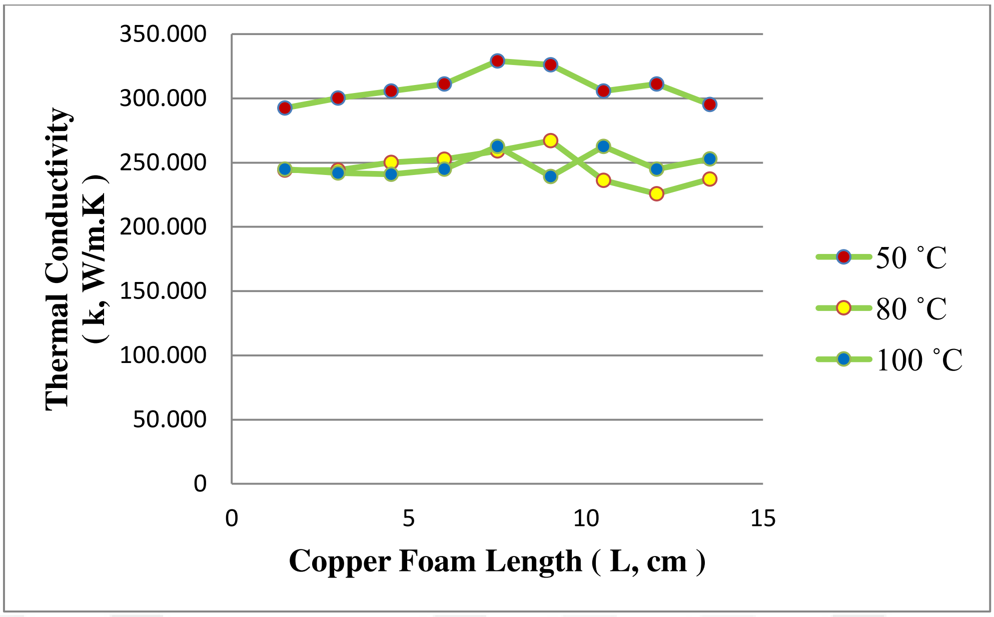

Figure 5.13 Thermal conductivity changes of the t = 3 mm Cu foam sample for ϴ = 30 min.

Results from the Figures 5.11, 5.12 and 5.13 give some informations; k values of the Cu foam samples change locally from point to point and depend on the ϴ which can be seen along the surface. It is clear from the figures that k values of the sample are highest for T_H = 50 ˚C and lowest for T_H = 80 ˚C. This situation shows the effects of the porous medium on k. k of the Cu foams show an increase depend on ϴ which changing from ϴ = 10 minutes to 30 minutes.

It is seen from the Figure 5.11 that, values of the k change between the (240 W/m.K – 275 W/m.K) for T_H = 50 ˚C, (130 W/m.K – 145 W/m.K) for T_H = 80 ˚C and (150 W/m.K – 190 W/m.K) for T_H = 100 ˚C Cu foam sample. Analysis results show the variations of the k are high for T_H = 50 ˚C and T_H = 100 ˚C and low for T_H = 80 ˚C along the sample surface. These variations imply the effects of the porous medium on local k changes depending on the heater temperatures.

Similarly, It is seen from the Figure 5.12 that, values of the k change between the (280 W/m.K – 312 W/m.K) for T_H = 50 ˚C, (140 W/m.K – 180 W/m.K) for T_H = 80 ˚C and (185 W/m.K – 225 W/m.K) for T_H = 100 ˚C Cu foam sample. Analysis results show the variations of the k are same for T_H = 80 ˚C and T_H = 100 ˚C and lower for T_H = 80 ˚C along the sample surface. These variations imply the effects of the porous medium on local k changes depending on the heater temperatures.

Finally, it is seen from the Figure 5.13 that, values of the k change between the (290 W/m.K – 330 W/m.K) for T_H = 50 ˚C, (220 W/m.K – 270 W/m.K) for T_H = 80 ˚C and (240 W/m.K – 260 W/m.K) for T_H = 100 ˚C Cu foam sample. Analysis results show the variations of the k are near for T_H = 50 ˚C and T_H = 80 ˚C and lower for T_H = 100 ˚C along the sample surface. In order to analyze the time dependent percentage change of the k values of the Cu foam samples, mean values of the 9 different k values are calculated and changes summarized for different T_H values in the Table 5.4.

Table 5.4 : Time dependent percentage changes of the mean thermal conductivity of the t = 3 mm Cu foam.

Cu Foam	**Temperatures (˚C)**	**10 Minutes (W/m.K)**	**20 Minutes (W/m.K)**	**30 Minutes (W/m.K)**
3 mm	50	260.840	294.205	308.599
	80	140.263	170.063	246.312
	100	164.949	208.268	248.322

It is seen from the table that percentage change of the mean k show some variations depend on the T_H. Thermal conductivity value of the sample is 308.599 W/m.K and highest for T_H = 50 ˚C. It is clear from the table that k values change negatively between the T_H = 50 ˚C - 80 ˚C at a rate of 46,2 %, 42,2 % and 20,2 % respectively. After T_H = 80 ˚C, changes are positively seen and highest for ϴ = 20 minutes.

These results show that at a specified foam thickness, effects of the T_H are high for local thermal conductivity changes of the samples.

Changes of the thermal conductivities of the 4 mm Cu foam sample at different T_H are given and results compared for ϴ = 10, 20 and 30 minutes and are shown in the Figures 5.14, 5.15 and 5.16.

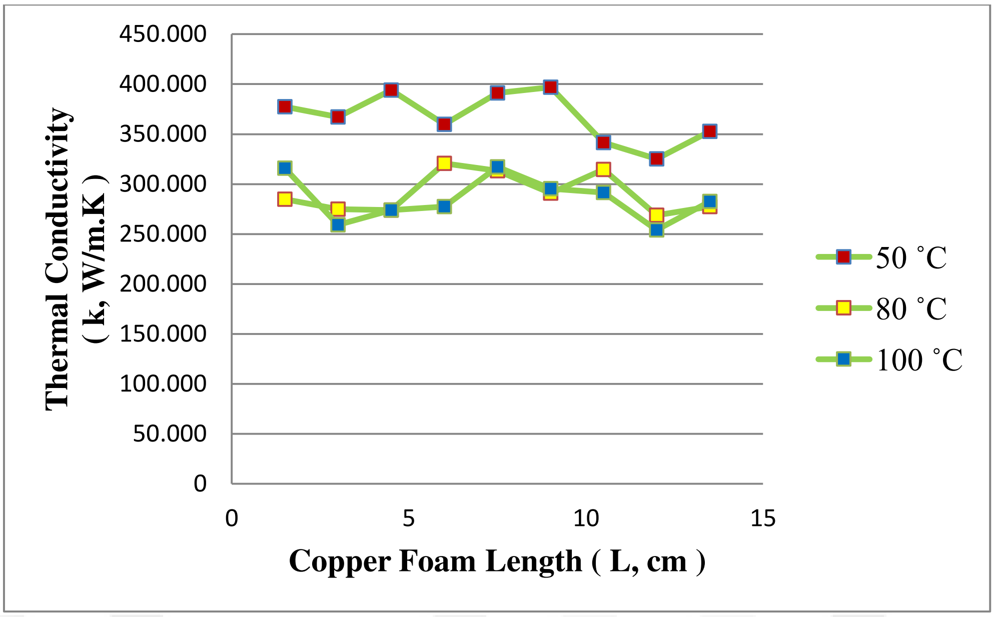

Figure 5.14 Thermal conductivity changes of the t = 4 mm Cu foam sample for ϴ = 10 min.

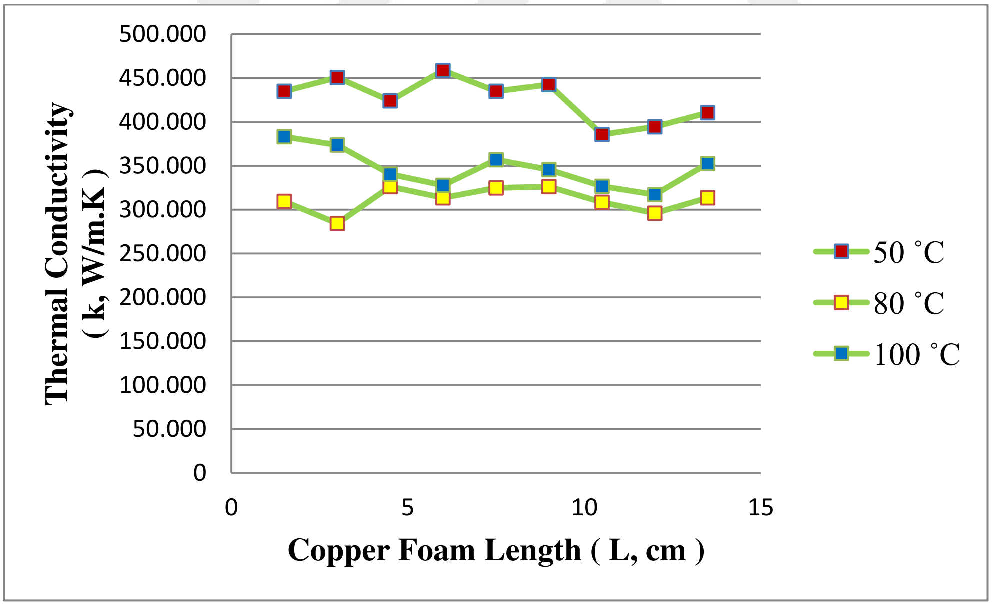

Figure 5.15 Thermal conductivity changes of the t = 4 mm Cu foam sample for ϴ = 20 min.

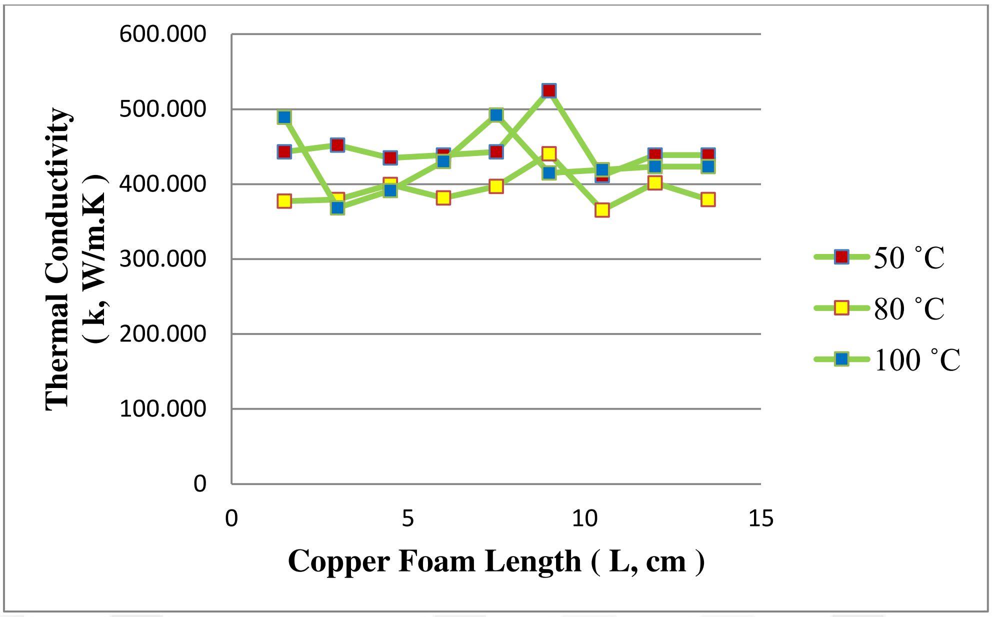

Figure 5.16 Thermal conductivity changes of the t = 4 mm Cu foam sample for ϴ = 30 min.

Results from the Figures 5.14, 5.15 and 5.16 give some informations; k values of the Cu foam samples change locally from point to point and depend on the ϴ which can be seen along the surface. It is clear from the figures that k values of the sample are highest for T_H = 50 ˚C and generally lowest for T_H = 80 ˚C. This situation shows the effects of the porous medium on k. k of the Cu foams show an increase with increasing ϴ which changing from ϴ = 10 minutes to 30 minutes.

It is seen from the Figure 5.14 that, values of the k change between the (325 W/m.K – 400 W/m.K) for T_H = 50 ˚C, (270 W/m.K – 320 W/m.K) for T_H = 80 ˚C and (250 W/m.K – 320 W/m.K) for T_H = 100 ˚C Cu foam sample. Analysis results show the variations of the k are high for T_H = 50 ˚C and T_H = 100 ˚C and low for T_H = 80 ˚C along the sample surface. Similarly, it is seen from the Figure 5.15 that, values of the k change between the (385 W/m.K – 460 W/m.K) for T_H = 50 ˚C, (280 W/m.K – 330 W/m.K) for T_H = 80 ˚C and (315 W/m.K – 385 W/m.K) for T_H = 100 ˚C Cu foam sample. Analysis results show the variations of the k are higher for T_H = 50 ˚C and T_H = 100 ˚C and lower for T_H = 80 ˚C along the sample surface. These variations imply the effects of the porous medium on local k changes depending on the heater temperatures.

Finally, It is seen from the Figure 5.16 that, values of the k change between the (410 W/m.K – 524 W/m.K) for T_H = 50 ˚C, (365 W/m.K – 440 W/m.K) for T_H = 80 ˚C and (360 W/m.K – 490 W/m.K) for T_H = 100 ˚C Cu foam sample. Analysis results show the variations of the k are near for T_H = 100 ˚C and T_H = 50 ˚C and lower for T_H = 80 ˚C along the sample surface. Mean values of the 9 different k values are calculated and changes summarized for different T_H in the Table 5.5.

Table 5.5 : Time dependent percentage changes of the mean thermal conductivity of the t = 4 mm Cu foam.

Cu Foam	**Temperatures (˚C)**	**10 Minutes (W/m.K)**	**20 Minutes (W/m.K)**	**30 Minutes (W/m.K)**
4 mm	50	367.301	426.265	447.348
	80	291.046	311.331	391.348
	100	285.298	347.070	428.070

It is seen from the table that percentage change of the mean k show some variations depend on the $T_{H.}$ Thermal conductivity value of the sample is 447.348 W/m.K and highest for T_H = 50 ˚C. It is clear from the table that k values change negatively between the T_H = 50 ˚C - 80 ˚C at a rate of 20,8 %, 27 % and 12,5 % respectively. After T_H = 80 ˚C, changes are positively seen and highest for ϴ = 20 minutes with 11,5 %. These results show that at a specified foam thickness, effects of the T_H are high for local thermal conductivity changes of the samples.

Changes of the thermal conductivities of the 5 mm Cu foam sample at different T_H are given and results compared for ϴ = 10, 20 and 30 minutes and are shown in the Figures 5.17, 5.18, and 5.19.

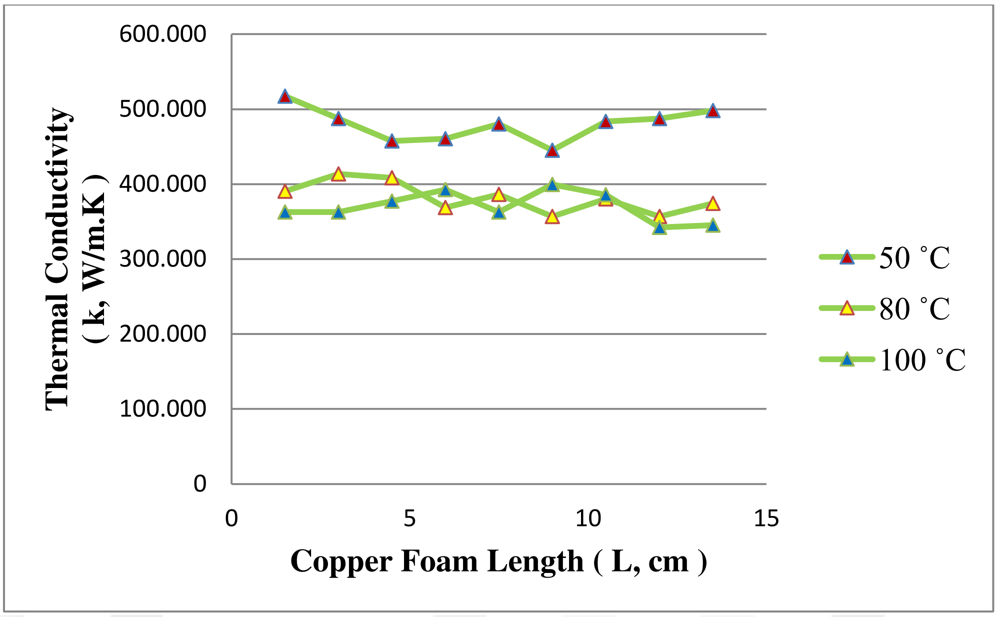

Figure 5.17 Thermal conductivity changes of the t = 5 mm Cu foam sample for ϴ = 10 min.

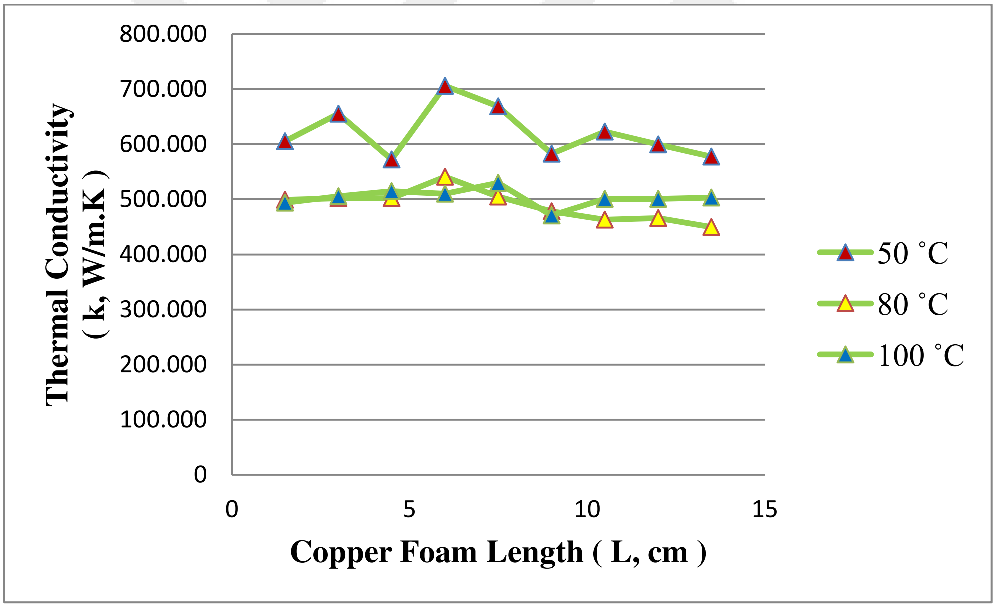

Figure 5.18 Thermal conductivity changes of the t = 5 mm Cu foam sample for ϴ = 20 min.

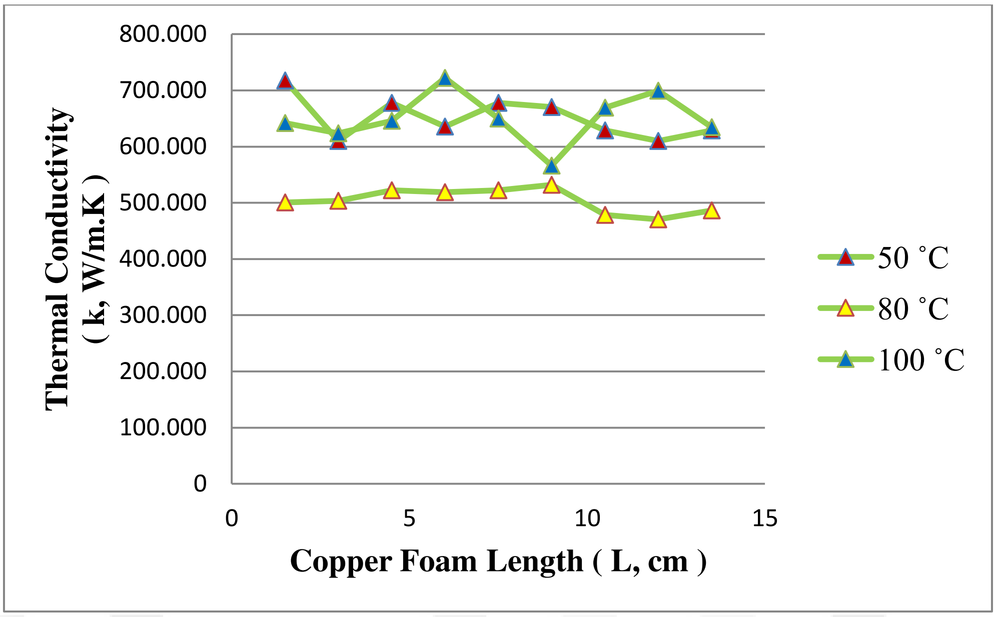

Figure 5.19 Thermal conductivity changes of the t = 5 mm Cu foam sample for ϴ = 30 min.

Results from the Figures 5.17, 5.18 and 5.19 give some informations; k values of the Cu foam samples change locally from point to point and depend on the ϴ which can be seen along the surface. It is clear from the figures that k values of the sample are highest for T_H = 50 ˚C and generally lowest for T_H = 80 ˚C. This situation shows the effects of the porous medium on k. k of the Cu foams show an increase depending on ϴ which changing from ϴ = 10 minutes to 30 minutes.

It is seen from the Figure 5.17 that, values of the k change between the (440 W/m.K – 517 W/m.K) for T_H = 50 ˚C, (350 W/m.K – 410 W/m.K) for T_H = 80 ˚C and (340 W/m.K – 400 W/m.K) for T_H = 100 ˚C Cu foam sample. Analysis results show the variations of the k are nearly same for T_H = 80 ˚C and T_H = 100 ˚C and higher for T_H = 50 ˚C along the sample surface. These variations imply the effects of the porous medium on local k changes depending on the heater temperatures.

Similarly, it is seen from the Figure 5.18 that, values of the k change between the (570 W/m.K – 670 W/m.K) for T_H = 50 ˚C, (450 W/m.K – 540 W/m.K) for T_H = 80 ˚C and (470 W/m.K – 530 W/m.K) for T_H = 100 ˚C Cu foam sample. Analysis results show the variations of the k are higher for T_H = 50 ˚C and T_H = 80 ˚C and lower for T_H = 100 ˚C along the sample surface.

Finally, it is seen from the Figure 5.19 that, values of the k change between the (610 W/m.K – 717 W/m.K) for T_H = 50 ˚C, (470 W/m.K – 530 W/m.K) for T_H = 80 ˚C and (560 W/m.K – 720 W/m.K) for T_H = 100 ˚C Cu foam sample. Analysis results show the variations of the k are highest for T_H = 100 ˚C and more near for T_H = 50 ˚C and T_H = 80 ˚C along the sample surface. Mean values of the 9 different k values are calculated and changes summarized for different T_H in the Table 5.6.

Table 5.6 : Time dependent percentage changes of the mean thermal conductivity of the t = 5 mm Cu foam.

Cu Foam	Temperatures (˚C)	10 Minutes (W/m.K)	20 Minutes (W/m.K)	30 Minutes (W/m.K)
5 mm	50	479.719	621.260	650.896
	80	381.768	489.508	503.869
	100	370.076	503.352	650.282

It is seen from the table that percentage change of the mean k show some variations depend on the T_H. Thermal conductivity value of the sample is 650.896 W/m.K and highest for T_H = 50 ˚C. It is clear from the table that k values change negatively between the T_H = 50 ˚C - 80 ˚C at a rate of 20,4 %, 21,2 % and 22,6 % respectively. After T_H = 80 ˚C, changes are positively seen and highest for ϴ = 30 minutes with 29 %.

These results show that at a specified foam thickness, effects of the T_H are high for local thermal conductivity changes of the samples.

Changes of the thermal conductivities of the 0.4 mm Cu foil sample at different T_H are given and results compared for ϴ = 10, 20 and 30 minutes and are shown in the Figures 5.20, 5.21 and 5.22.

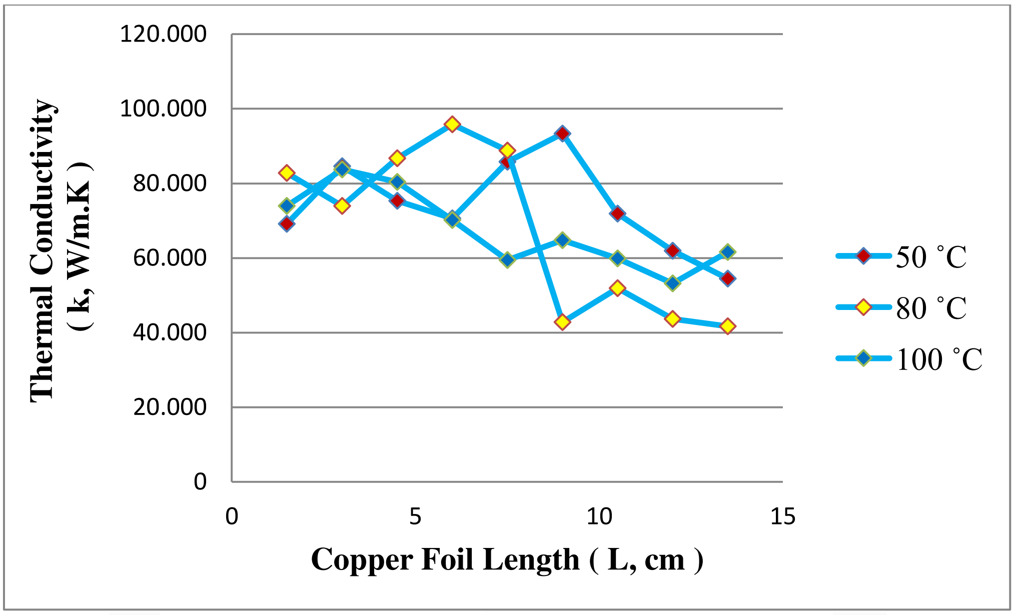

Figure 5.20 Thermal conductivity changes of the t = 0.4 mm Cu foil sample for ϴ = 10 min.

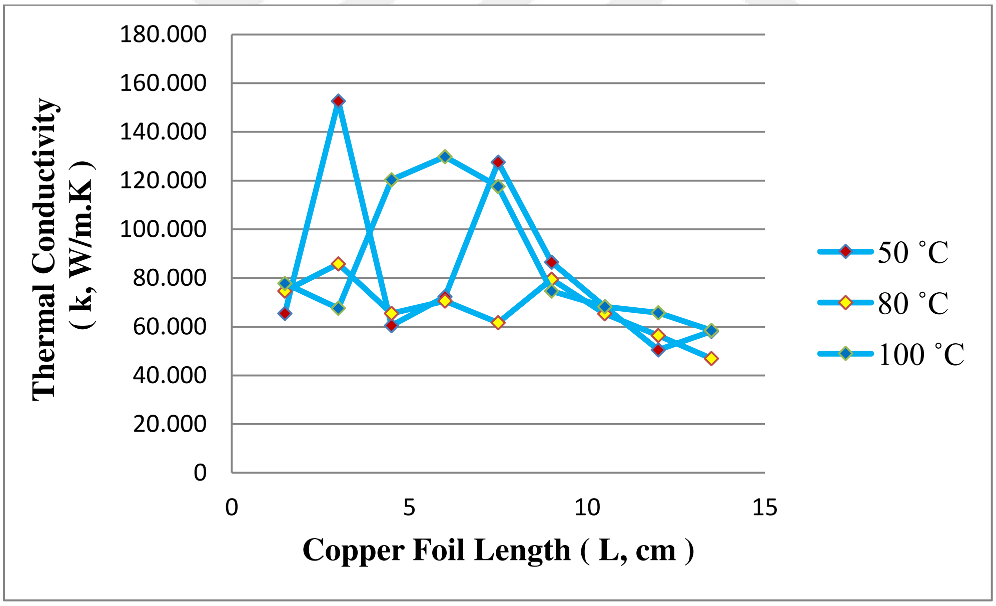

Figure 5.21 Thermal conductivity changes of the t = 0.4 mm Cu foil sample for ϴ = 20 min.

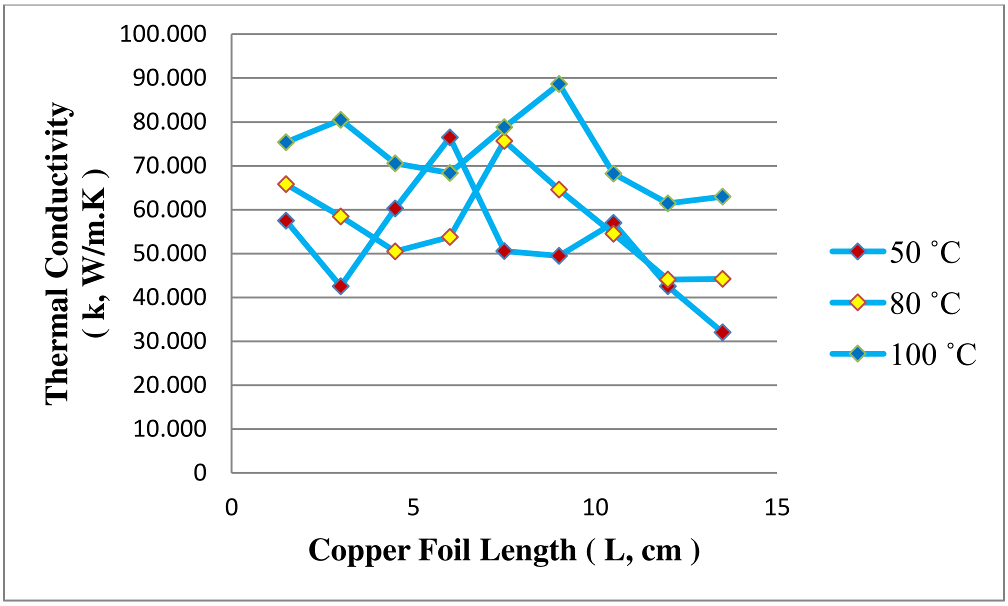

Figure 5.22 Thermal conductivity changes of the t = 0.4 mm Cu foil sample for Θ = 30 min.

Analysis results from the Figures 5.20, 5.21 and 5.22 show that some irregularities can be seen because of the Cu foil surface structures. Generally, k change shows near or similar profiles in the first and last region / distances of the material.

It is seen from the Figure 5.20 that k is between 40 W/m.K ≤ k ≤ 96 W/m.K, from the Figure 5.21, k is between 50 W/m.K ≤ k ≤ 150 W/m.K and from the Figure 5.22 k is between 30 W/m.K ≤ k ≤ 90 W/m.K.

Mean values of the k and changes in percent are given in the Table 5.7.

Table 5.7 : Time dependent percentage changes of the mean thermal conductivity of the Cu foil reference item

Cu Foil	Temperatures (˚C)	10 Minutes (W/m.K)	20 Minutes (W/m.K)	30 Minutes (W/m.K)
0.4 mm	50	72.584	86.991	51.087
	80	64.066	67.146	58.131
	100	75.715	82.483	97.116

It is seen from the table that percentage change of the mean k show some variations depend on the T_H. Thermal conductivity value of the sample is 97.116 W/m.K and highest for T_H = 100 ˚C. It is clear from the table that k values change negatively between the T_H = 50 ˚C - 80 ˚C at a rate of 11,7 %, 22,8 % respectively. After T_H = 80 ˚C, changes are positively seen and highest for ϴ = 30 minutes with 67 %.

Changes of the thermal conductivities of the 0.4 mm Cu foil with holes reference items at different T_H are given and results compared for ϴ = 10, 20 and 30 minutes and are shown in the Figures 5.23, 5.24 and 5.25.

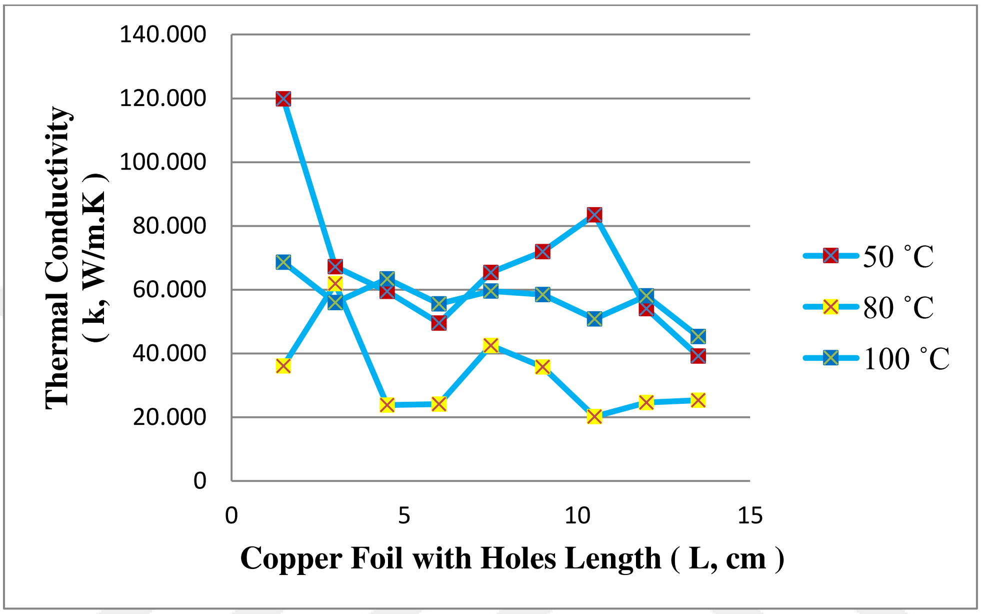

Figure 5.23 Thermal conductivity changes of the t = 0.4 mm Cu foil with holes for ϴ = 10 min.

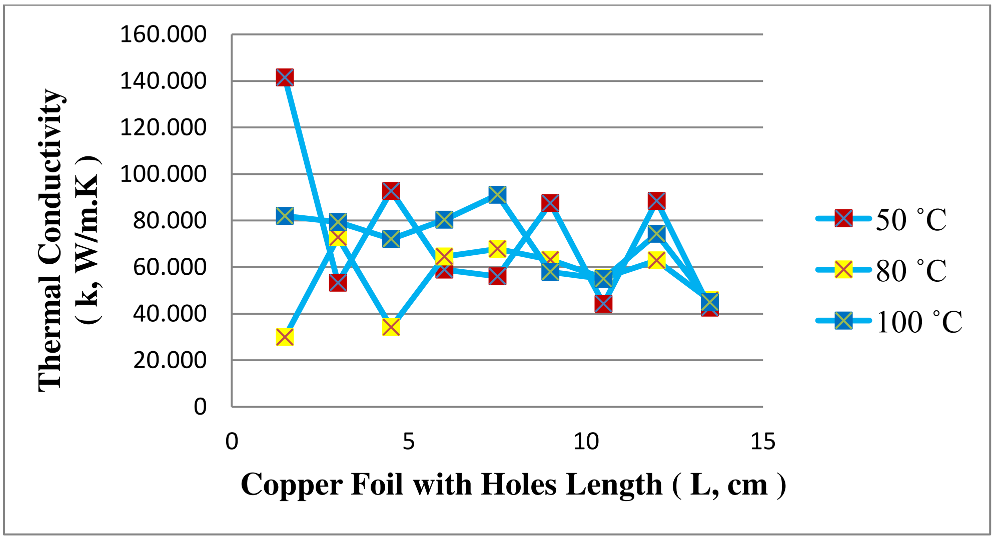

Figure 5.24 Thermal conductivity changes of the t = 0.4 mm Cu foil with holes for ϴ = 20 min.

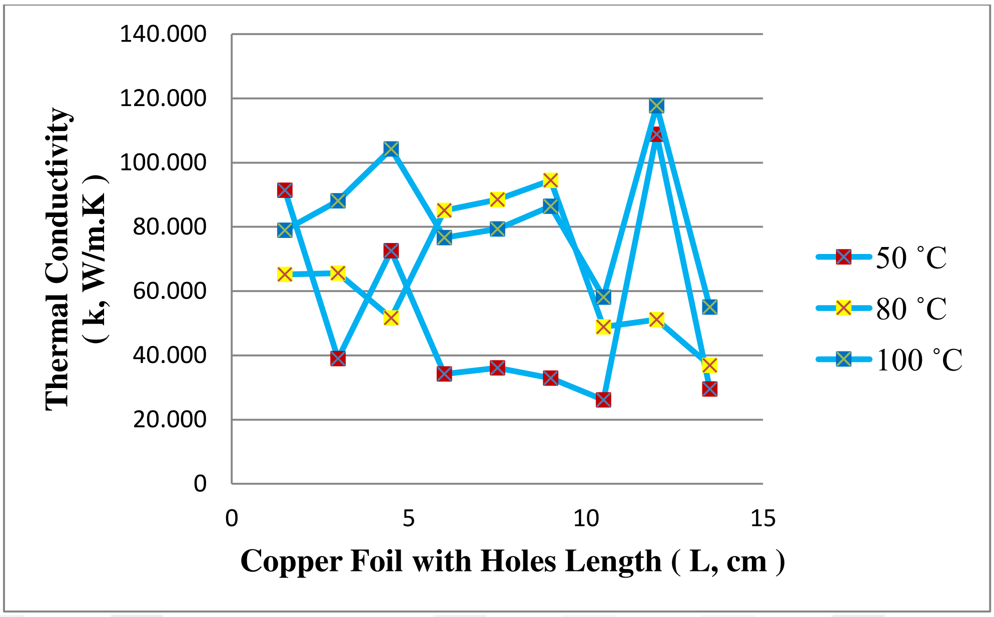

Figure 5.25 Thermal conductivity changes of the t = 0.4 mm Cu foil with holes for ϴ = 30 min.

Analysis results from the Figures 5.23, 5.24 and 5.25 show that some irregularities can be seen because of the Cu foil surface structures. Generally, k change shows near or similar profiles in the first and last region / distances of the material.

It is seen from the Figure 5.23 that k is between 20 W/m.K ≤ k ≤ 120 W/m.K, from the Figure 5.24, k is between 30 W/m.K ≤ k ≤ 140 W/m.K and from the Figure 5.25 k is between 25 W/m.K ≤ k ≤ 120 W/m.K.

Mean values of the k and changes in percent are given in the Table 5.8.

Table 5.8 : Time dependent percentage changes of the mean thermal conductivity of the Cu foil reference items with holes

Cu Foil with Holes	**Temperatures (˚C)**	**10 Minutes (W/m.K)**	**20 Minutes (W/m.K)**	**30 Minutes (W/m.K)**
0.4 mm	50	68.096	73.892	52.283
	80	32.699	55.166	65.262
	100	57.301	70.752	82.724

It is seen from the table that percentage change of the mean k show some variations depend on the $T_{H.}$ Thermal conductivity value of the sample is 82.724 W/m.K and highest for T_H = 100 ˚C. It is clear from the table that k values change negatively between the T_H = 50 ˚C - 80 ˚C at a rate of 52 %, 25,3 % respectively. After T_H = 80 ˚C, changes are positively seen and highest for ϴ = 10 minutes with 75,2 %.

As a result, time dependent thermal conductivity changes of the different thicknesses of Cu foams and Cu foils are given in the above figures. Analysis results and temperature effects based on T_H are summarized and listed as follows ;

1. Thermal conductivities of the Cu foam samples change with different T_H of 50 ˚C ≤ T_H ≤ 100 ˚C depending on the ϴ. Changes of k are irregular depending on samples t and ϴ.
2. Percentage changes of the k of the Cu foam and Cu foil samples show some different variations depending on t, ϴ and T_H.
3. From the results, effects of the T_H with changing time periods based on the Cu foams and Cu foils thicknesses on heat transfer are vital for heat source based heat transfer researches and applications.

5.3 Time Dependent Heat Capacity Changes of The Tested Copper Foam Samples

In chapter 2, basic terminology of the heat capacity of porous metal foams are given. As stated before, heat capacity is known as the internal energy of a system, or the systems microscopic kinetic and potential energy. Heat capacity or thermal capacity C, is a measurable physical quantity of a substance that characterizes the amount of heat needed to change the temperature of the substance to a given degree, in other words the ratio between the amount of heat transferred to the sample Q, and the resulting increase in temperature ΔT, by the absorbed heat is previously given in the Equation (2.12).

$$C = Q / \Delta T \qquad (2.12)$$

Where, C is heat capacity (J/K), Q is heat transferred by conduction (J), ΔT is temperature difference (K).

In Equation 2.12, Q values are calculated with same method stated before in section 5.2 by using the Equation 5.3. Calculated Q values are converted to energy unit by multiply with ϴ. As well as, ΔT values are formulated with the Equation 5.6.

$$\Delta T = (T_{m,upper} + T_{m,contact}) / 2 - T_{f,cf} \quad (5.6)$$

Where, $T_{m,upper}$ is upper surface mean temperature (˚C), $T_{m,contact}$ contact surface mean temperature of the sample (˚C) and $T_{f,cf}$ is final temperature of the Cu foam sample after the specified time period (˚C).

It is important to observe the heat capacity of the porous materials for defining the heat transfer characteristics of the materials. In this section, time dependent heat capacity changes of the Cu foam samples with respect to different thicknesses and heater temperatures are given. Depending on the t and ϴ, 9 C values are calculated for different T_H. Calculated C values are given in the Table 5.9.

Table 5.9 : Heat capacity values of the Cu foam samples at different T_H

Heat Capacity (C) Table					
T_H (˚C)	**Cu Foam Thickness (mm)**	**Time Periods ϴ, (min)**	**Q (J)**	**ΔT (K)**	**C (J/K)**
50	3	10	72,391	284.95	**254.048**
		20	137,269	281.2	**488.154**
		30	197,217	280.3	**703.592**
	4	10	72,860	284.45	**256.143**
		20	137,425	282.5	**486.460**
		30	197,217	280.6	**702.840**
	5	10	72,626	282.7	**256.901**
		20	137,269	280.85	**488.762**
		30	197,687	279.15	**708.175**
80	3	10	112,696	295.1	**381.890**
		20	207,391	289.95	**715.264**
		30	293,947	286.95	**1.024.384**
	4	10	114,260	295.75	**386.340**
		20	211,304	289.75	**729.263**
		30	296,766	286.5	**1.035.832**
	5	10	113,869	290.6	**391.841**
		20	208,174	286.25	**727.245**
		30	294,183	282.5	**1.041.356**
100	3	10	140,087	302.15	**463.634**
		20	255,130	295	**864.847**
		30	356,868	290.15	**1.229.943**
	4	10	139,226	299.1	**465.483**
		20	253,878	291.65	**870.488**
		30	354,990	286.9	**1.237.330**
	5	10	139,852	294.75	**474.477**
		20	253,878	289	**878.470**
		30	355.696	286.1	**1.243.258**

It is obvious from the table that, heat capacities of the samples increase depend on the T_H and ϴ. C values change between 250 J/K ≤ C ≤ 710 J/K for T_H = 50 ˚C, 380 J/K ≤ C ≤ 1042 J/K for T_H = 80 ˚C and 460 J/K ≤ C ≤ 1245 J/K for T_H = 100 ˚C. C values are highest for T_H = 100 ˚C. It is also important to note that, at the same T_H, thickness effects are low, there are small differences. These results show the heat capacity properties of the Cu foam samples are higher at high T_H.

5.3.1 Effects Of The Thickness on Heat Capacity Changes For The Tested Copper Foam Samples

In this section, time dependent heat capacity changes of the Cu foam samples are analysed with respect to different Cu foam thicknesses for different T_H and results are shown and compared in the Figures 5.26, 5.27 and 5.28.

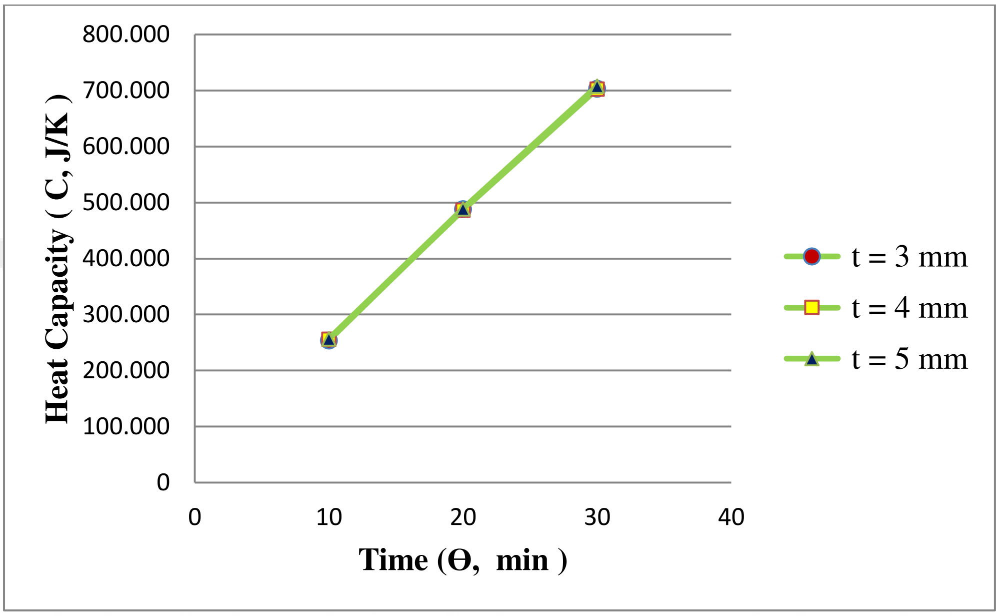

Figure 5.26 Time dependent heat capacity variations of the Cu foams at $T_H = 50$ ˚C

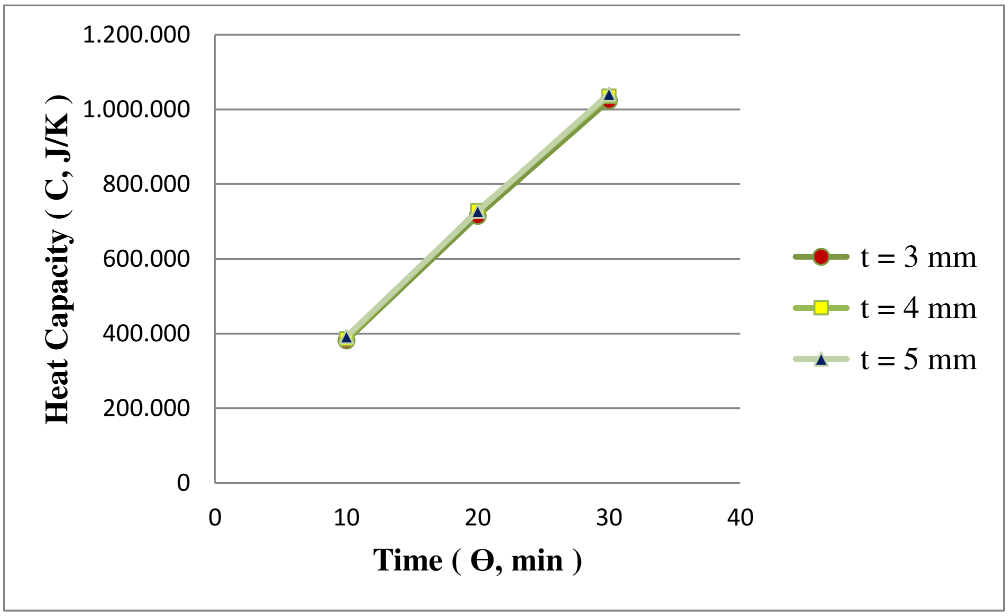

Figure 5.27 Time dependent heat capacity variations of the Cu foams at $T_H = 80$ ˚C

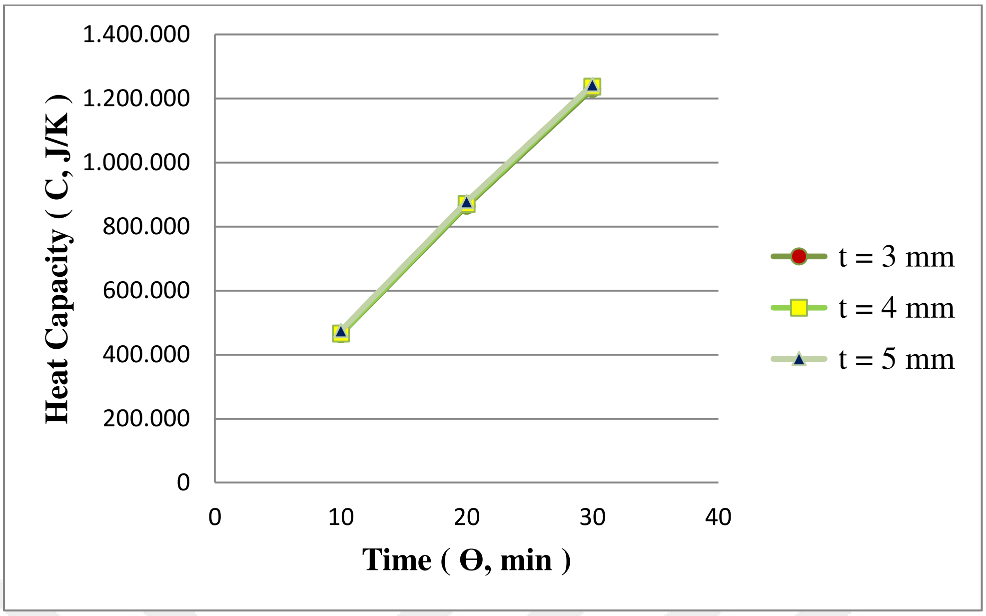

Figure 5.28 Time dependent heat capacity variations of the Cu foams at T_H = 100 ˚C

As can be seen from the Figures 5.26 through 5.28, effects of the t are low for the specified T_H. Differences depending on the Θ for T_{H} = 50 ˚C , 80 ˚C and 100 ˚C are (2.85 J/K – 4.5 J/K), (9.9 J/K – 17 J/K) and (11 J/K – 13 J/K) respectively.

5.3.2 Effects Of The Temperatures on Heat Capacity Changes For The Tested Copper Foam Samples

Similarly, time dependent heat capacity changes of the Cu foam samples are analyzed with respect to different T_H and results are shown in the Figures 5.29, 5.30, 5.31 and 5.32.

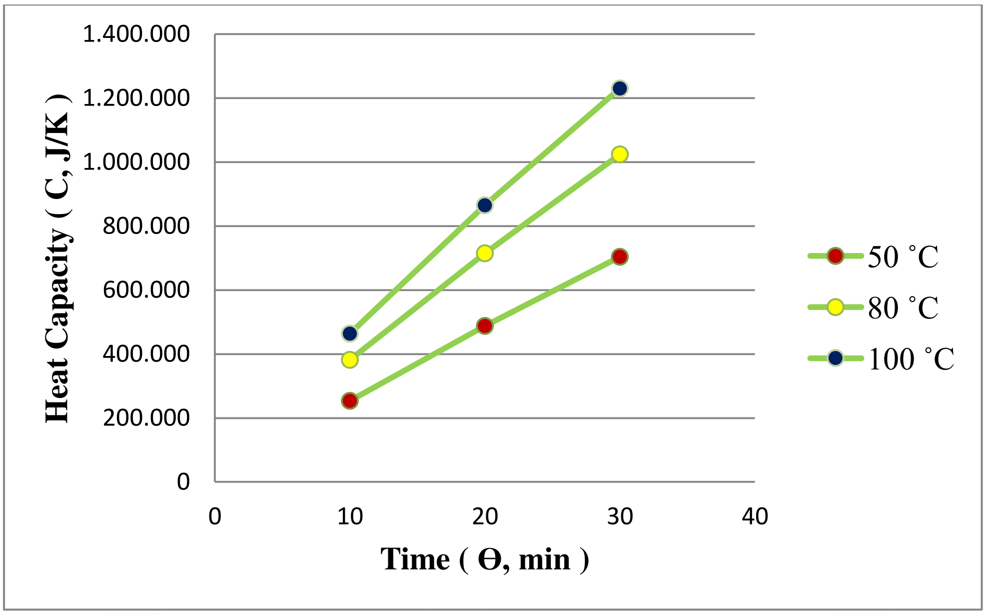

Figure 5.29 Time dependent heat capacity variations of the t = 3 mm Cu foam sample

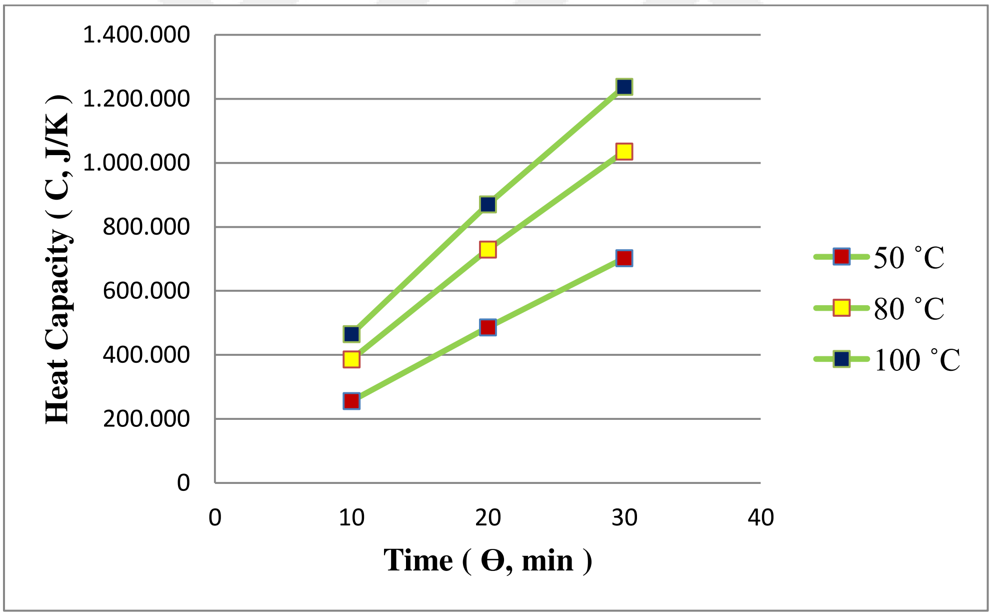

Figure 5.30 Time dependent heat capacity variations of the t = 4 mm Cu foam sample

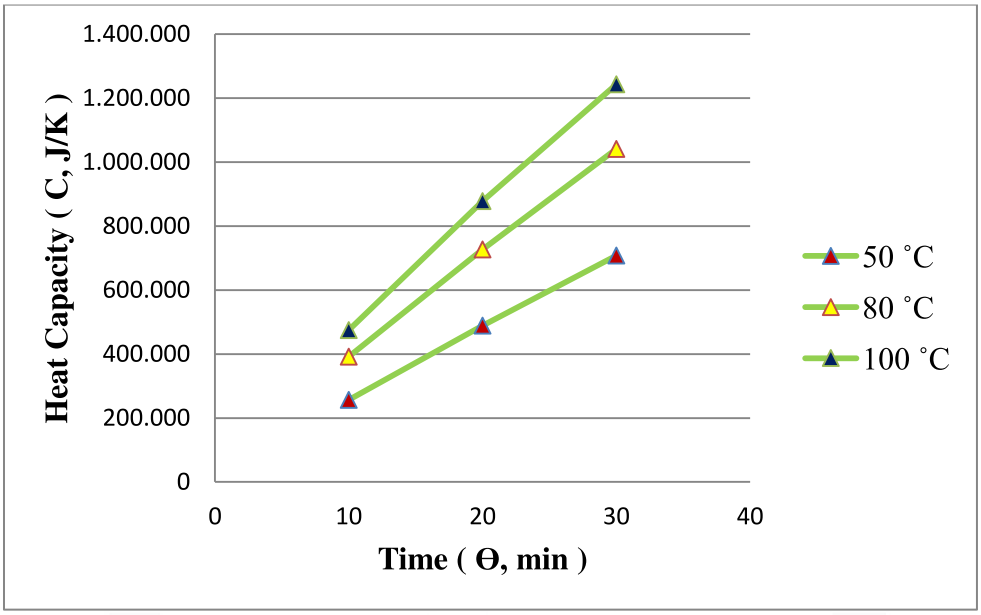

Figure 5.31 Time dependent heat capacity variations of the t = 5 mm Cu foam sample

Analysis results from the Figures 5.29 through 5.31 show that, effects of the T_H and Θ on the C are high. On the other hand, effects of the t on the C change are small. Time dependent variations of C values of t = 3 mm Cu foam sample change between 254 J/K ≤ C ≤ 704 J/K for $T_{H=}$ 50 ˚C, 380 J/K ≤ C ≤ 1025 J/K for $T_{H=}$ 80 ˚C and 463 J/K ≤ C ≤ 1230 J/K for $T_{H=}$ 100 ˚C.

Time dependent variations of C values of t = 4 mm Cu foam sample change between 250 J/K ≤ C ≤ 703 J/K for $T_{H=}$ 50 ˚C, 386 J/K ≤ C ≤ 1035 J/K for $T_{H=}$ 80 ˚C and 465 J/K ≤ C ≤ 1240 J/K for $T_{H=}$ 100 ˚C, and finally, time dependent variations of C values of t = 5 mm Cu foam sample change between 256 J/K ≤ C ≤ 709 J/K for $T_{H=}$ 50 ˚C, 390 J/K ≤ C ≤ 1040 J/K for $T_{H=}$ 80 ˚C and 470 J/K ≤ C ≤ 1245 J/K for $T_{H=}$ 100 ˚C.

Lastly, Figure 5.32 presented the all C values of the samples as a function of varying times.

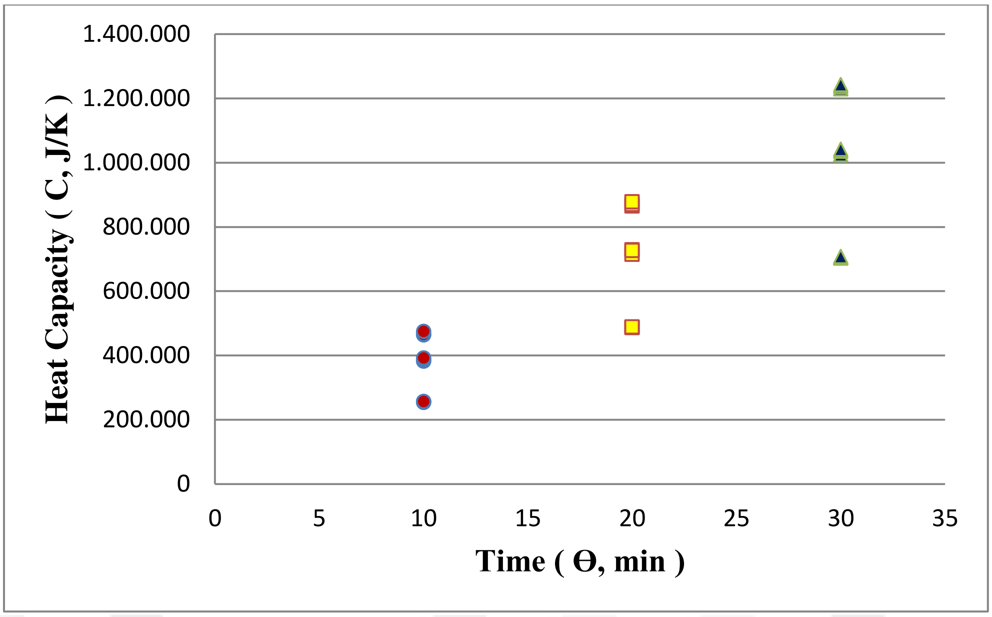

Figure 5.32 Time dependent heat capacity distributions of the Cu Foam samples

Results show that, there are some similarities and differences depending on the Θ. It is clear from the figure, C values are more near to each other which approximately change between the 200 J/K ≤ C ≤ 500 J/K for 10 minutes and more far to each other which change between the 700 J/K ≤ C ≤ 1300 J/K for 30 minutes.

As a result of the all analysis, time dependent heat capacity changes of the Cu foam samples are given in the above figures. Analysis results are summarized and listed as follows;

1. Heat capacity values of the Cu foams at a given T_H for different thicknesses are nearly same, there are small differences but increase with Θ. For that reason, from the figures, it is obvious that effects of the thicknesses are lowest. As can be seen from the Figures 5.26 through 5.28, differences for C values depending on the Θ for $T_{H=}$ 50 ˚C, 80 ˚C and 100 ˚C are (2.85 J/K – 4.5 J/K), (9.9 J/K – 17 J/K) and (11 J/K – 13 J/K) respectively.

2. Depending on the T_H, heat capacities of the Cu foam samples show some changes with respect to Θ. At high T_H, C values are highest compared with other T_H results.

3. Depending on the T_H, differences between the heat capacities of the samples are lowest for Θ = 10 min. After Θ =10 min, differences can be seen morely.

4. Finally, it can be seen from the Figure 5.32 that C values are more near to each other which approximately change between the 200 J/K $\leq$ C $\leq$ 500 J/K for 10 min. and more far to each other which change between the 700 J/K $\leq$ C $\leq$ 1300 J/K for 30 min.

5.4 Time Dependent Thermal Diffusivity Changes of The Tested Copper Foam Samples

In chapter 2, basic definitions of the thermal diffusivity of porous metal foams are given. As stated before, thermal diffusivity of a material is the thermal inertia of that material. It can be understood as the ability of a material to conduct heat, relative to the heat stored per unit mass or volume. In other words, defines the speed of heat propagation by conduction during changes of temperature. Thermal diffusivity of a material can be defined as the thermal conductivity divided by the product of specific heat capacity and density which expressed mathematically in the Equation 2.13 as follow;

$$\alpha = k / (\rho . C_p) \qquad (2.13)$$

where, α is thermal diffusivity (m^2/s) or (mm^2/s), k is thermal conductivity W/(m.K), ρ is density (kg/m^3), C_p is specific heat capacity J/(kg.K).

In equation 2.13, k values are previously calculated in section 5.2, ρ values of the samples calculated by using the equation 3.1 in chapter 3 and C_p values are found by dividing the C values of the sample to the mass values of the samples stated in the Table 3.2. 9 α values are calculated for each T_H.

It is important to analyse the thermal diffusivity values of the Cu foam samples for defining the thermal characteristics. For this aim, in this section, time dependent thermal diffusivity changes of the Cu foam samples with respect to different t and T_H are given. Calculated α values are given in the Table 5.10 as follows,

Table 5.10 : Thermal diffusivity values of the Cu foams at different T_H

Thermal Diffusivity (α) Table						
T_H (˚C)	**Cu Foam Thickness** (mm)	**Time Periods** Ɵ, (min)	**k** (W/(m.K))	**ρ** (kg/m3)	**Cp** (J/(kg.K))	**α** (mm²/s)
50	3	10	260.840	715.555	26,299	**13.861**
		20	294.205	715.555	50,533	**8.136**
		30	308.599	715.555	72,836	**5.921**
	4	10	367.301	639.444	22,254	**25.811**
		20	426.265	639.444	42,264	**15.773**
		30	447.348	639.444	61,063	**11.457**
	5	10	479.719	616.444	18,522	**42.015**
		20	621.260	616.444	35,239	**28.600**
		30	650.896	616.444	51,058	**20.680**
80	3	10	140.263	715.555	39,533	**4.958**
		20	170.063	715.555	74,044	**3.210**
		30	246.312	715.555	106,044	**3.246**
	4	10	291.046	639.444	33,565	**13.560**
		20	311.331	639.444	63,359	**7.684**
		30	391.348	639.444	89,994	**6.800**
	5	10	381.768	616.444	28,251	**21.922**
		20	489.508	616.444	52,433	**15.145**
		30	503.869	616.444	75,079	**10.887**
100	3	10	164.949	715.555	47,995	**4.803**
		20	208.268	715.555	89,529	**3.251**
		30	248.322	715.555	127,323	**2.726**
	4	10	285.298	639.444	40,442	**11.032**
		20	347.070	639.444	75,629	**7.177**
		30	428.070	639.444	107,500	**6.227**
	5	10	370.076	616.444	34,209	**17.549**
		20	503.352	616.444	63,336	**12.892**
		30	650.282	616.444	89,636	**11.769**

It is obvious from the table that, thermal diffusivities of the samples increase depending on the increasing t. α values change between the 5 $mm^2/s \leq \alpha \leq 42$ mm^2/s for T_H = 50 ˚C, 3 $mm^2/s \leq \alpha \leq 22$ mm^2/s for T_H = 80 ˚C and 2 $mm^2/s \leq \alpha \leq 18$ mm^2/s for T_H = 100 ˚C. α values are highest for T_H = 50 ˚C. It is also important to note that, at the same T_H, thickness effects are high, there are some differences. These results show the thermal diffusivity properties of the Cu foam samples are higher at low T_H.

Analysis results compared and effects of the t and T_H are given in the following sections in detail.

5.4.1 Effects Of The Thickness on Thermal Diffusivity Change For The Tested Copper Foam Samples

In this section, time dependent thermal diffusivity changes of the Cu foam samples are analysed with respect to different Cu foam thicknesses for different T_H and results are shown in the Figures 5.33, 5.34 and 5.35.

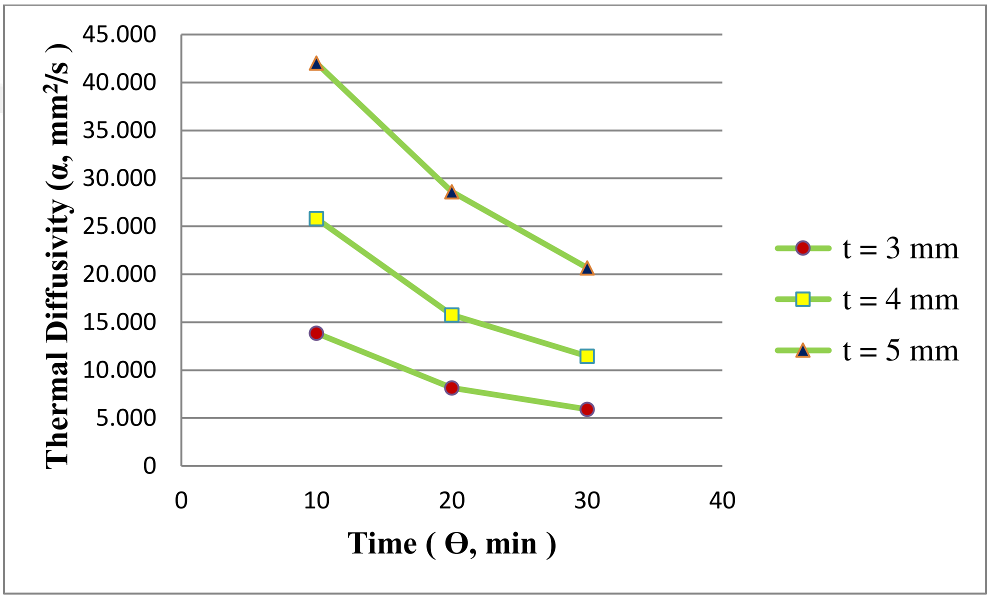

Figure 5.33 Time dependent thermal diffusivity variations of the Cu foams at $T_H = 50$ ˚C

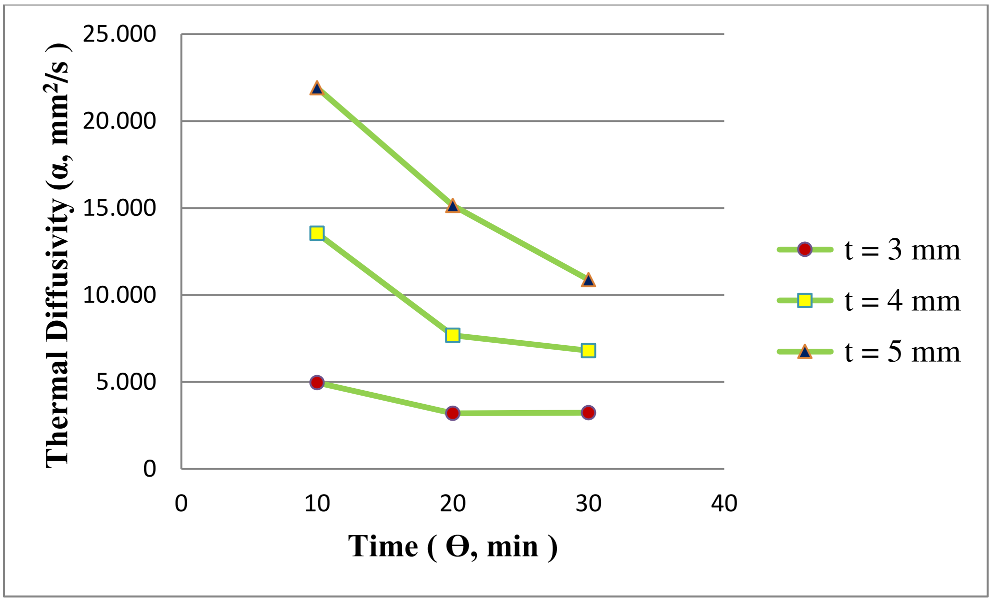

Figure 5.34 Time dependent thermal diffusivity variations of the Cu foams at $T_H = 80$ ˚C

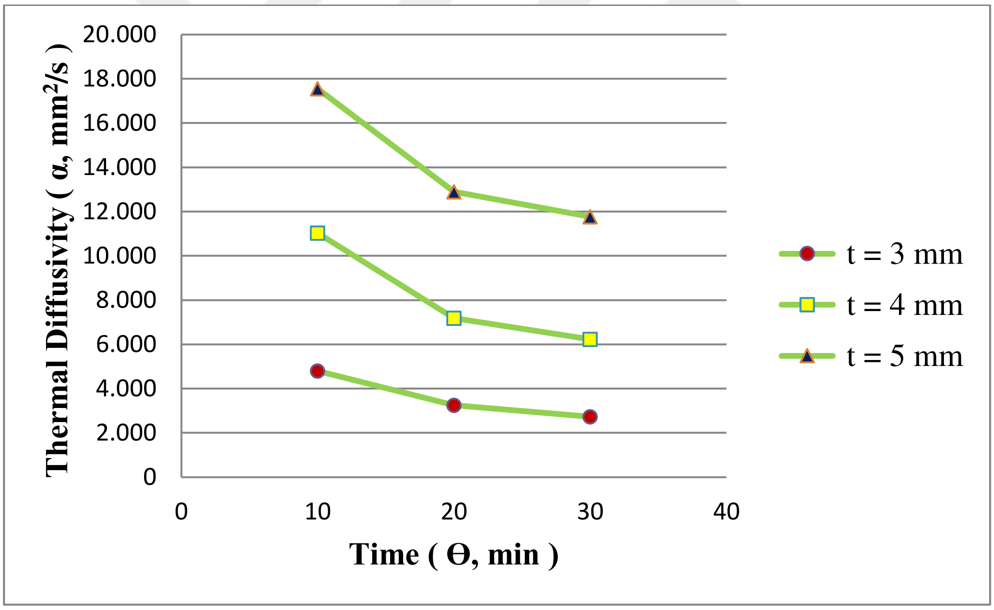

Figure 5.35 Time dependent thermal diffusivity variations of the Cu foams at $T_H = 100$ ˚C

Analysis results from the Figure 5.33 through 5.35 show that, α values of the samples decrease depending on the Θ. α values of the 5 mm thickness Cu foam sample are higher than the other samples. α values of the samples change between the 8 $mm^2/s \leq \alpha \leq 14$ mm^2/s for t = 3 mm, 11 $mm^2/s \leq \alpha \leq 26$ mm^2/s for t = 4 mm and 20 $mm^2/s \leq \alpha \leq 42$ mm^2/s for t = 5 mm at $T_H = 50$ ˚C. Similarly, α values of the samples change between the 3 $mm^2/s \leq \alpha \leq 5$ mm^2/s for t = 3 mm, 6 $mm^2/s \leq \alpha \leq 14$ mm^2/s for t = 4 mm and 10 $mm^2/s \leq \alpha \leq 22$ mm^2/s for t = 5 mm at $T_H = 80$ ˚C. Finally, α values of the samples change between the 3 $mm^2/s \leq \alpha \leq 5$ mm^2/s for t = 3 mm, 6 $mm^2/s \leq \alpha \leq 12$ mm^2/s for t = 4 mm and 10 $mm^2/s \leq \alpha \leq 18$ mm^2/s for t = 5 mm at $T_H = 100$ ˚C. It is also important to note that, α values decrease with increasing T_H.

5.4.2 Effects of The Temperatures on Thermal Diffusivity Change For The Tested Copper Foam Samples

Similarly, time dependent thermal diffusivity changes of the Cu foam samples are analyzed with respect to different T_H and results are shown in the Figures 5.36, 5.37, 5.38 and 5.39.

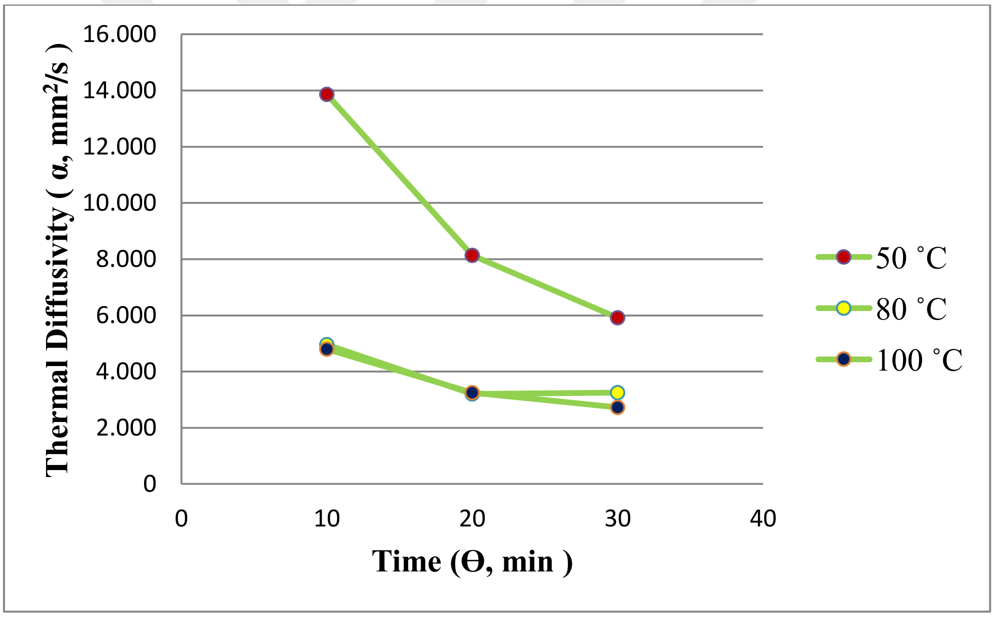

Figure 5.36 Time dependent thermal diffusivity variations of the t = 3 mm Cu foam

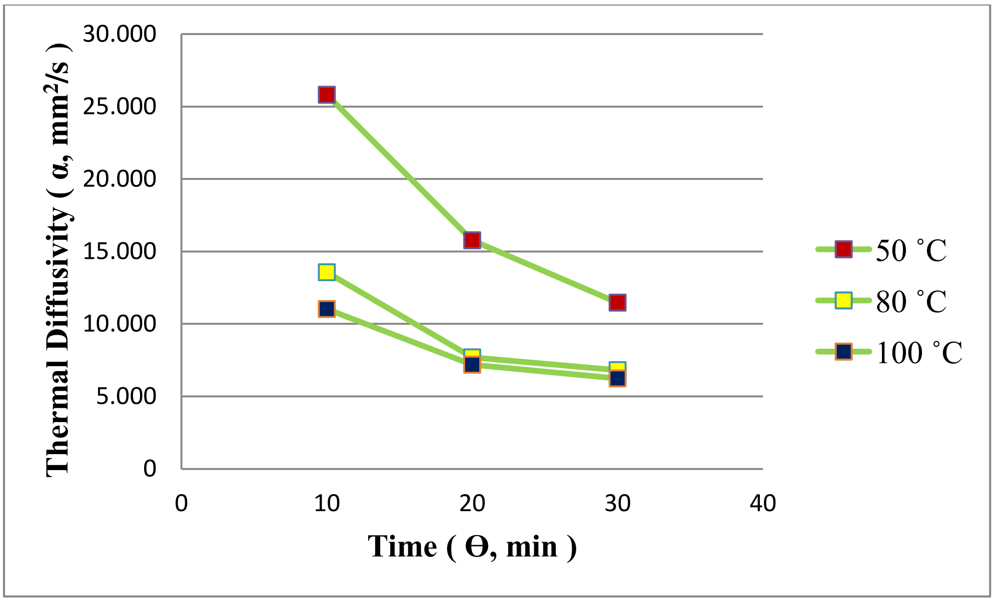

Figure 5.37 Time dependent thermal diffusivity variations of the t = 4 mm Cu foam

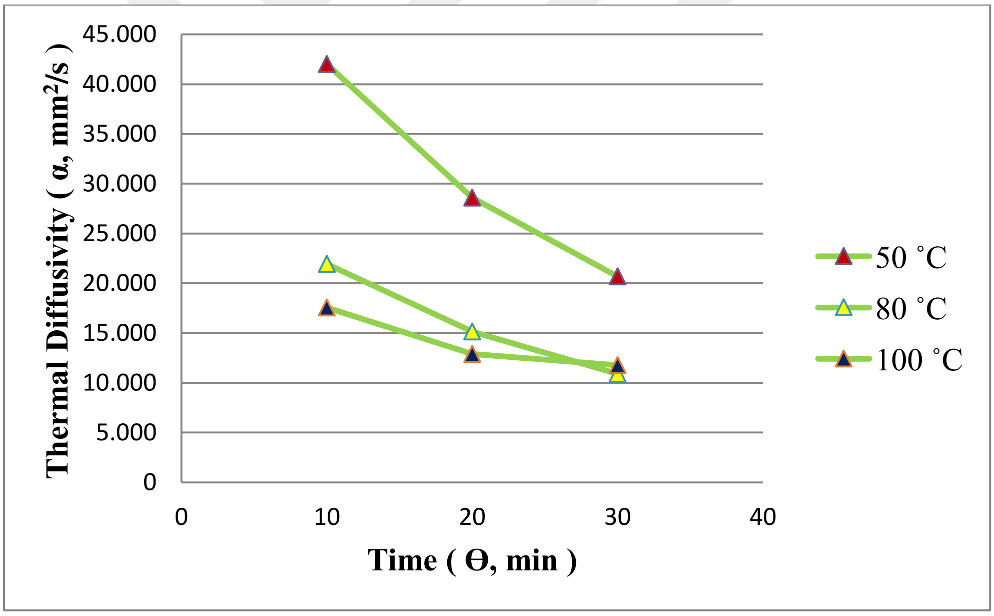

Figure 5.38 Time dependent thermal diffusivity variations of the t = 5 mm Cu foam

It is obvious from the Figure 5.36 through 5.38, depending on the T_H, α values show some variations. From the Figure 5.36, difference in α values between the T_H = 50 ˚C - 100 ˚C is 14.8 mm^2/s for ϴ = 10 min, 5 mm^2/s for ϴ = 20 min and 3.3 mm^2/s for ϴ = 30 min.

Likely, from the Figure 5.37, difference in α values between the T_H = 50 ˚C - 100 ˚C is 8.9 mm^2/s for ϴ = 10 min, 8.7 mm^2/s for ϴ = 20 min and 5.2 mm^2/s for ϴ = 30 min.

Finally, from the Figure 5.38, difference in α values between the T_H = 50 ˚C - 100 ˚C is 24.5 mm^2/s for ϴ = 10 min, 15.7 mm^2/s for ϴ = 20 min and 8.9 mm^2/s for ϴ = 30 min. From the results, it can be say that the effects of the T_H are more clear between the T_H = 50 ˚C - 80 ˚C, and T_H = 50 ˚C - 100 ˚C. It is seen that there is a little difference between T_H = 80 ˚C - 100 ˚C.

Lastly, Figure 5.39 presented the distribution of the all α values of the Cu foam samples as a function of the varying times.

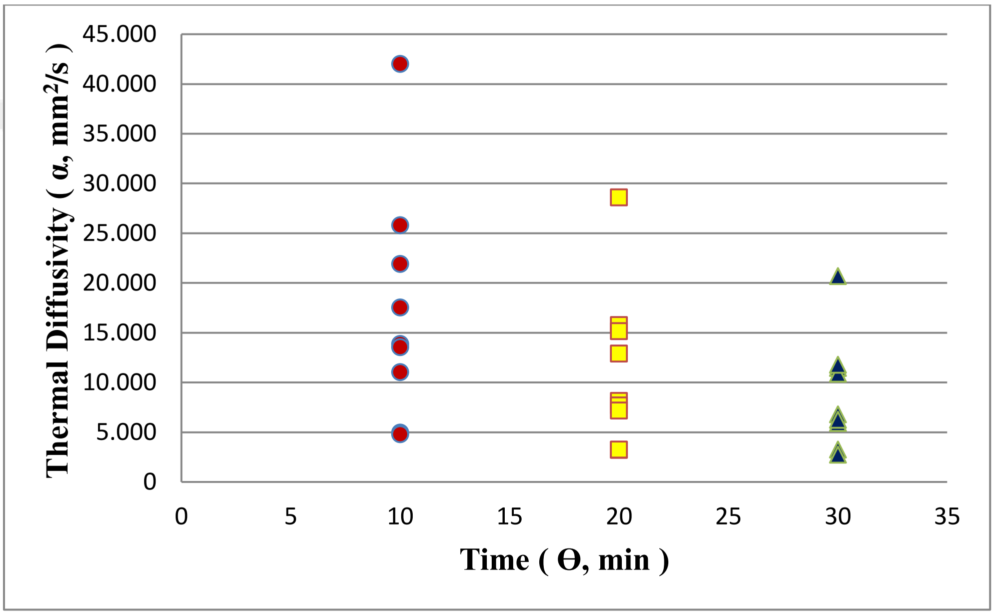

Figure 5.39 Time dependent thermal diffusivity distributions of the Cu Foams

Results from the Figures 5.39 show that, there are some similarities and differences can be seen depending on the ϴ. For example, α values change between the 5 $mm^2/s \leq \alpha \leq$ 43 mm^2/s for 10 min, 4 $mm^2/s \leq \alpha \leq$ 28 mm^2/s for 20 min and 3 $mm^2/s \leq \alpha \leq$ 21 mm^2/s for 30 min. These results show the variation range of the α is highest for ϴ = 10 min and lowest for ϴ = 30 min.

As a result, time dependent α changes of the Cu foam samples are given in the above figures. Analysis results are summarized and listed as follows;

1. Thermal diffusivity values of the Cu foams at a given T_H increase with Cu foam thickness but decrease with increasing ϴ. For that reason, from the figures, it is obvious that effects of the thickness are high.
2. Depend on the T_H, α values of the Cu foam samples show some differences. α values are highest at T_H = 50 ˚C compared with other T_H and nearly same for T_H = 80 ˚C and 100 ˚C. On the other hand, time dependent α changes of Cu foams are more rapid and highest at T_H = 50 ˚C.
3. Finally, it can be seen from the last figure that α ranges and values of the Cu foam samples decrease with increasing ϴ.

5.5 Effects of The Cooling Time on Thermal Profiles of The Tested Cu Foam Samples

In this section, in order to define the cooling performance of the Cu foam samples, analysis of effects of the cooling times on thermal profiles of the tested Cu foam samples are presented. Test samples' contact surfaces, which exposed to T_H = 80 ˚C and 100 ˚C through heating process for ϴ = 10 min, are located on reference plate of white paper as a cooling medium until the contact surface temperature comes to T_R values. Thermal views of the contact surfaces are taken periodically for ϴ = 0, 3, 6 and 10 minutes. Thermal profiles are shown and compared in Figures 5.40 through 5.45.

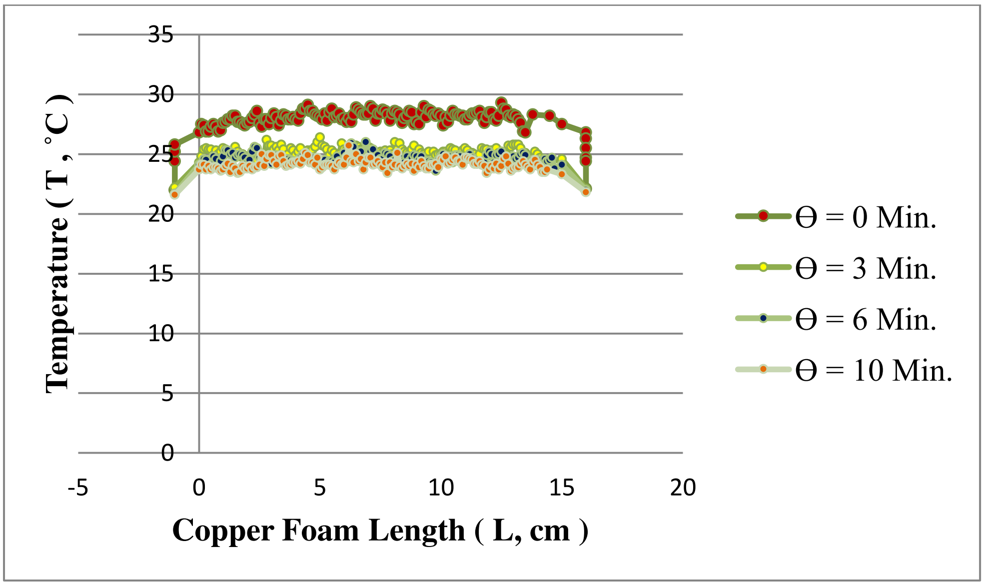

Figure 5.40 Thermal profiles of 3 mm thickness Cu foam sample at T_H = 80 ˚C as a function of ϴ.

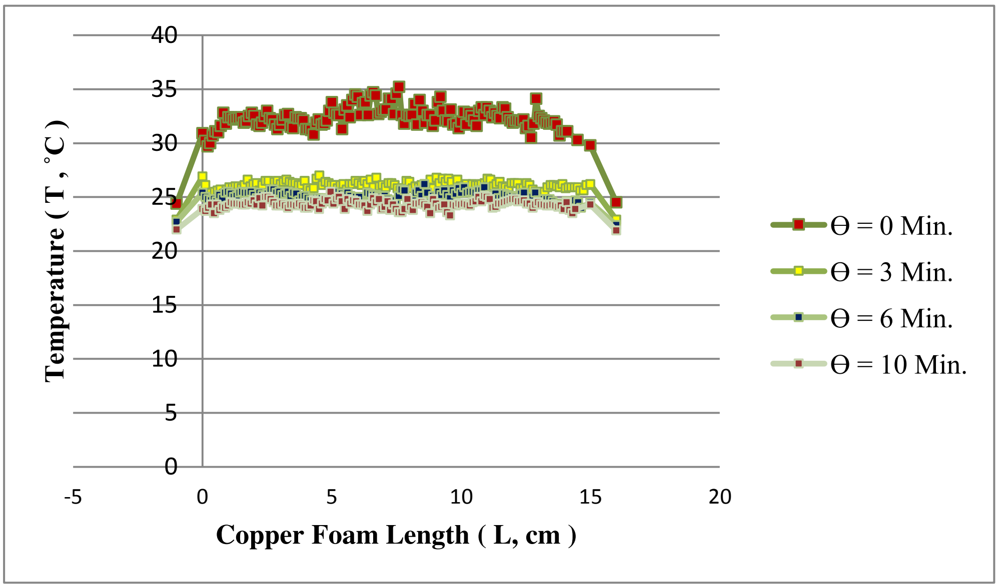

Figure 5.41 Thermal profiles of 4 mm thickness Cu foam sample at T_H = 80 ˚C as a function of ϴ.

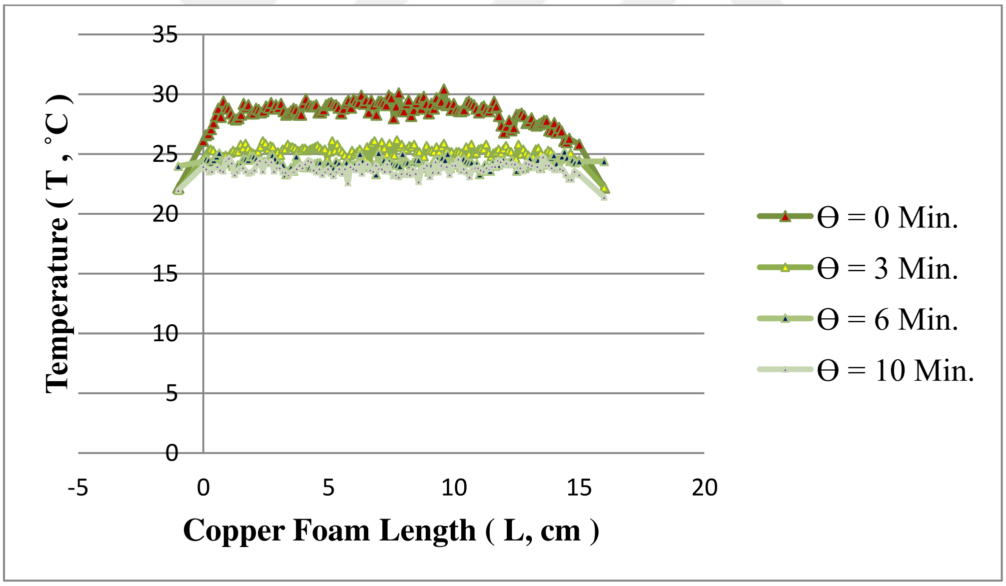

Figure 5.42 Thermal profiles of 5 mm thickness Cu foam sample at T_H = 80 ˚C as a function of ϴ.

It is obvious from the Figures 5.40 through 5.42 that, thermal profiles of the samples show high temperature values at ϴ = 0 min. After the 0.min, thermal profiles show near temperature values depending on the increasing ϴ. $T_{m,\ contact}$ values for ϴ = 0, 3, 6 and 10 min. are 27.8 ˚C, 25.1 ˚C, 24.5 ˚C and 24.1 ˚C for t = 3 mm Cu foam sample.

Similarly, $T_{m, contact}$ values for t = 4 mm Cu foam sample are 32.3 ˚C, 26.1 ˚C, 25.1˚C and 24.2 ˚C.

Finally, $T_{m, contact}$ values for t = 5 mm Cu foam sample are 28.5 ˚C, 25.2 ˚C, 24.2˚C and 23.7 ˚C. Analysis results indicates that $T_{m,contact}$ value of the 4 mm Cu foam is higher than the other thicknesses of the sample. Thermal profiles for T_H = 100 ˚C are shown and compared in Figures 5.43 through 5.45.

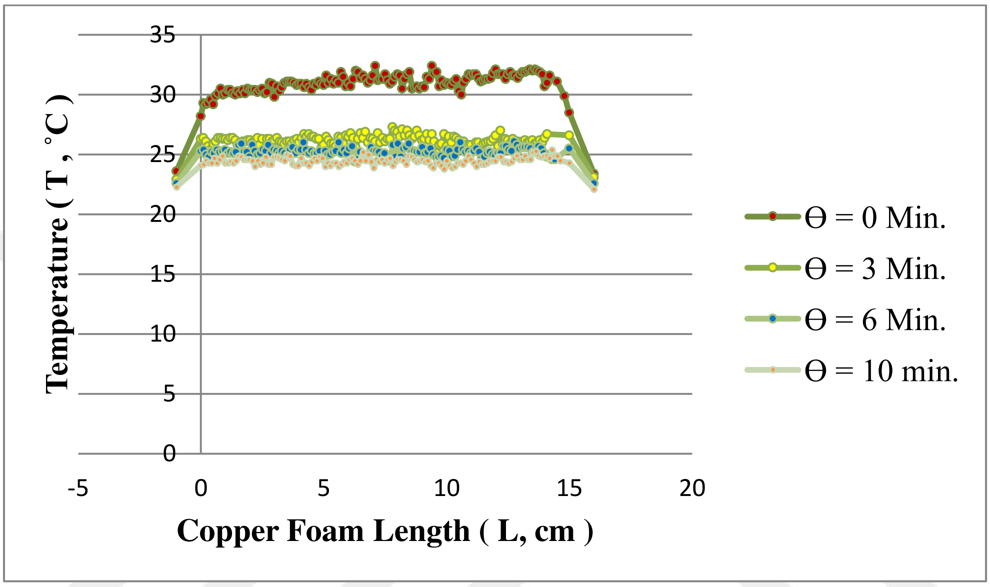

Figure 5.43 Thermal profiles of 3 mm thickness Cu foam sample at T_H = 100 ˚C as a function of Θ.

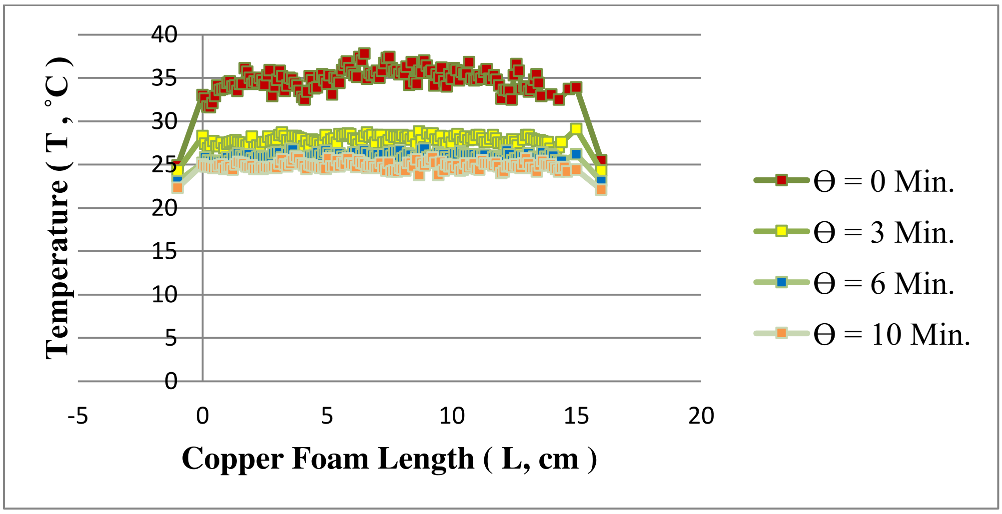

Figure 5.44 Thermal profiles of 4 mm thickness Cu foam sample at T_H = 100 ˚C as a function of Θ.

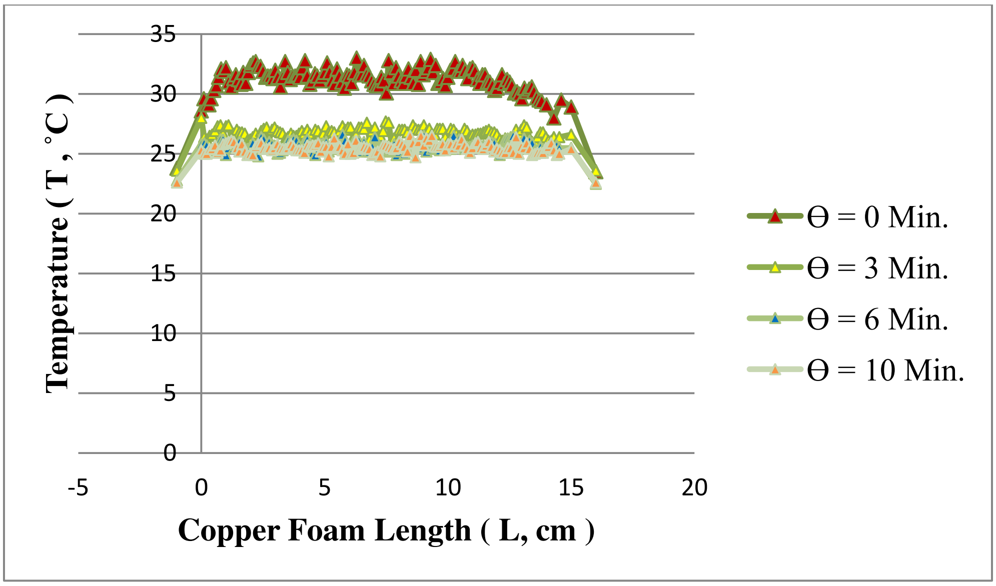

Figure 5.45 Thermal profiles of 5 mm thickness Cu foam sample at T_H = 100 ˚C as a function of ϴ.

It is obvious from the Figures 5.43 through 5.45 that, thermal profiles of the samples show high temperature values at ϴ = 0 min. After the 0.min, thermal profiles show near temperature values depend on the ϴ. $T_{m, contact}$ values for ϴ = 0, 3, 6 and 10 min. are 30.8 ˚C, 26.1 ˚C, 25 ˚C and 24.4 ˚C for t = 3 mm Cu foam sample.

Similarly, $T_{m, contact}$ values for t = 4 mm Cu foam sample are 34.6 ˚C, 27.5 ˚C, 25.9˚C and 24.8 ˚C.

Finally, $T_{m, contact}$ values for t = 5 mm Cu foam sample are 31.1 ˚C, 26.8 ˚C, 25.7˚C and 25.5 ˚C. Analysis results indicates that $T_{m,contact}$ value of the 4 mm Cu foam is higher than the other thicknesses of the sample.

Analysis results showed the effects of the cooling time on the thermal profile of the Cu foam samples as a function of T_H, t and ϴ. In another words, effects of the porous medium on the cooling performance are described in detail.

Time dependent $T_{m, contact}$ values from the Figures 5.40 through 5.45 are summarized in the Table 5.11

Table 5.11 : Time dependent contact surface mean temperature values of the Cu foam samples

T_H (˚C)	Cu Foam Thickness, t (mm)	Contact Surface Mean Temperature, $T_{m,contact}$ (˚C)			
		Ɵ = 0 Min.	Ɵ = 3 Min.	Ɵ = 6 Min.	Ɵ = 10 Min.
80	3	28.1	25.2	24.6	24.1
	4	32.3	26.1	25.1	24.2
	5	28.5	25.2	24.2	23.8
100	3	30.8	26.1	25	24.4
	4	34.6	27.5	25.9	24.8
	5	31.1	26.8	25.7	25.5

It is clear from the Table 5.11 that, contact surface temperature values of the sample decrease depending on the increasing Ɵ. Percentage change rate of the contact surface temperature in 10 minutes at T_H = 80 ˚C for t = 3 mm, 4 mm and 5 mm Cu samples are % 14.2, % 25 and % 16.5. For T_H = 100 ˚C, these values are % 20.8, % 28.3 and % 18 respectively.

It is clearly seen from the results that change rate is higher for T_H = 100 ˚C. It is also important to note that t = 4 mm Cu foam sample shows the highest temperature change rate and temperature values depending on the Ɵ compared with other Cu foam samples. In addition to the these results, $T_{m,contact}$ values are higher at T_H = 100 ˚C. After Ɵ = 6. minutes, contact surface temperatures of the samples nearly come to the T_R. Temperature differences and changes can be easily seen for Ɵ = 0. minutes. These results showed the effects of the T_H, t and Ɵ on the heat transfer from the Cu foam surface.

5.6 Conclusion

In the first section of the this chapter, investigations of the thermal characteristics of the Cu foam samples and Cu foil reference items are presented in detail. It is obvious that to define the thermal characteristics of a material, analyses of thermal conductivity, heat capacity and thermal diffusivity are important and key parameters. For this aim, in the each section, effects of the t, T_H and Θ are sensitively considered. Analysis results are given and summarized at the end of the each sections.

Results indicates that there are large differences between Cu foam samples and Cu foil reference items k values due to effects of the porous medium. For example, conclusions ;

For k :

- Time dependent k values of t = 3 mm Cu foam sample change between 260 W/m.K ≤ k ≤ 309 W/m.K for T_H = 50 ˚C, 140 W/m.K ≤ k ≤ 247 W/m.K for T_H = 80 ˚C and 160 W/m.K ≤ k ≤ 250 W/m.K for T_H = 100 ˚C.
- Time dependent k values of t = 4 mm Cu foam sample change between 360 W/m.K ≤ k ≤ 450 W/m.K for T_H = 50 ˚C, 290 W/m.K ≤ k ≤ 392 W/m.K for T_H = 80 ˚C and 285 W/m.K ≤ k ≤ 430 W/m.K for T_H = 100 ˚C.
- Time dependent k values of t = 5 mm Cu foam sample change between 479 W/m.K ≤ k ≤ 651 W/m.K for T_H = 50 ˚C, 380 W/m.K ≤ k ≤ 504 W/m.K for T_H = 80 ˚C and 370 W/m.K ≤ k ≤ 650 W/m.K for T_H = 100 ˚C.
- Time dependent k values of t = 0.4 mm Cu foil reference sample change between 50 W/m.K ≤ k ≤ 87 W/m.K for T_H = 50 ˚C, 58 W/m.K ≤ k ≤ 68 W/m.K for T_H = 80 ˚C and 75 W/m.K ≤ k ≤ 98 W/m.K for T_H = 100 ˚C.
- Time dependent k values of t = 0.4 mm Cu foil with holes reference sample change between 52 W/m.K ≤ k ≤ 74 W/m.K for T_H = 50 ˚C, 32

W/m.K ≤ k ≤ 66 W/m.K for T_H = 80 ˚C and 57 W/m.K ≤ k ≤ 83 W/m.K for T_H = 100 ˚C.

Time dependent variations of the thermal conductivity of the different thicknesses of porous copper foam samples change between 140 W/m.K ≤ k ≤ 651 W/m.K and 32 W/m.K ≤ k ≤ 98 W/m.K for copper foil reference item samples. It is obvious from the results that porous copper foam samples have much higher thermal conductivity values than copper foil reference item samples. This situations indicate the effects of the porous medium on thermal conductivity and also show effects of the t, T_H and Θ on k between the porous and non-porous medium in terms of thermal performances.

For C :

Heat capacity values of the Cu foams at a given T_H for different thicknesses are nearly same, there are small differences but increase with increasing Θ. For that reason, it is obvious that effects of the thicknesses are lowest. As can be seen from the Figures 5.26 through 5.28, differences for C values depending on the Θ for $T_{H=}$ 50 ˚C, 80 ˚C and 100 ˚C are (2.85 J/K – 4.5 J/K), (9.9 J/K – 17 J/K) and (11 J/K – 13 J/K) respectively.

Time dependent variations of C values of t = 3 mm Cu foam sample change between 254 J/K ≤ C ≤ 704 J/K for $T_{H=}$ 50 ˚C, 380 J/K ≤ C ≤ 1025 J/K for $T_{H=}$ 80 ˚C and 463 J/K ≤ C ≤ 1230 J/K for $T_{H=}$ 100 ˚C.

Time dependent variations of C values of t = 4 mm Cu foam sample change between 250 J/K ≤ C ≤ 703 J/K for $T_{H=}$ 50 ˚C, 386 J/K ≤ C ≤ 1035 J/K for $T_{H=}$ 80 ˚C and 465 J/K ≤ C ≤ 1240 J/K for $T_{H=}$ 100 ˚C.

Time dependent variations of C values of t = 5 mm Cu foam sample change between 256 J/K ≤ C ≤ 709 J/K for $T_{H=}$ 50 ˚C, 390 J/K ≤ C ≤ 1040 J/K for $T_{H=}$ 80 ˚C and 470 J/K ≤ C ≤ 1245 J/K for $T_{H=}$ 100 ˚C.

Heat capacity values of the porous copper foam samples change between 250 J/K ≤ C ≤ 1245 J/K and 255 J/K ≤ C ≤ 1270 J/K for copper foil reference item samples depending on the different parameters of T_H, t and Θ. Results show that there is a little difference between the test samples.

For α :

α values of the samples change between the 8 $mm^2/s \leq \alpha \leq 14$ mm^2/s for t = 3 mm, 11 $mm^2/s \leq \alpha \leq 26$ mm^2/s for t = 4 mm and 20 $mm^2/s \leq \alpha \leq 42$ mm^2/s for t = 5 mm at T_H = 50 ˚C.

Similarly, α values of the samples change between the 3 $mm^2/s \leq \alpha \leq 5$ mm^2/s for t = 3 mm, 6 $mm^2/s \leq \alpha \leq 14$ mm^2/s for t = 4 mm and 10 $mm^2/s \leq \alpha \leq 22$ mm^2/s for t = 5 mm at T_H = 80 ˚C.

Finally, α values of the samples change between the 3 $mm^2/s \leq \alpha \leq 5$ mm^2/s for t = 3 mm, 6 $mm^2/s \leq \alpha \leq 12$ mm^2/s for t = 4 mm and 10 $mm^2/s \leq \alpha \leq 18$ mm^2/s for t = 5 mm at T_H = 100 ˚C. It is also important to note that, α values decrease with increasing T_H.

As a result, thermal diffusivity of the porous copper foam samples change between 3 $mm^2/s \leq \alpha \leq 42$ mm^2/s and 0.1 $mm^2/s \leq \alpha \leq 0.8$ mm^2/s for copper foil reference item samples depending on the different parameters of T_H, t and Θ. These results show that speed of heat propagation inside the porous copper foam samples is much higher than the copper foil reference item samples.

For Cooling Time :

In the second section of the chapter, a detailed analyses and results of the effects of the cooling times on the thermal profiles of the Cu foam test samples are given. Time dependent temperature variations and percentage change rate for all conditions are shown.

Contact surface temperature values of the samples decrease depending on the increasing Θ. Percentage change rate of the contact surface temperature in 10 minutes at T_H = 80 ˚C for t = 3 mm, 4 mm and 5 mm Cu samples are % 14.2, % 25 and % 16.5. For T_H = 100 ˚C, these values are % 20.8, % 28.3 and % 18 respectively.

All experimental analysis results showed the thermal conductivity, heat capacity properties of the Cu foam samples are high, on the other hand, α values are lower. it is seen from the results that cooling time of the Cu foam samples is short. As a result, Cu foam materials can be used as a heat sink and good candidate for cooling purpose studies for many engineering and technological fields.

CHAPTER 6

SUGGESTIONS FOR FUTURE INVESTIGATIONS

In this thesis, heat transfer characteristics of porous metal foams are experimentally and theoretically investigated. Copper metal foams are selected for conducted studies. All thermal image analyses of the samples as a function of different parameters are presented in detail. In order to define the thermal characteristics of the copper foam sample, thermal conductivity, heat capacity and thermal diffusivity analyses are given for different cases. Experimental results show the effects of the porous medium on heat transfer. The results revealed that, micro-structure of the porous medium can have a significant effect on heat transfer. Especially, particular attentions are given to define the thermal characteristics of the material for further heat transfer investigations in many engineering fields. Some suggestions are summarized and listed for future investigations ;

- Optimising the design and production of porous metal foam structures for enhanging the heat transfer in micro channel.
- Investigating the effects of the micro / nano porous metal foams on heat transfer.
- Defining the relationship between geometrical properties and optimal heat transfer.
- Developing the new models to deal with the fluid and thermodynamic challenges for complex porous structures.
- Defining the thermal and material characteristics of the porous mediums for different cases and applications.
- Developing the innovative porous metal foams for maximazing the heat transfer, especially for solving the cooling problems in many engineering fields.

REFERENCES

[1] N.Dukhan, 2013. 'Metal foams: fundamentals and applications', Lancaster, PA: DEStech Publications, Inc.

[2] M. F. Ashby., A. G. Evans., N. A. Fleck, L. J. Gibson., J. W. Hutchinson and H. N. G. Wadley. 2000. 'Metal foams: a design guide', Burlington: Butterworth-Heinemann.

[3] J. Banhart. (2001). 'Manufacture, characterisation and application of cellular metals and metal foams', *Progress Material Science.* **46**, (6), 559–632.

[4] J. Banhart., M. Ashby and N. Fleck. (1999). 'Metal foams and porous metal structures', Breman, Germany, MIT.

[5] Xu, H. J., Qu, Z. G. & Tao, W. Q. (2011b). Thermal Transport Analysis in Parallel-plate Channel Filled with Open-celled Metallic Foams, *International Communications in Heat and Mass Transfer*, Vol.38, No.**7**, (August 2011), pp. 868-873, ISSN 0735-1933.

[6] Banhart, J. (2001). Manufacture, characterisation and application of cellular metals and metal foams, *Progress in Materials Science*, Vol.46, No.**6**, (2001), pp. 559-632, ISSN 0079- 6425.

[7] Xu, H. J., Qu, Z.G. & Tao, W. Q. (2011a). Analytical Solution of Forced Convective Heat Transfer in Tubes Partially Filled with Metallic Foam Using the Two-equation Model, *International Journal of Heat and Mass Transfer*, Vol. 54, No.**17-18**, (May 2011), pp. 3846–3855, ISSN 0017-9310.

[8] Xu, H. J., Qu, Z. G. & Tao, W. Q. (2011b). Thermal Transport Analysis in Parallel-plate Channel Filled with Open-celled Metallic Foams, *International Communications in Heat and Mass Transfer*, Vol.38, No.**7**, (August 2011), pp. 868-873, ISSN 0735-1933.

[9] Xu, H. J., Qu, Z. G., Lu, T. J., He, Y. L. & Tao, W. Q. (2011c). Thermal Modeling of Forced Convection in a Parallel Plate Channel Partially Filled with Metallic Foams, *Journal of Heat Transfer*, Vol.133, No.**9**, (September 2011), pp. 092603.1-092603.9, ISSN 0022- 1481.

[10] S.D. Schampheleire, P. D. Jaeger., H. Huisseune., B. Ameel., C. T'Joen., K.K. Kerpel., M. D. Paepe. (2013). Thermal hydraulic performance of 10 PPI aluminium foam as alternative for louvered fins in an HVAC heat exchanger, *Applied Thermal Engineering* **51** 371–382.

[11] A. Muley., C. Kiser., B. Sundén., R. K. Shah. (2012). Foam heat exchangers: a technology assessment, *Heat Transfer Engineering* **33** (1) 42–51.

[12] K. Boomsma., D. Poulikakos., F. Zwick. (2003). Metal foams as compact high performance heat exchangers, *Mechanics Material.* **35** (12) 1161–1176.

[13] F. Barari., E. M. E. Luna., R. Goodall., R. Woolley. (2013). Metal foam regenerators; heat transfer and storage in porous metals, *J. Material. Research.* **28** (17) 2474–2482.

[14] M. Odabaee., K. Hooman. (2011). Application of metal foams in air-cooled condensers for geothermal power plants: an optimization study, *Int. Commun. Heat Mass Transfer* **38** 838–843.

[15] W.H.Hsieh., J. Y. Wu., W. H. Shih., W. C. Chiu. (2004). Experimental investigation of heat transfer characteristics of aluminium-foam heat sinks, *Int. J. Heat Mass Transfer* **47** 5149–5157.

[16] B. Ozmat., B. Leyda., B. Benson. (2004). Thermal applications of open-cell metal foams, *Material Manufacturing Processes* **19** (5) 839–862.

[17] C. Hutter., D. Buchi., V. Zuber., P. R. Rohr. (2011). Heat transfer in metal foams and designed porous media, *Chemical. Engineering Science.* **66** 3806–3814.

[18] C. T'Joen., P. D. Jaeger., H. Huisseune., S. V. Herzeele., N. Vorst., M. D. Paepe. (2010). Thermo-hydraulic study of a single row heat exchanger consisting of metal foam covered round tubes. *Int. J. Heat Mass Transfer.* **53** 3262–3274.

[19] M. Odabaee., S. Mancin., K. Hooman. (2013). Metal foam heat exchangers for thermal management of fuel cell systems – an experimental study, *Experimental Thermal Fluid Science.* **51** 214–219.

[20] Jörg Ettrich. (2014). fluid flow and heat transfer in cellular solid, PhD. thesis book.

[21] Dai, Z., Nawaz, K., Park, Y. G., Bock, J., and Jacobi, A. M. (2010). "Correcting and extending the Boomsma-Poulikakos effective thermal conductivity model for three-dimensional, fluid-saturated metal foams." *International Communications in Heat and Mass Transfer,* Vol. **37**, pp. 575-580.

[22] Mahjoob, S., and Vafai, K. (2008). "A synthesis of fluid and thermal transport models for metal foam heat exchangers," *International Journal of Heat and Mass Transfer,* Vol. **51**, pp. 3701-3711.

[23] Krishnan, S., Murthy, J. Y., and Garimella, S. V. (2006). "Direct Simulation of Transport in Open-Cell Metal Foam," *Journal of Heat Transfer*, Vol. **28**, pp. 793-800.

[24] Schmierer,E.N., Razani, A., Keating, S., and Melton, T. (2004). "Characterization of high porosity open-celled metal foam using computed tomography," *American Society of Mechanical Engineers, Heat Transfer Division, HTD*, Vol. **375**, pp. 415-424.

[25] Saadatfar, M., Garcia-Moreno, F., Hutzler, S., Sheppard, A. P., Knackstedt, M. A., Banhart (2009). "Imaging of metallic foams using X-ray micro-CT," *Colloids and Surfaces A: Physicochemical and Engineering Aspects,* Vol. **344** pp. 107-112.

[26] Bodla, K. K., Murthy, J. Y., and Garimella, S. V. (2010). "Microtomography-based simulation of transport through open-cell metal foams," *Numerical Heat Transfer, Part A: Application.* Vol. **58**, pp. 527-544.

[27] J. -M. Hugo, F. Topin. 2011. Metal foams design for heat exchangers: structure and effectives transport properties, in: Heat and Mass Transfer in Porous Media, Springer-Verlag, pp. 219e244.

[28] Purdue University, Suresh Garimella, Director, 765.494.5621, (CTRC)

[29] Bhattacharya, A., Calmidi, V. V., and Mahajan, R. L. (2002). "Thermophysical properties of high porosity metal foams", *International Journal of Heat and Mass Transfer,* Vol. **45**, pp. 1017-103.

[30] Calmidi, V. V. (1998). Transport Phenomena in high porosity metal foams, Ph.D. Thesis, University of Colorado, Boulder, CO.

[31] Girlich, D., Hackeschmidt, K., and Kühn, C. (2005). Bestimmung des konvektiven Wärmeübergangs offenporiger Metallschäume". In: Konstruktion Heft 1/2, pp. 1–10.

[32] Girlich, D., Kühn, C., and Hackeschmidt, K. (2004). Berechnung des Druckverlustes für offenporigen Metallschäume. In: Zeitschrift Konstruktion Heft 4.

[33] Boomsma, K, S. (2002). Metal Foams as Novel Compact High Performance Heat Exchangers for the Cooling of Electronics. PhD Thesis. ETH Zürich.

[34] Alvarez-Hernandez, A. R. (2005). Combined flow and heat transfer characterization of open cell aluminum foams. Master Thesis. University of Puerto Rico.

[35] Cruz Ruiz, E. (2004). Modelling of Heat Transfer in Open Cell Metal Foams. Master Thesis. University of Puerto Rico.

[36] N. Dukhan., K. C. Chen, (2007). Heat transfer measurements in metal foam subjected to constant heat flux, *Experimental Thermal Fluid Science.* **32** 624–631.

[37] N. Dukhan., P. D. Quiñones-Ramos., E. Cruz-Ruiz., M. Vélez-Reyes., E. P. Scott. (2005). One dimensional heat transfer analysis in open-cell 10-ppi metal foam, *Int. J. Heat Mass Transfer* **48** 5112–5120.

[38] D. DeWitt., F. Incropera, T., Bergman and A. Lavine. 2007. 'Introduction to heat transfer': Hoboken, NJ, John Wiley & Sons

[39] I. Kurtbas., N. Celik., I. Dinçer (2010). Exergy transfer in a porous rectangular channel, *Energy* **35** 451.

[40] I. Ghosh. (2009). How good is open-cell metal foam as heat transfer surface, Trans. ASME: *J. Heat Transfer* **131** 101004-1–101004-8.

[41] S. Mancin., C. Zilio., A. Cavallini., L. Rossetto. (2010). Heat transfer during air flow in aluminum foams, *Int. J. Heat Mass Transfer* **53** 4976–4984.

[42] S. Mancin., C. Zilio., A. Diani., L. Rossetto. (2013). Air forced convection through metal foams: experimental results and modeling, *Int. J. Heat Mass Transfer* **62** 112–123.

[43] C. Zhao., H. Hodson., T. Kim., T. Lu. (2004). Thermal transport in high porosity cellular metal foams, *J. Thermophysics. Heat Transfer* **18** 309–317.

[44] A. Cavallini., S. Mancin., L. Rossetto., C. Zilio. (2009). Air flow in aluminum foam: heat transfer and pressure drops measurements, *Exp. Heat Transfer* **23** 94–105.

[45] Lu, T. (2002). Ultralight porous metals: from fundamentals to applications, *Acta Mechanica Sinica, Chinese J. Mech*, vol.**18**, pp.457-479.

[46] Calmidi, V. V, and Mahajan, R. L. (1999). The effective thermal conductivity of high porosity fibrous metal foams, *J. Heat Transfer*, vol. **121**, pp. 466-471.

[47] Hsieh, W. H., Wu, J. Y., Shih, W. H., and Chiu, W. C. (2004). "Experimental investigation of heat transfer characteristics of aluminum-foam heat sink," *International Journal of Heat and Mass Transfer,* Vol. **47**, pp. 5149–5157.

[48] Boomsma, K., and Poulikakos, D. (2001). "On the effective thermal conductivity of a three dimensionally structured fluid-saturated metal foam," *International Journal of Heat and Mass Transfer,* Vol. **44**, pp. 827–836.

[49] Nawaz, K., Bock, J., and Jacobi, A. M. (2010). "Experimental studies to evaluate the use of metal foams in highly compact air-cooling heat exchangers," *13th International Refrigeration and Air Conditioning Conference, July 12th- 16th, Purdue University Lafayette, IN.*

[50] Moofat., R. J. Eaton, J. K., and Onstad, A. (2009). "A method for determining the heat transfer properties of foam-fins," *ASME Journal of Heat Transfer*, Vol. **13.1**.

[51] Calmidi, V. V., and Mahajan, R. L. (2000). "Forced convection in high porosity metal foams," *ASME Journal of Heat Transfer,* Vol. **122**, pp. 557–565.

[52] H. R. Seyf and M. Layeghi. (2010). 'Numerical analysis of convective heat transfer from an elliptic pin fin heat sink with and without metal foam insert', *J. Heat Transfer.* **132**, (7), DOI 071401-1–071401-9.

[53] C. Y. Zhao., T. Kim., T. J. Lu and H. P. Hodson. (2004). 'Thermal transport in high porosity cellular metal foams', *J. Thermophysics Heat Transfer* **18**, (3), 309–317.

[54] S. Mancin., C. Zilio., A. Diani and L. Rossetto (2012). ‘Experimental air heat transfer and pressure drop through copper foams’, *Experimental Thermal Fluid Science*, **36**, 224–232.

[55] A. Tamayol and K. Hooman (2011). ‘Thermal assessment of forced convection through metal foam heat exchangers’, *J. Heat Trans*fer **133**, (11), 111801-1–111801-7. DOI 10.1115/1.4004530.

[56] Long, Y. 2009. Physical Properties of Materials. Changsha, China: Central south univeristy press.

[57] White, M. A. 2011. Physical Properties of Materials. Boca Raton, FL, USA: CRC Press, Taylor & Francis Group.

[58] C. T. Hsu., P. Cheng., K. W. Wong. (1994). Modified ZehnereSchlunder models for stagnant thermal conductivity of porous media, *Int. J. Heat Mass Transfer* **37** (17) 2751e2759.

[59] V. V. Calmidi., R. L. Mahajan. (1999). The effective thermal conductivity of high porosity fibrous metal foams, *ASME J. Heat Transfer* **121** 466e471.

[60] Kaviany, M. 1995. Principles of Heat Transfer in Porous Media. New York, USA: Springer-Verlag.

[61] Jiang, C. -H., et al. (2010). Thermodynamic properties and heat capacities of Co (BTC)_{1/3} (DMF) (HCOO). *Journal of Thermal Analysis and Calorimetry.* **102**(3): p. 1087-1093.

[62] Song, L. -F., et al. (2010). Heat capacities and thermodynamic properties of MgBTC. *Journal of Thermal Analysis and Calorimetry.* **101**(1): p. 365-370.

[63] Song, L. -F., et al. (2010). Heat capacities and thermodynamic properties of a novel mixed-ligands MOFs. *Journal of Thermal Analysis and Calorimetry*. **100**(2): p. 679-684.

[64] Zhou, Y.-X., et al., Heat capacities and thermodynamic properties of M(HBTC)(4,4′-bipy)·3DMF (M = Ni and Co). *Journal of Thermal Analysis and Calorimetry*. p. 1-6.

[65] Thomas, L. C. Making accurate DSC and MDSC, Specific Heat Capacity Measurement with the Q1000 T zero DSC.

[66] Kerrisk J. F. (1971). "Thermal Diffusivity of Heterogeneous Materials", *Journal of Applied Physics,* vol. **42(1)**, pp. 267-271.

[67] Katsunori, Inoue. (1991). Thermal Diffusivity Measurement of Porous Materials, *Transactions of JWRI*, vol. **20(1)** pp. 35 – 40.

[68] García, E., Osendi, M. I. and Miranzo, P. (2002). Thermal Diffusivity of Porous Codierite Ceramic Burners, *Journal of Applied Physics***,** vol. **92(5)**, pp. 2346 – 2349.

[69] Barea, R. et al. (2005). Thermal Conductivity of Highly Porous Mullite Material, *Acta Materialia***,** vol.**53**, pp. 3313 – 3318.

[70] Öchsner, A., Masakazu, Tane. and Hideo, Nakajima. (2006). Prediction of Thermal Properties of Lotus-Type and Quasi-Isotropic Porous Metals: Numerical and Analytical Methods, *Materials Letters*, vol. **60**, pp. 2690 – 2694.

[71] Parker W. J., Jenkins, R. J., Butler, C. P. and Abbot, G. L. (1961). "Flash method of determining thermal diffusivity, heat capacity and thermal conductivity", *Journal of Applied Physics*, vol. **32**, pp. 1679-1684.

[72] Boomsma, K., Poulikakos, D., and Zwick, F. (2003). Metal foams as compact high performance heat exchanger, *J. Mech. Mater*. **35**, 1161–1176.

[73] Jiang, P., Li, M., Lu, T., Yu, L., and Ren, Z. (2004). Experimental research on convection heat transfer in sintered porous plate channels, *Int. J. Heat Mass Transfer*, **47**, 2085–2096.

[74] Tzeng, S., and Jeng, T. (2006). Convective heat transfer in porous channels with 90-deg turned flow, *Int. J. Heat Mass Transfer*, **49**, 1452–1461.

[75] Mohammed, H. A., and Salman, Y. K. (2007). Experimental investigation of mixed convection heat transfer for thermally developing flow in a horizontal circular cylinder, *Appl. Therm. Eng.*, **27**, 1522–1533.

[76] Kurtbas, I., and Celik, N. (2009). Experimental investigation of forced and mixed convection heat transfer in a foam-filled horizontal rectangular channel, *Int. J. Heat Mass Transfer,* **52**, 1313–1325.

[77] Wu, H., and Wang, R. (2010). Convective heat transfer over a heated square porous cylinder in a channel, *Int. J. Heat Mass Transfer*, **53**, 1927–1937.

[78] Kamath, P. M., Balaji, C., and Venkateshan, S. (2011). Experimental investigation of flow assisted mixed convection in high porosity foams in vertical channels, *Int. J. Heat Mass Transfer*, **54**, 5231–524.

[79] T. M. Jeng., S. C. Tzeng., et Y. C. Yang. (2014). Experimental study of heat transfer characteristics in a 180-deg round turned channel with discrete aluminum-foam blocks, *Int. J. Heat Mass transfer*. **52** 133-141.

[80] S. Mancin., C. Zilio., A. Cavallini., L. Rossetto. (2010). Pressure drop during air flow in aluminum foams, *Int. J. Heat Mass transfer*. **53** 3121-3130.

[81] Handbook of Chemistry and Physics, Chemical Rubber Publishing Co., Cleveland Ohio.

[82] Holman, J. P. 2001. Experimental Methods for Engineers, 7th ed., McGraw-Hill International Edition, New York, USA.

APPENDICES

THERMAL IMAGES AND HISTOGRAM TEMPERATURE VIEWS OF THE COPPER FOAM SAMPLES

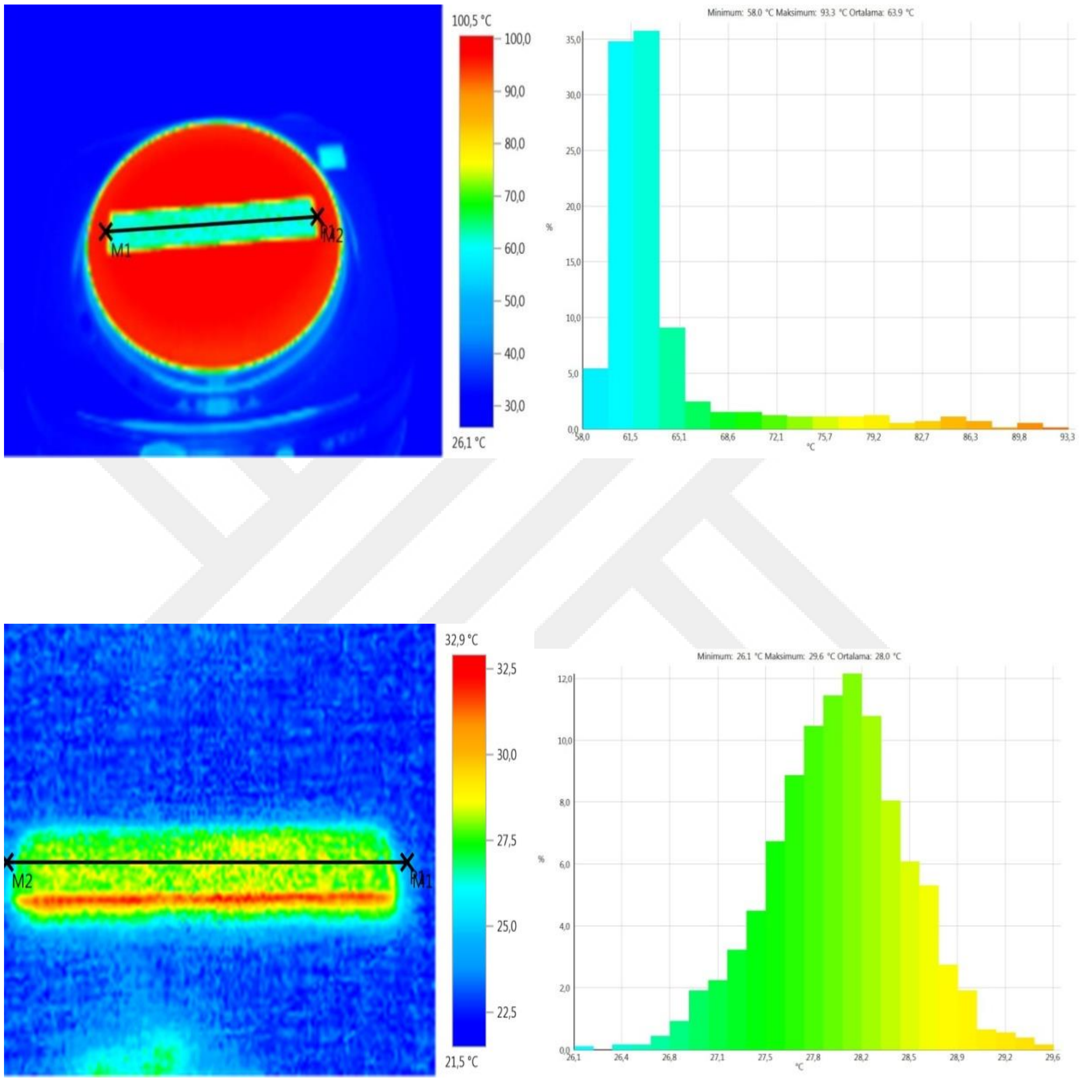

Figure A1 Thermal images and histogram profiles of the t = 3 mm Cu foam for Ө = 10 minutes time periods at $T_H = 80$ ˚C

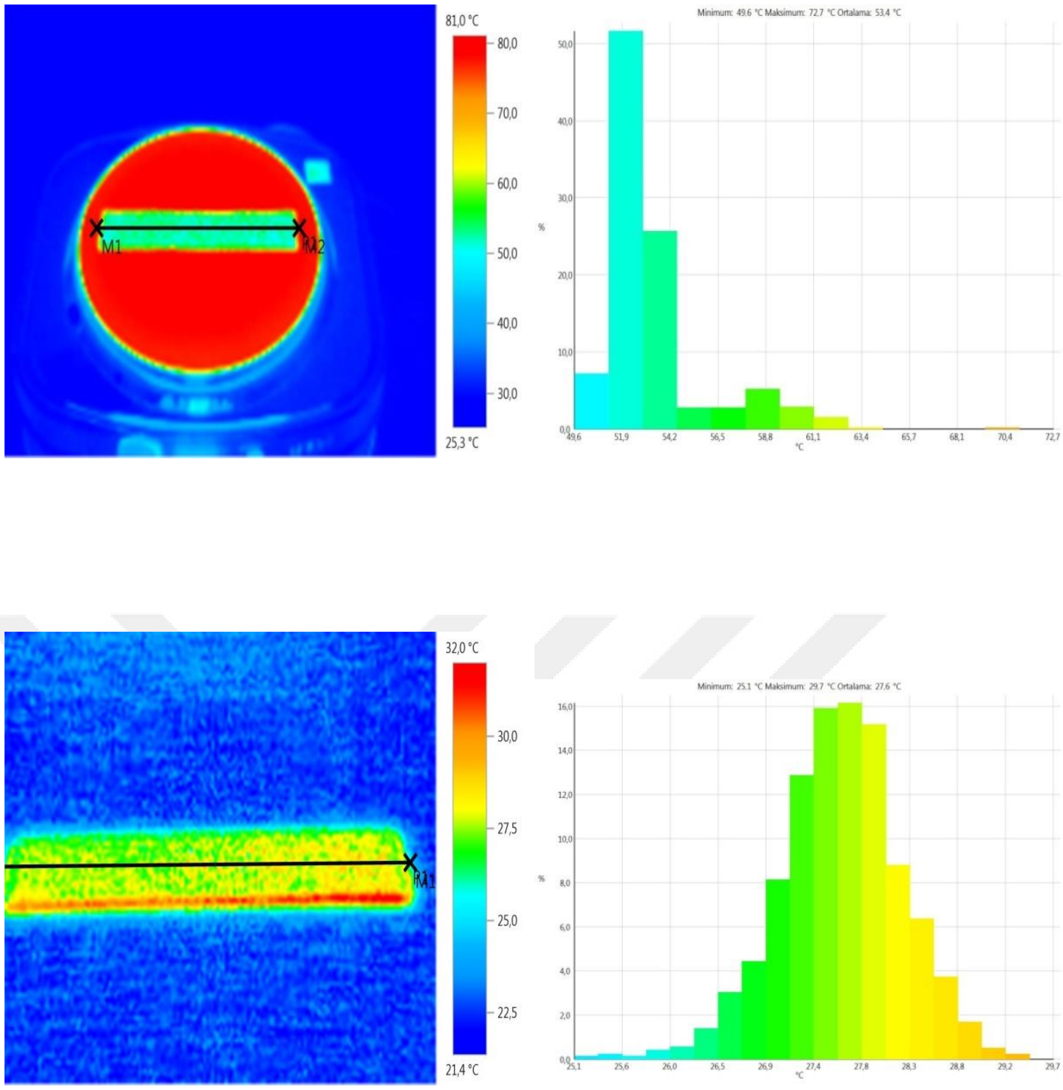

Figure A2 Thermal images and histogram profiles of the t = 3 mm Cu foam for ϴ = 20 minutes time periods at $T_H = 80$ ˚C

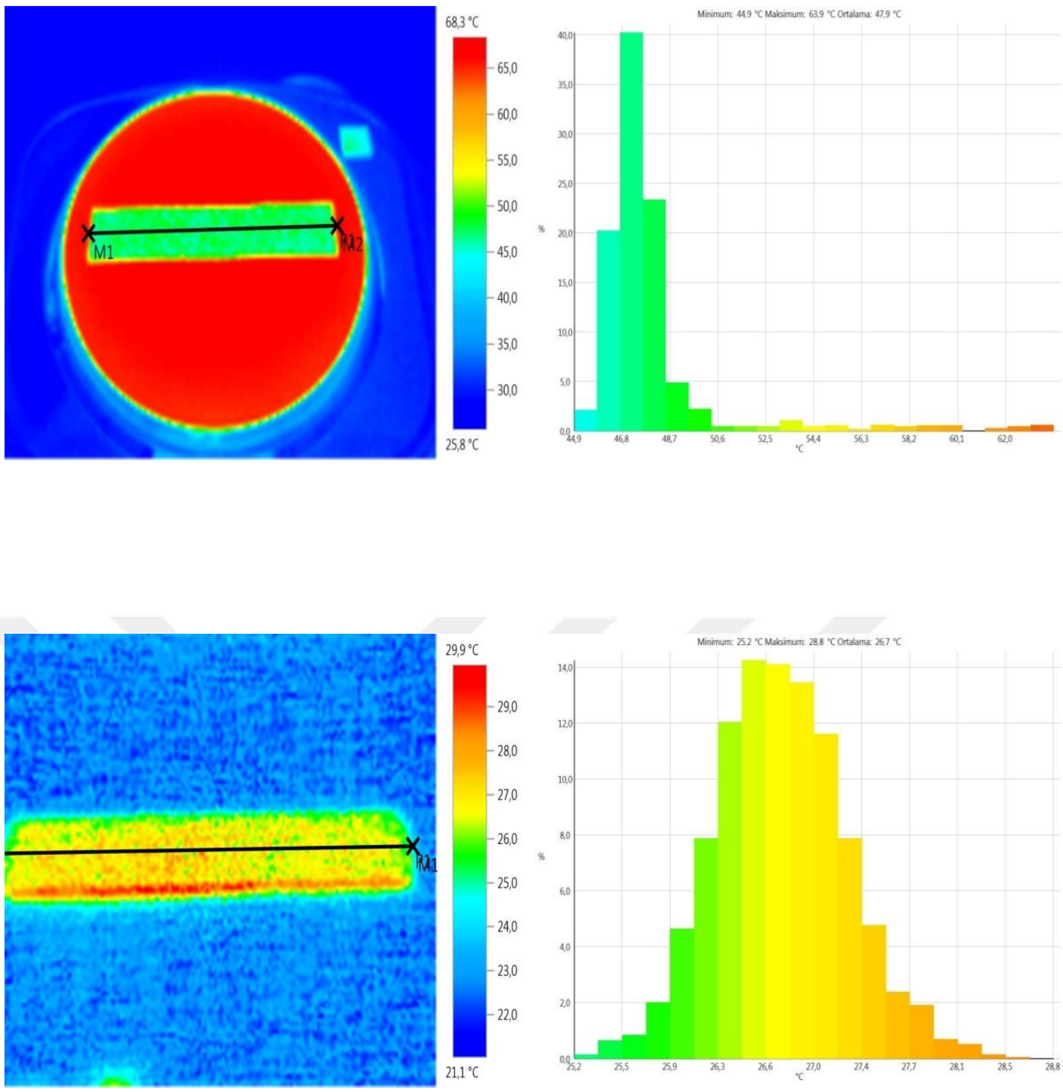

Figure A3 Thermal images and histogram profiles of the t = 3 mm Cu foam for Θ = 30 minutes time periods at $T_H = 80$ ˚C

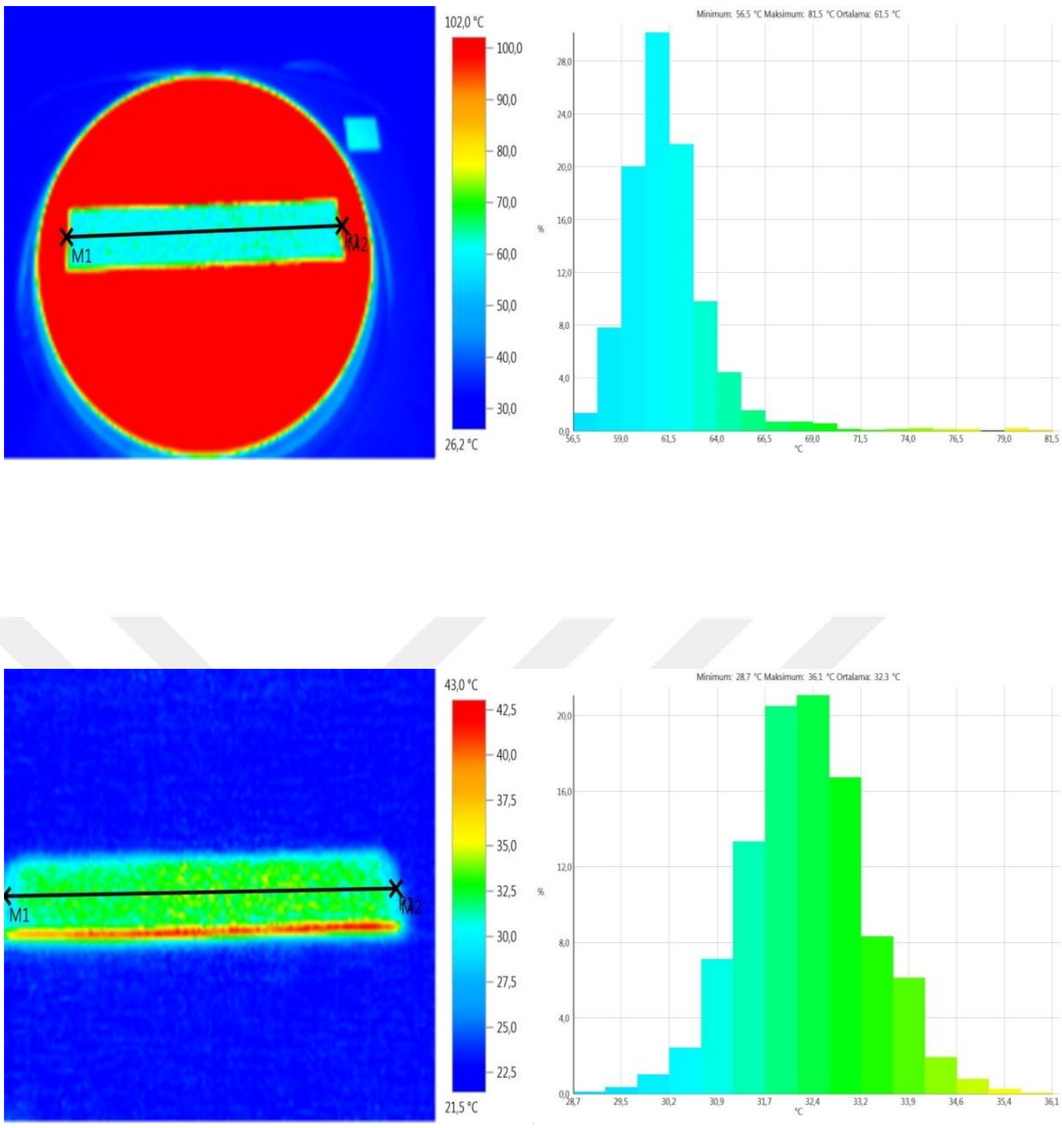

Figure A4 Thermal images and histogram profiles of the t = 4 mm Cu foam for ϴ = 10 minutes time periods at T_H = 80 ˚C

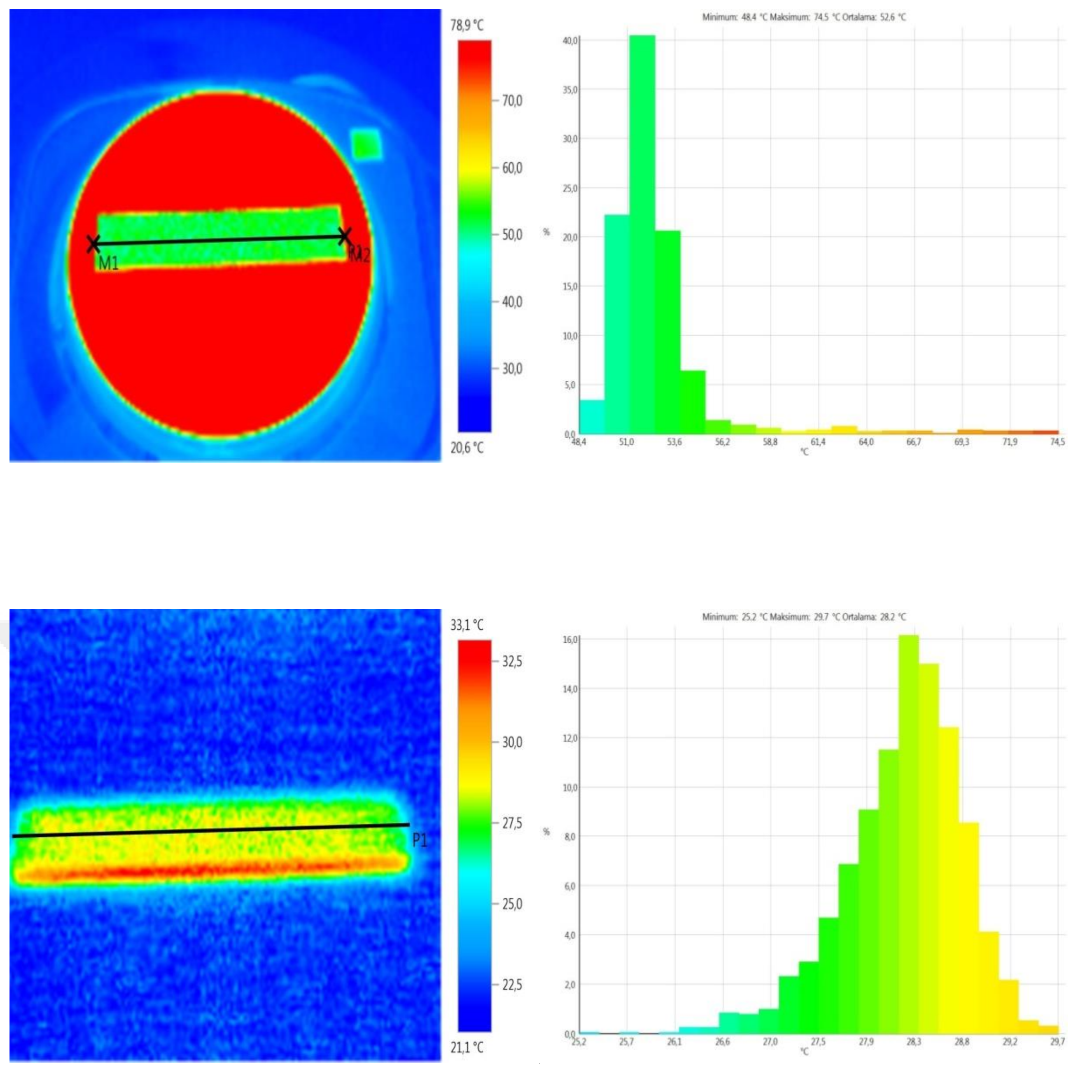

Figure A5 Thermal images and histogram profiles of the t = 4 mm Cu foam for ϴ = 20 minutes time periods at T_H = 80 ˚C

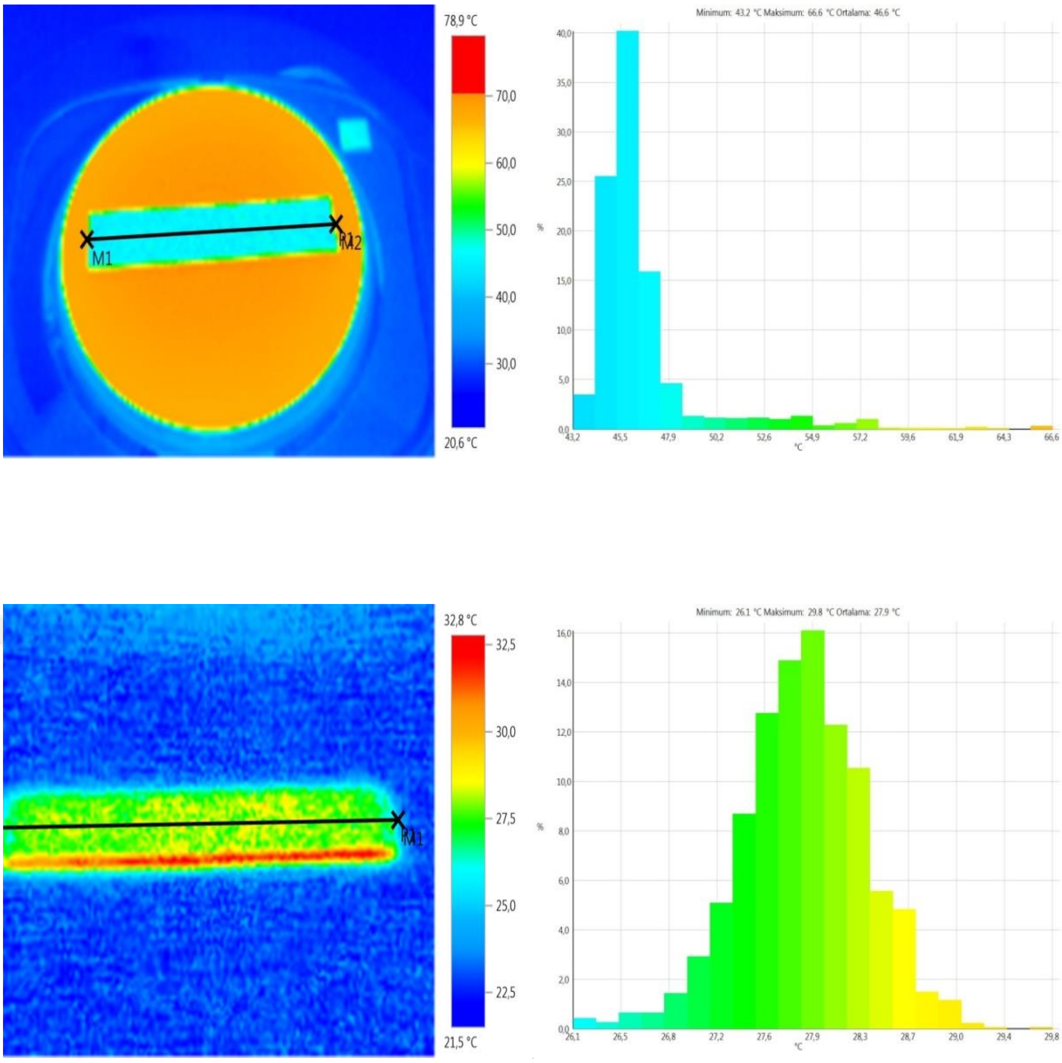

Figure A6 Thermal images and histogram profiles of the t = 4 mm Cu foam for Θ = 30 minutes time periods at $T_H = 80$ ˚C

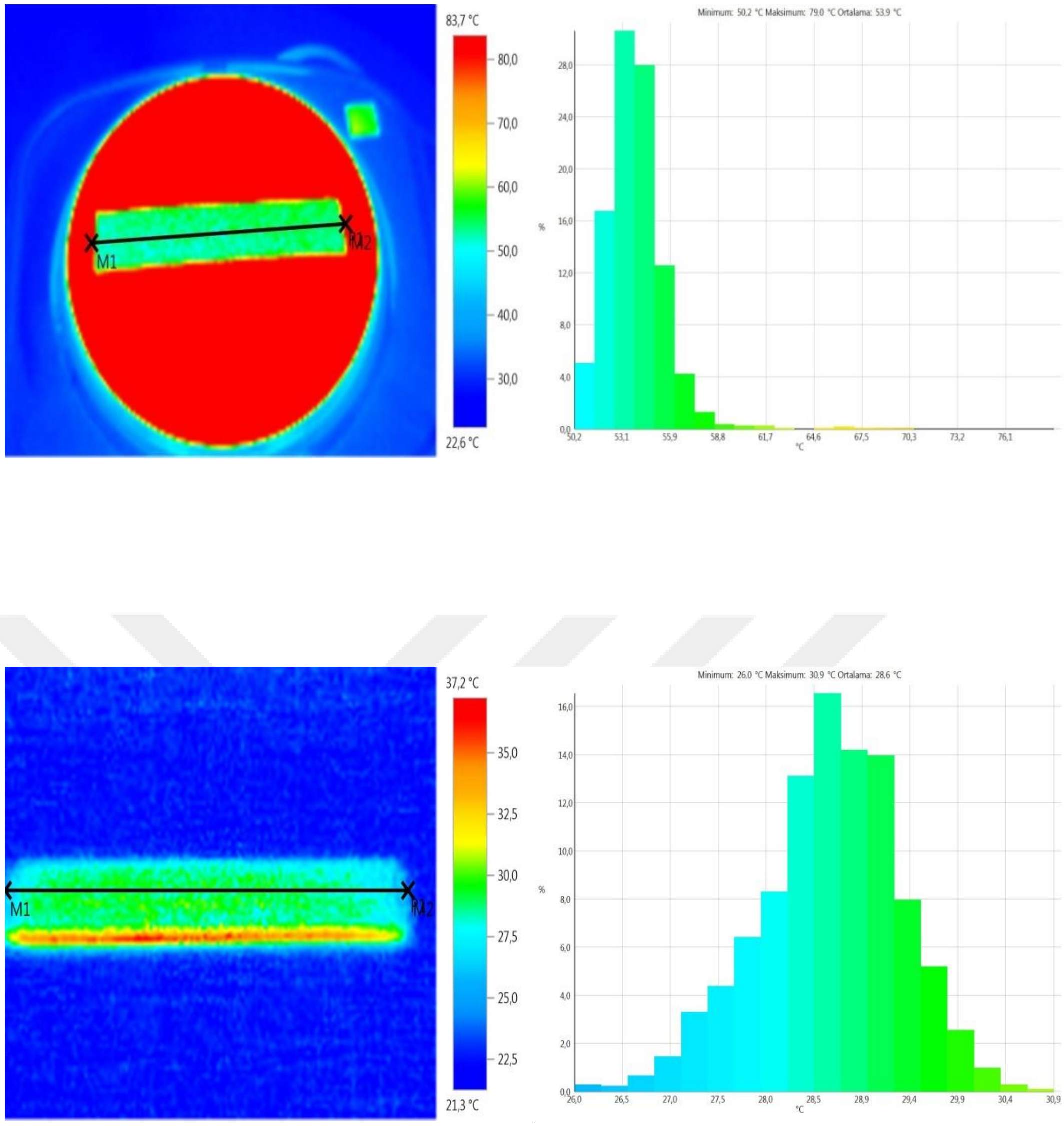

Figure A7 Thermal images and histogram profiles of the t = 5 mm Cu foam for Θ = 10 minutes time periods at $T_H = 80$ ˚C

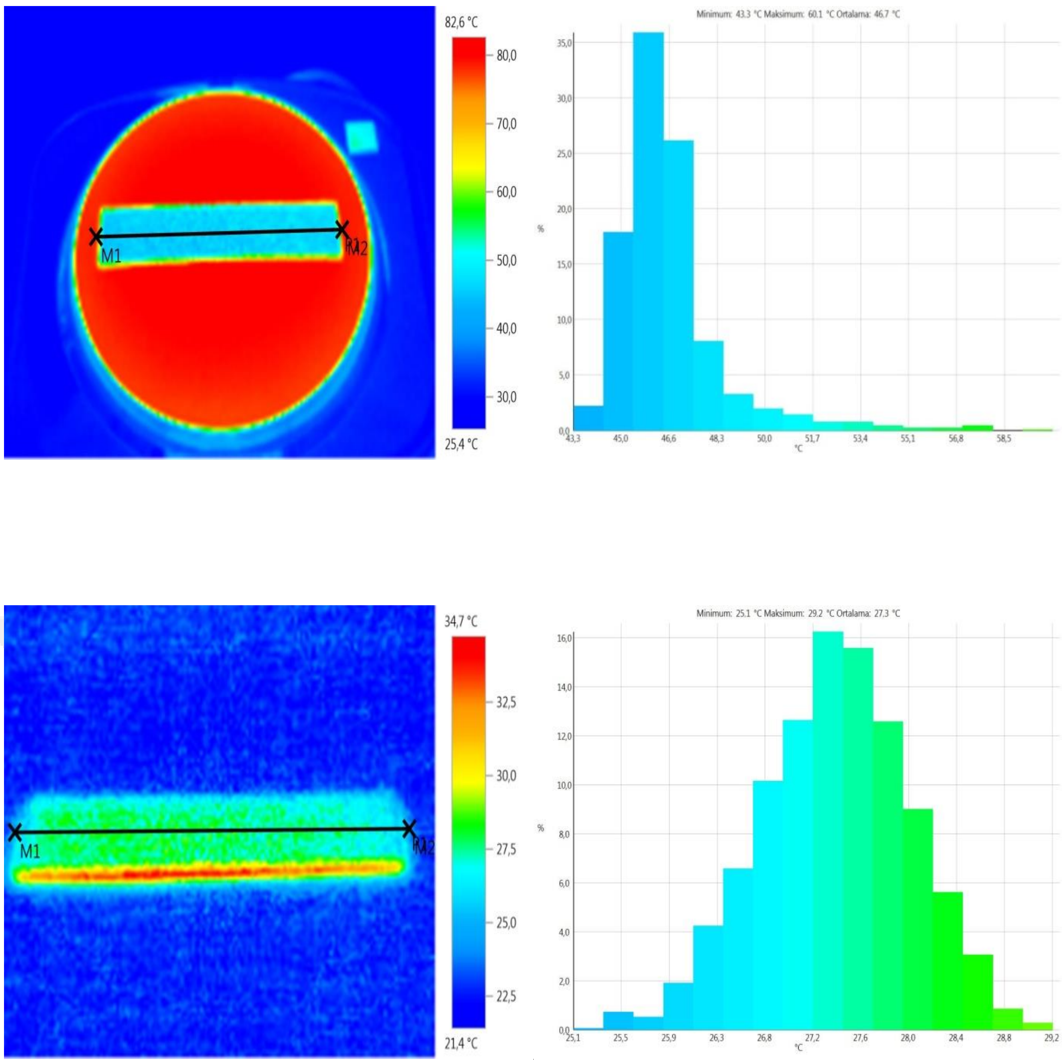

Figure A8 Thermal images and histogram profiles of the t = 5 mm Cu foam for ϴ = 20 minutes time periods at $T_H = 80$ ˚C

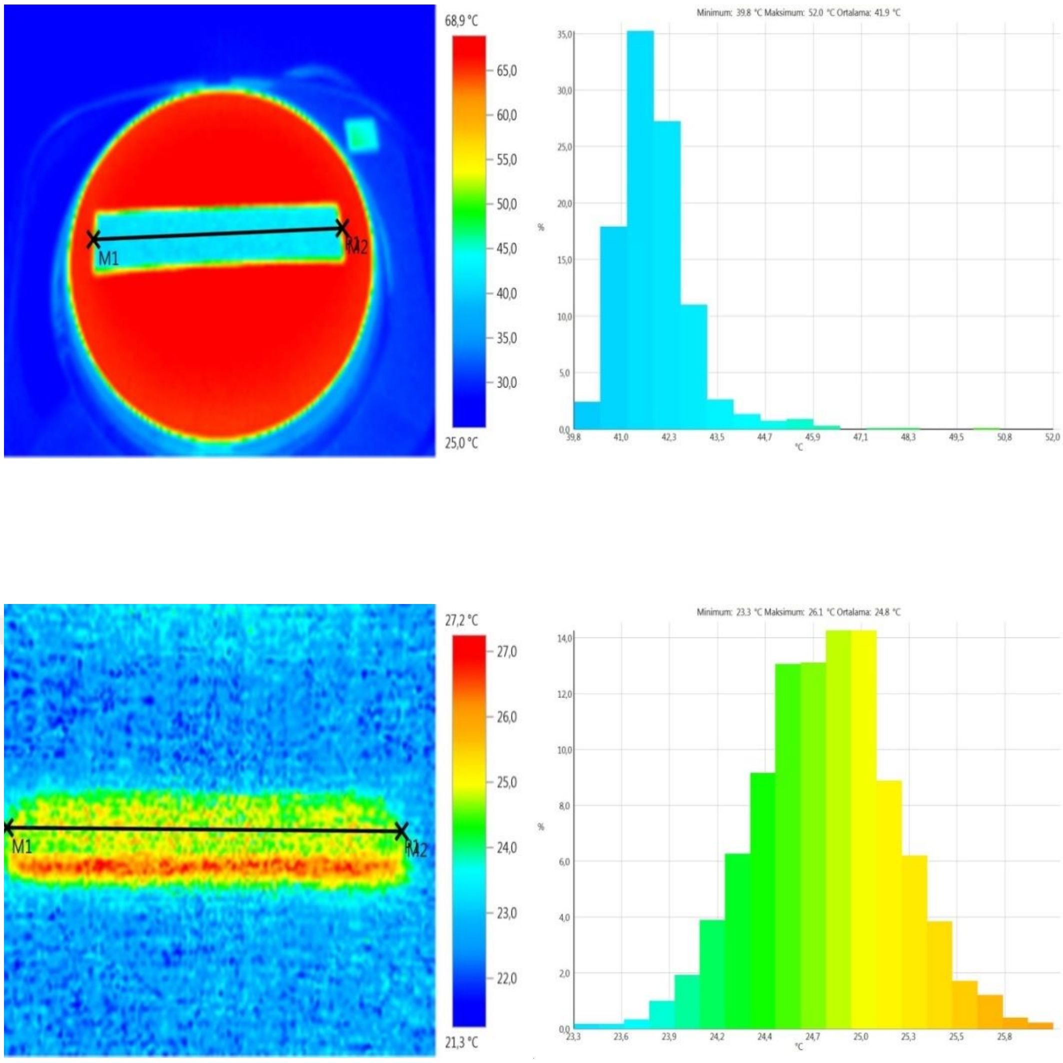

Figure A9 Thermal images and histogram profiles of the t = 5 mm Cu foam for ϴ = 30 minutes time periods at $T_H = 80$ ˚C

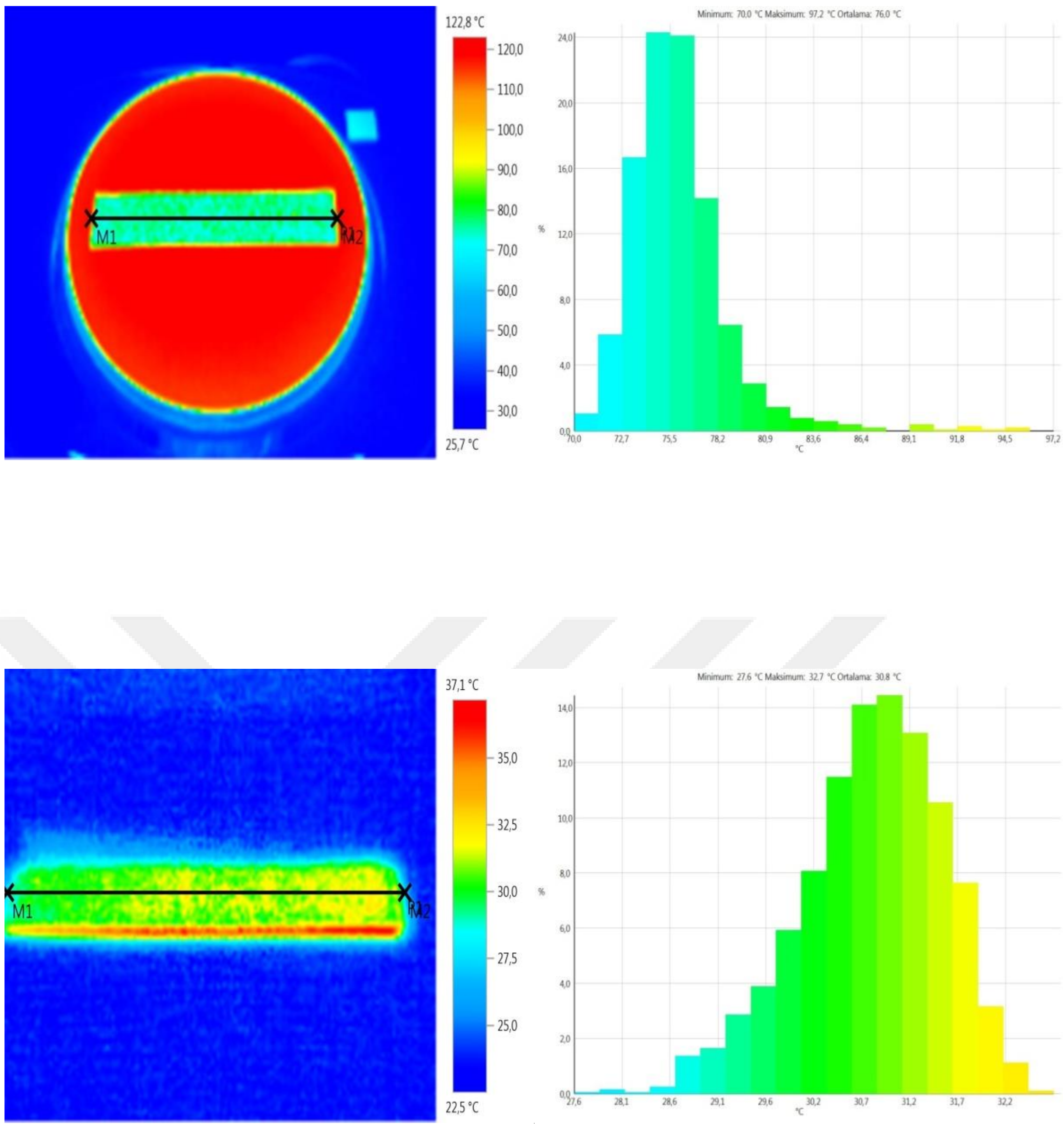

Figure A10 Thermal images and histogram profiles of the t = 3 mm Cu foam for ϴ = 10 minutes time periods at T_H = 100 ˚C

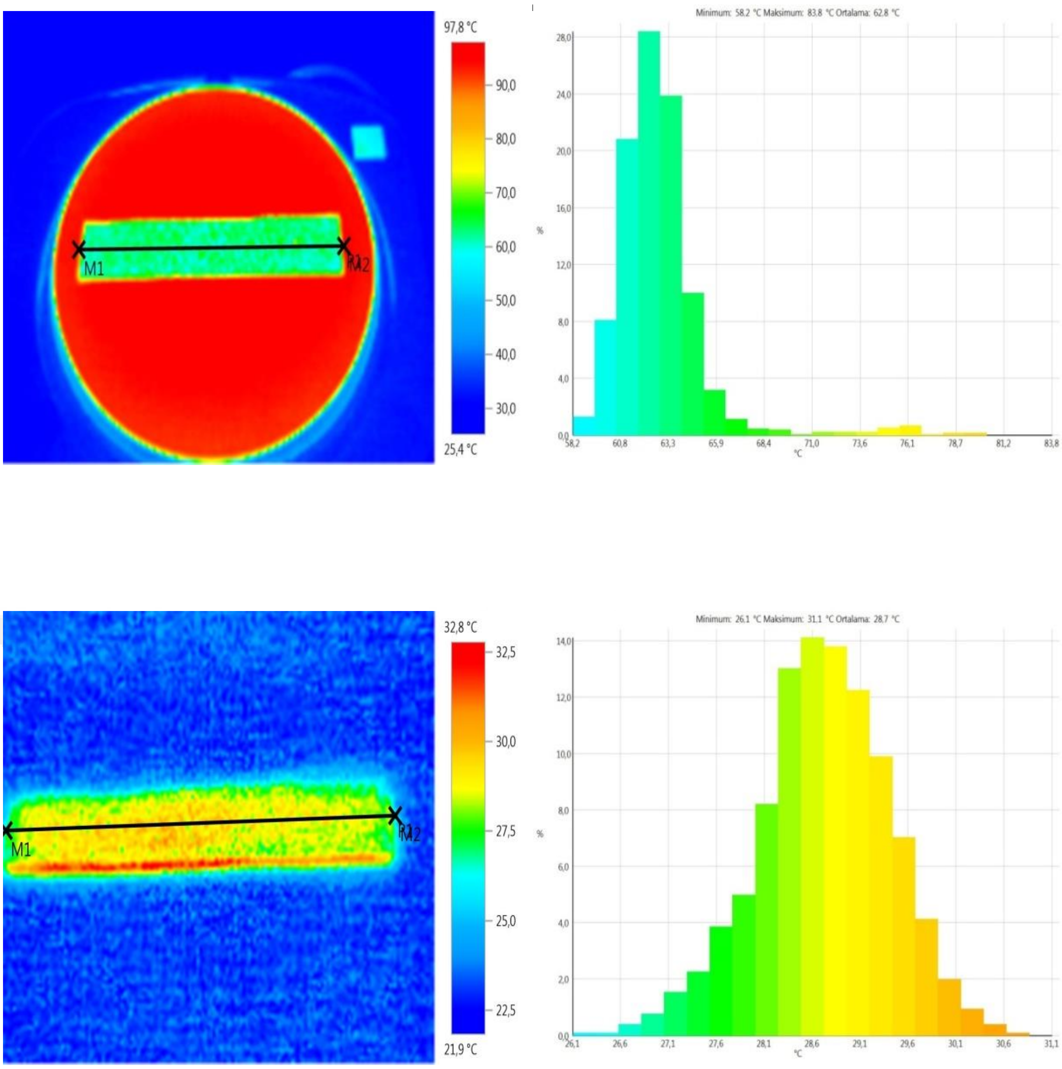

Figure A11 Thermal images and histogram profiles of the t = 3 mm Cu foam for ϴ = 20 minutes time periods at T_H = 100 ˚C

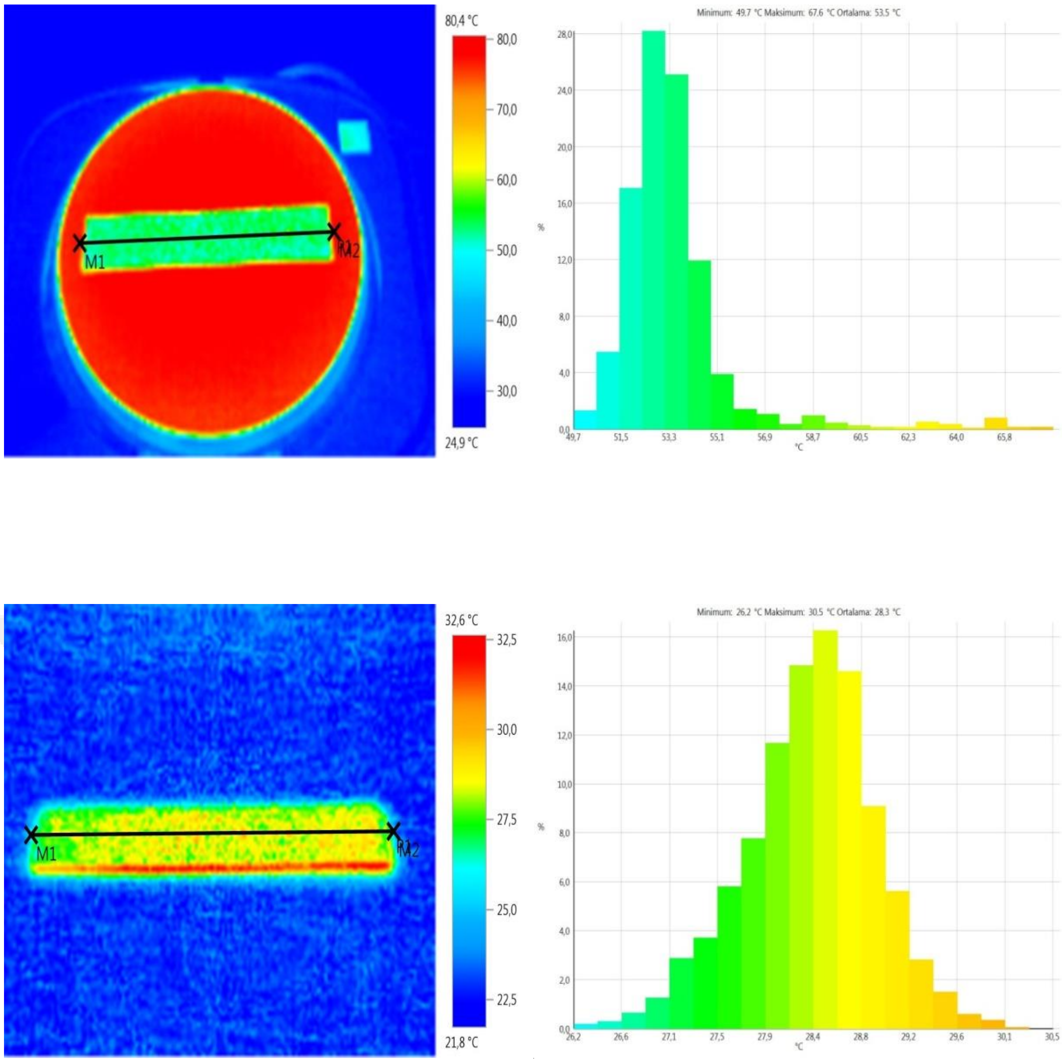

Figure A12 Thermal images and histogram profiles of the t = 3 mm Cu foam for ϴ = 30 minutes time periods at T_H = 100 ˚C

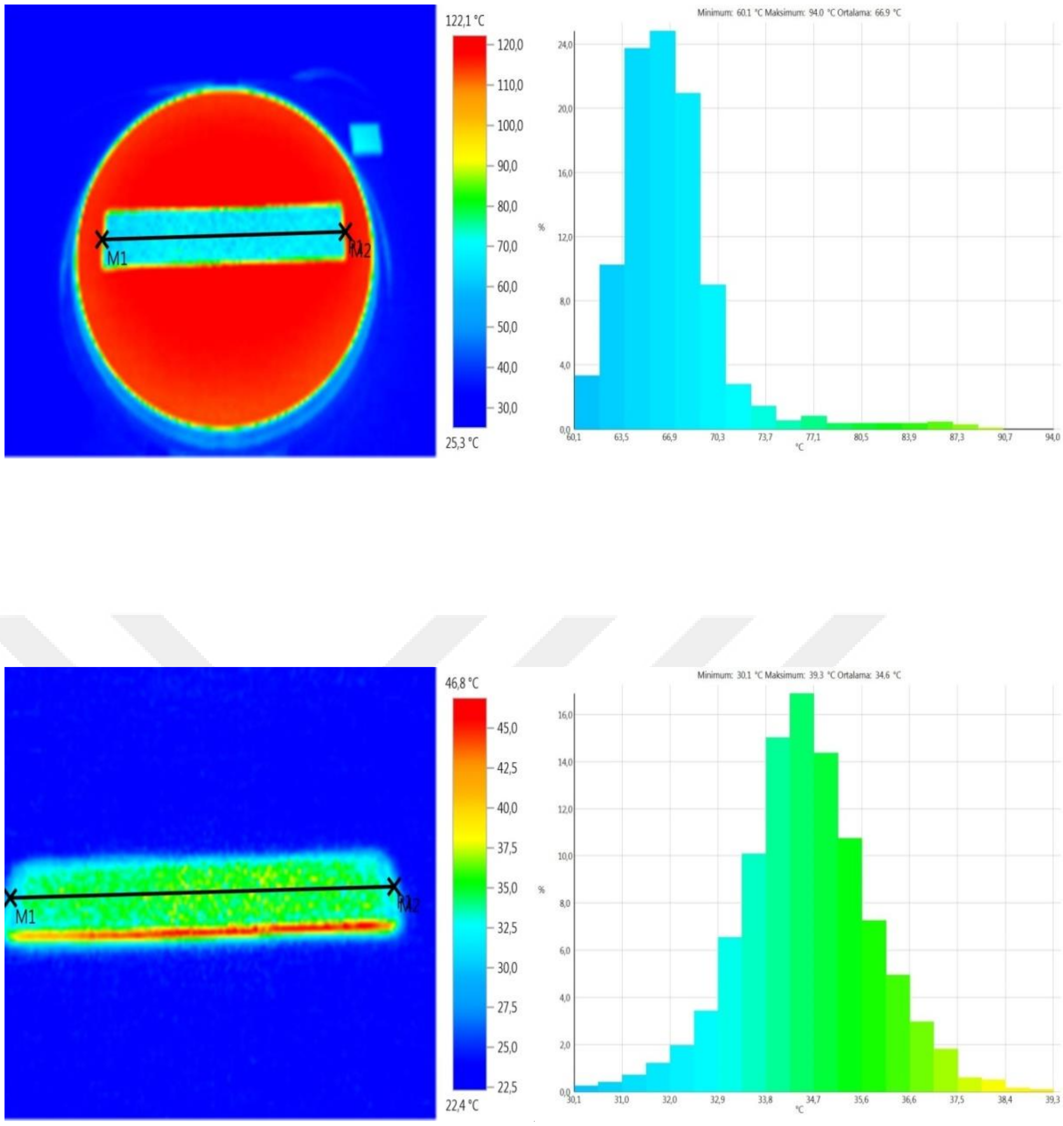

Figure A13 Thermal images and histogram profiles of the t = 4 mm Cu foam for ϴ = 10 minutes time periods at T_H = 100 ˚C

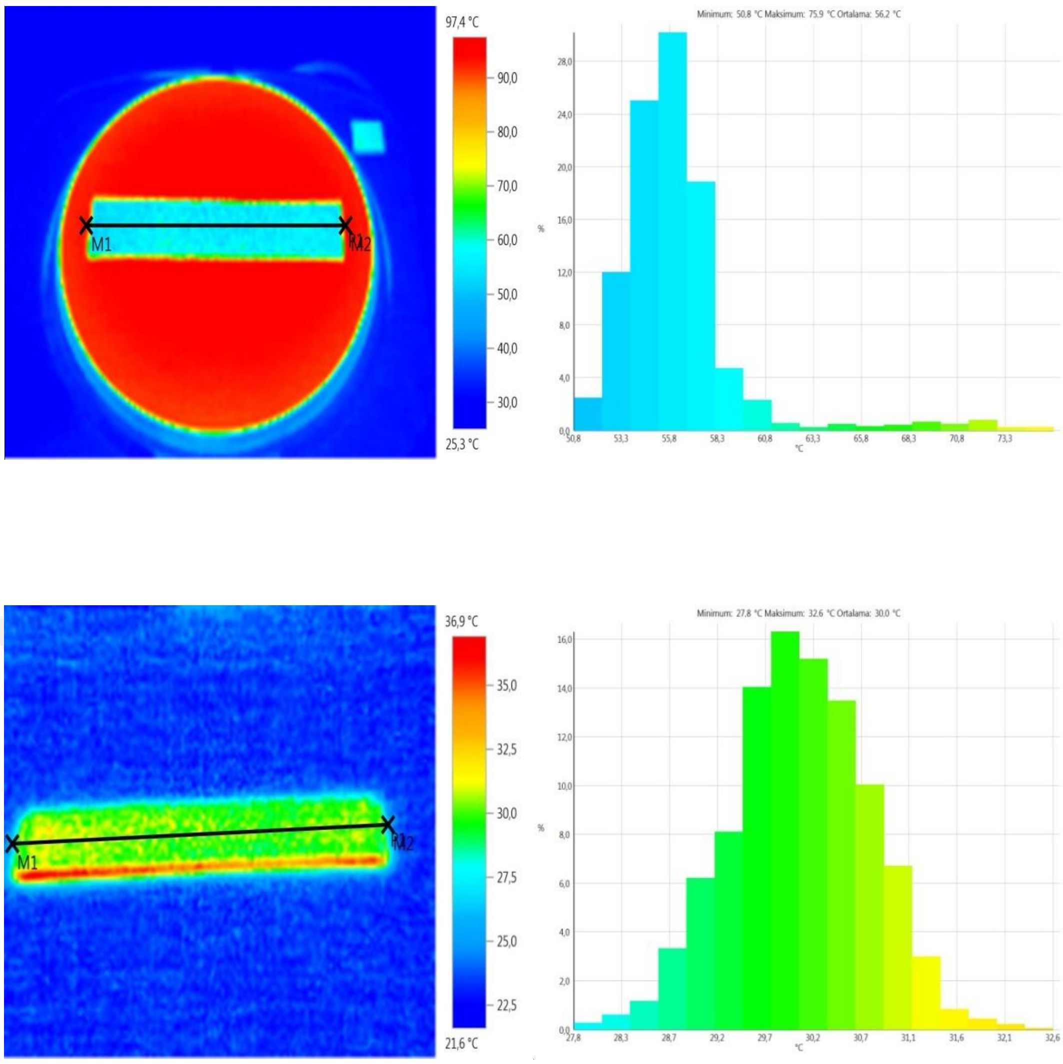

Figure A14 Thermal images and histogram profiles of the t = 4 mm Cu foam for ϴ = 20 minutes time periods at $T_H = 100$ ˚C

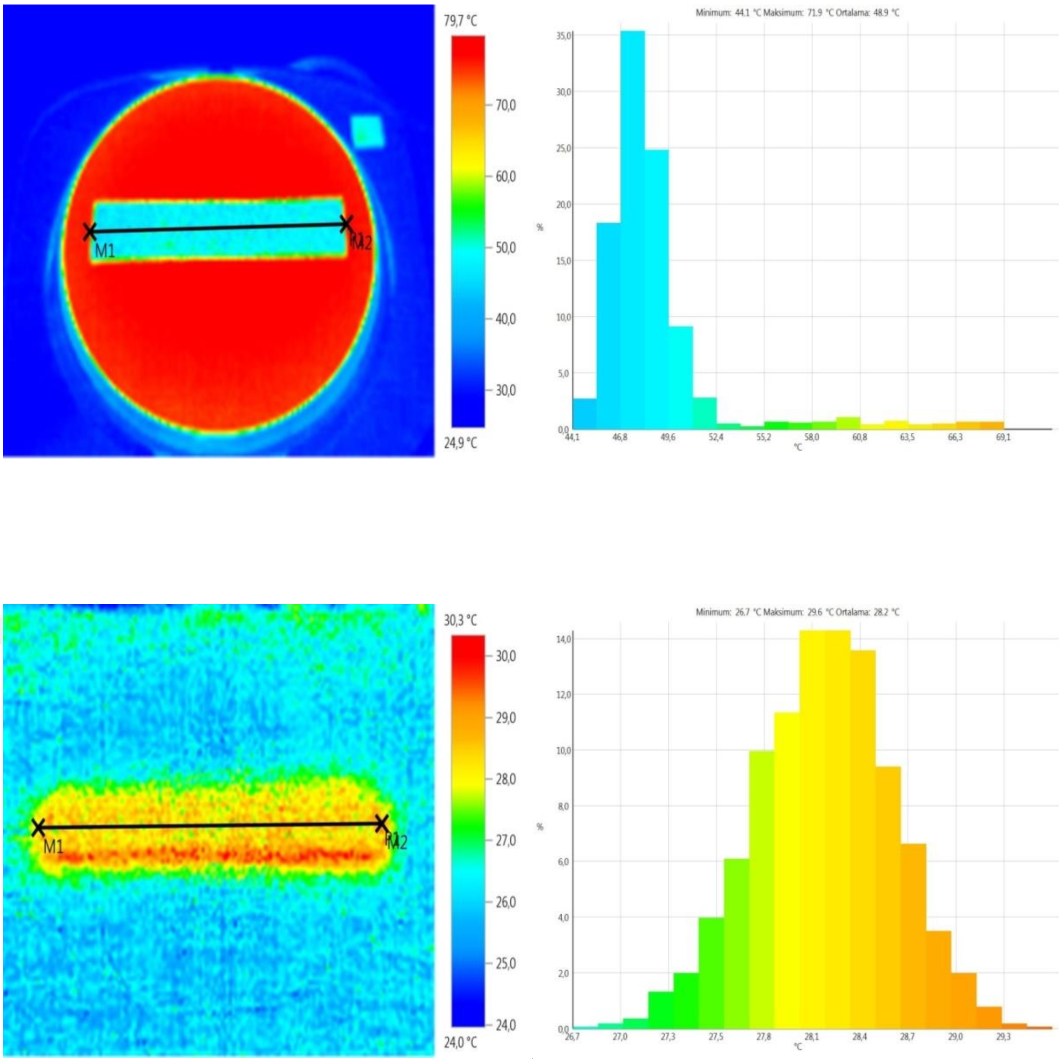

Figure A15 Thermal images and histogram profiles of the t = 4 mm Cu foam for ϴ = 30 minutes time periods at T_H = 100 ˚C

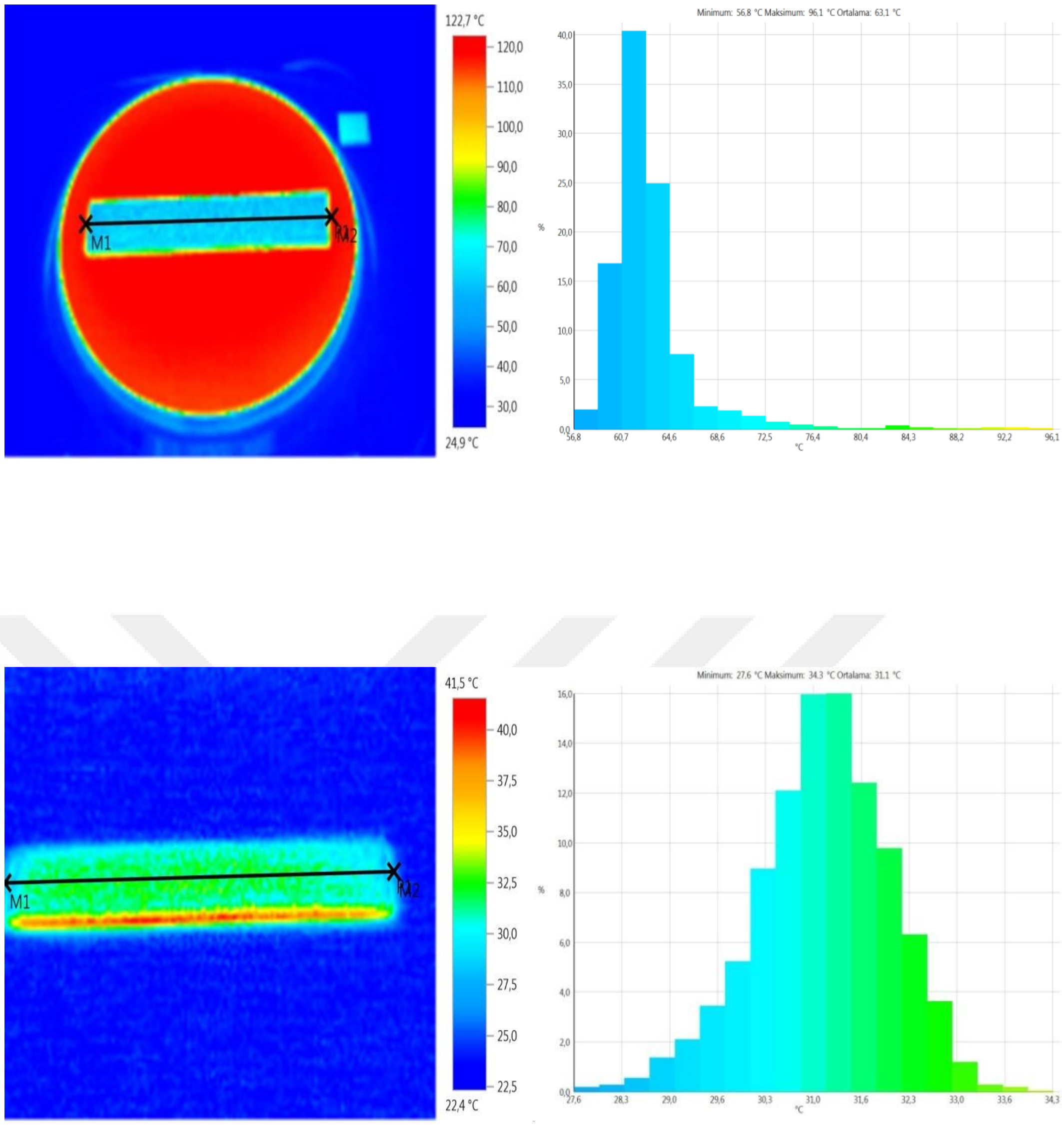

Figure A16 Thermal images and histogram profiles of the t = 5 mm Cu foam for Θ = 10 minutes time periods at T_H = 100 ˚C

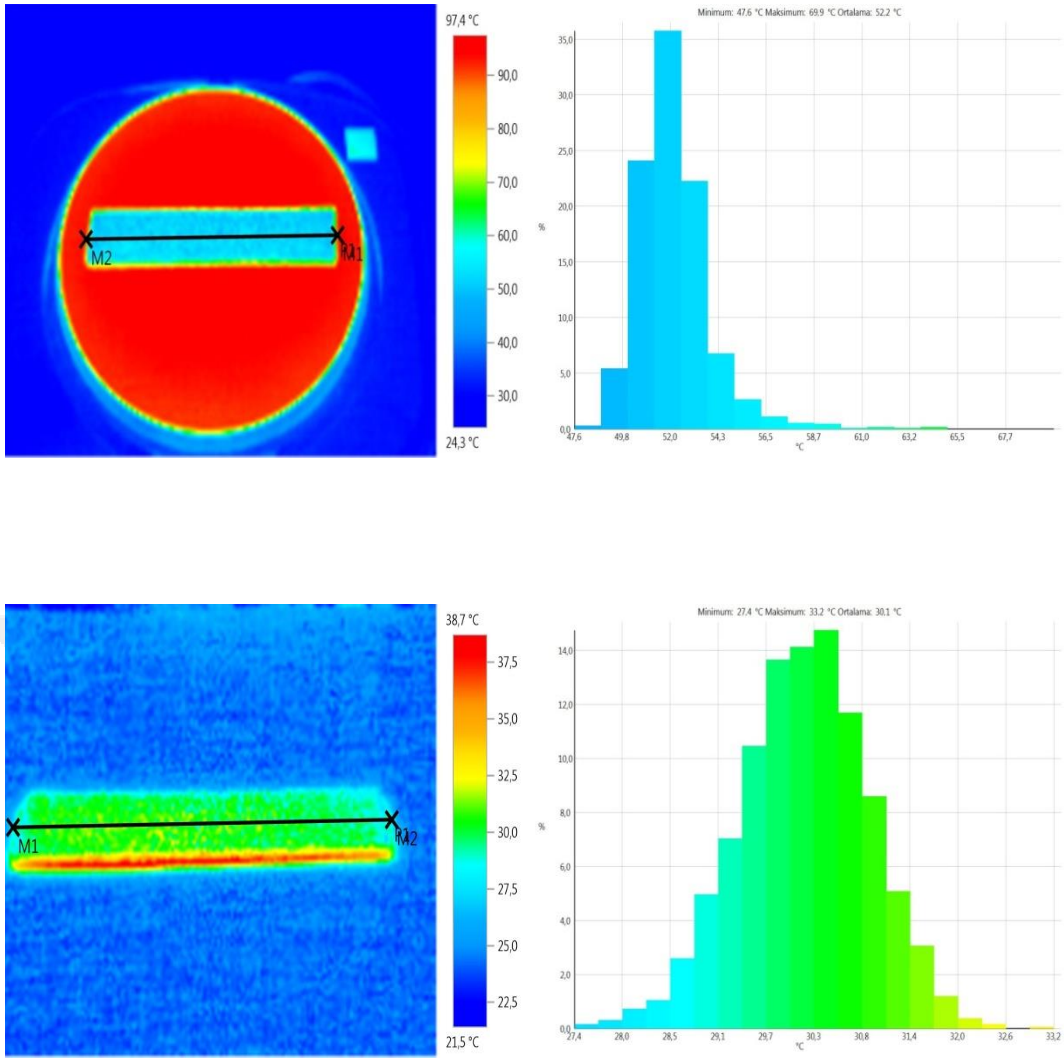

Figure A17 Thermal images and histogram profiles of the t = 5 mm Cu foam for ϴ = 20 minutes time periods at $T_H = 100$ ˚C

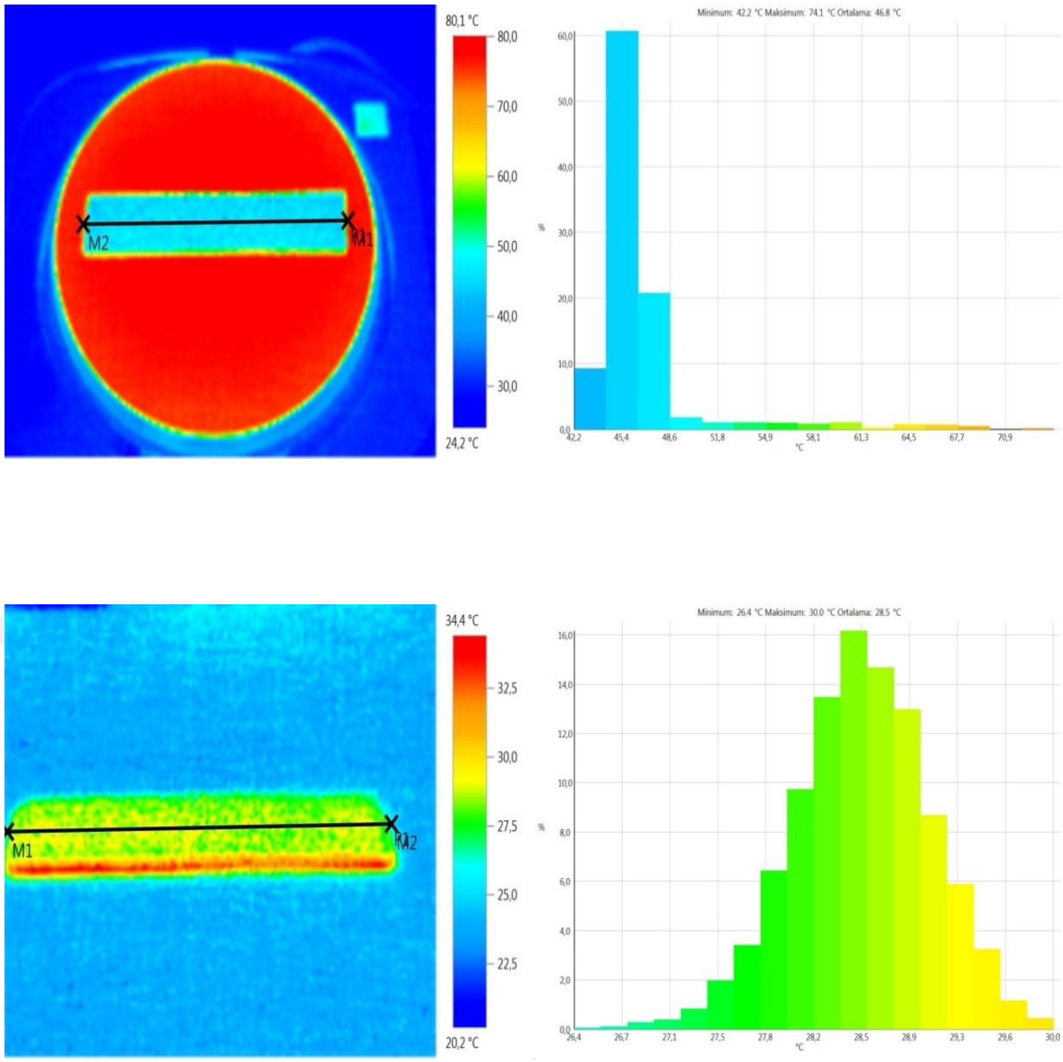

Figure A18 Thermal images and histogram profiles of the t = 5 mm Cu foam for ϴ = 30 minutes time periods at T_H = 100 ˚C

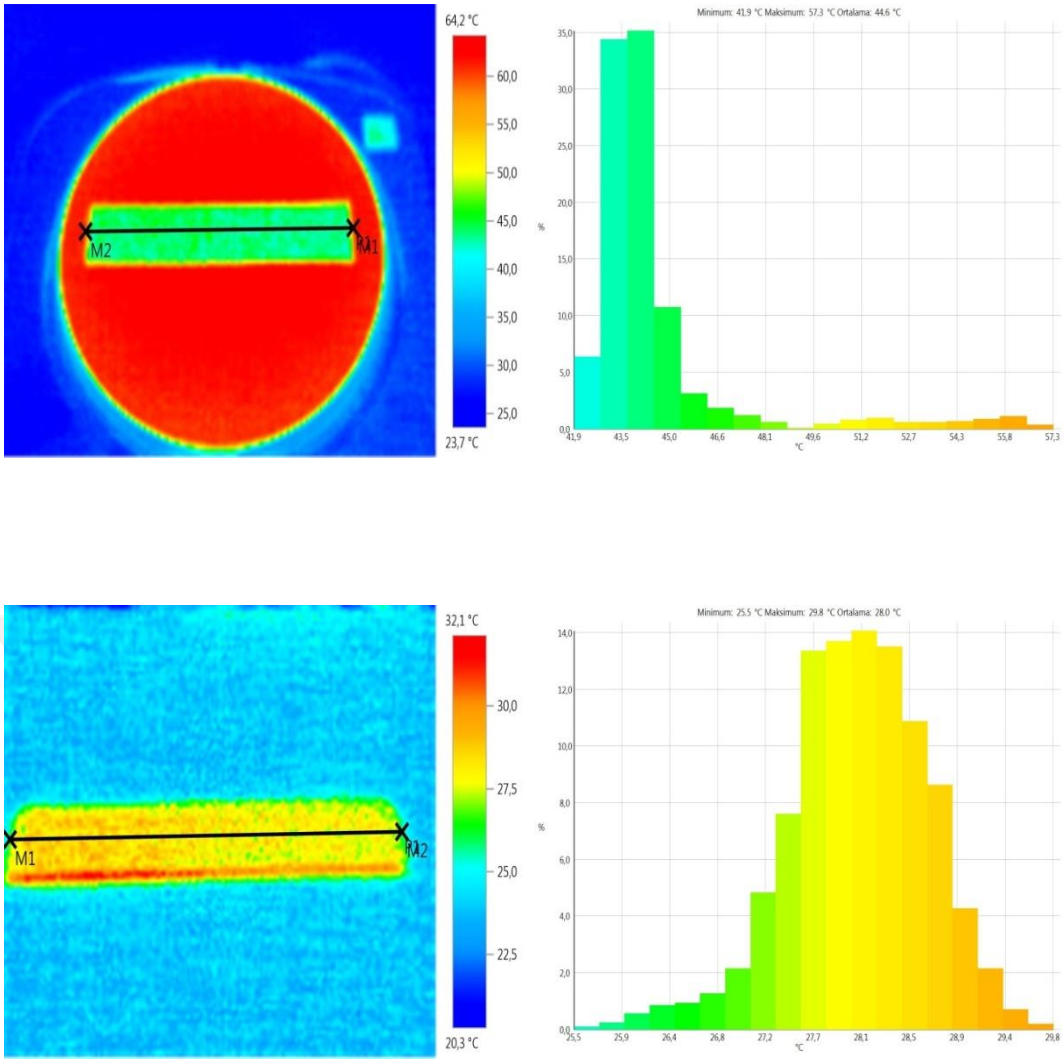

Figure A19 Thermal images and histogram profiles of the t = 3 mm Cu foam for ϴ = 10 minutes time periods at $T_H = 50$ ˚C

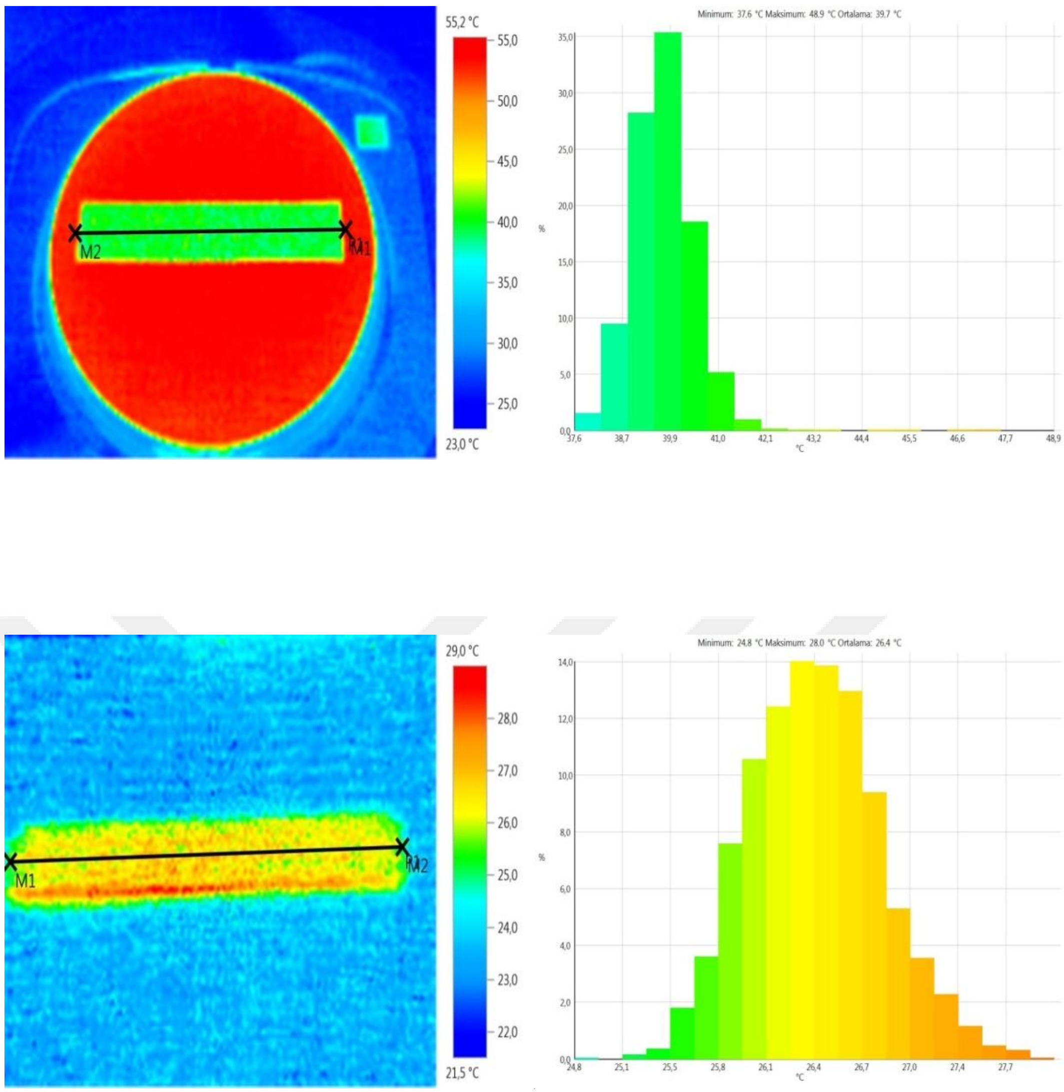

Figure A20 Thermal images and histogram profiles of the t = 3 mm Cu foam for ϴ = 20 minutes time periods at $T_H = 50$ ˚C

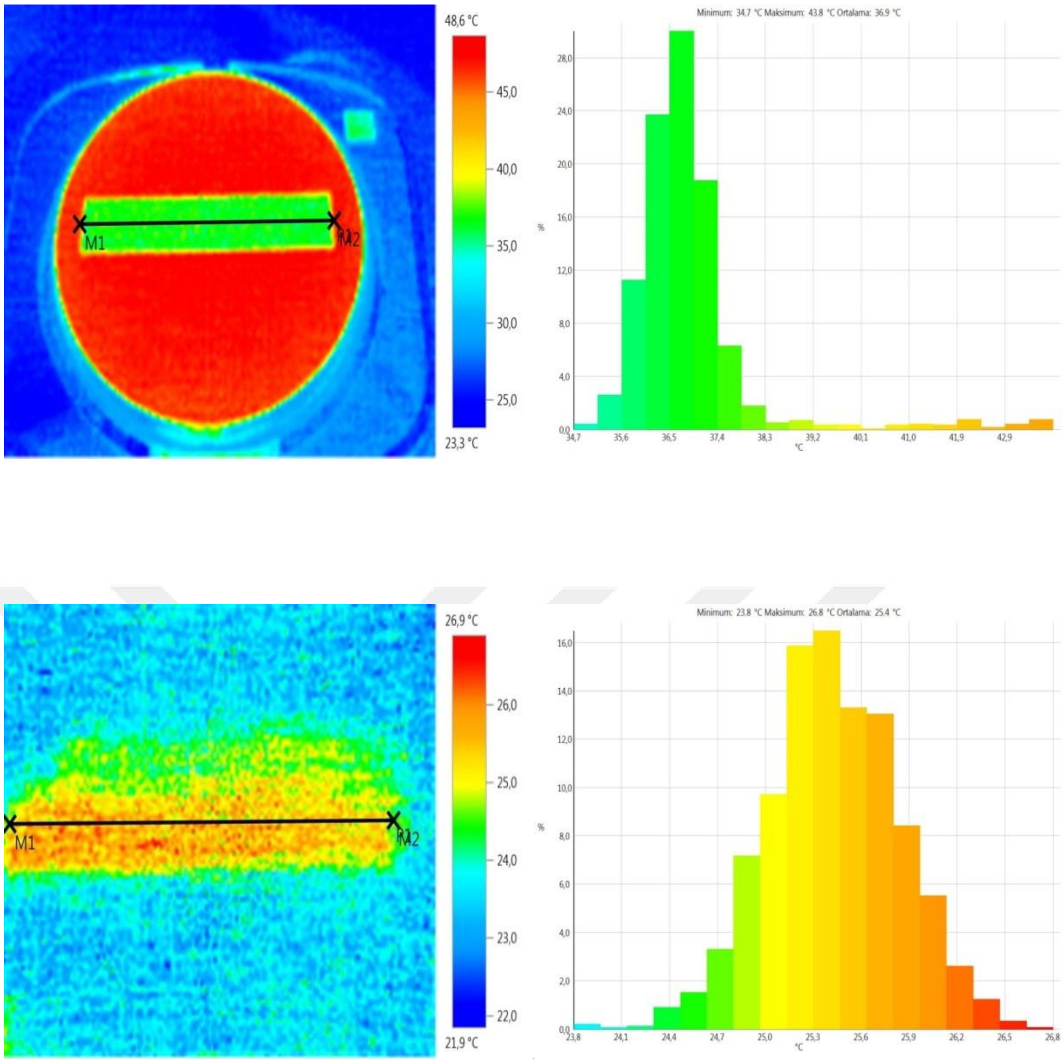

Figure A21 Thermal images and histogram profiles of the t = 3 mm Cu foam for Θ = 30 minutes time periods at $T_H = 50$ ˚C

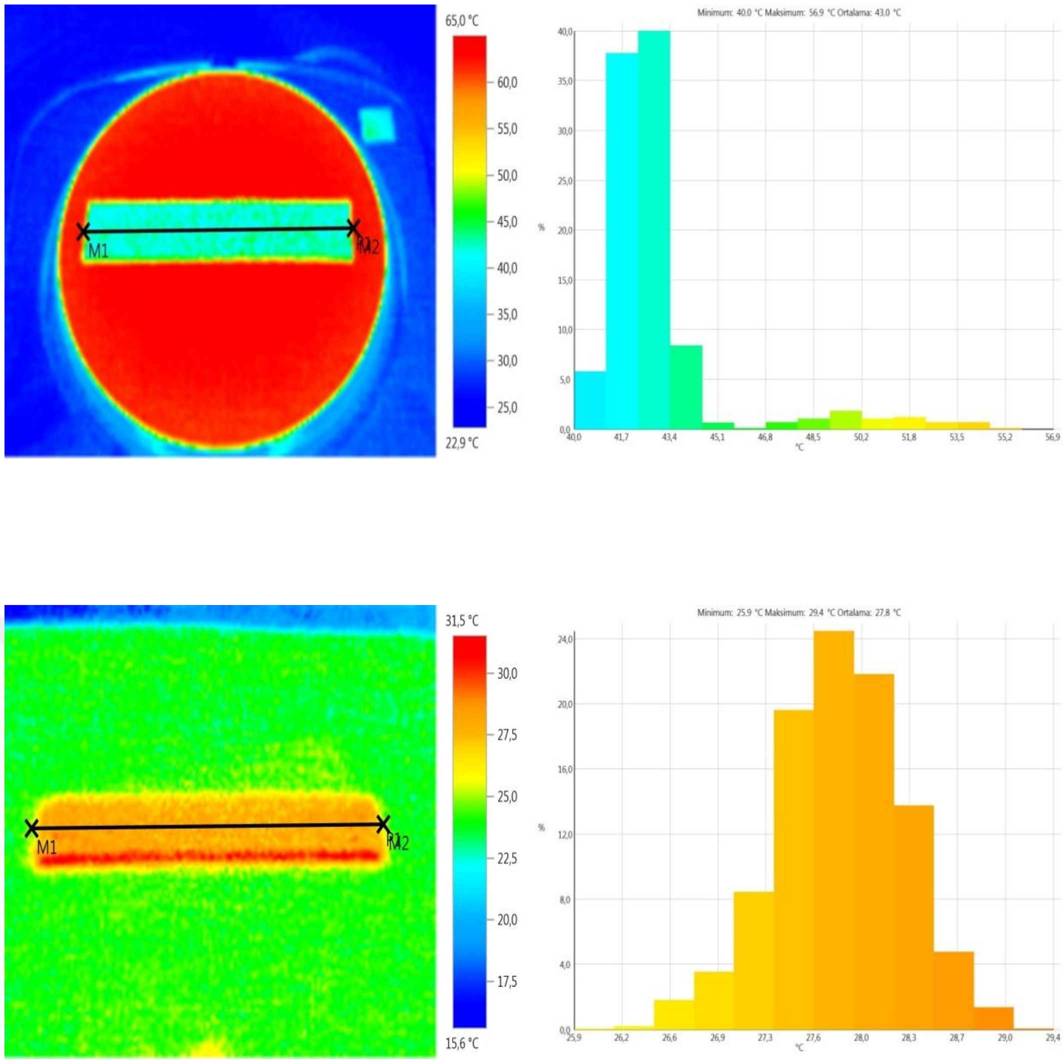

Figure A22 Thermal images and histogram profiles of the t = 4 mm Cu foam for Θ = 10 minutes time periods at $T_H = 50$ ˚C

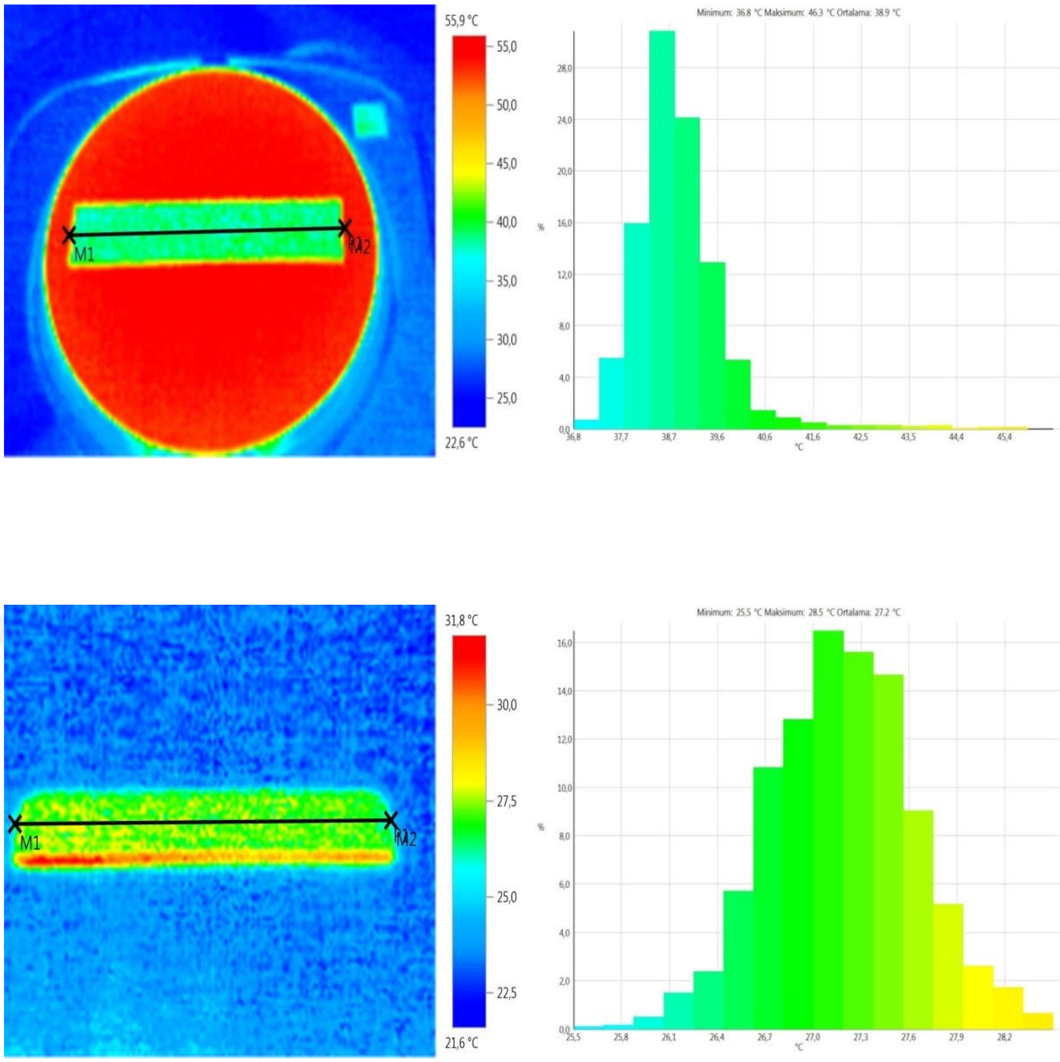

Figure A23 Thermal images and histogram profiles of the t = 4 mm Cu foam for ϴ = 20 minutes time periods at $T_H = 50$ ˚C

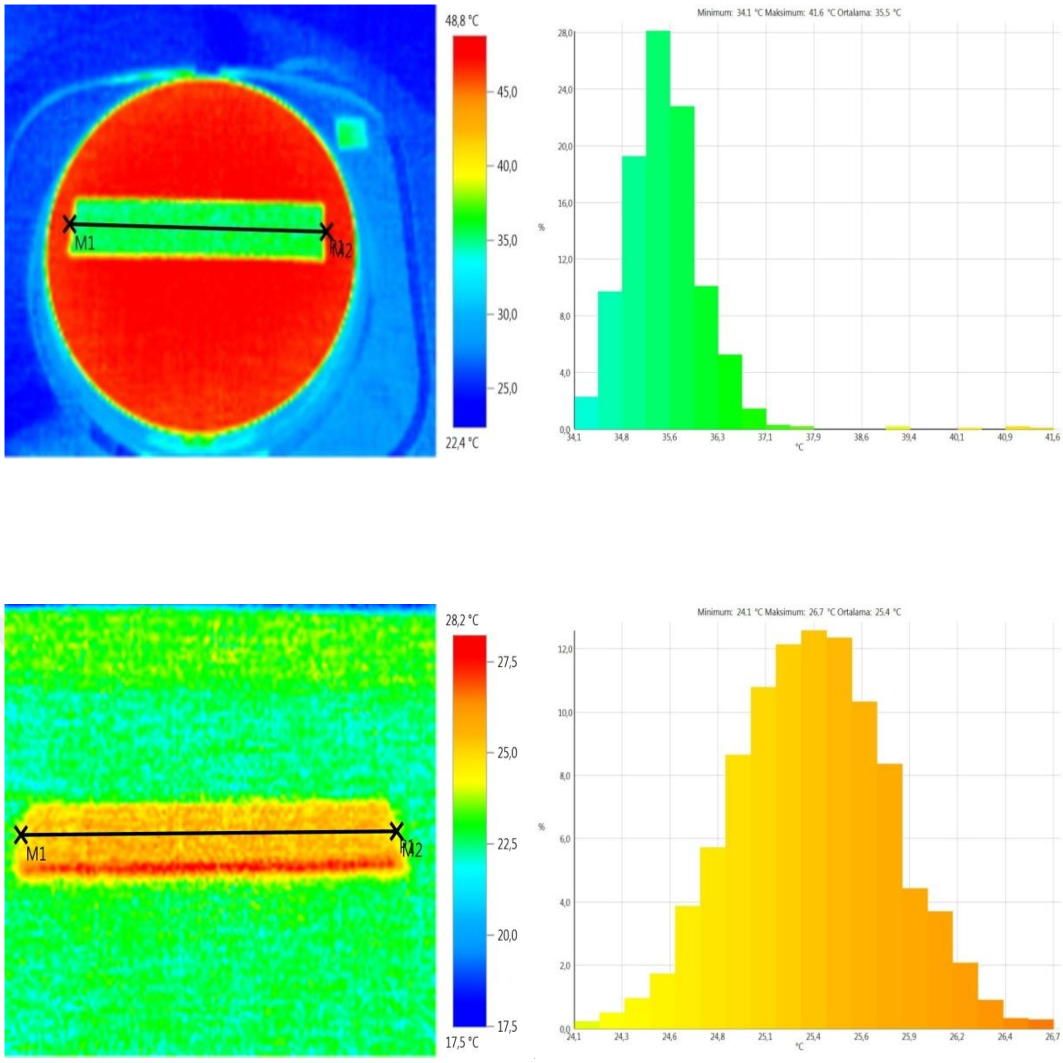

Figure A24 Thermal images and histogram profiles of the t = 4 mm Cu foam for ϴ = 30 minutes time periods at T_H = 50 ˚C

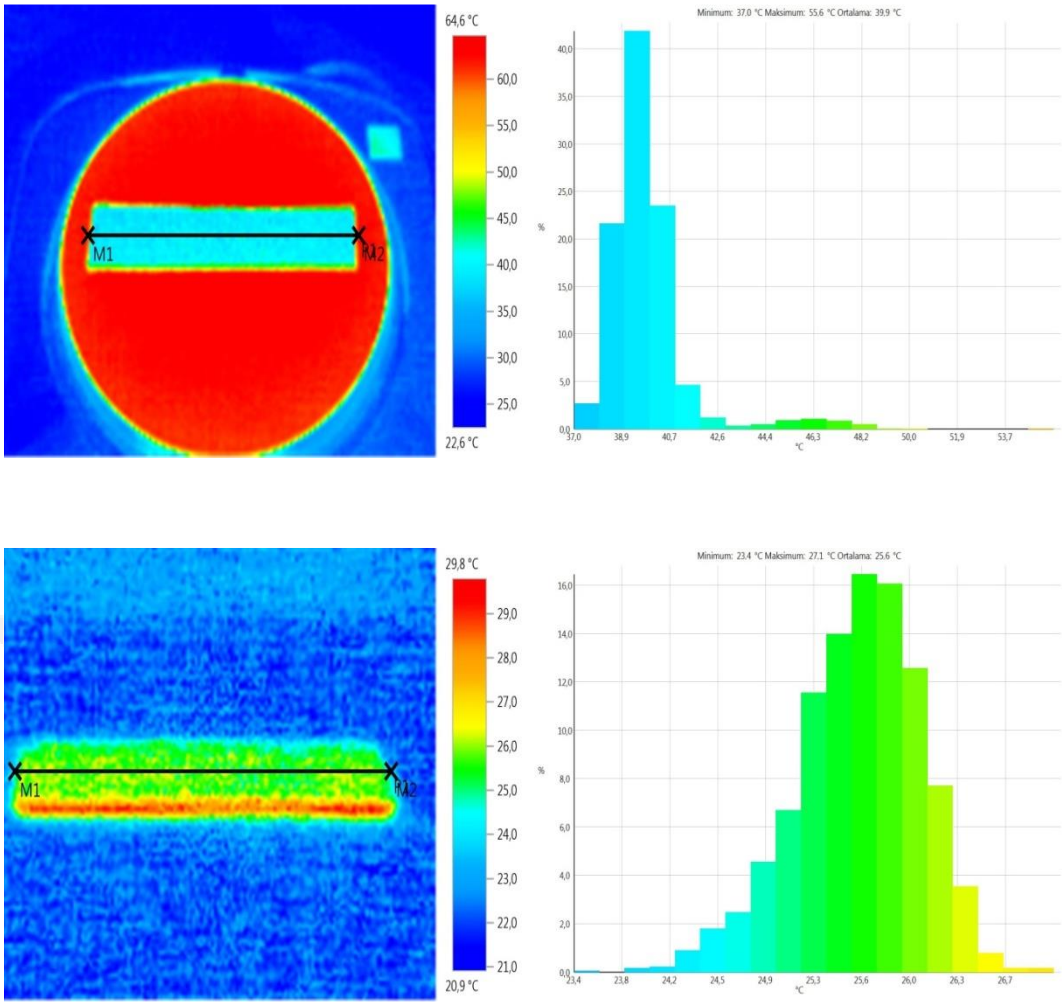

Figure A25 Thermal images and histogram profiles of the t = 5 mm Cu foam for ϴ = 10 minutes time periods at $T_H = 50$ ˚C

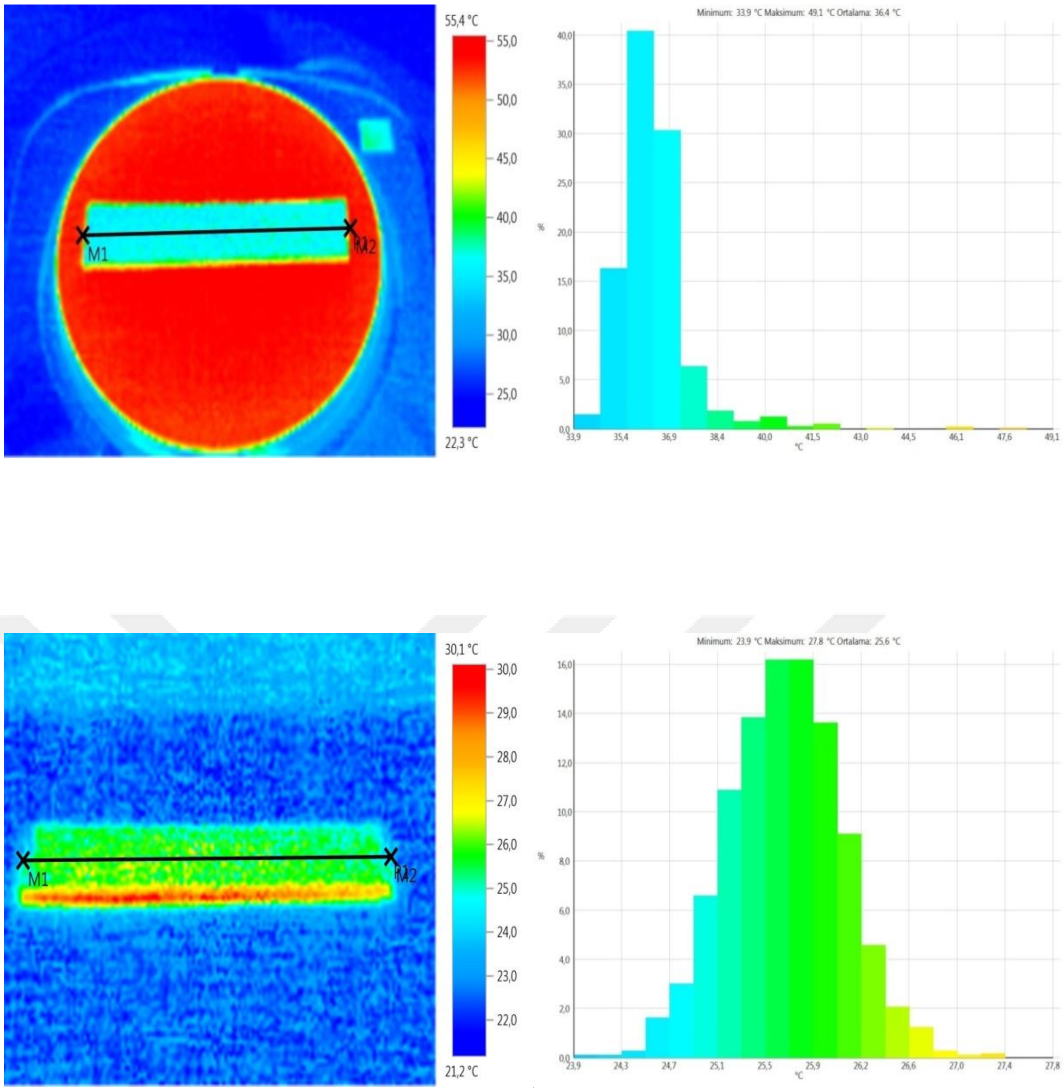

Figure A26 Thermal images and histogram profiles of the t = 5 mm Cu foam for Θ = 20 minutes time periods at $T_H = 50$ ˚C

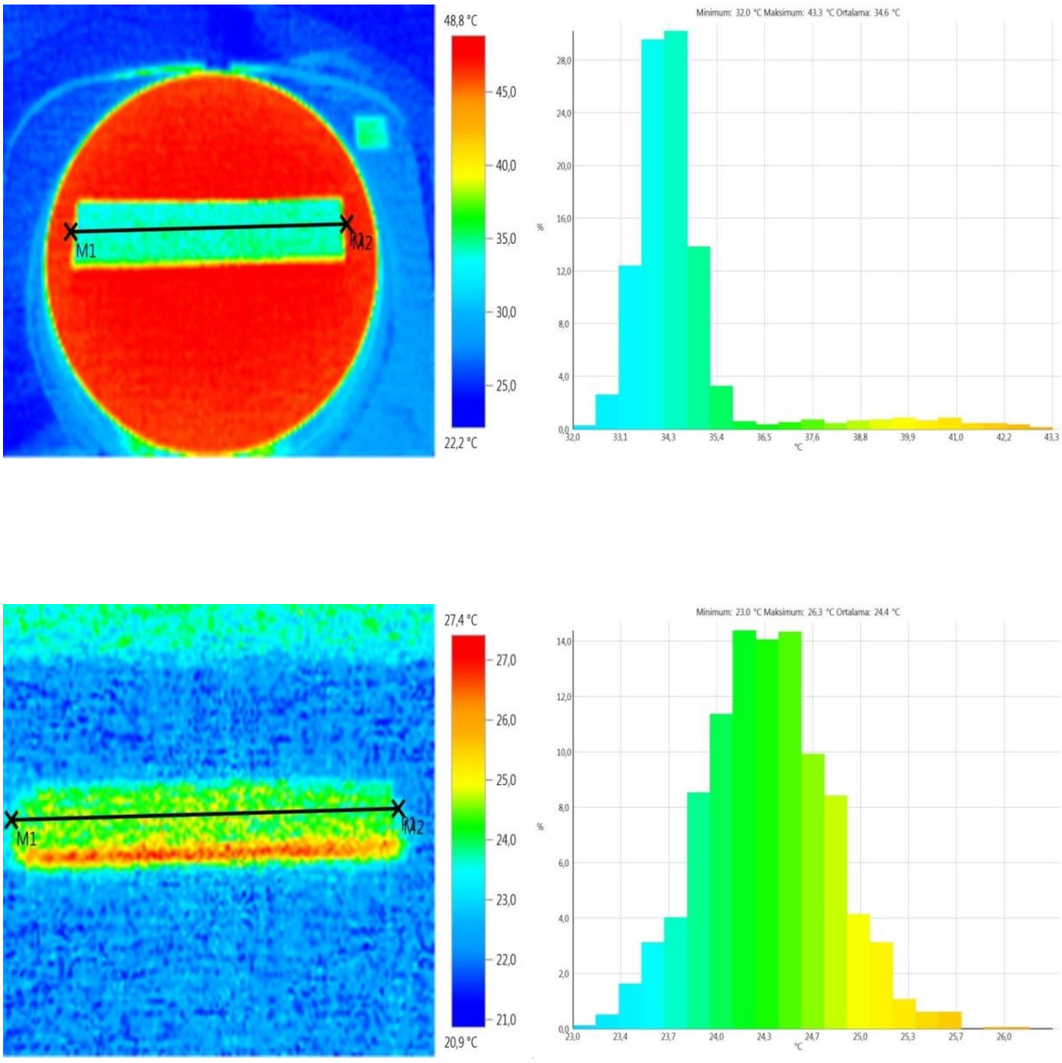

Figure A27 Thermal images and histogram profiles of the t = 5 mm Cu foam for Θ = 30 minutes time periods at $T_H = 50$ ˚C